

Technical specifications of freight string transport system for highly efficient transportation of bulk commodities



Contents

1. Introduction.....	3
2. Mounted STS	6
2.1. Weight and Dimensional Parameters of Motorail Freight Wagon	7
2.2. The Provision of Ore Transportation in the Volume of 50 mln t/year.....	8
2.3. Wheels Size of Motorail Freight Wagon	12
2.4. Gauge and Freight Wagon Cross-Sectional Dimensions.....	15
2.5. Capacity of Autonomous Power Supply System.....	18
2.6. Location of Diesel-Electric Aggregates in a Motorail.....	22
2.7. Motorail Stability Rating.....	22
2.8. Specifications of a Motorail with Load Capacity of 160tons Intended for Ore Transportation.....	25
2.9. STU Motorail Fuel Efficiency.....	27
2.10. Analysis of String-Rail (“Longitudinal Sleeper”) Located on Elastic Subgrade.....	28
2.11. Static Analysis of a String-Rail on an Elevated Section of a Track.....	48
2.12. Analysis of Rail Motor-Vehicle Train Dynamic Interaction on an Elevated Section of STS Track Structure.....	67
2.13. Analysis of Dynamic Interaction of a Rail Motor-Vehicle Train and Ground Sections of STS Track Structure.....	78
2.14. Conclusions on Mounted STS	86
3. Suspended STS	88
3.1. Unicars Weight and Dimensional Parameters	88
3.2. The Provision of Ore Carriage in the Volume of 50 mln t/year.....	95
3.3. Capacity of Autonomous Power Supply System.....	99
3.4. Specifications of Suspended STS Unicar with Load Capacity of 15 Tons Intended for Ore Transportation	101
3.5. Fuel Efficiency of a Suspended STS Unicar.....	102
3.6. Automatic Control System of Suspended STS.....	103
3.7. Static Analysis of a String-Rail on a Suspended Section of a Track Structure.....	104
3.8. Conclusions on Suspended STS.....	130
4. Conclusions.....	132
5. List of References	132



1. Introduction

Australia is rich in mineral resources. It owns large share of world reserves (18% of zinc, 33% of lead, 37% of nickel, 39% of rutile, 41% of zircon, 95% of tantalum and 40% of uranium). Australia is ranked 4th place in the world in production of coal and 1st place in its export. In the production of iron ore it takes third place in the world.

Currently, revenue growth of Australian mining industry is provided by rapid economic growth in Asia. Thus, economic growth in China leads to increase of steel, nickel, copper, chark and other minerals demand. An increase of middle class and urbanization takes place in China. Every year 35-40 million of Chinese migrate from rural to urban areas. They need household items, home appliances. The network of water pipes and sewage systems have to be expanded. It results in sustainable expansion of mining products market of Australia.

However, there are some limitations in export of mining products from Australia. First of all, it is undeveloped infrastructure (roads and ports). String Transport Unitsky helps to remove this limitation.

String Transport Unitsky (STU), as well as, for example, road and rail transport, has its own variety, freight STU. Freight STU might be used for different purposes. The most perspective purpose of freight STU is bulk cargo transportation (coal, ore, gravel, sand, etc.)

Freight STU may be of several types:

- suspended (a rolling stock is hanged up to the bottom of a string-rail track structure);
- mounted (a rolling stock is placed on the top of a string-rail track structure);
- traction and braking forces are implemented with the help of driving wheels;
- traction and braking forces are implemented with the help of traction rope;
- with electrical contact system or without it (for example, driven by diesel-electric unit).

Each type of freight STU might be efficient for different purposes.

Thus, the use of a traction rope (see Fig. 1.1) is most appropriate for the carriage of goods in the automatic mode at relatively short distances (up to 10 km) in mountainous areas, where track slopes in the vertical plane can reach 45°.

Suspended STU (see Fig. 1.2) is more versatile and may have wider application. It can be used to solve local problems, such as transportation of goods overcoming several barriers up to 1 km (rivers, lakes, swamps, ravines, quarries, etc.), and it can also be used to transport goods for hundreds of kilometers. At relatively low traffic volumes (5-6 million tons per year, for example, construction of dams) a rolling stock should be managed by a driver. At significant traffic volumes transportation process should be fully automated. Freight STU assumes, if necessary, locating of terminal stations in the sea at a distance of 5-10 km from the shore to the sea depth of 20-25 m, which minimizes expensive works of dredging (see. Fig. 1.3).



Fig. 1.1. Traction rope version of freight suspended STU



Fig. 1.2. The version of freight suspended STU with a driver

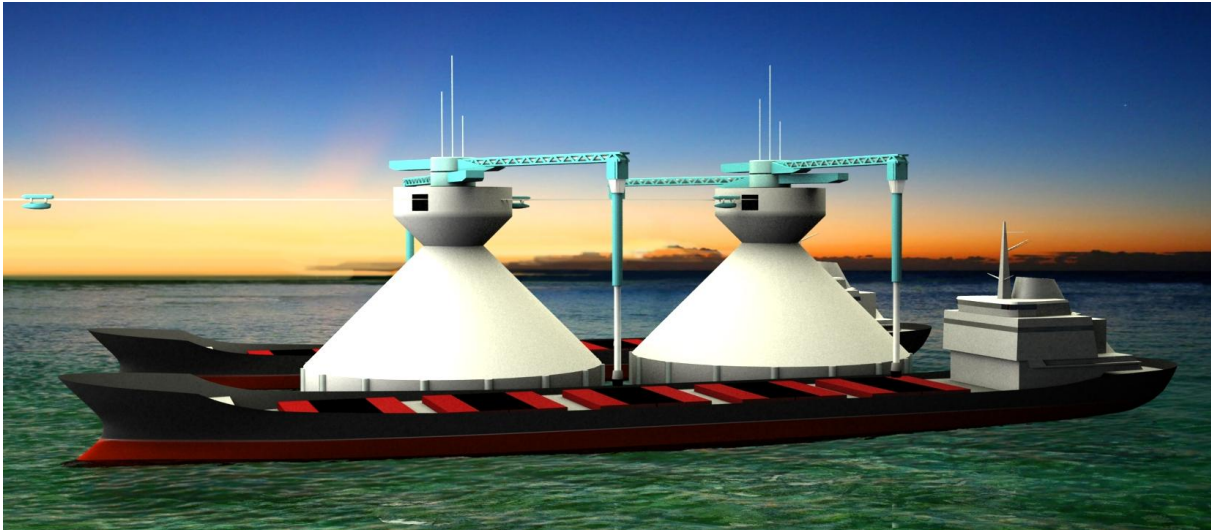


Fig. 1.3. Freight suspended STU assumes location of terminal stations in the sea at a distance of 5-10 km from the shore

Track structure of mounted STU may withstand significant load and at the same time develop high speed rates (up to 120 km/h and even more). Thus, high-speed mounted STU will successfully solve a problem of transportation of goods in large quantities (50 million tons per year and more) to the long distances (see Fig.1.4).



Fig. 1.4. Freight mounted STU

This technical proposal was developed to make preliminary design, analysis and evaluation of bulk carriage concept, in particular iron ore transportation (including stamped iron ore, see Fig. 1.5) by freight STU for the conditions of Australia (hereinafter referred to as STS). Both suspended and mounted STS are taken into consideration in this technical proposal. Estimated productivity of both STS versions is 50 million tons per year.



Fig.1.5. Stamped iron ore ready for smelting

A number of STS know-how (including illustrations, concepts, methods of calculation, technical and economic parameters) have been disclosed in this proposal. Since it is the know-how, which is the basis of STS technology capitalization providing its high market value, all the information contained in this proposal is confidential.

2. Mounted STS

The concept of mounted STS is transportation of bulk materials over a string-rail track structure with the help of speed multijointed rail cars (motorails), adapted for loading and off-loading of cargo on the move at special terminal stations.

A motorail consists of several wagons, driven by multiple-unit system. There is a head wagon (single or joint), freight wagons (the number of wagons depends on load capacity of a motorail) and a hind wagon (single or joint).

Power supply units, fuel tanks and other equipment are located in a head and a hind wagon. Driver's place is in a head wagon.

Freight wagons are motorized and are equipped with self-dumping cabins. The process of off-loading is implemented through bottom hatches. The concept assumes complete automation of transportation process.

String-rail track structure of mounted STS is the form of wire or cable bridges with prestressed cable, wired to the cable-stayed girder, which serves as railway for motorails.

String-rail track structure of mounted STS, depending on the terrain, consists of several sections. There are elevated sections (string-rail is mounted on the supports). There are also sections built in the form of longitudinal sleeper, which rest on the ground as on elastic foundation. In this case a string-rail is wired to the leveled and compact ground, and only rail top juts out of the ground.



2.1. Weight and Dimensional Parameters of Motorail Freight Wagon

Admissible axial load on track and wagon base size (taking into account calculated norms of freight mounted STU-STs) are accepted as initial data for evaluative definition of weight and dimensional parameters of freight wagon.

Calculated admissible wheels axial load on track is 30 000 N (15 000 N – per one string rail), wheels base size is 2 000 mm.

2.1.1. Wagon Load Capacity

Wagon load capacity is determined from the formula:

$$P = p_o \cdot m_o / (1 + k_t) \cdot g = 30000 \cdot 2 / (1 + 0.5) \cdot 9.8 = 4081 \text{ kg,}$$

where:

$p_o = 30\,000 \text{ N}$ is axial load;

$m_o = 2$ is axle number;

$g = 9.81 \text{ m/s}^2$ is acceleration of gravity;

$k_t = 0.5$ is tare coefficient (on pre-design stage is accepted as equal to the average roofed railway hoppers tare coefficient (on the average approx. 0,4) and dump wagons (on the average approx. 0.6).

Wagon load capacity is accepted equal to $P = 4,0 \text{ t}$.

2.1.2. Wagon Weight

Dead weight of the wagon (tare) will be $T = P \cdot k_t = 4.0 \cdot 0.5 = 2.0 \text{ t}$.

Total weight (gross weight) of a wagon will be $M = P + T = 4.0 + 2.0 = 6.0 \text{ t}$.

2.1.3. The Volume of the Iron Ore Loaded to the Wagon Body

The calculated volume v of ore loaded to the wagon body can be determined from the following formula:

$$v = P / \rho, \text{ m}^3$$

where ρ is a bulk density, t/m^3 .

Iron ore bulk density depends on ore intended use (for example, sintered iron ore production, open-hearth or blast-furnace process of steel production) and may vary from 2.4 to 2.8 t/m^3 . To calculate the body volume we take the density of 2.5 t/m^3 which is relevant for fine-crushed ore (fineness of approx. 25 mm), which is largely distributed by Australian mine companies.

In this case calculated volume of the loaded iron ore will be:

$$v = 4.0 / 2.5 = 1.6 \text{ m}^3.$$

2.1.4. Freight Wagon Length

To provide uniform loading of a track structure by multijointed motorail in motion the interval between the wheels of adjacent wagons should be equal to the wagon base (2 000 mm). In this case the overall length of freight wagon will be 4 000 mm (see Fig. 2.1), and the rate of 3 900 mm may be accepted as the size of wagon inner length.

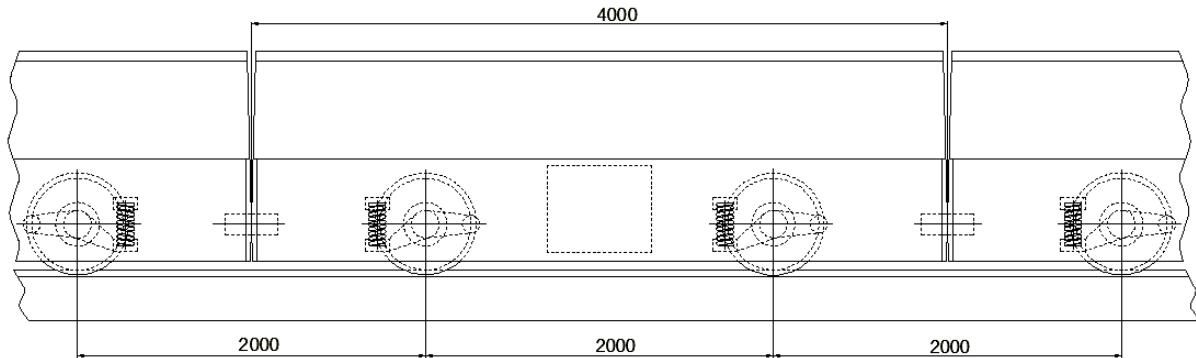


Fig. 2.1. Uniform loading of a track structure by a motorail

2.2. The Provision of Ore Transportation in the Volume of 50 mln t/year

There are four stages in the process of ore transportation:

- loading of ore to the moving at a low speed motorail at a loading terminal station (0.5–2.0 m/sec);
- transportation of ore by a motorail to an off-loading terminal station (80–120 km/h);
- off-loading of ore by moving at a low speed motorail at the off-loading terminal station (0.5–2.0 m/sec);
- moving of an empty motorail to the loading terminal station (80–120 km/h).

To carry 50 million tons of ore per year motorail loading and off-loading on terminal stations should be provided with a productivity of at least 1.65 t/sec (in conditions of working on a triple-shift basis with 20 minutes breaks between the shifts, without regard to the time lost due to the moving of not only freight wagons and keeping safe distance between motorails on terminal stations).

2.2.1. Loading

The most efficient way of motorail loading seems to be implemented on the motorail move. As an example we can consider the simplest method, when loading process is similar to the ore loading process from a storage bin to a ribbon conveyor. In our case the motorail itself will act as a conveyor. It is known that under uniform motion of bulk load (in our case it is ore) the productivity of vehicle is equal to the weight of load going through its cross section per time unit. So we can determine the appropriate motorail low speed necessary for loading from the formula:

$$V_{\text{н}} = Q / A_{\text{r}} \cdot \rho = 1.65 / 0.41 \cdot 2.5 = 1.61 \text{ m/sec},$$

where

$Q = 1.65 \text{ t/sec}$ is transport system productivity;

$A_{\text{r}} = v / L = 1.6 / 3.9 = 0.41 \text{ m}^2$ is cross sectional area of load in the body of the motorail freight wagon,

where:

$v = 1.6 \text{ m}^3$ is ore calculated volume loaded to the freight wagon (see Art. 2.1.3);

$L = 3.9 \text{ m}$ is inner length of the motorail freight wagon body (see Art.2.1.4).

Fig. 2.2, 2.3 and 2.4 listed below represent motorail loading process on the terminal station.

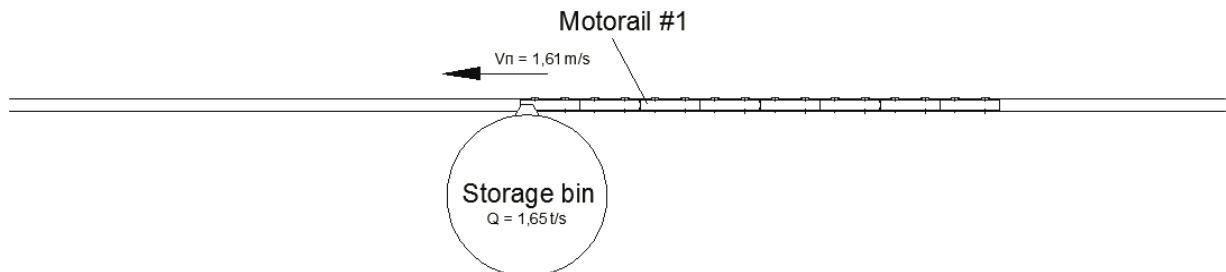


Fig. 2.2. Bin delivery unit is switched on and ore loading process with the productivity of 1,65 t/sec to the freight wagons of the motorail #1 moving at a speed of 1.61 m/sec takes place

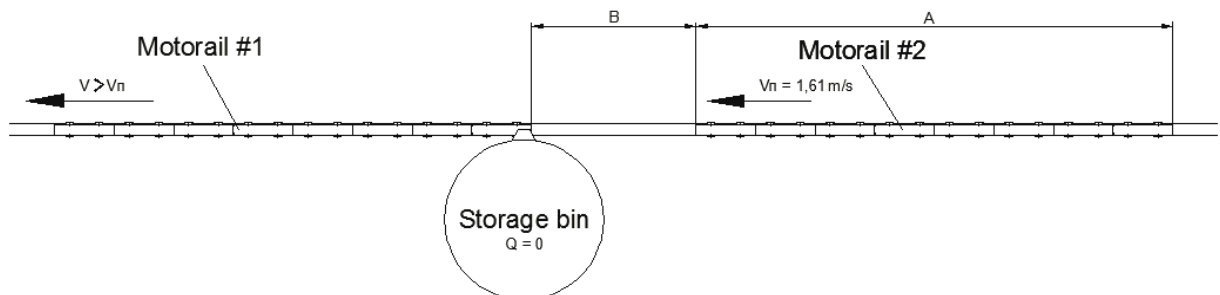


Fig. 2.3. Ore loading from a storage bin to the motorail #1 is completed. The motorrail #1 starts speeding-up. Bin delivery unit is switched off till motorail #2 arrives.

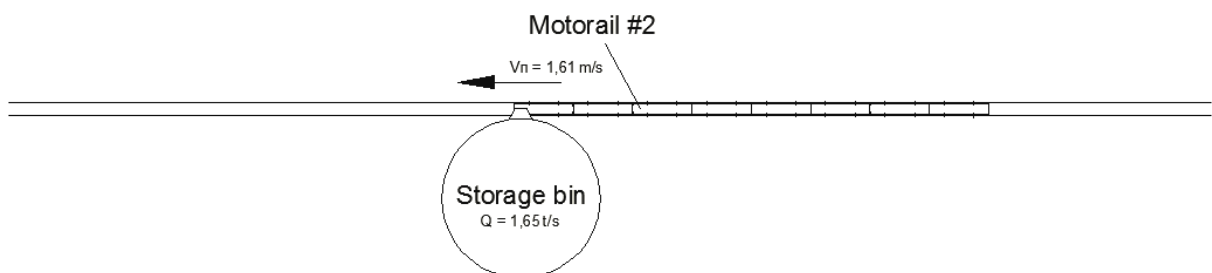


Fig. 2.4. Bin delivery unit is switched on and ore loading process with the productivity of 1,65 t/sec to the freight wagons of the motorail #2 moving at a speed of 1.61 m/sec takes place.

Motorrail traffic interval is determined from:

$$\Delta T = (A + B) / V_n, \text{ sec (the results see in Tab. 2.1)}$$

where

A is motorrail length, m (see Fig.2.3);

B is safe distance between motorrails on a terminal station, m (see Fig.2.3).

The motorrail length can be determined from the formula:



$$A = (P_{\Pi} / P) \cdot L_B + L_1 + L_2, \text{ m (see Fig. 2.1)}$$

where

P_{Π} is motorail load capacity (see Fig. 2.1);

$P = 4 \text{ t}$ is wagon load capacity;

$L_B = 4 \text{ m}$ is freight wagon overall length (see Art.2.1.4);

$L_1 = 9 \text{ m}$ is the head jointing wagon overall length (the amount is recommended on the basis of predesign of a track structure);

$L_2 = 9 \text{ m}$ is the hind jointing wagon overall length (the amount is recommended on the basis of predesign of a track structure).

Minimal safe distance B should exceed the motorail length of braking which value can be determined from the formula offered by European Standard EN 13452-1 for rail transport:

$$S = V_o \cdot t_e + V_o^2 / (2 \cdot a_e) = 1.61 \cdot 2 + 1.61^2 / (2 \cdot 1) = 4.52 \text{ m,}$$

where

$V_o = 1.61 \text{ m/sec}$ is initial speed (corresponds to loading speed);

$t_e = 2 \text{ sec}$ is equivalent damping time in accordance with EN 13452-1 safety standards;

$a_e = 1 \text{ m/sec}^2$ is equivalent speed reduction in accordance with EN 13452-1 safety standards.

Safe distance is taken as equal to approximately two S:

$$B = S \cdot 2 = 9 \text{ m.}$$

Knowing traffic interval we can determine annual productivity of transport system for different motorail load capacity rates (in conditions of working on a triple-shift basis with 20 minutes breaks between the shifts) from the formula:

$$Q_r = P_{\Pi} \cdot 30222000 / \Delta T, \text{ mln. t/year,}$$

where 30 222 000 is the number of working seconds per year.

The calculated results of the motorail lengths, traffic intervals and annual productivity of STS transport system for motorails with different load capacity are represented in Tab. 2.1.

Table 2.1

Motorail length, traffic intervals and annual productivity of transport system at ore loading and off-loading motorail speed of 1,61 m/sec for motorails of different load capacity

The motorail load capacity (P_{Π}), t	A, m	ΔT , sec	Q_r , mln. t/year
100	118	77.6	40.0
160	178	114.9	42.0
200	218	139.7	43.3
260	278	177.0	44.4
300	318	201.8	44.9



Table 2.1 shows that at motorail loading speed of 1.61 m/sec the motorail loading capacity should be considerably increased (up to 500 tons and more) to achieve annual productivity of 50 mln. t/year. In return it leads to excessive increase of motorail length, relayed capacity and overall sizes of autonomous electric supply system power equipment, which makes no sense when there is small cross-section area of load in the motorail freight wagon body. To achieve mentioned annual productivity it is reasonable to increase motorail loading speed to the extent of practical recommendations.

Loading speed limit can be estimated under the level of present bulk conveyors because the motorail loading principle is similar to the ore loading process from a bin to a conveyor. Existing ore loading automatic equipment provide the conveyor speed of approx. 6 m/sec.

2.2.2 Off-Loading

Motorail off-loading is implemented on the move by opening hatches on a signal to hatch hold-down (or by its runover). Hatch doors also return to their initial position on the move by runover to hold-down rolling batteries.

Ropeway operational experience (the version when wagonettes are being off-loaded through bottom hatches) shows that it is undesirable to increase off-loading speed on the move more than the rate of 2 m/s [1]. Taking it into account, motorails traffic interval will depend on the off-loading time of bulk.

Traffic intervals and annual productivity of STS transport system at ore loading and off-loading speed of 2.0 m/sec for motorails of different load capacity are represented in Tab.2.2. Motorails with load capacity exceeding 160 t at ore loading and off-loading speed of 2 m/sec provide more than 50 mln t/year annual productivity (in conditions of working on a triple-shift basis with 20 minutes breaks between the shifts).

Table 2.2

Motorail length, traffic intervals and annual productivity of STS transport system at ore loading and off-loading motorail speed of 2,0 m/sec for different rates of motorails load capacity

The motorail load capacity (P_n), t	A, m	ΔT, sec	Q_r, mln. t/year
100	118	64	47.2
160	178	94	51.4
200	218	114	53.0

2.2.3 Number of Motorails and Average Speed on a Track

The number of motorails involved in a carriage process depends on an average motorails speed on a track, its load capacity with intended transport system productivity and carriage distance. Tab.2.3 shows the number of motorails with load capacity of 160 t which are involved in ore transportation on 100 km distance with annual productivity of 51 mln t/year (three average speed rates on a track are represented).



Table 2.3

The number of motorails with load capacity of 160 t which are involved in STS ore transportation on 100 km distance with annual productivity of 51 mln t/year

An average motorail speed, km/h	The number of motorails involved
50	154
100	77
150	52

Choosing an average motorail speed it is reasonable to take speed rate of about 100 km/h. First of all due to industry-standard production of breaking equipment designed for freight automobile and rail transport (trams). If electric machines built in wheels (motors-in-wheel) are used as traction electric motors, maximum angular frequency of revolution won't let the average speed exceed the rate of 100 km/h. It should be mentioned that motorail energetic efficiency will go down when the speed is increased. To define optimal speed rate providing the whole transport system (including rolling stock, track and infrastructure) with minimum costs, it is necessary to make complex analysis of transportation costs (energy, amortization, wages, etc.).

2.3. Wheels Size of Motorail Freight Wagon

2.3.1. Wheel Tread Diameter

Wheel diameter can be determined on the basis of contact resistance. There are two contact versions depending on the wheel rim and rail form:

- line contact (contact patch is close to rectangular shape);
- point contact (contact patch is close to ellipse shape).

The first version can be applied to freight STU in case of cylinder wheel rolling on a flat rail top. The second version can be applied to freight STU in case of cylinder wheel rolling on a raised rail top. Ropeway operational back-ground [2] shows that track resistance at point contact is 1.5 times higher than it is at line contact (with the same load and wheel diameter). Taking into account the recommendations [2], to increase STU efficiency wagon wheels are at least of 450 mm diameter, and the rail top in the middle of it has a flat strip not less than 20 mm wide (see Fig. 4.1).

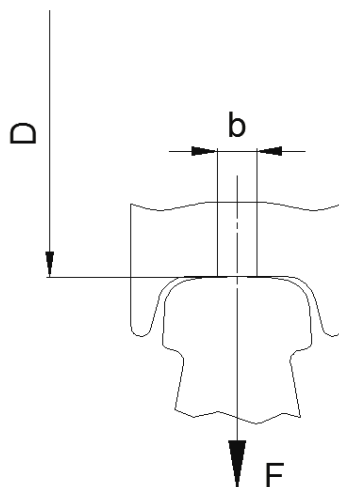


Fig. 2.5. Wheel and rail top contact



In this case contact stress will be the following:

$$\sigma_k = 272 \cdot 10^3 (F/(D \cdot b))^{1/2} = 272 \cdot 10^3 (14700/(0.45 \cdot 0.02))^{1/2} = 347621250 \text{ Pa,}$$

where

$F = M \cdot g / 4 = 6000 \cdot 9.8 / 4 = 14700 \text{ N}$ is load per wheel;

$D = 0.45 \text{ m}$ is wheel rolling surface diameter;

$b = 0.02 \text{ m}$ is the width of a flat strip on the rail top (the length of a contact line);

$M = 6000 \text{ kg}$ is the total (gross) weight of a freight wagon.

Admissible contact stress rates for steel rails in case of line contact are represented in Tab. 2.4.

Admissible contact stress rates for steel wheels in case of line contact are represented in Tab. 2.5.

Table 2.4

Admissible contact stress rates for steel rails (line contact)

Steel Grade	Hardness, HB, not less than	$[\sigma_k]$, MPa
Carbonaceous of ordinary quality		
Ст3	130	400
Ст5	140	450
14Г	130	460
14Г2	140	480
24Г	140	500
Carbonaceous and manganous of high quality		
45	229	570
60Г	260	650
35Г2	225	650
Rail		
M71	217	600
M75	245	770

Table 2.5

Admissible contact stress rates for steel wheels (line contact)

Steel Grade	Rim hardness (normalization), HB	$[\sigma_k]$, MPa
45	217	450
50Г2	241	550
65Г	260	600
40XH	255	550

In the presence of tangential forces (tractive or breaking force) the rates represented in Tab. 2.4 and 2.5 must be decreased. Reduction value depends on tangential to normal force ratio (see Tab. 2.6).

Table 2.6

Admissible contact stresses for steel wheels (line contact)

Tangential to normal force ratio	0.0	0.1	0.15	0.2	0.25	0.3
Admissible stresses decrease, %	0.0	2	4	6	10	15-20

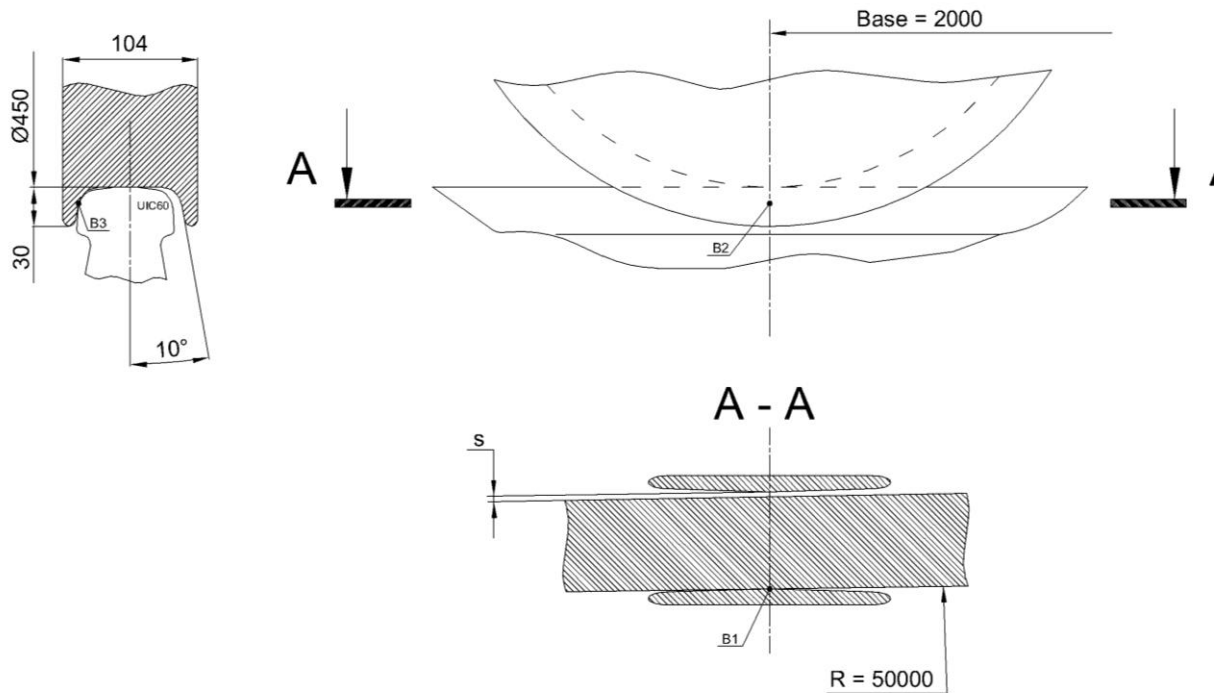


Fig.2.7. For rounding 50 m diameter curves with 2 m base a deflection angle of bearing rib external edge should be not less than 10° . S size (equal to 8 mm) is a tolerance zone of wheel and rail positional relationship.

2.4. Gauge and Freight Wagon Cross-Sectional Dimensions

2.4.1. Motorail Height

To create optimal loading conditions wagon height should be approximately the same throughout the whole motorail length. Taking into account motorail low silhouette specified by small cross-section area of load in freight wagon body, driver's cab dimensions should be approximately the same as they are in motor car driver's cabin. In accordance with VDA 239-01 Code [3] the motor car driver's cabin height may vary from 1180 mm (compact motor car) to 1280 mm (big motor car). In motorail cabin we can accept the largest height of 1200 mm and in freight wagon body (taking into account hard bottom) we can accept the height of 1100 mm.

2.4.2. Body Width

Ore volume loaded to the freight wagon is equal to 1.6 m^3 (see Art. 2.1.3). To use totally wagon (and the whole motorail) nominal load capacity freight bodies volume should exceed the ore load volume. Rail transport operational back-ground shows that even at the most accurate loading the volume of the wagon is utilized at only 90-95percent of its potential. It happens because the wagon is not fully loaded at its flank sides and to their whole height due to the load angle of repose [4]. The freight wagon body volume can be determined from the formula used for rail dump wagons volume determination:

$v_r = v \cdot k_H = 1.6 \cdot 1.25 = 2 \text{ m}^3$ is the freight wagon body volume,

where:

$k_H = 1.1 - 1.25$ is dump wagons coefficient of fullness (taking into account freight wagon retreating edges and high loading speed (2 m/sec); on pre-design stage we accept the coefficient equal to 1.25).

In this case the freight wagon body inner width may be determined from the following relation:

$$b = v_r / (L \cdot h) = 2 / (3.9 \cdot 1.1) = 0.47 \text{ m,}$$

where:

L = 3.9 m is inner length of the freight wagon body;

h = 1.1 is inner height of the freight wagon body.

2.4.3. Overall Width and Gauge of a Freight Wagon

Gauge and freight wagon overall width and dimensions are determined from pre-design taking into account the following data:

-body inner width is equal to 470 mm;

-wheel overall width is equal to 110 mm;

-wheel rolling circle diameter should be no less than 450 mm;

-bearing rib height is equal to 30 mm;

-overall dimensions of electromagnetic brake produced by Mayr (diameter - 200 mm, width – 100 mm);

-traction motors overall sizes by initially estimated starting torque are accepted on the level of installed power of 5-6 kW per one wheel.

Pre-design results are outlined in Fig. 2.8 (motors-in-wheel serving as traction motors) and in Fig. 2.9 (series produced asynchronous motors version).

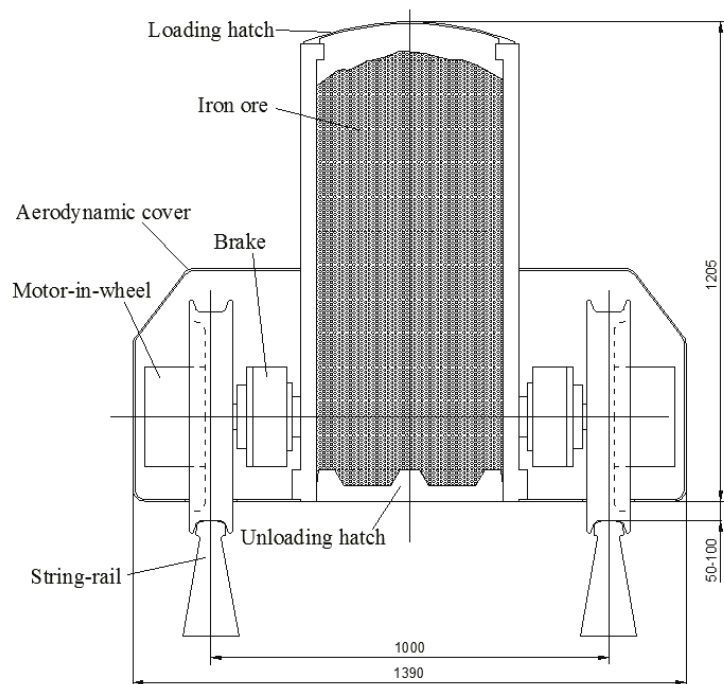


Fig. 2.8. Freight wagon cross section (motor-in-wheel version)

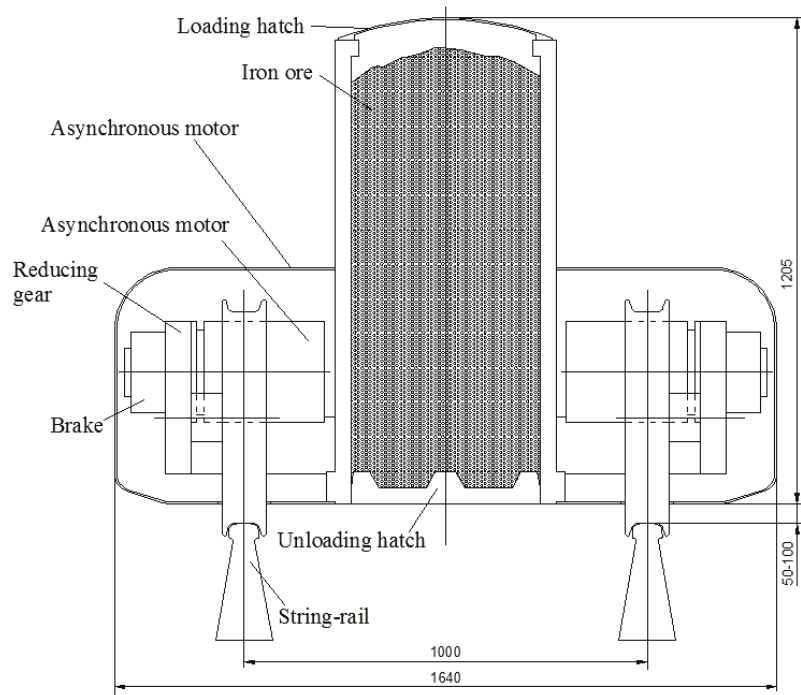


Fig. 2.9. Freight wagon cross section (asynchronous motors version)

When series manufactured asynchronous motors serve as traction motors, freight wagon (and the whole motorail) overall width will be 250 mm larger, and reducing gear will appear in a drive between a wheel and a motor. But series manufactured motors are cheap (300 – 400 \$), have long operation life (not less than 30 000 hours) and are easily obtainable.

2.4.4. Head and Hind Wagon Cross Section

Head and hind wagon cross section dimensions and configuration are determined by pre-design on the basis of the following parameters:

- gauge size (1000 mm);
- freight wagon overall width (in particular 1390 mm for motor-in-wheel version);
- necessary space for power equipment accommodation (efficient generating capacity diapason of 100-150 kW within 700-800 mm width). Head wagons follow VDA 239-01 Code. According to it typical space width for a driver in a motor car should be approximately 735 mm.

Pre-design results of head wagon cross-section are represented in Fig.2.10.

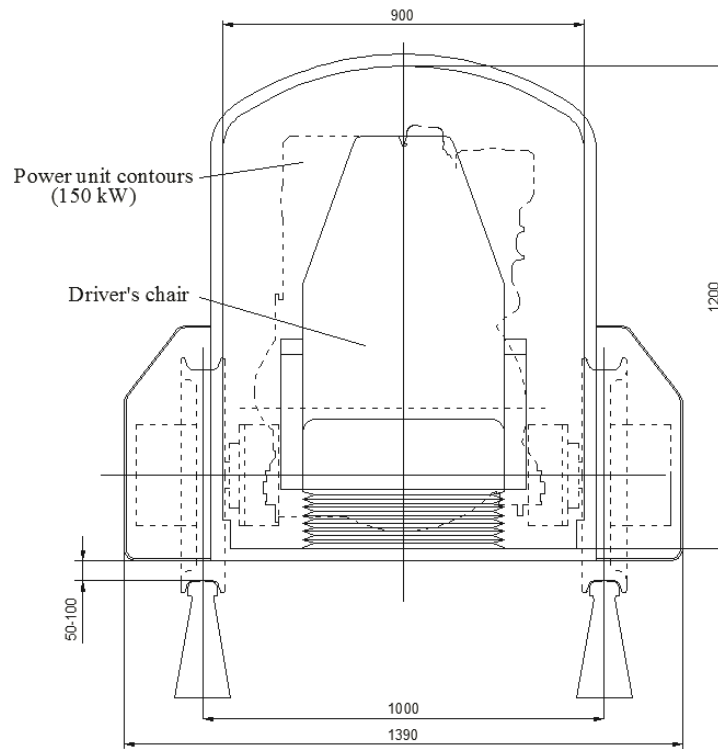


Fig. 2.10. Head wagon cross-section (in a driver's place)

2.5. Capacity of Autonomous Power Supply System

According to a layout arrangement to make autonomous power supply system more safe there should be two (or even more) diesel-power generators able to interact or function by themselves.

In the article autonomous power supply equipment (diesel engines) total capacity is estimated on the basis of traction dynamical analysis assigned for the motorail with 160 t load capacity providing maximum ore transportation speed of about 120 km/h.

2.5.1. The Power Required for Moving of a Loaded Motorail

Power required for moving (effective power) can be determined from the formula:

$$N_n = (F_1 + F_2) \cdot V = (4008 + 1768) \cdot 33.4 = 192918 \text{ W},$$

where:

$V = 33.4 \text{ m/s}$ (120 km/h) is motorail maximum working speed.

Analysis of the values used in the N_n determination formula:

1) $F_1 = M_n \cdot g \cdot f = 255600 \cdot 9.8 \cdot 0.0016 = 4008 \text{ N}$ is motorail wheels drag force,

where:

$M_n = M \cdot n_1 + 0.65 \cdot M \cdot n_2 = 6000 \cdot 40 + 0.65 \cdot 6000 \cdot 4 = 255600 \text{ kg}$ is motorail total weight;

$f = 0.0016$ is coefficient of steel wheel rolling resistance in line contact and $D > 450 \text{ mm}$ [2];

n_1 is the number of freight wagons in motorail formation;

n_2 is the number of head and hide wagons in motorail formation;



2) $F_2 = 0.5 \cdot \rho_B \cdot A_{\Pi} \cdot C_x \cdot V^2 = 0.5 \cdot 1.204 \cdot 1.4 \cdot 1.88 \cdot 33.4^2 = 1\,768$ N is motorail air resistance,

where:

$\rho_B = 1.204$ kg/m³ is sea level atmospheric density at a temperature of + 20° C;

$A_M = 1.4$ m² is the head wagon maximum frontal area;

$C_x = 1.88$ is air resistance coefficient.

Air resistance coefficient is calculated from the formula [2]:

$$C_x = C_f \cdot (S_{\text{поб}} / A_M) \cdot \eta_c \cdot \eta_M \cdot 1.5 = 0.00177 \cdot (860/1.4) \cdot 1.1 \cdot 1.05 \cdot 1.5 = 1.88$$

where:

$S_{\text{поб}} = 860$ m² is motorail side area;

$\eta_c = 1.1$ is adjustment coefficient depending on a motorail relative length A/d (where A is the length of a train, and d is an equivalent diameter of a train) [2];

$\eta_M = 1.05$ is adjustment coefficient depending on a head wagon forebody extension [2].

Coefficient of air and train's lateral surface friction can be determined from Prandtl-Schlichting formula [2] (referring to plain and even wagon wall surface):

$$C_f = 0.455 / (\log R_e)^{2.58} = 0.455 / (8.581)^{2.58} = 0.00177,$$

where:

$R_e = V \cdot A / \nu = 33.4 \cdot 178 / 1.56 \cdot 10^{-5} = 3811 \cdot 10^5$ is Reynolds number;

$V = 33.4$ m/sec (120 km/h) is motorail maximum working speed;

$\nu = 1.56 \cdot 10^{-5}$ m²/s is air kinematic viscosity at a temperature of + 20° C.

2.5.2. Total Capacity on Crankshaft of Power Equipment

Total capacity on crankshaft of power equipment can be determined from the formula:

$$N = N_{\Pi} / (\eta_p \cdot \eta_{\text{д}} \cdot \eta_{\text{п}} \cdot \eta_{\text{г}} \cdot (1 - \eta_{\text{в}}) \cdot \cos\varphi) = 192918 / (0.96 \cdot 0.88 \cdot 0.94 \cdot 0.9 \cdot (1 - 0.1) \cdot 0.95) = 315\,741 \text{ W},$$

where:

$\eta_p = 0.96$ is reducing gear efficiency coefficient (two gearing);

$\eta_{\text{д}} = 0.88$ is traction motor efficiency coefficient;

$\eta_{\text{п}} = 0.94$ is traction converter efficiency coefficient;

$\eta_{\text{г}} = 0.9$ is generator efficiency coefficient;

$\eta_{\text{в}} = 0.1$ is power equipment ventilating losses;

$\cos\varphi = 0.95$ is phase shift.

2.5.3. Total Capacity Sufficiency Check

To check sufficiency of power equipment total capacity (speaking about ore transportation at an average speed of 100 km/h at a distance of 100 km) motorail travelling time and distance are determined on speed-up, uniform motion and braking areas (taking into account drive minimum capacity of 315.7 kW).

**2.5.3.1. Motorail Distance and Travelling Time in a Speed-up Area**

Speed-up area distance and time are determined on the basis of traction-dynamic analysis (see Tab. 2.7).

Table 2.7

Changes of speed rates, acceleration, speed-up time and distance on a motorail speed-up area (N = 315.7 W)

V, km/h	V, m/s	a, m/ s ²	t _v , sec	S _v , m
0	0	0	0	0
2	0.556	0.600	0.926	0.257
4	1.111	0.600	1.852	1.029
6	1.667	0.438	2.923	2.516
8	2.222	0.324	4.381	5.351
10	2.778	0.256	6.294	10.135
12	3.333	0.211	8.672	17.401
14	3.889	0.179	11.525	27.702
16	4.444	0.154	14.864	41.615
18	5.000	0.135	18.702	59.738
20	5.556	0.120	23.051	82.694
22	6.111	0.108	27.927	111.135
24	6.667	0.097	33.343	145.740
26	7.222	0.089	39.316	187.219
28	7.778	0.081	45.863	236.317
30	8.333	0.075	53.000	293.814
32	8.889	0.069	60.748	360.530
34	9.444	0.064	69.126	437.329
36	10.000	0.059	78.156	525.121
38	10.556	0.055	87.861	624.870
40	11.111	0.052	98.267	737.593
42	11.667	0.048	109.399	864.374
44	12.222	0.045	121.286	1006.364
46	12.778	0.042	133.960	1164.789
48	13.333	0.040	147.454	1340.963
50	13.889	0.038	161.805	1536.293
52	14.444	0.035	177.052	1752.292
54	15.000	0.033	193.238	1990.590
56	15.556	0.031	210.411	2252.953
58	16.111	0.030	228.622	2541.295
60	16.667	0.028	247.928	2857.700
62	17.222	0.026	268.392	3204.445
64	17.778	0.025	290.082	3584.027
66	18.333	0.023	313.076	3999.197
68	18.889	0.022	337.460	4452.995
70	19.444	0.021	363.327	4948.796
72	20.000	0.020	390.787	5490.369
74	20.556	0.018	419.961	6081.937
76	21.111	0.017	450.984	6728.265



V, km/h	V, m/s	a, m/ s ²	t _v , sec	S _v , m
78	21.667	0.016	484.015	7434.753
80	22.222	0.015	519.232	8207.565
82	22.778	0.014	556.841	9053.783
84	23.333	0.013	597.084	9981.605
86	23.889	0.012	640.242	11000.595
88	24.444	0.012	686.645	12122.016
90	25.000	0.011	736.691	13359.261
92	25.556	0.010	790.856	14728.435
94	26.111	0.009	849.723	16249.152
96	26.667	0.008	914.011	17945.639
98	27.222	0.007	984.626	19848.322
100	27.778	0.007	1062.728	21996.149
102	28.333	0.006	1149.840	24440.116
104	28.889	0.005	1248.009	27248.828
106	29.444	0.005	1360.084	30517.681
108	30.000	0.004	1490.197	34384.929
110	30.556	0.003	1644.666	39061.924
112	31.111	0.003	1833.870	44895.718
114	31.667	0.002	2076.671	52516.962
116	32.222	0.001	2413.123	63264.721
118	32.778	0.001	2955.223	80882.993
120	33.333	0.000	4316.240	125872.142

According to analysis the speed of 118 km/h on plain horizontal area was chosen because maximum working speed of 120 km/h may be achieved only at a distance which exceeds 100 km. To achieve the speed of 118 km/h (taking into account motorail drive capacity of 315.7 kW) starting distance is equal to $S_{y118} = 80\,883$ m and time is equal to $t_{y118} = 2\,955$ sec (see bold print line in Tab. 2.7).

2.5.3.2. Motorail Distance and Travelling Time on a Braking Area

Motorail distance and travelling time on a braking area are determined from well-known formulas:

$$S_{T118} = a \cdot t_{T118}^2 / 2 = 1 \cdot 32.8^2 / 2 = 537 \text{ m,}$$

where:

$a = 1 \text{ m/s}^2$ is acceleration of motorail service braking;

$t_{T118} = 32.8 / a = 32.8$ s is braking time.

2.5.3.3. Motorail Distance and Travelling Time at uniform speed of 118km/h

Motorail distance rate (taking into account uniform speed rate of 118 km/h) is determined by the following way: the total distance of 100 km minus acceleration and braking rates of a distance,

$$S_{p118} = 100000 - S_{y118} - S_{T118} = 100000 - 80882,993 - 537.2 = 18579.8 \text{ m}$$

$$t_{p118} = S_{p118} / 32.778 = 18579.8 / 32.778 = 566.8 \text{ s}$$

Average speed of ore transportation at a distance of 100 km can be determined from the formula:

$$V_{cp} = (S_{y118} + S_{p118} + S_{T118}) / (t_{y118} + t_{p118} + t_{T118}) = 100000 / (2955.223 + 566.8 + 32.778) = 28.1 \text{ m/sec (101 km/h).}$$

Thus, an average speed of ore transportation at a distance of 100 km as $N = 315.7$ kW will be 101 km/h.

For reasons of fuel efficiency power equipment total capacity is assigned 25-30 per cent more, because minimum fuel consumption of any motor can be achieved when it is not functioning at its total capacity (70-75 per cent of generating capacity). As the result power equipment total generating capacity should be something like $N = 450$ kW.

2.5.4. Total Capacity Reserve of Motorail Autonomous Power Equipment

To provide an average speed of ore transportation in terms of tractive resistance increase (head wind, upgrade) without fuel efficiency worsening and without decrease of autonomous power supply system operation life, it is reasonable to have not less than 25 per cent capacity reserve (at that N total capacity will be approx. equal to 600 kW). Analyses prove that having such reserve of power equipment total capacity motorail can accelerate to the speed of 120 km/h in a head wind of 15 m/s without decrease of its fuel efficiency.

2.6. Location of Diesel-Electric Aggregates in a Motorail

Diesel-electric aggregates (DEA) and their primary systems location in motorail head and hind wagon groups is determined by pre-design on the basis of UKA diesel-electric aggregate with generating capacity of 120 kW at head wind of 15 m/s. The UKA diesel-electric aggregate is produced by Hörmann IMG, Germany.

Pre-design results are represented in Fig. 2.11

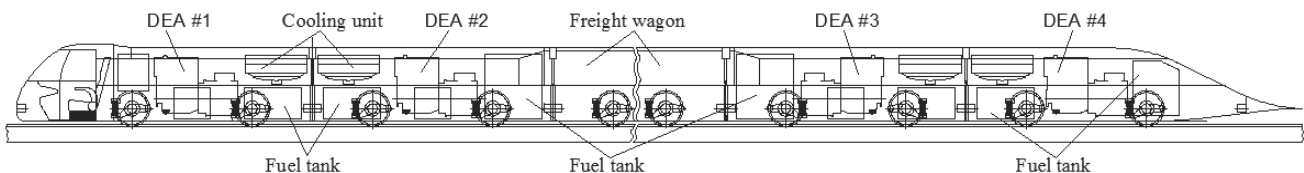


Fig. 2.11. Diesel-electric aggregates and their primary systems location in head and hind wagon groups of 160 t load capacity motorail.

2.7. Motorail Stability Rating

Motorail turnover stability rating depends on the influence of crosswind force and on motorail passing of curved sections.

2.7.1. Maximum Admissible Speed of Stormy Crosswind Speed

Maximum admissible stormy crosswind speed can be determined from the motorail balance equation. Design model of maximum admissible crosswind speed determination is represented in Fig. 2.12.

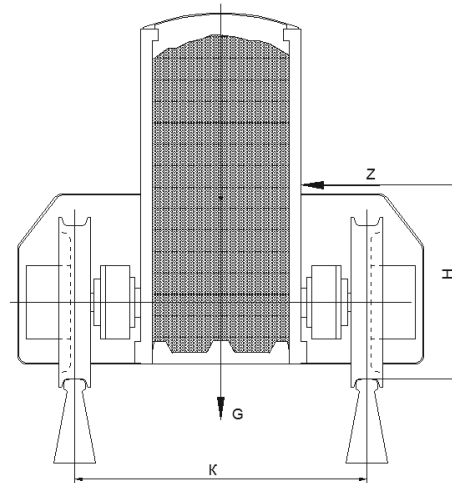


Fig. 2.12. Design model of maximum admissible crosswind speed determination

The motorail balance equation can be represented in the following way:

$$G \cdot K / 2 - Z \cdot H = 0,$$

where:

$G = m \cdot g$ is the motorail gravity force (empty or loaded), N (see Tab. 2.8);

$K = 1.0$ m is gauge width;

m is motorail weight (dead or total weight), kg (see Tab. 2.8);

H is the distance between the centre of effort of motorail side area and the rail top, m (see Tab. 2.8);

$Z = 0.5 \cdot \rho_B \cdot A_{\bar{6}} \cdot C_y \cdot V_{\bar{6}}^2$ is crosswind force, N,

where:

$A_{\bar{6}} = 214.5$ m² is the motorail cross-section area;

$C_y = 1$ is the motorail side air resistance coefficient.

If we insert the formula defining crosswind force to the motorail balance equation, the crosswind admissible speed can be determined:

$$V_{\bar{6}} = (G \cdot K / 2 / (0.5 \cdot \rho_B \cdot A_{\bar{6}} \cdot C_y \cdot H))^{0.5}, \text{ m/s.}$$

The results of analysis see in Tab. 2.8.

Table 2.8

Crosswind admissible speed $V_{\bar{6}}$

m, kg	G, N	H, m	$V_{\bar{6}}$, m/s (km/h)	Remarks
95 600 (empty)	936 880	0.7	72 (259)	According to Saffir-Simpson storm scale the highest grade storm (#5) speed is equal to 250 km/h.
255 600 (loaded)	2 504 880	0.65	98 (352)	

2.7.2. Estimate of Motorail Stability While Passing Curved Sections

To estimate motorail stability when it passes curved sections of a track the following parameters should be determined:

- minimum radius of turnaround section where motorail traffic is possible at a maximum operational speed of 120 km/h;
- motorail maximum speed on curved sections of a track with assumed minimum radius of 50 m (for example, a turnaround section).

Design model of motorail stability estimate while passing curved sections of a track is represented in Fig. 2.13. Above mentioned values are determined from solution of motorail balance on a curved track section equation:

$$G \cdot K / 2 - Y \cdot J = 0,$$

where:

$Y = m \cdot V^2 / r$ is inertia centrifugal force, N;

J is a distance of motorail centre of mass to the rail top (empty or load) (see Tab. 2.9).

2.7.2.1. Minimum Radius of a Curved Track Section at motorail speed of 120 km/h

Minimum radius of a curved track section can be determined from the motorail balance equation. The model designed for determination of minimum radius of a curved track section is represented in Fig.2.13.

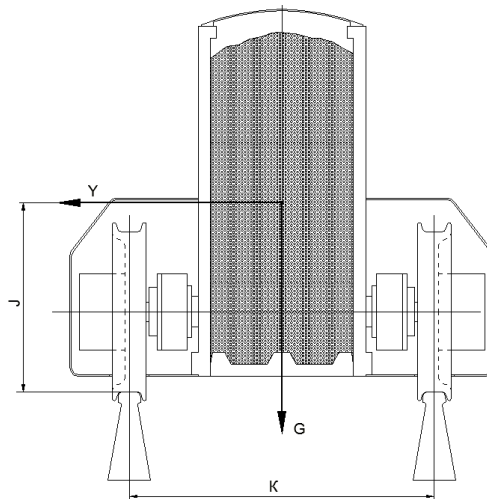


Fig. 2.13. The model designed for the estimate of motorail stability while passing curved track sections

When we solve motorail balance equation taking into account inertia centrifugal force formula, it is possible to determine minimum radius value of a curved track section:

$$r = m \cdot V^2 \cdot J / (G \cdot K / 2), \text{ m.}$$

See the results in Tab. 2.9.

Table 2.9

Minimum radius (r) of a curved track section where the motorail can move at its maximum operational speed of 120 km/h

m, kg	G, N	J, m	r, m
95 600 (empty)	936 880	0.65	147.5
255 600 (loaded)	2 504 880	0.6	136.0



2.7.2.2. Maximum Motorail Speed on Curved Track Sections with Minimum Radius Accepted As 50 m

When we solve motorail balance equation taking into account inertia centrifugal force formula, we can also determine maximum motorail speed rate on curved track sections with accepted minimum radius equal to 50 m:

$$V = (G \cdot Y/2 \cdot r / (m \cdot J))^{0.5}, \text{ m/s.}$$

See the results in Tab. 2.10.

Table 2.10

Maximum motorail speed rate on curved track sections with accepted minimum radius $r = 50 \text{ m}$ (for example, in a turnaround section)

m, kg	G, N	J, m	V, m/sec (km/h)
95 600 (empty)	936 880	0.65	19.5 (70.2)
255 600 (loaded)	2 504 880	0.6	20.5 (73.8)

2.8. Specifications of a Motorail with Load Capacity of 160tons Intended for Ore Transportation

Basic specifications of the motorail with load capacity of 160 t (see Fig. 2.14) are represented in Tab.2.11.

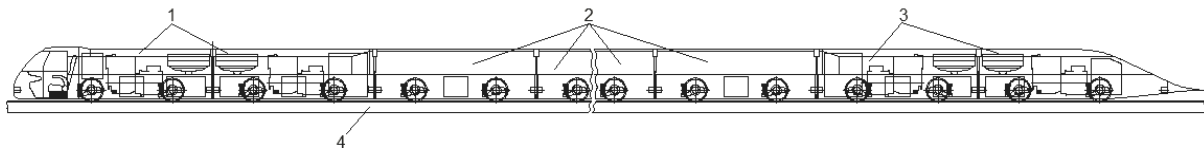


Fig.2.14. STU freight motorail with load capacity of 160 t designed for ore transportation: 1 –head wagons joint; 2 – freight wagons; 3 – hind wagons joint; 4 – track structure



Table 2.11

Motorail Specifications

No.	Specification	Specification values (description)
1	Load capacity, t	160
2	Dead weight, t	95.6
3	Body capacity, m ³	80
4	Overall dimensions, mm: - length - width - height (from rail top, empty)	178 000 1390 (1640 with asynchronous traction motors) 1 305
5	Gauge, mm	1 000
6	Clearance, mm	50-100
7	Wagon base, mm	2000
8	Load on track: - axial, t - linear, t/m	3.0 1.5
9	Number of freight wagons	40
10	Maximum operational speed, km/h	120
11	Time of acceleration to the maximum speed, minutes: - 70% load of diesel-electric aggregates - 100% load of diesel-electric aggregates	19 10
12	Maximum climbing ability, %: - loaded with 160 t - empty	2.8 (1.6 with asynchronous traction motors) 10.0
13	Braking distance (initial speed of 120 km/h), m	621
14	Driving system	Diesel-electric (the version manufactured by Hörmann IMG, Germany)
15	Fuel consumption (1 ton of ore transportation at a distance of 1 km, g /t ×km)	4.2
16	Brake system: - service - parking (emergency)	electrodynamic electromechanical (the version manufactured by Mayr, Germany)
17	Ore loading	Through upper hatches at a speed of 2 m/sec
18	Ore off-loading	Through bottom hatches at a speed of 2 m/sec
19	Minimum radius of turnaround section, m	50
20	Minimum radius on route, m	150
21	Maximum admissible crosswind speed, km/h	259
22	Number of drivers (if they are necessary)	1
23	Traffic in automatic (semi-automatic) mode	provided



2.9. STU Motorail Fuel Efficiency

Fuel consumption during transportation of 1 ton of iron ore at a distance of 1 km for STU motorail with load capacity of 160 t is 4.2 g/t×km. This rate is lower than an average fuel consumption of ore transportation by a conventional railroad. For example, while transporting ore by railset of 40 dumpcars with load capacity of 60 t at an average speed of 100 km/h, its fuel consumption will exceed the above mentioned rate by 15percent. It’s interesting to compare fuel consumption of STS motorail and “Road trains” which are widely used in Australia in transporting different goods, including ore (see Fig. 2.15).

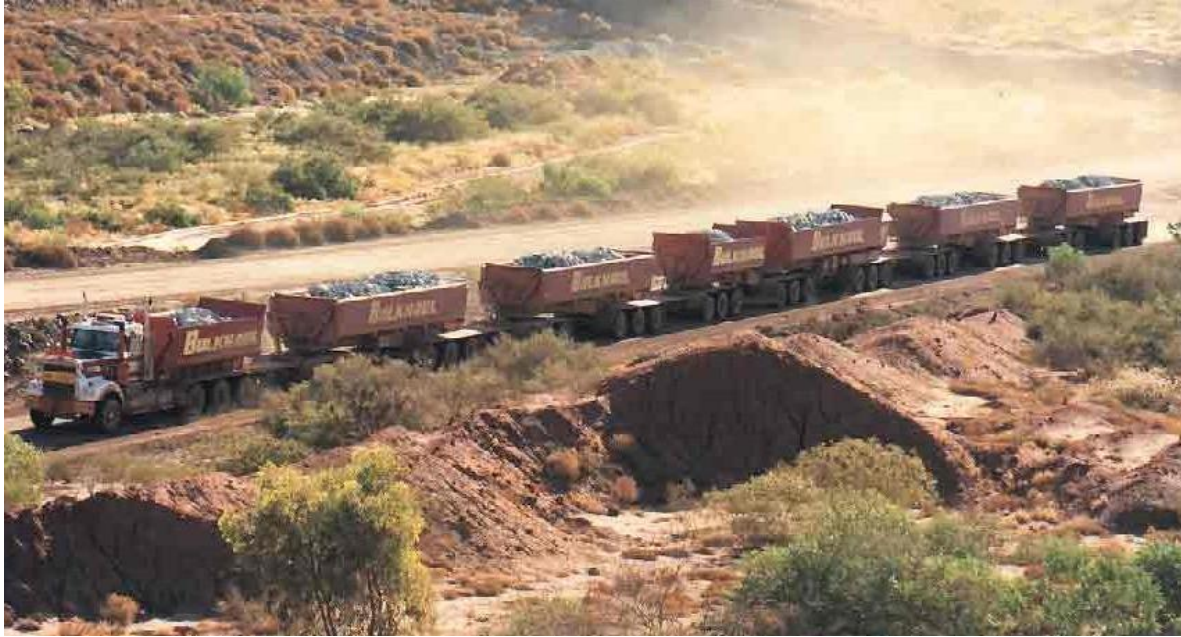


Рис. 2.15. “Road trains” are widely used in Australia for mining transportation

Tab. 2.12 represents diesel fuel consumption of “Road train” and STS motorails having the same load capacity (160 t) while transporting 1 mln tons of load at a distance of 100 km.

Table 2.12

Comparative table of “Road train” and STS motorail fuel consumption while transporting 1 mln tons of load at a distance of 100 km

Motorail	Fuel consumption while transporting 1 mln tons of load at a distance of 100 km, tons		
	Asphalt covering	Pressed gravel surfacing	STS track
«Road train»	2375*	3125*	-
STS	-	-	650*

*taking into account diesel motors fuel consumption of 210 g/kW×h

2.10. Analysis of String-Rail (“Longitudinal Sleeper”) Located on Elastic Subgrade

Analysis of pressure on the ground under a string-rail flange, bending moment and bending stress is carried out on basis of three rail type versions: the original version, the version based on the use of P50-type rail and the optimized version. On the basis of original version we can also make analysis of how string stress influences rail deflection and bending moment in it. The calculation was carried out on the basis of finite-element analysis. The models were processed on PC using the finite-element complex Femap with NX Nastran.

2.10.1. Original Version

Normalized to steel cross section of a string-rail wired to the ground is represented in Fig. 2.16.

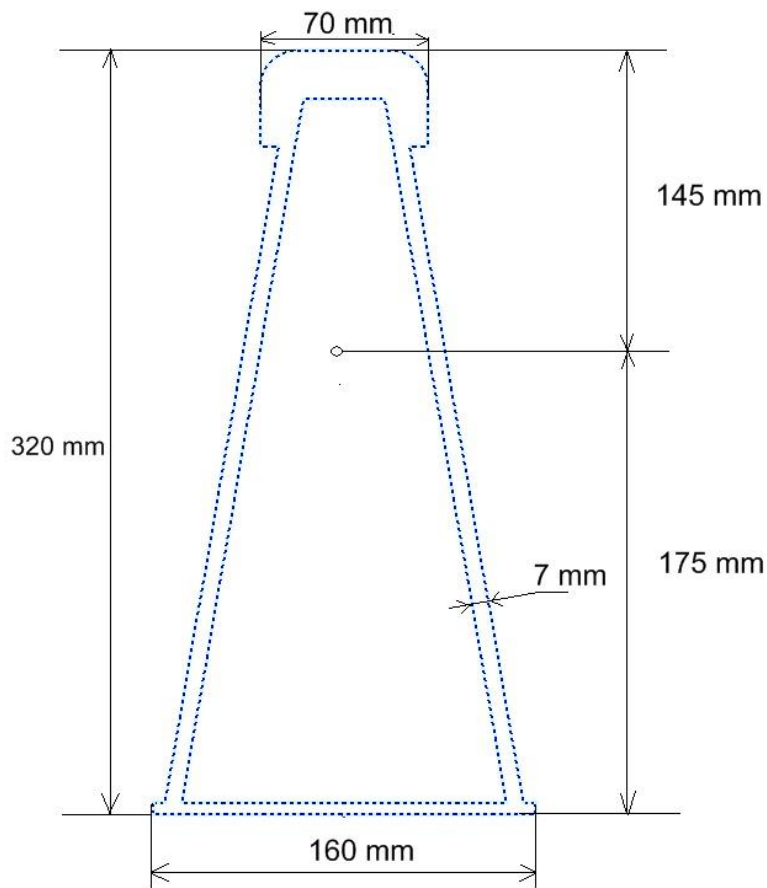


Fig.2.16 Normalized to steel cross section of a string-rail

Initial Data

Normalized to steel string-rail area (with allowance to concrete): $A = 66.2 \text{ cm}^2$.

$E = 2 \cdot 10^{11} \text{ Pa}$ is elasticity modulus of rail steel.

$J = 8.5 \cdot 10^{-5} \text{ m}^4$ is inertia moment of a normalized to steel rail section.

$E \cdot J = 1.7 \cdot 10^7 \text{ N} \cdot \text{m}^2$.

$P = 20\,000 \text{ N}$ is one wheel pressure force (there is one or two wheels (arranged at a distance of 0.75 m from each other) on a rail of infinite length).



$b = 0.16$ m is width of a rail flange.

$\rho = 110$ kg/m is linear density (mass) of rail.

k is compliance coefficient of elastic subgrade (ground) . The coefficient is equal in value to the force applied to 1cm^2 of subgrade area to make ground sit of 1 cm.

$k_{\pi} = k \cdot b$ – coefficient of subgrade reaction.

Analytical Dependencies

Maximum rail (subgrade) deformation caused by single force:

$$Y = 0.354 \frac{P}{\sqrt[4]{k^3 b^3 EJ}}$$

Maximum rail bending moment caused by single force:

$$M = 0.354 \cdot P \cdot \sqrt[4]{\frac{EJ}{kb}}$$

Maximum pressure on the ground under a rail flange (under P force):

$$p = 0.354 \cdot P \cdot \sqrt[4]{\frac{k}{b^3 EJ}}$$

The Results of Analysis

Given results are analyzed on basis of two variants. In first variant the rail is influenced by one wheel single force ($P = 20\,000$ N), and in the second variant the rail is influenced by forces of two wheels arranged at a distance of 0.75 m one from another ($2P = 2 \times 20\,000$ N).

The First Variant ($P = 20\,000$ N is when the rail is influenced by one wheel single force)

Tab. 2.13 represents all basic values for three types of ground of various densities.

Fig.2.17 represents the diagram of bending moments in a string-rail lying on a firm ground.

Fig.2.18 represents the diagram of pressure on the ground under a rail flange lying on a firm ground.

Fig.2.19 represents the diagram of pressure on the ground under a rail flange lying on a moderately firm ground.

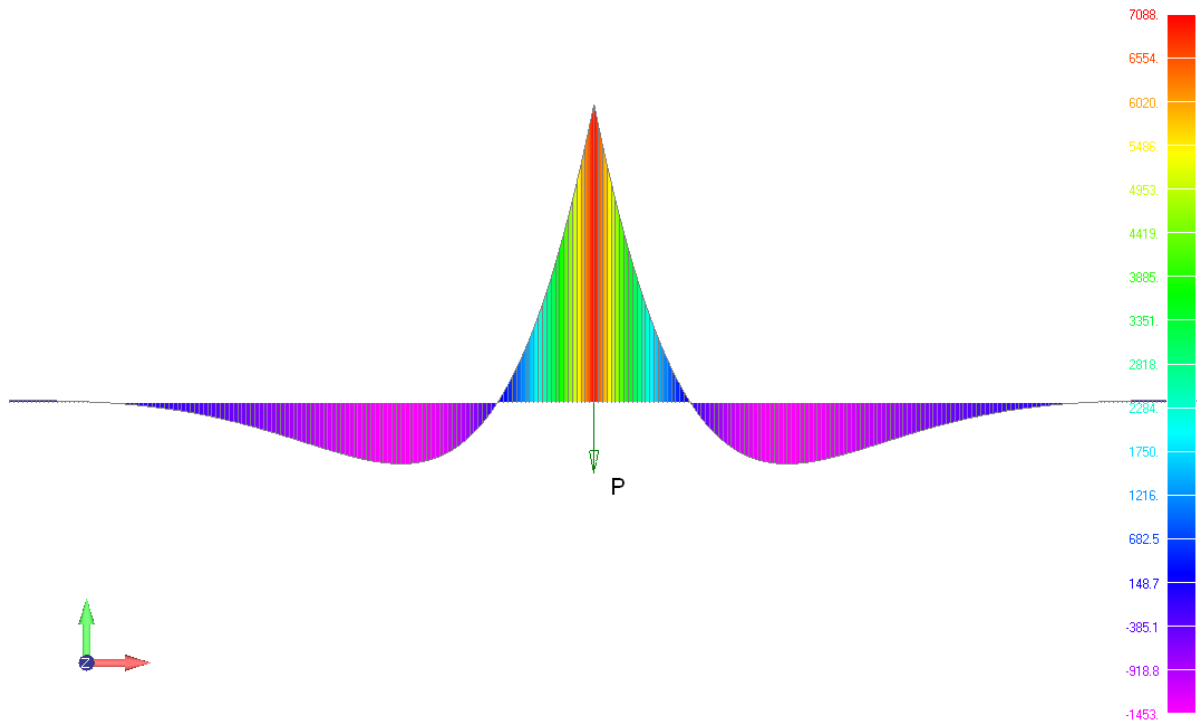
Fig.2.20 represents the diagram of pressure on the ground under a rail flange lying on a loose ground

Table 2.13

The Values of Single Force Effect

Type of Ground	Subgrade compliance coefficient, N/m^3 (kgf/cm^3)	Maximum bending moment, $N \cdot m$, and max. subgrade deformation (mm)	Max. bend stress, MPa		Max. pressure on the ground under a rail flange, N/m^2 (kgf/cm^2)
			Top of rail	Bottom of rail	
Firm ground	10^8 (10)	7088 (0.52)	-12.3 +2.5	+14.5 -3.0	52000 (0.52)
Moderately firm ground	$5 \cdot 10^7$ (5.0)	8461 (0.89)	-14.6 +3.0	+17.3 -3.55	44500 (0.445)
Loose ground	$5 \cdot 10^6$ (0.5)	15140 (5.53)	-26.2 +5.43	+30.9 -6.4	27650 (0.2765)

The pressure on the ground under a string-rail is equal to the following product: (Subgrade deformation) x (Compliance coefficient of elastic subgrade).


 Fig. 2.17 The diagram of bending moments ($N \cdot m$) in a string-rail lying on a firm ground

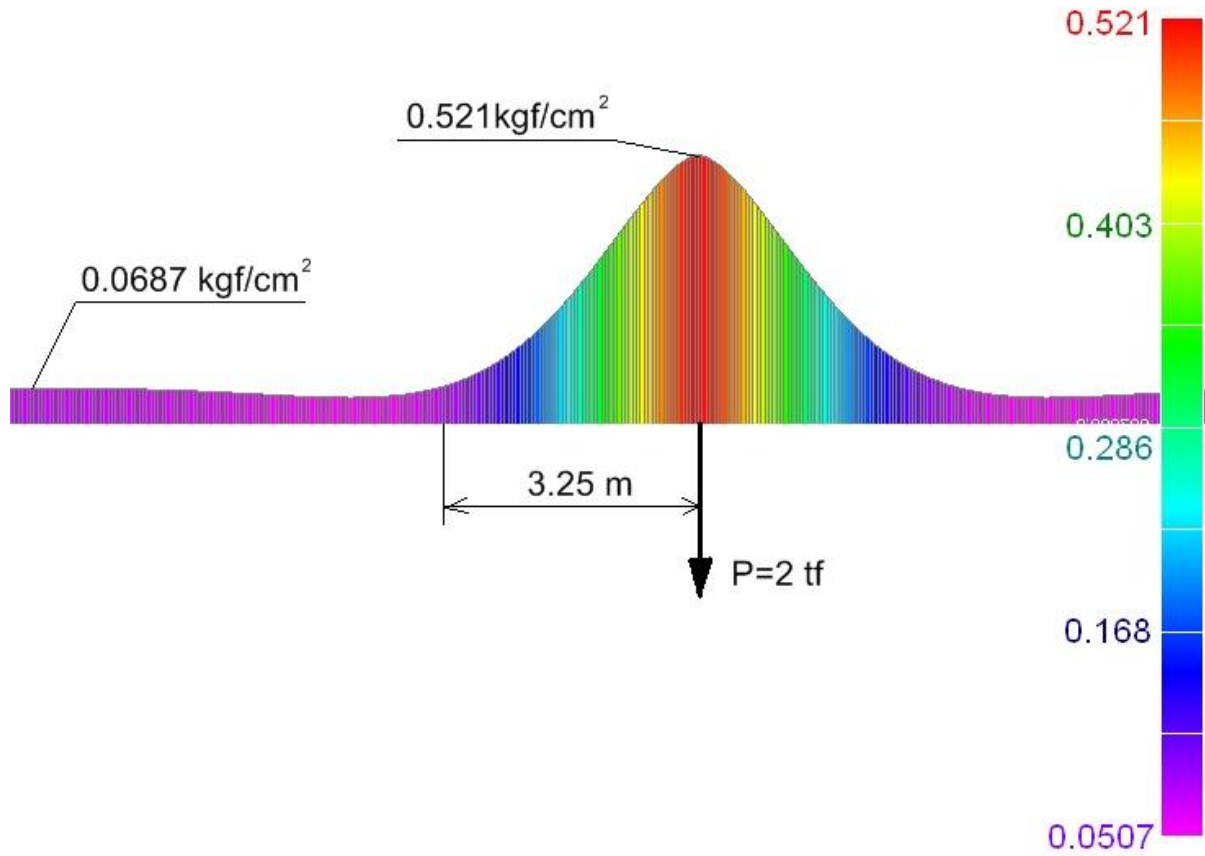


Fig.2.18. The diagram of pressure on the ground under a rail flange (kgf/cm^2) lying on a firm ground

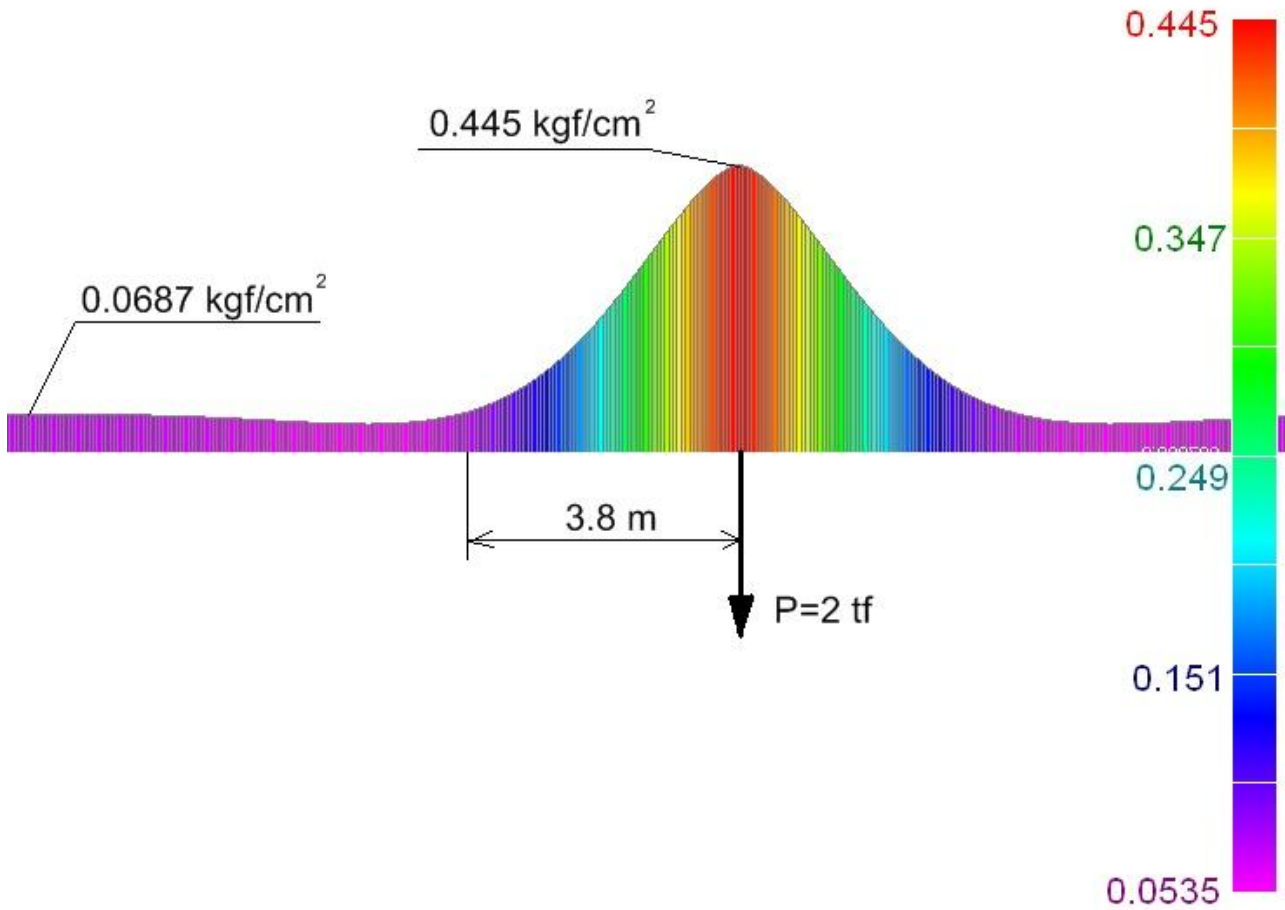


Fig. 2.19. The diagram of pressure on the ground under a rail flange (kgf/cm^2) lying on a moderately firm ground

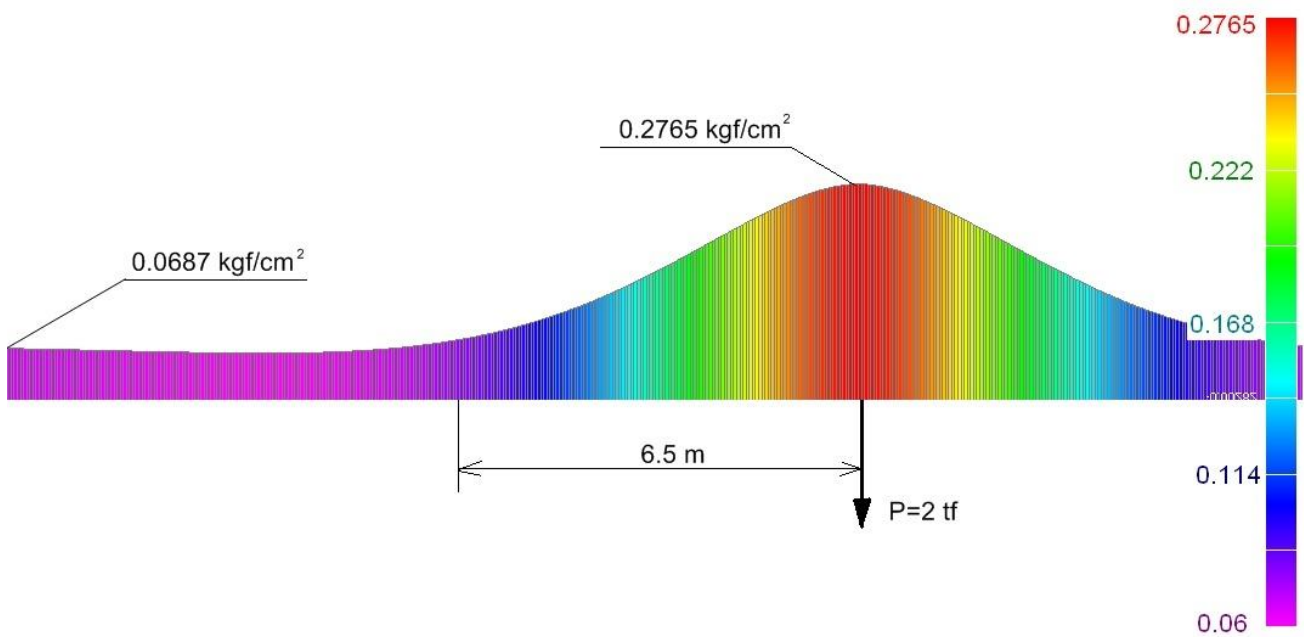


Fig. 2.20. The diagram of pressure on the ground under a rail flange (kgf/cm^2) lying on a loose ground



The Second Variant The rail is influenced by forces of two wheels arranged at a distance of 0,75 m one from another ($2 P = 2 \times 20\,000\text{ N}$).

Tab. 2.14 represents all basic values for three types of ground of various densities.

Fig. 2.21 represents the diagram of bending moments in a string-rail lying on a firm ground.

Fig. 2.22 represents the diagram of pressure on the ground under a rail flange lying on a firm ground.

Fig.2.23 represents the diagram of pressure on the ground under a rail flange lying on a moderately firm ground.

Fig.2.24 represents the diagram of pressure on the ground under a rail flange lying on a loose ground

Table 2.14

The Values Resulted From Two Wheels Force Effect

Type of Ground	Subgrade compliance coefficient, N/m^3 (kgf/cm^3)	Maximum bending moment, $\text{N}\cdot\text{m}$, and max. subgrade deformation (mm)	Max. bend stress, MPa		Max. pressure on the ground under a rail flange, N/m^2 (kgf/cm^2)
			Top of rail	Bottom of rail	
Firm ground	10^8 (10)	8 610 (0.9)	-14,9 +4.7	+17.7 -5.5	90 300 (0.903)
Moderately firm ground	$5 \cdot 10^7$ (5.0)	11100 (1.56)	-19,1 +5.75	+22.6 -6.8	78000 (0.78)
Loose ground	$5 \cdot 10^6$ (0.5)	23700 (9.54)	-41.0 +10.7	+48.4 -12.6	47700 (0.48)

The pressure on the ground under a string-rail is equal to the following product: (Subgrade deformation) x (Compliance coefficient of elastic subgrade).

The comparative analysis represented in Fig. 2.13 and 2.14 proves that maximum pressure exerted on the ground by a motorail with coupled wheels (arranged at a distance of 0.75 m one from another) will 1.7 times exceed the pressure on the ground by a one-wheel motorail, regardless of the type of ground. Therefore, while motorail designing the wheels should be arranged regularly, without wheels approach one to another.

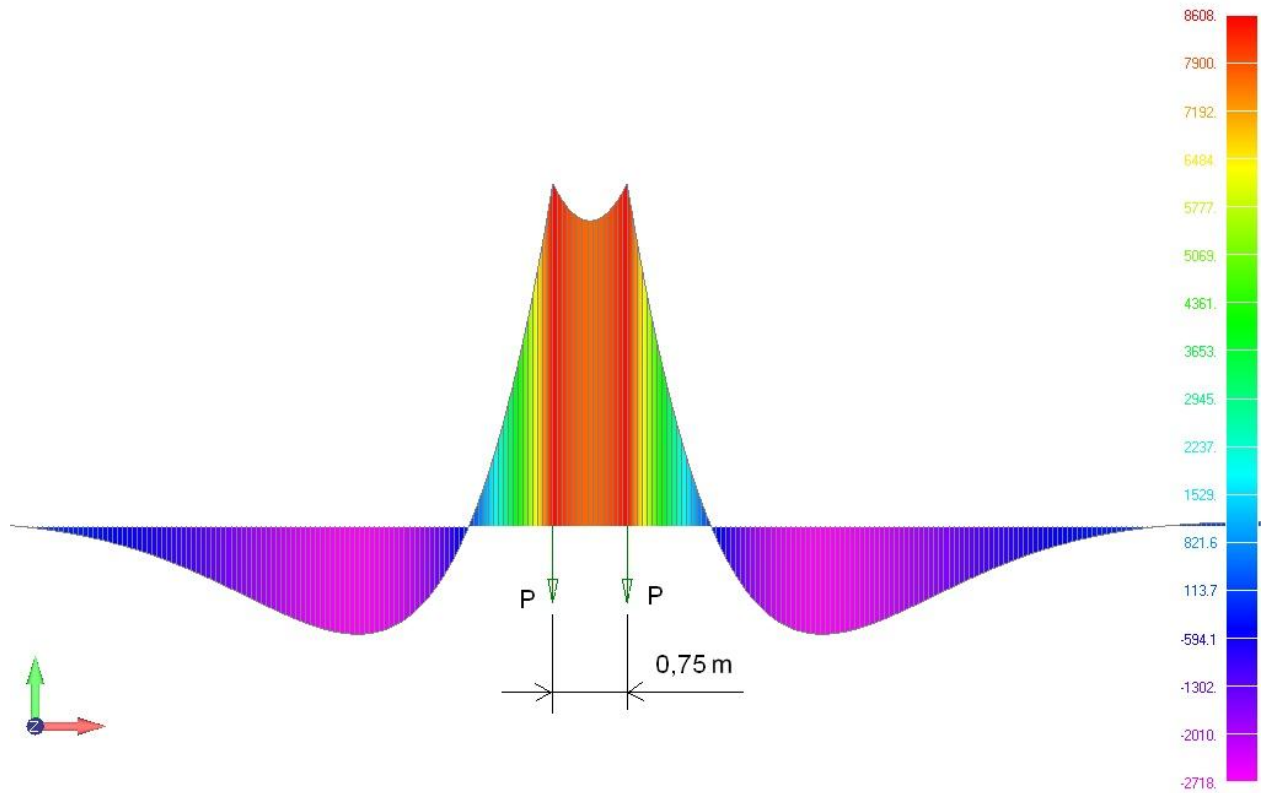


Fig. 2.21. The diagram of bending moments (N·m) in a string-rail lying on a firm ground

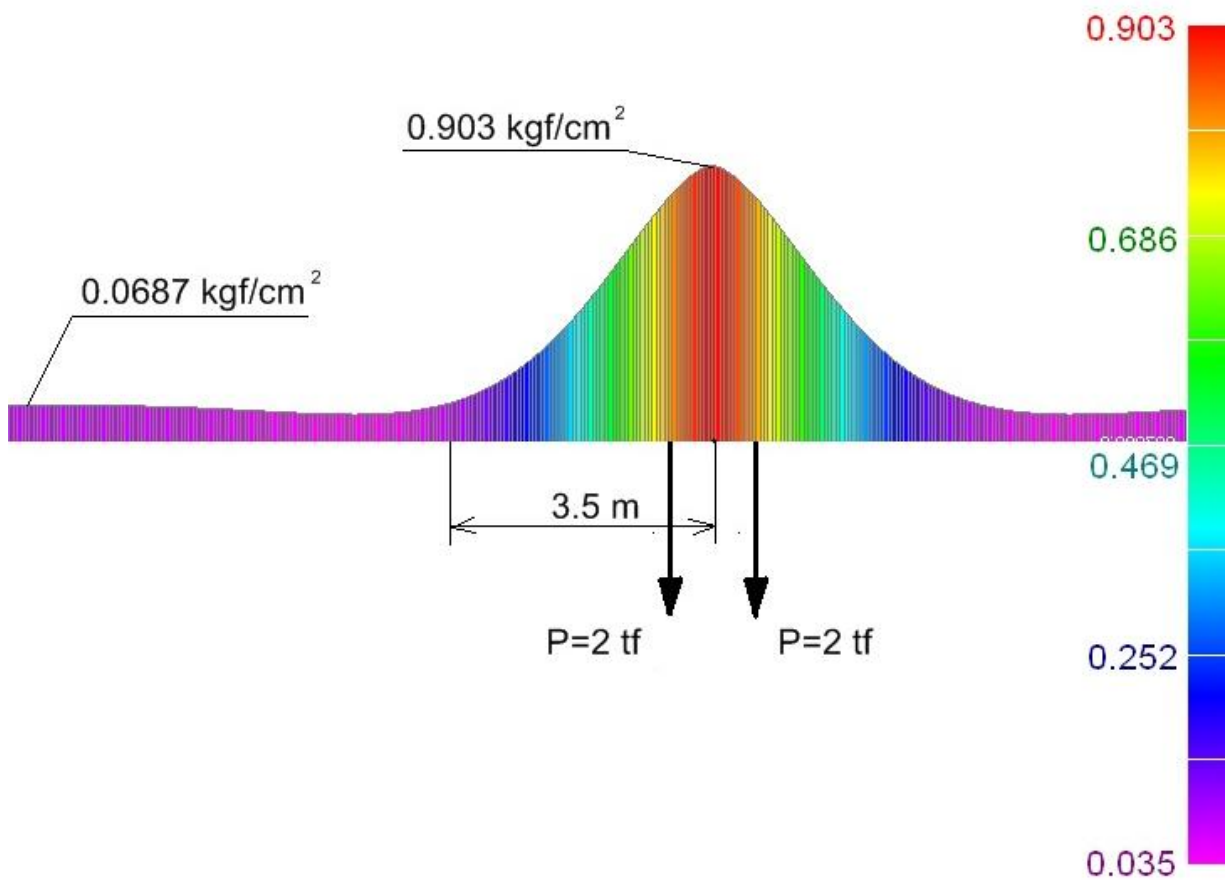


Fig. 2.22. The diagram of pressure on the ground under a rail flange (kgf/cm^2) lying on a firm ground

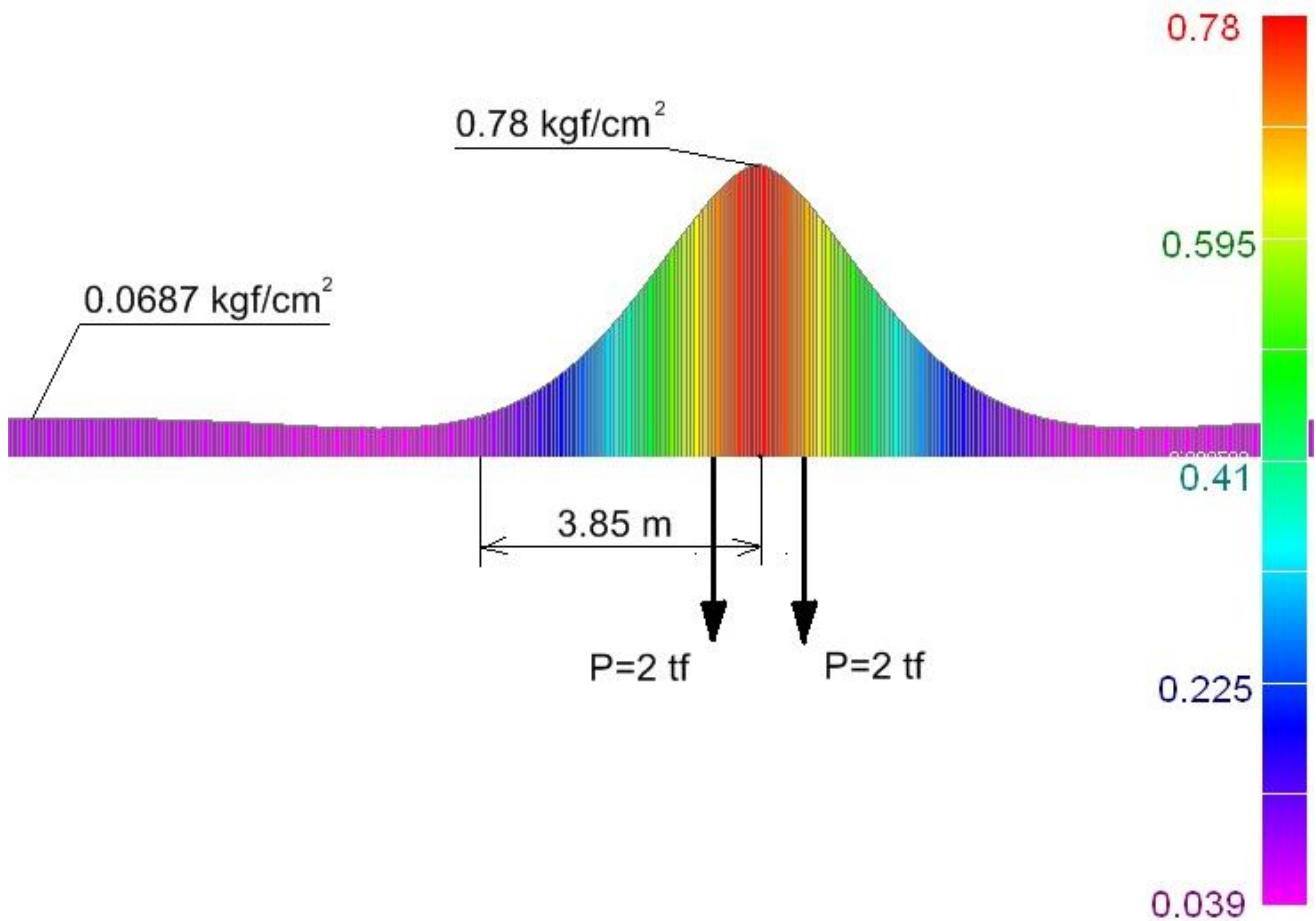


Fig. 2.23. The diagram of pressure on the ground under a rail flange (kgf/cm^2) lying on a moderately firm ground

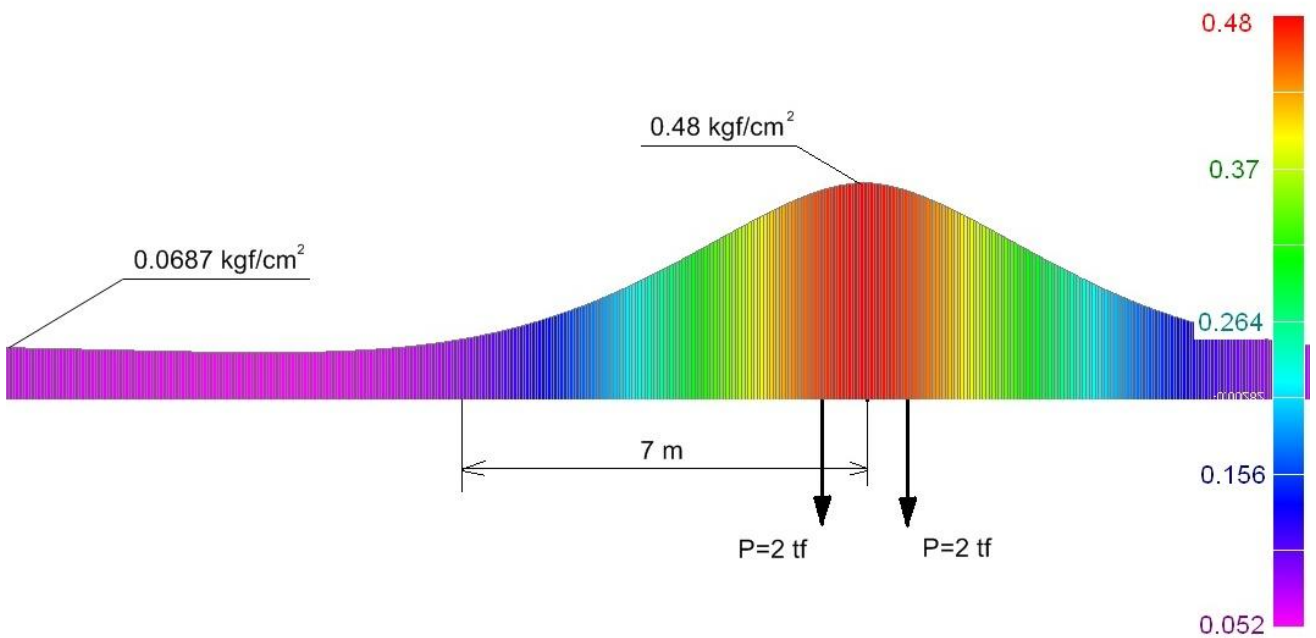


Fig. 2.24. The diagram of pressure on the ground under a rail flange (kgf/cm^2) lying on a loose ground

2.10.2. The Version Based on the Use of P-50-Type Rail Produced in Russia

Cross section of P50-type rail (Russia) is represented in Fig. 2.25.

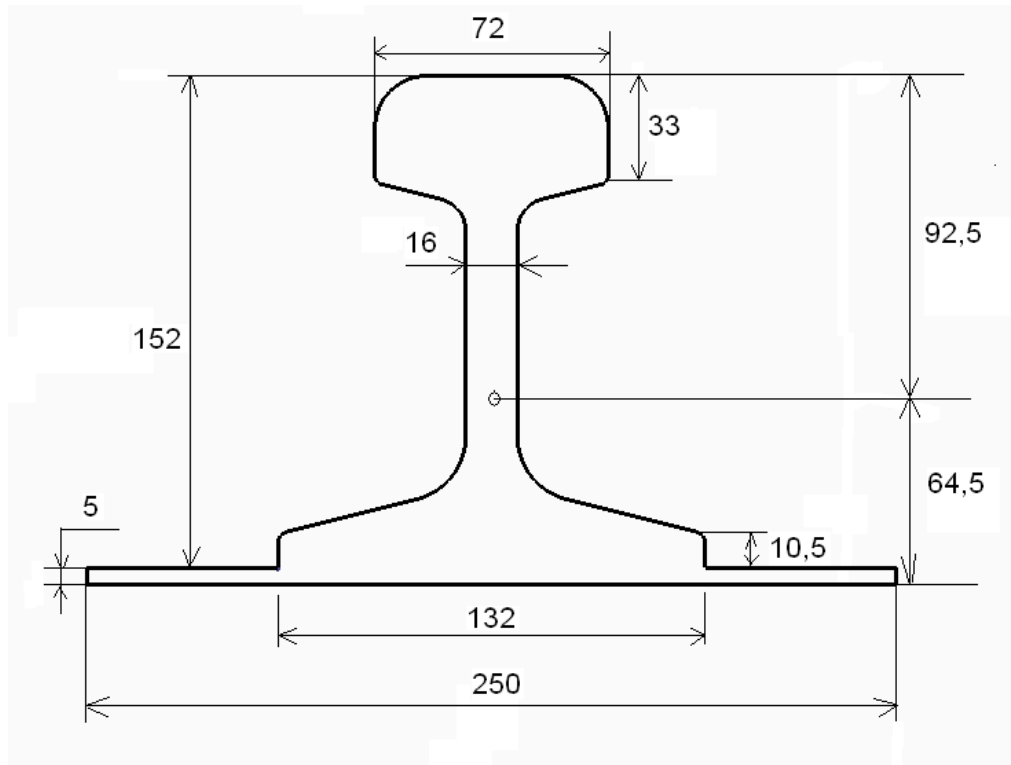


Fig. 2.25. Cross section of a string-rail based on P50-type rail with a plate welded to the bottom

Initial Data on a Rail

Normalized to steel string-rail cross-section area: $A = 78 \text{ cm}^2$.

$E = 2 \cdot 10^{11} \text{ Pa}$ is elasticity modulus of rail steel.

$J = 2.61 \cdot 10^{-5} \text{ m}^4$ is inertia moment of a normalized to steel rail section.

$E \cdot J = 5.22 \cdot 10^6 \text{ N} \cdot \text{m}^2$.

$b = 0.25 \text{ m}$ is width of a rail flange.

$\rho = 61 \text{ kg/m}$ is linear density (mass) of a rail.

k is compliance coefficient of elastic subgrade (ground). The coefficient is equal in value to the force applied to 1 cm^2 of subgrade area to make ground sit of 1 cm.

$k_n = k \cdot b$ is coefficient of subgrade reaction.

Initial Data on Weight Load of a Motorail Moving on a Rail-Track Structure

The schematic view of rail loading by a motorail is represented in Fig.2.26.

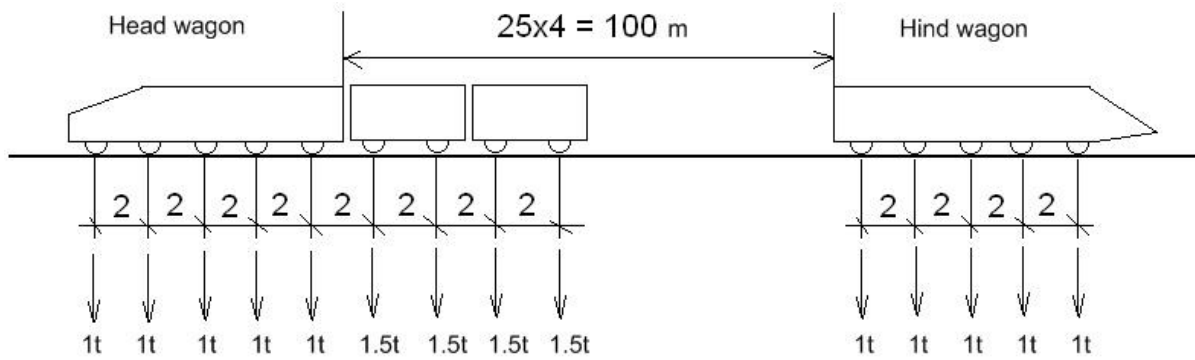


Fig. 2.26. The schematic view of rail loading by a motorail

The pressure resulted from one wheel of head and hind wagons is $P_1 = 10\ 000\ \text{N}$.

The pressure resulted from one wheel of freight wagons is $P_2 = 15\ 000\ \text{N}$.

The Results of Analysis

Tab.2.15 represents all basic values resulted from vertical load of a motorail on three types of ground of various densities.

Fig.2.27 represents the diagram of the motorail lengthwise pressure on the ground under a rail flange lying on a firm ground.

Fig.2.28 represents the diagram of pressure on the ground under a rail flange lying on a firm ground towards head and hind freight wagons

Fig.2.29 represents the diagram of pressure on the ground under a rail flange lying on a moderately firm ground.

Fig.2.30 represents the diagram of pressure on the ground under a rail flange.

Table 2.15

The Values Resulted From Motorail’s Vertical Load

Type of Ground	Subgrade compliance coefficient, N/m^3 (kgf/cm^3)	Maximum bending moment, $\text{N}\cdot\text{m}$, and max. subgrade deformation (mm)	Max. bend stress, MPa		Max. pressure on the ground under a rail flange, N/m^2 (kgf/cm^2)
			Top of rail	Bottom of rail	
Firm ground	10^8 (10)	2594 (0.369)	-9.07 +4.1	+6.4 -2.9	36900 (0.369)
Moderately firm ground	$2.5 \cdot 10^7$ (2.5)	2902 (1.36)	-10.14 +4.34	+7.15 -3.06	34000 (0.34)
Loose ground	$5 \cdot 10^6$ (0.5)	3379 (6.6)	-11.8 +6.2	+8.33 -4.36	33000 (0.33)

The pressure on the ground under a rail is equal to the following product: (Subgrade deformation) x (Compliance coefficient of elastic subgrade).

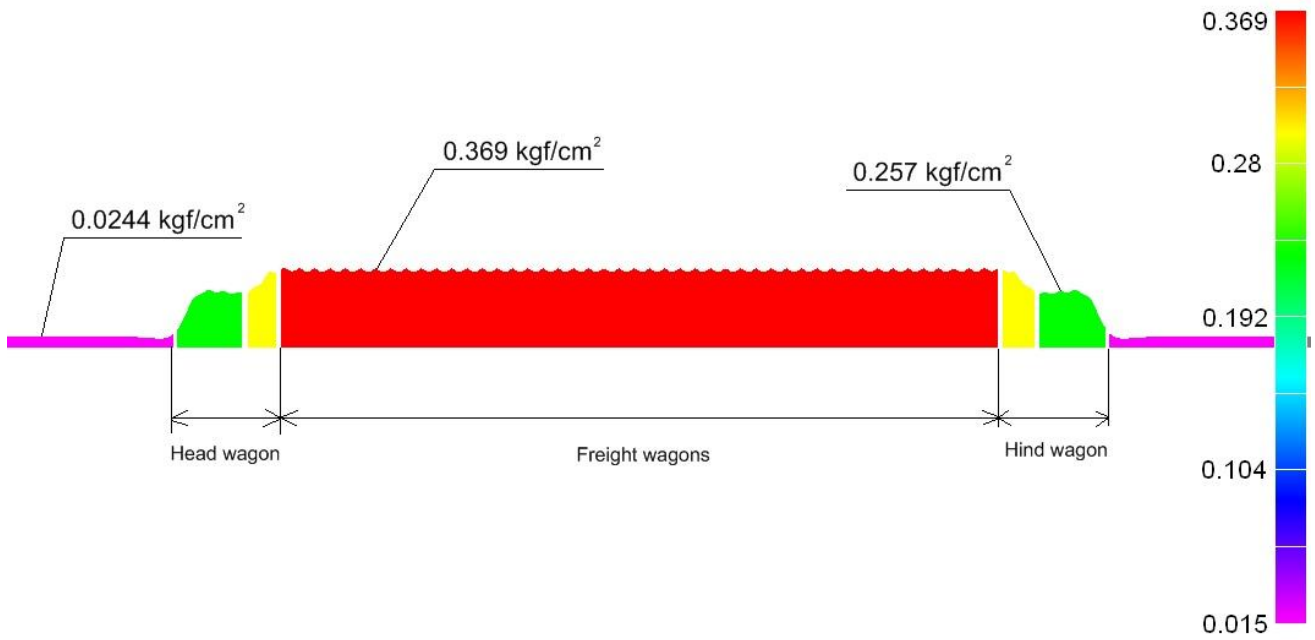


Fig. 2.27. The diagram of the pressure on the ground under a rail flange (kgf/cm^2) along the whole length of a motorail (firm ground: $k = 10 \text{ kgf/cm}^2$)

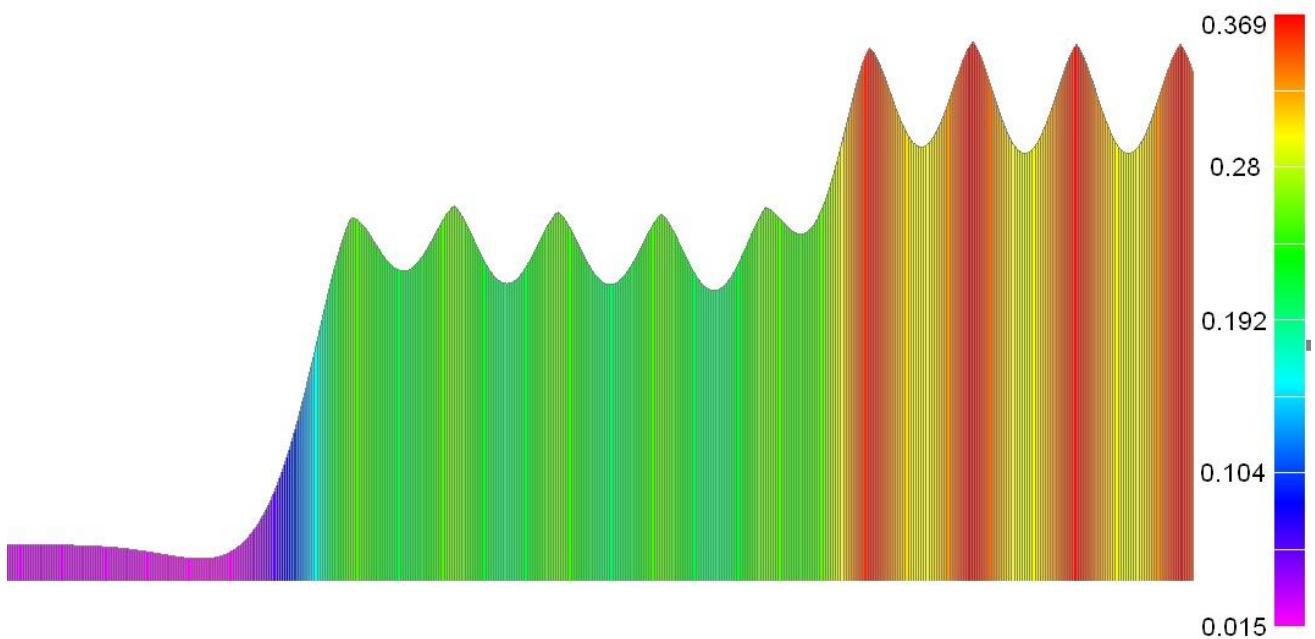


Fig. 2.28. The diagram of the pressure on the ground under a rail flange (kgf/cm^2) for a head and the first freight wagons (firm ground: $k = 10 \text{ kgf/cm}^2$)

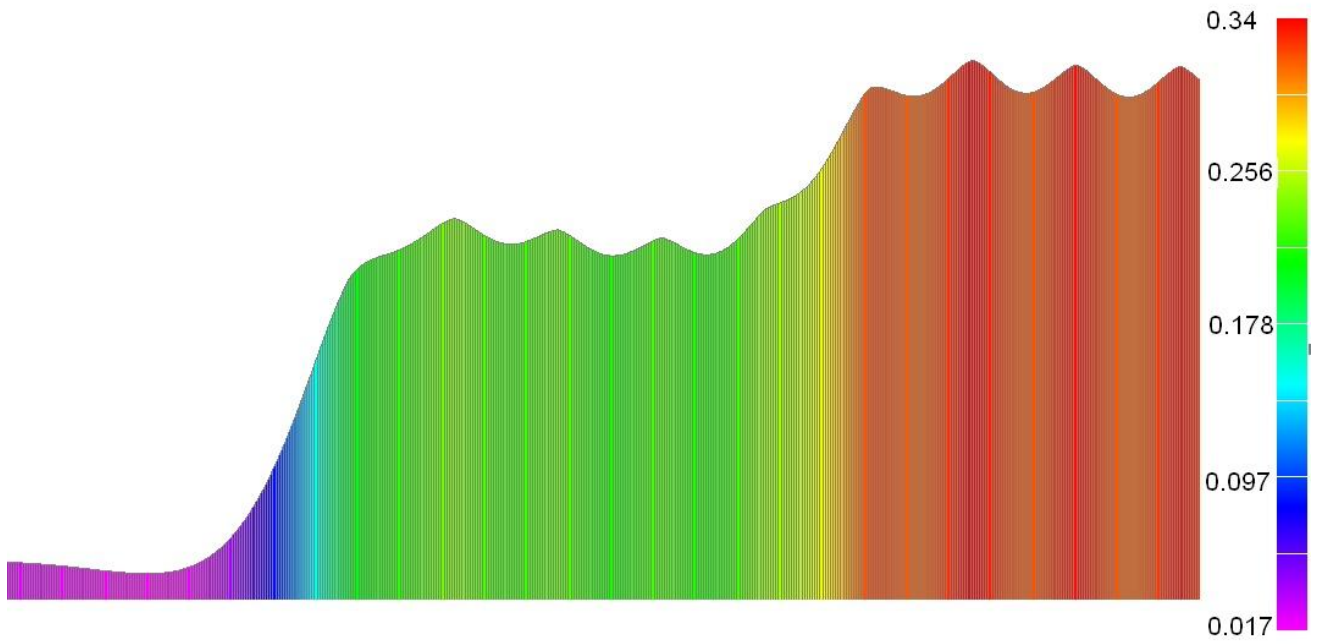


Fig. 2.29. The diagram of the pressure on the ground under a rail flange (kgf/cm²) for a head and the first freight wagons (moderately firm ground: $k = 2.5 \text{ kgf/cm}^2$)

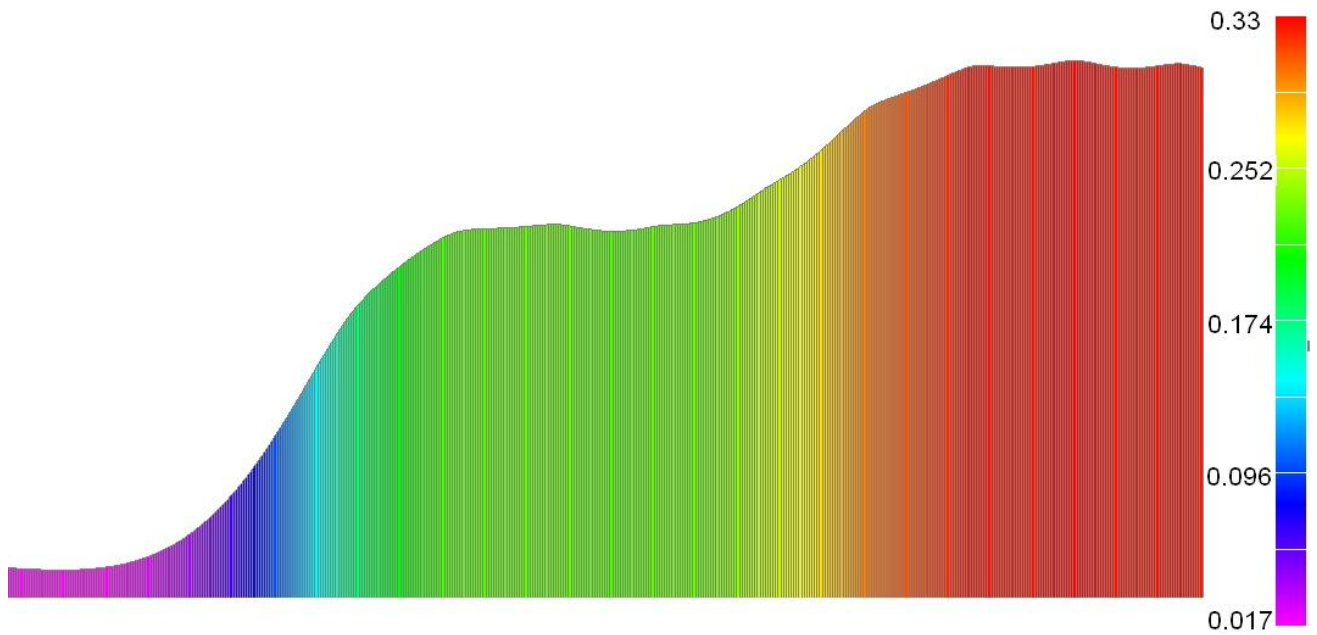


Fig. 2.30. The diagram of the pressure on the ground under a rail flange (kgf/cm²) for a head and the first freight wagons (loose ground: $k = 0.5 \text{ kgf/cm}^2$)

2.10.3. The Optimized Version

Cross section of the optimized version of a string-rail is represented in Fig. 2.31.

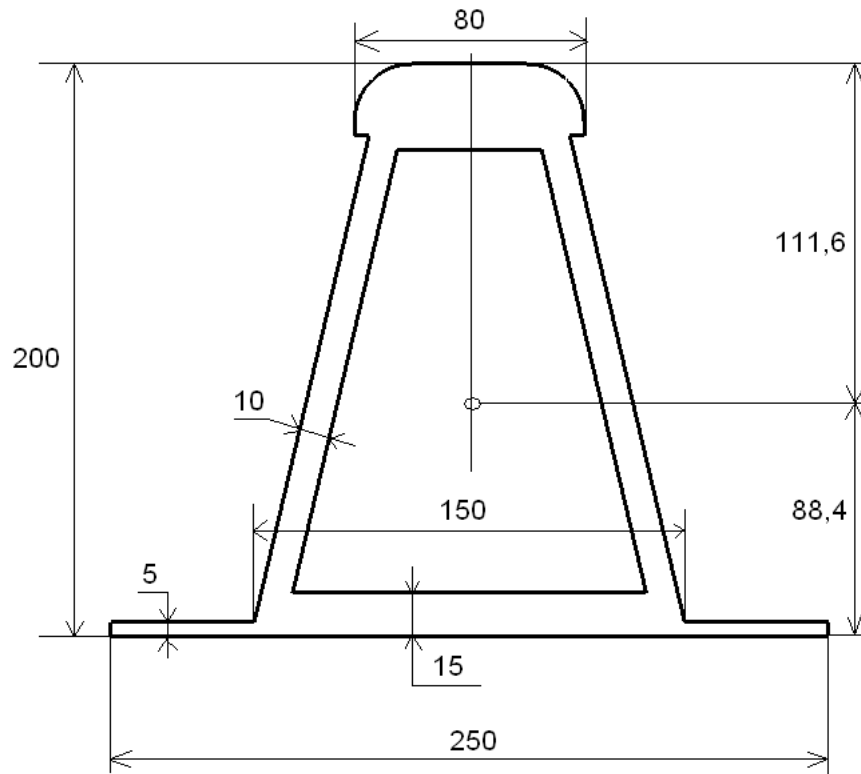


Fig. 2.31. Cross section of the optimized version of a string-rail

Initial Data on a String-Rail

Normalized to steel string-rail area is $A = 83 \text{ cm}^2$.

$E = 2 \cdot 10^{11} \text{ Pa}$ is elasticity modulus of rail steel.

$J = 4.546 \cdot 10^{-5} \text{ m}^2$ is inertia moment of a normalized to steel rail section.

$E \cdot J = 9.092 \cdot 10^6 \text{ N} \cdot \text{m}^2$.

$b = 0.25 \text{ m}$ is width of a rail flange.

$\rho = 81.1 \text{ kg/m}$ is linear density (mass) of a rail.

k is compliance coefficient of elastic subgrade (ground). The coefficient is equal in value to the force applied to 1 cm^2 of subgrade area to make ground sit of 1 cm.

$k_n = k \cdot b$ is coefficient of subgrade reaction.



Initial Data on Weight Load of a Motorail

The schematic view of string-rail loading by a motorail is represented in Fig.2.32.

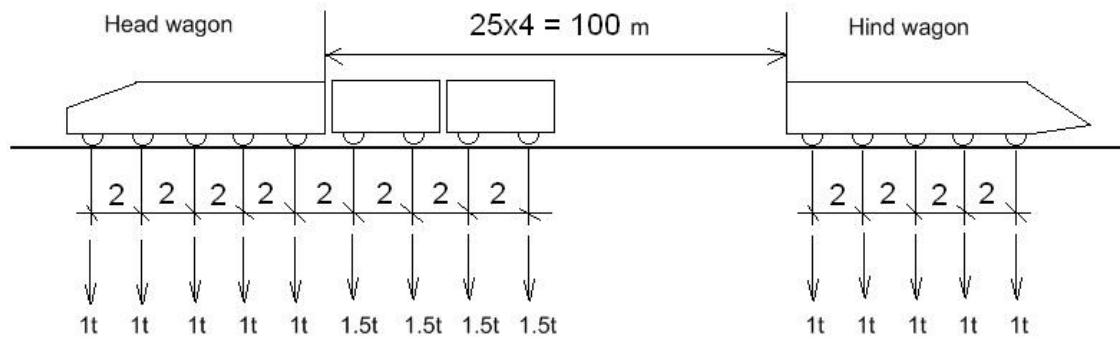


Fig. 2.32. The schematic view of string-rail loading by a motorail

The pressure resulted from one wheel of head and hind wagons is $P_1 = 10\ 000\ N$.
 The pressure resulted from one wheel of freight wagons is $P_2 = 15\ 000\ N$.

The Results of Analysis

Tab. 2.16 represents all basic values resulted from vertical load of a motorail on three types of ground of various densities.

Table 2.16

The Values Resulted From Motorail’s Vertical Load

Type of ground	Subgrade compliance coefficient, N/m^3 (kgf/cm^3)	Maximum bending moment, $N\cdot m$, and max. subgrade deformation (mm)	Max. bend stress, MPa		Max. pressure on the ground under a rail flange, N/m^2 (kgf/cm^2)
			Top of rail	Bottom of rail	
Firm ground	10^8 (10)	2713 (0.362)	-2.97 +6.66	+5.28 -2.355	36200 (0.362)
Moderately firm ground	$2.5 \cdot 10^7$ (2.5)	3036 (1.37)	-7.45 +3.095	+5.91 -2.45	34250 (0.3425)
Loose ground	$5 \cdot 10^6$ (0.5)	3775 (6.74)	-9.26 +5.6	+7.35 -4.43	33700 (0.337)

The pressure on the ground under a string-rail is equal to the following product: (Subgrade deformation) x (Compliance coefficient of elastic subgrade).



Taking into account the data, listed in Tab. 2.16, it follows that ground pressure under a rail bottom, wired to the ground (this rail serves as longitudinal sleeper, which distributes the load along the track) is not high (0.33 – 0.36 kgf/cm²). In conventional rail roads there is larger pressure on the ground (0.6-0.8 kgf/cm²), though there are assembled rails and sleepers and sand and road cap. The abovementioned ground pressure is much lower in comparison with ground pressure caused by foundations of buildings, which have lifetime of dozens and hundreds of years. It assumes high reliability and durability of string-rail track structure wired to the ground.

2.10.4. Influence of String Tension

The influence of string tension on string-rail deflection (vertical deformations) and its bending moments is analyzed. The case when an endless rail is influenced by two forces of two wheels, situated at a distance of 0.75 m, is considered. Decrease of ground pressure under rail bottom, caused by increase of string tension is estimated. Analysis is carried out considering string tension of 0-1000 ton-force, for EJ from 10⁶ to 10⁸ N·m² and for three types of ground (k = 0.5 kgf/cm³, 5 kgf/cm³ and 10 kgf/cm³).

The Results of Analysis

The results of analysis are represented in the following graphs:

- A) for loose ground (Fig. 2.33 – 2.35);
- B) for moderately firm ground (Fig. 2.36 – 2.38);
- C) for firm ground (Fig.2.39 – 2.41).

A) Loose Ground

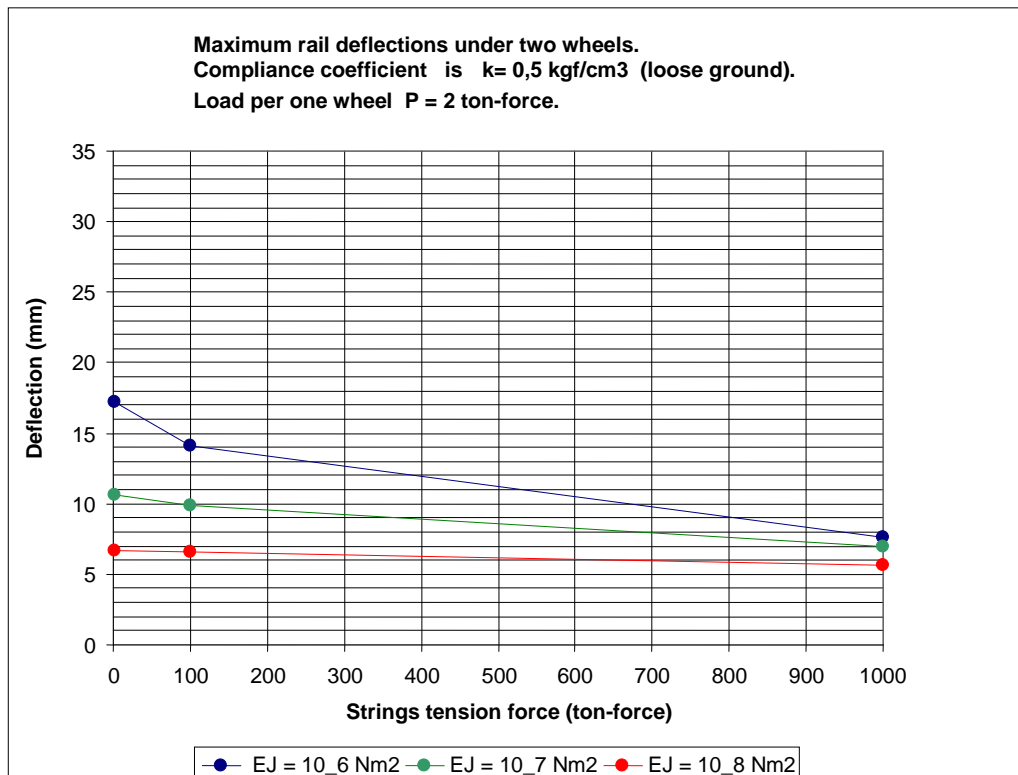


Fig. 2.33

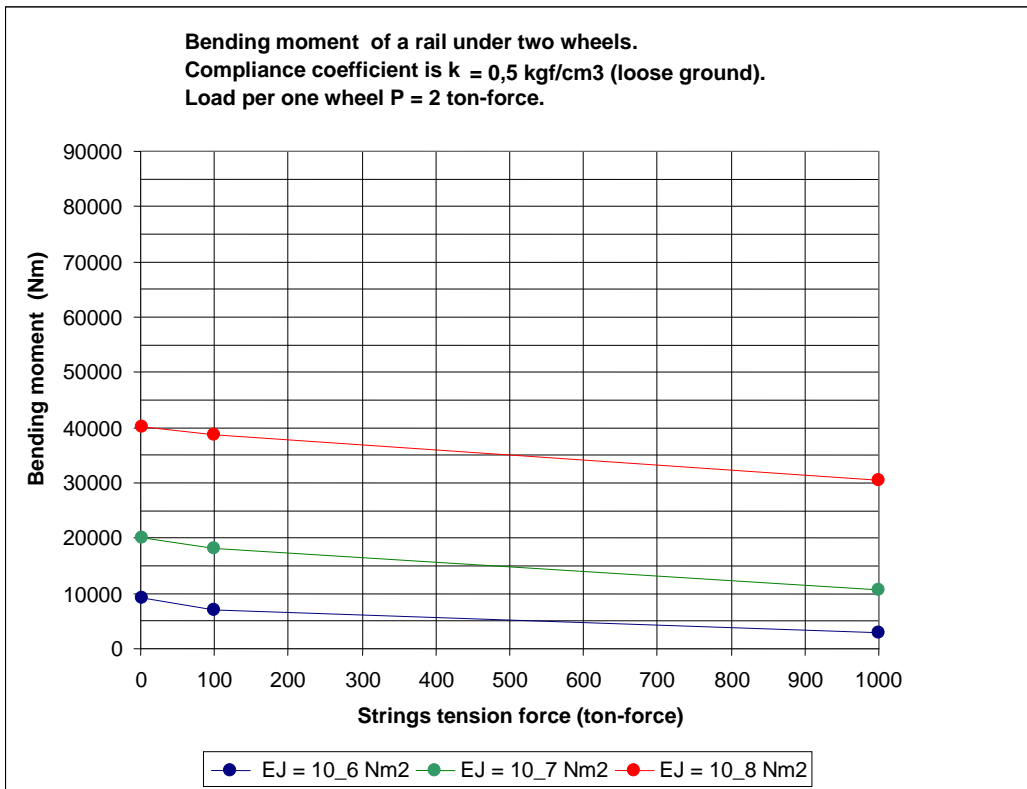


Fig. 2.34

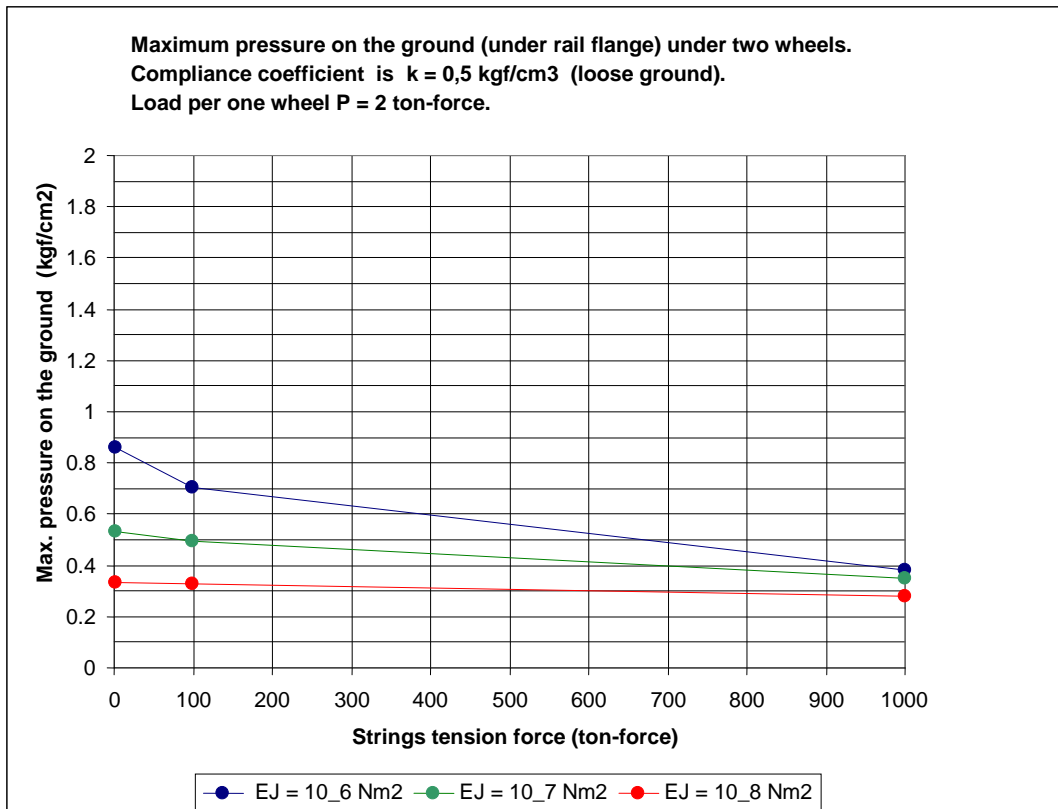


Fig. 2.35



B) Moderately Firm Ground

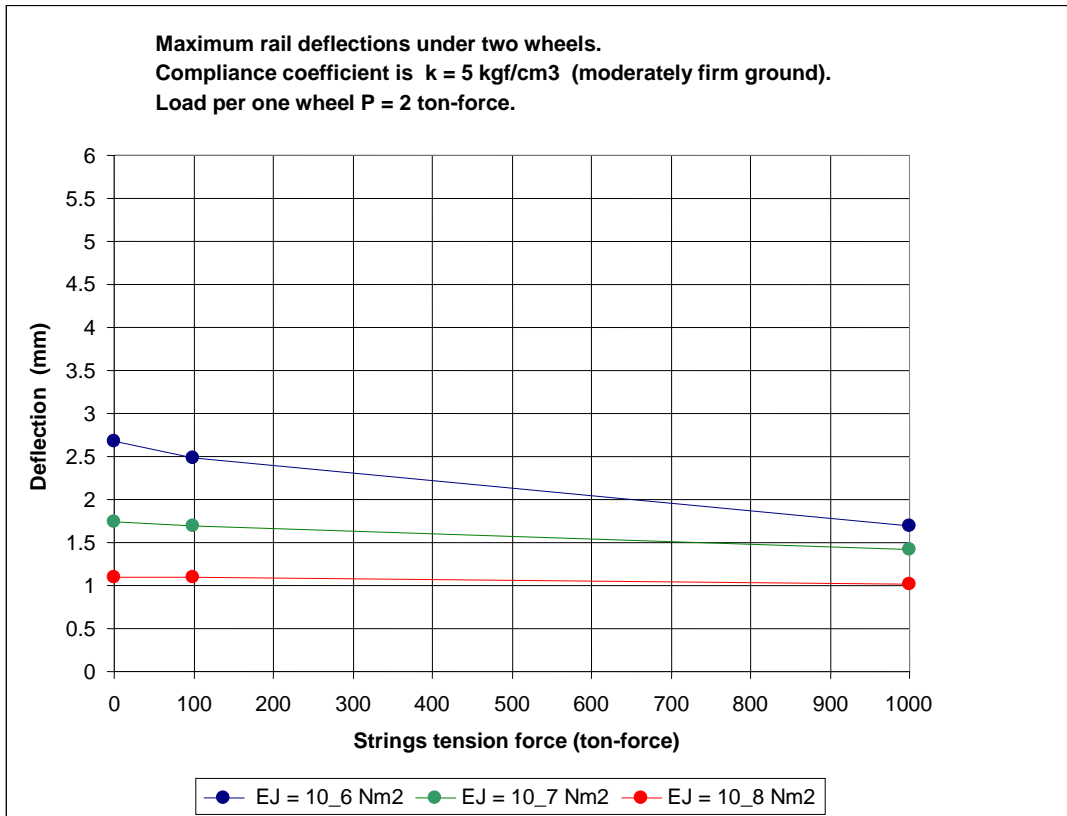


Fig. 2.36

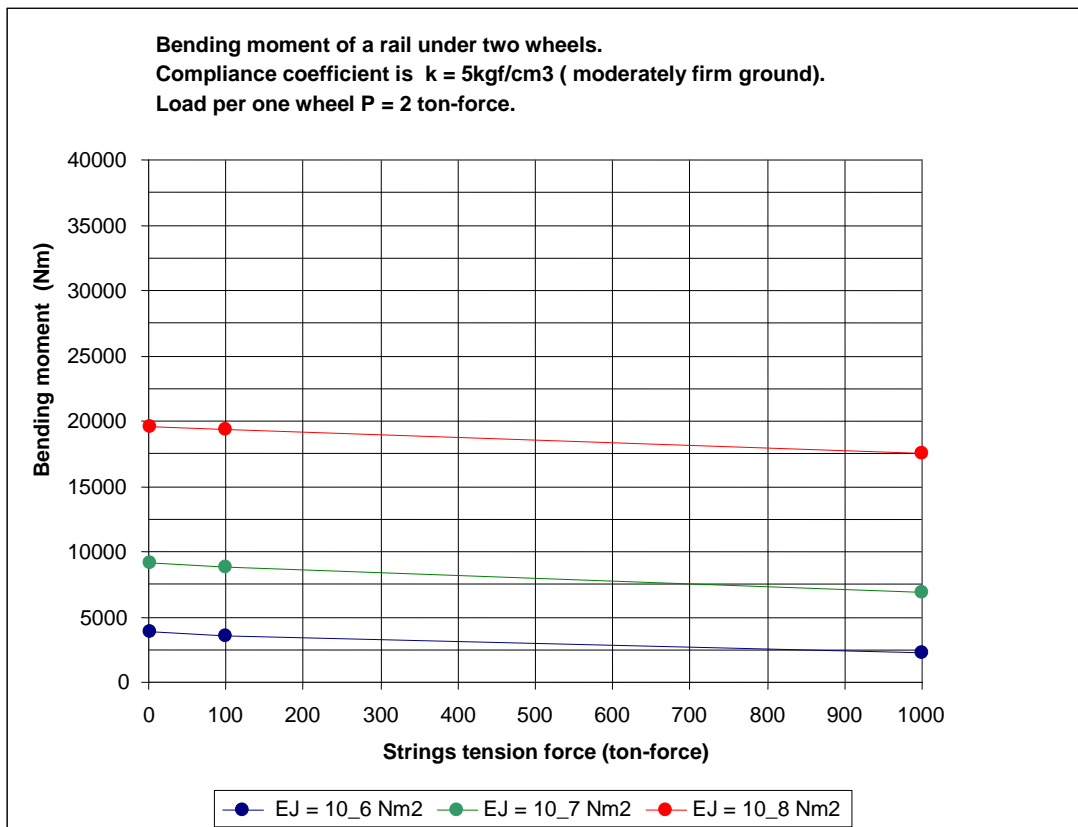


Fig. 2.37

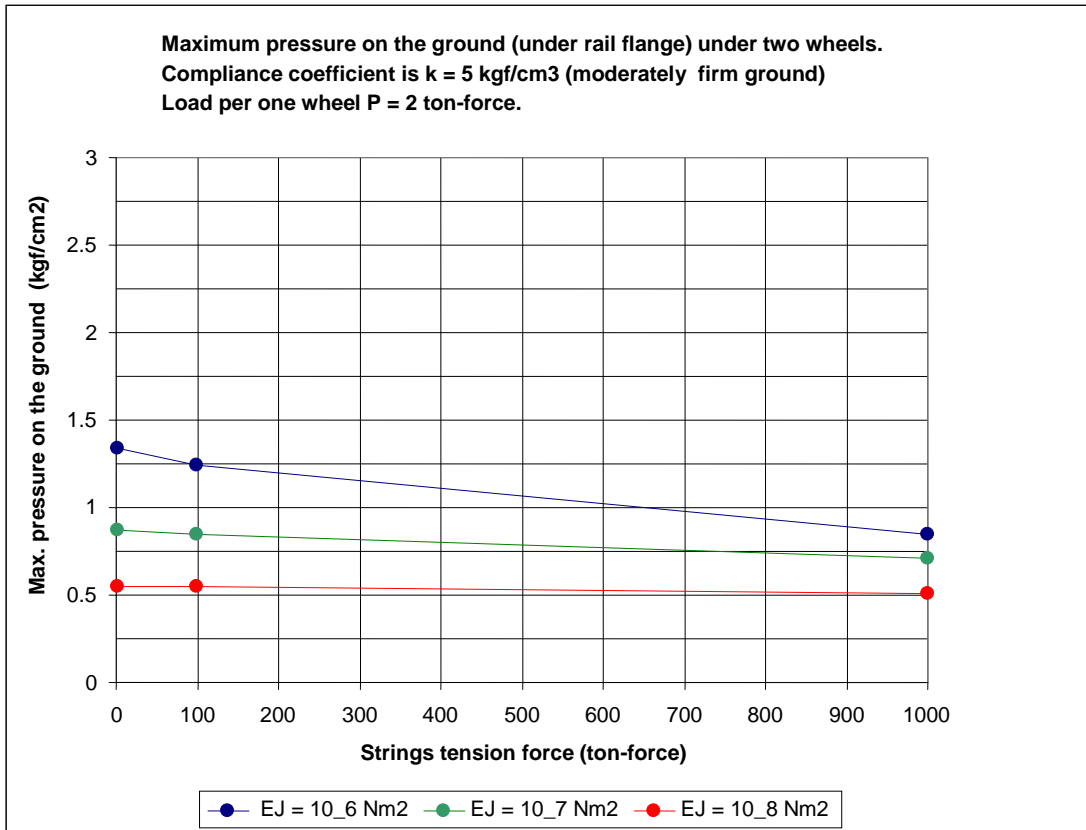


Fig. 2.38

C) Firm Ground

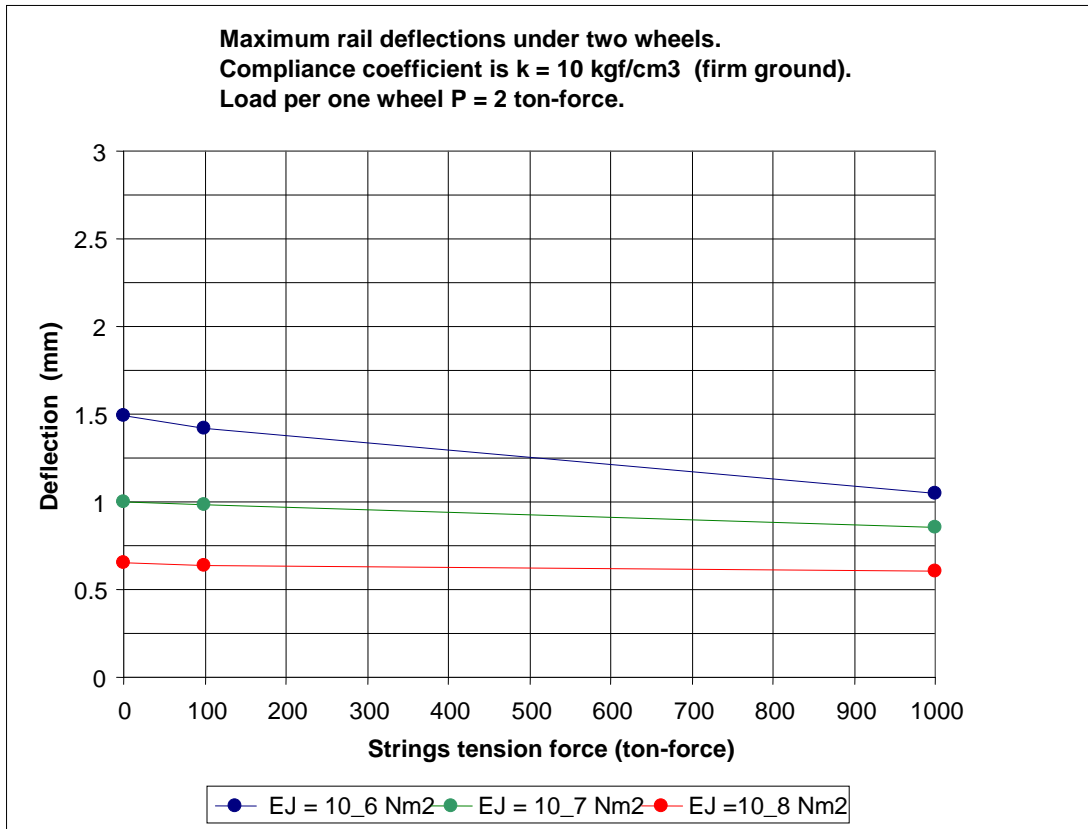


Fig. 2.39

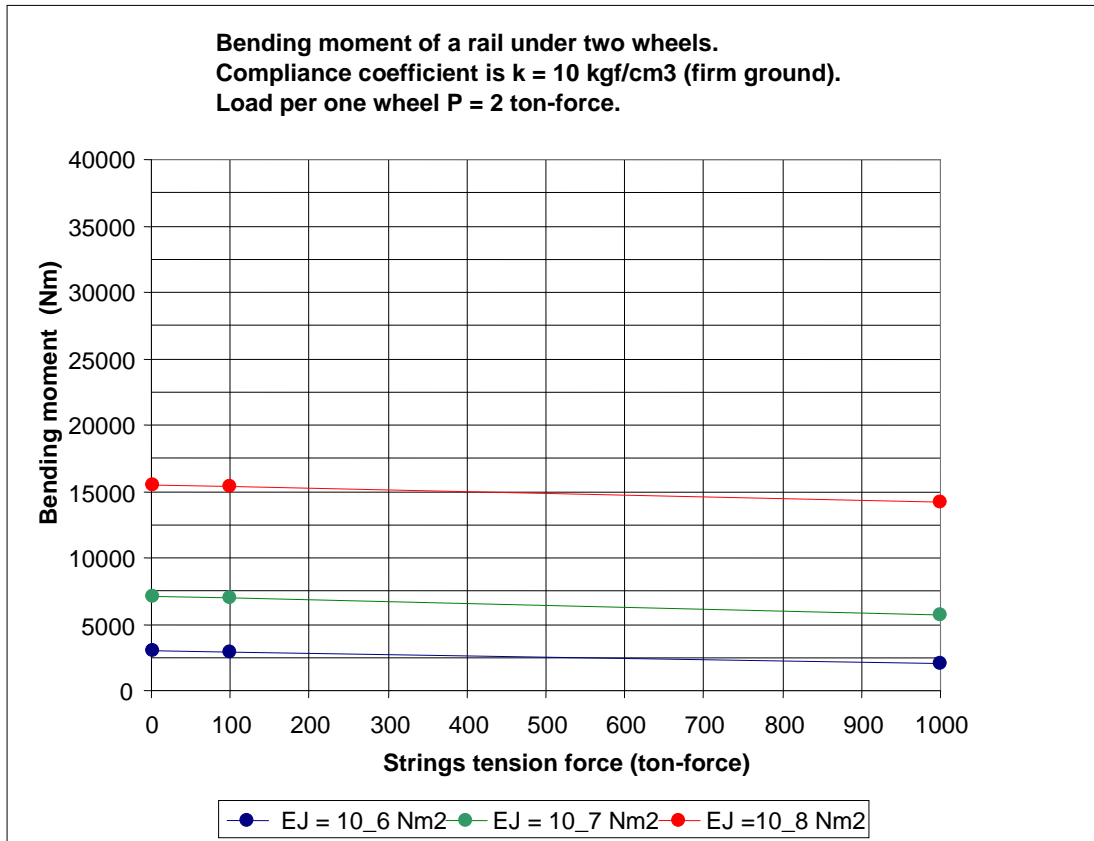


Fig. 2.40

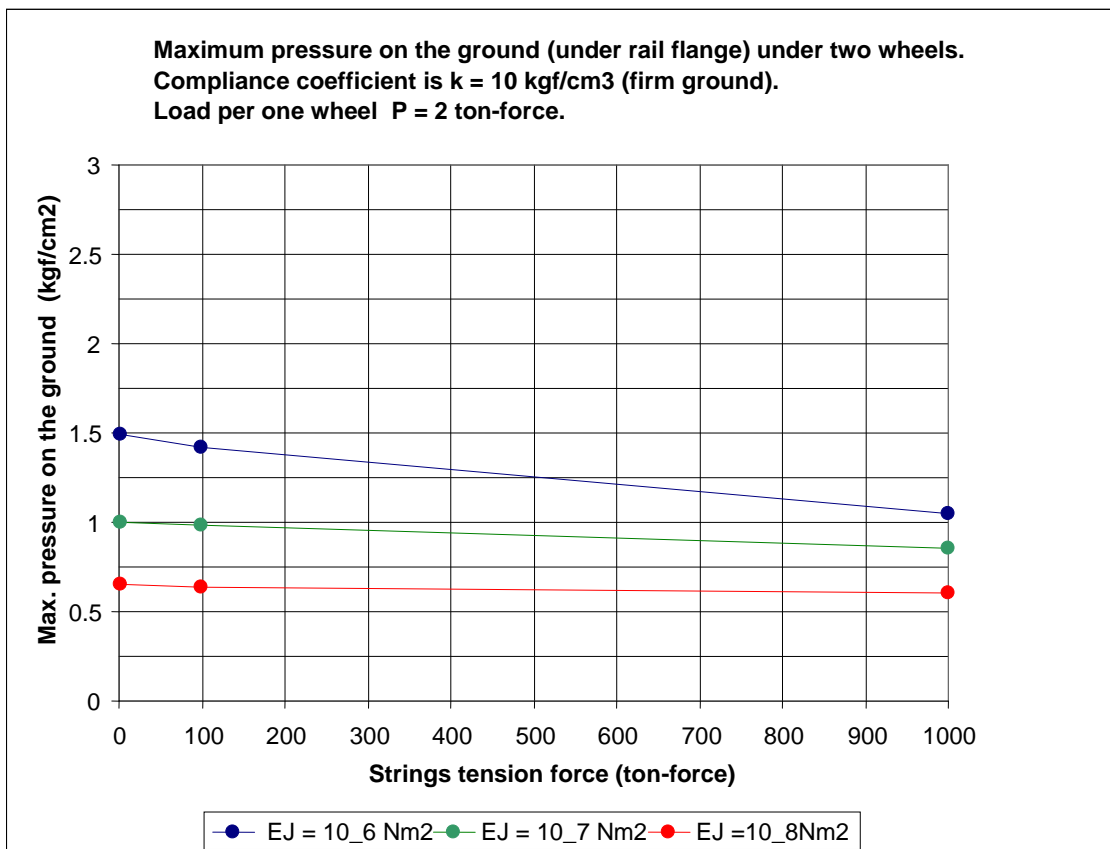


Fig. 2.41



The results of analysis prove that on loose ground and in terms of small bending stiffness of a rail strings should be considerably stressed. In such case string should be stressed up to 100 tons per one rail.

General view of STS with double-track wired to the ground is represented in Fig. 2.42 – 2.44



Fig. 2.42. General view of double-track STS located on “the first level”

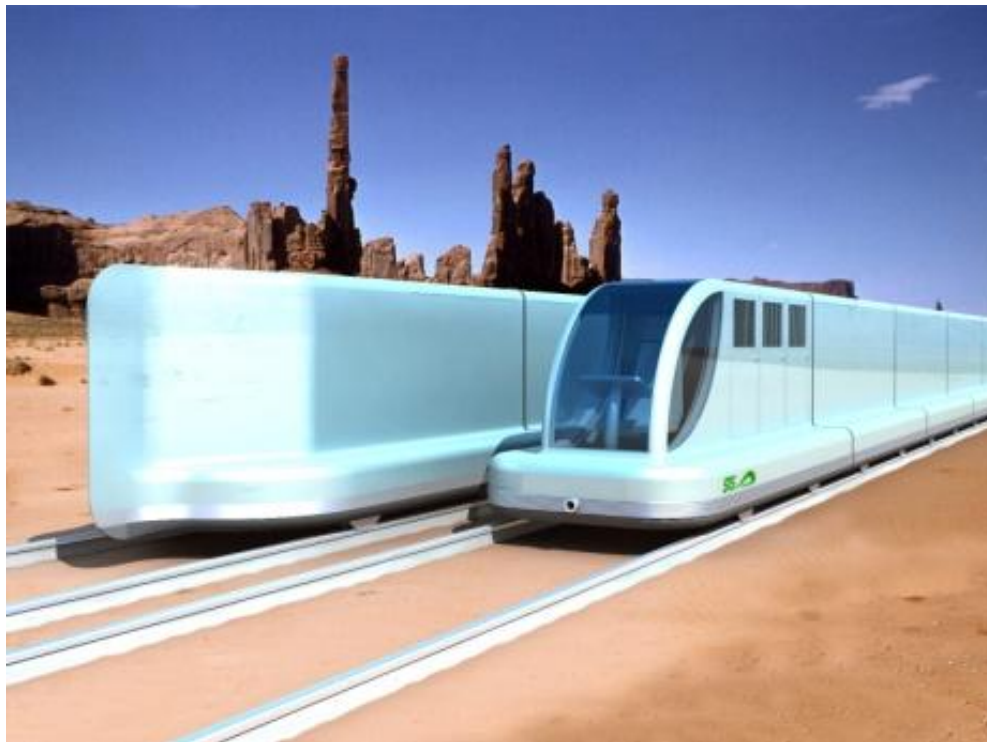


Fig. 2.43. General view of double-track STS located on “the first level”

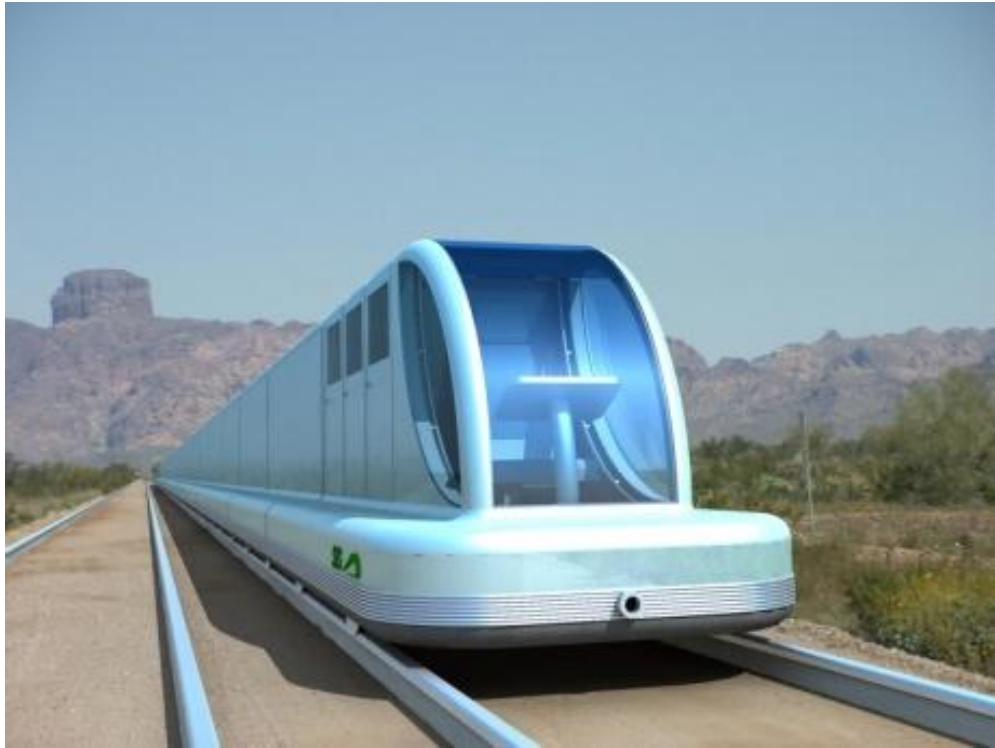


Fig. 2.44. General view of double-track STS located on “the first level”

2.11. Static Analysis of a String-Rail on an Elevated Section of a Track

On an elevated section of a track string-rail’s stiffness, strength and endurance are tested.

2.11.1. Stiffness and Strength Analysis

String-Rail Initial Data:

Normalized to steel string-rail area:

$A = 115\text{cm}^2$ (for stiffness analysis);

$A = 66\text{ cm}^2$ (for strength analysis).

$E = 2 \cdot 10^{11}$ Pa is elasticity modulus of rail steel.

Inertia moment of a normalized to steel rail section:

$J = 1.94 \cdot 10^{-4}\text{ m}^4$ (for stiffness analysis)

$J = 1.31 \cdot 10^{-4}\text{ m}^4$ (for strength analysis).

$E \cdot J = 3.88 \cdot 10^7\text{ N} \cdot \text{m}^2$ (for stiffness analysis)

$E \cdot J = 2.62 \cdot 10^7\text{ N} \cdot \text{m}^2$ (for strength analysis).

$\rho = 150\text{ kg/m}$ is linear density (mass) of a rail.

String-rail cross-section is represented for stiffness analysis (Fig. 2.45) and for strength analysis (Fig. 2.46).

The schematic view of an elevated track section is represented on Fig. 2.47.

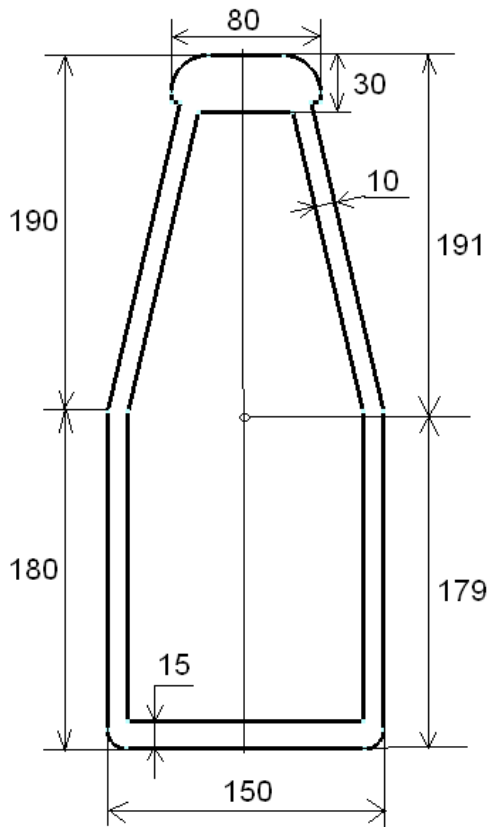


Fig. 2.45. Cross section of normalized steel rail for stiffness analysis (with account of concrete inside of the rail)

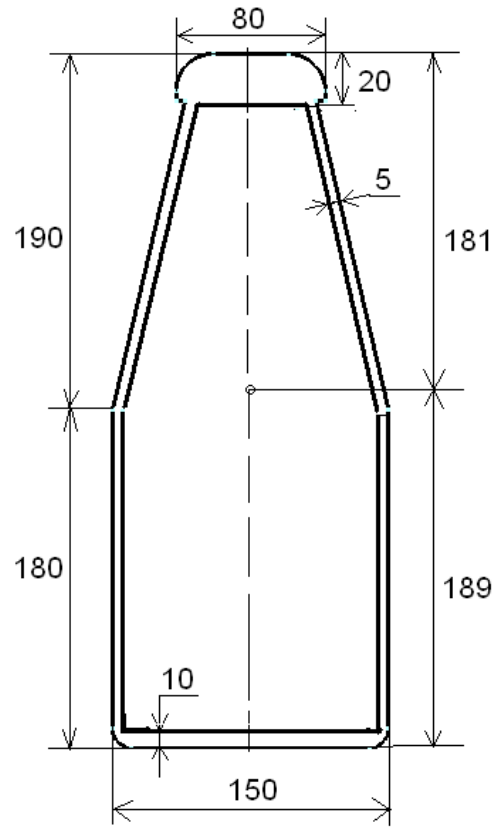


Fig. 2.46. Rail cross section for strength analysis (regardless to concrete inside of the rail)

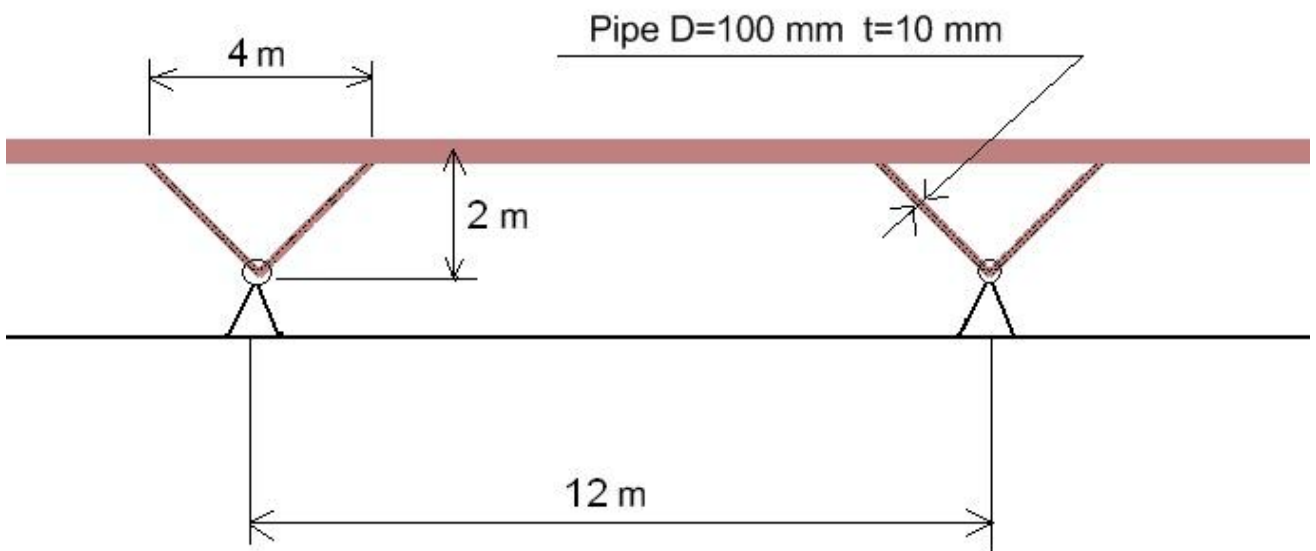


Fig. 2.47. The schematic view of an elevated track section

Initial Data on Motorail's Weight Load

The schematic view of string-rail loading by a motorail is represented in Fig.2.48.

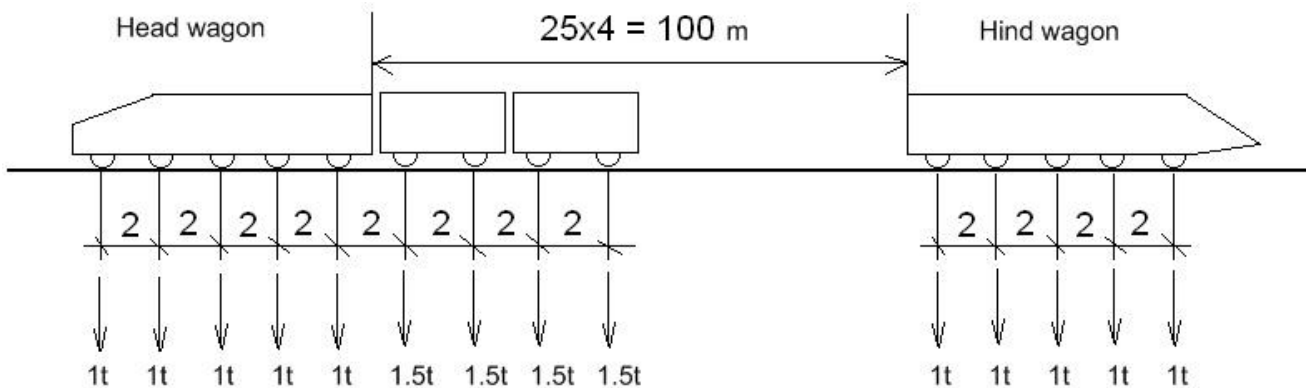


Fig. 2.48. The schematic view of string-rail loading by a motorail

The pressure resulted from one wheel of head and hind wagons is $P_1 = 10\,000\text{ N}$.

The pressure resulted from one wheel of freight wagons is $P_2 = 15\,000\text{ N}$.

The Results of Analysis

Fig.2.49 represents the diagrams of deflections along the whole length of a train.

Fig.2.50 represents the diagrams of bending moments along the whole length of a train.

Fig.2.51 represents the diagrams of stress caused by bending of a rail top.

Fig.2.52 represents the diagram of stress caused by bending of a rail bottom.

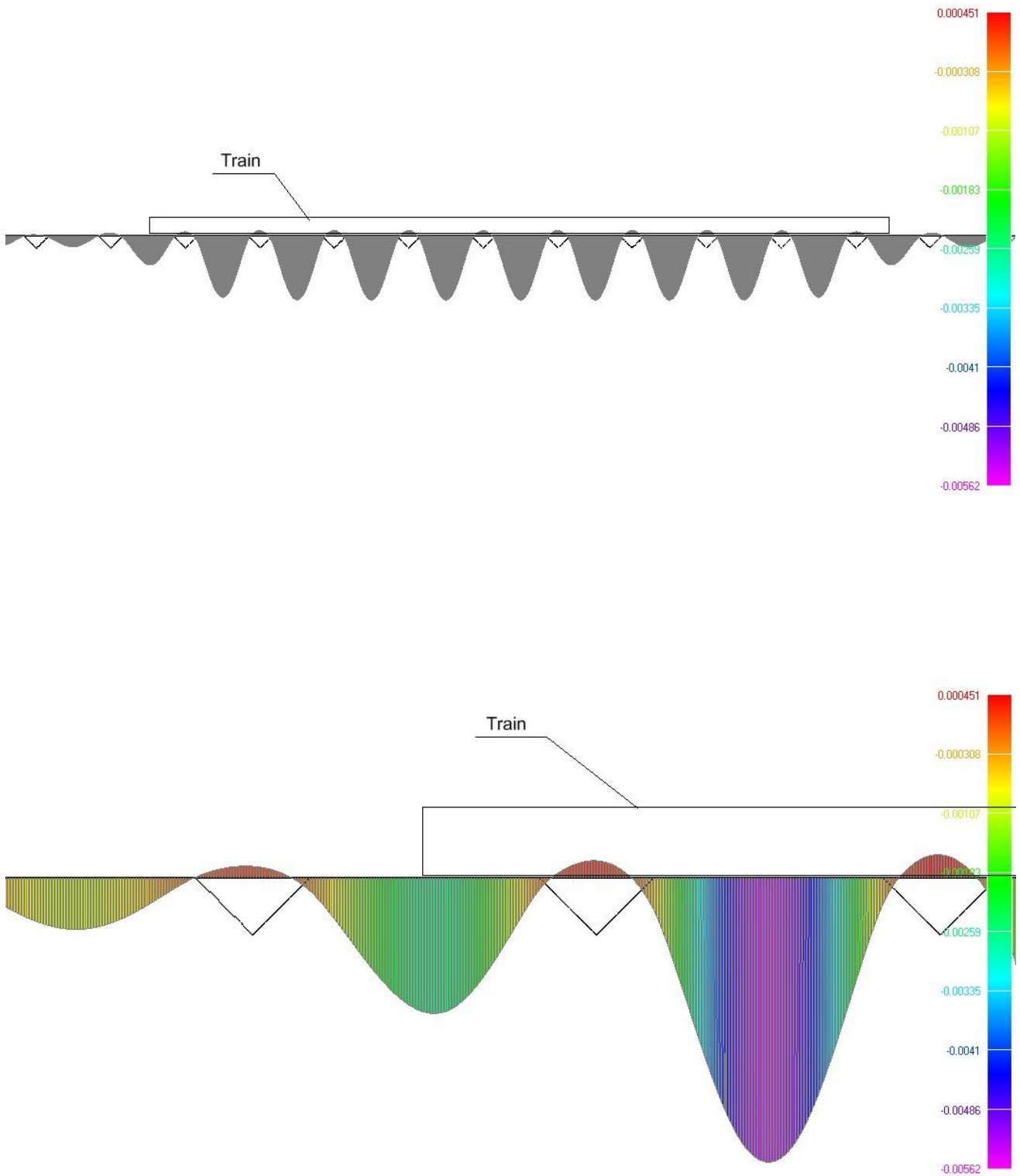


Fig. 2.49. The diagram of span bending (meters) along the whole length of a train. (maximum deflection is 5,62 mm): the upper diagram represents span bending above the whole train body, the lower diagram represents span bending above the forebody of a train

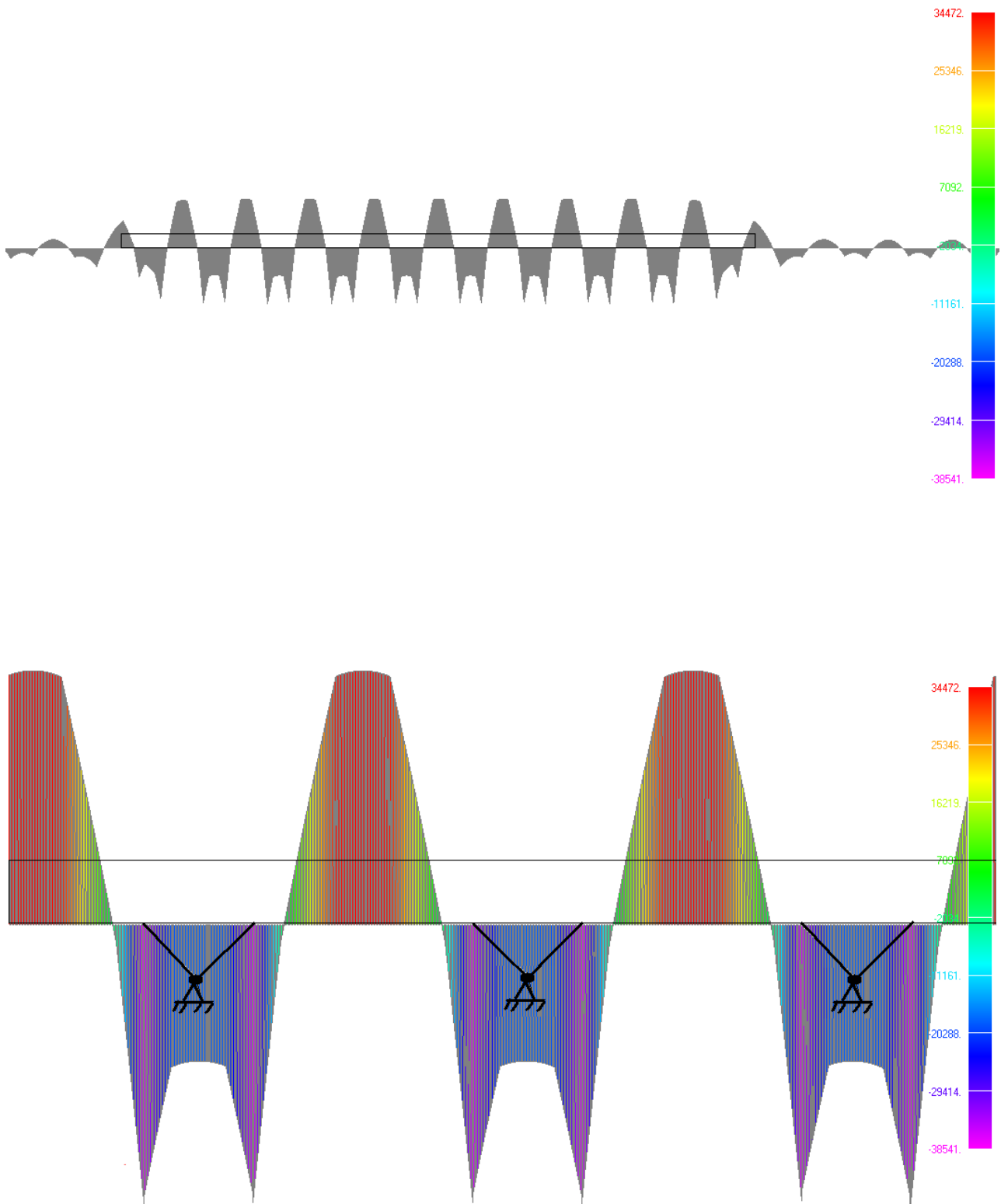


Fig. 2.50. The diagram of bending moments along the whole length of a train (maximum torque is 34470 N·m, minimum torque is 38540 N·m)

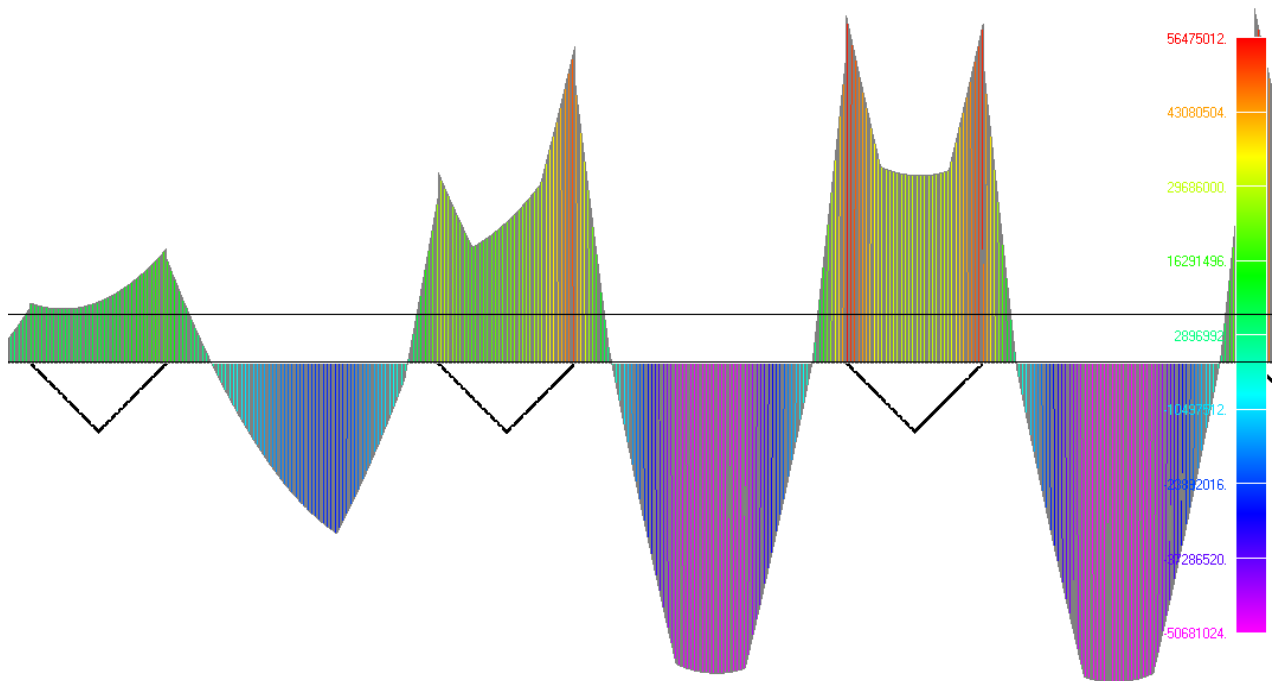


Fig. 2.51. The diagram of stress caused by bending (Pa) of a rail top.

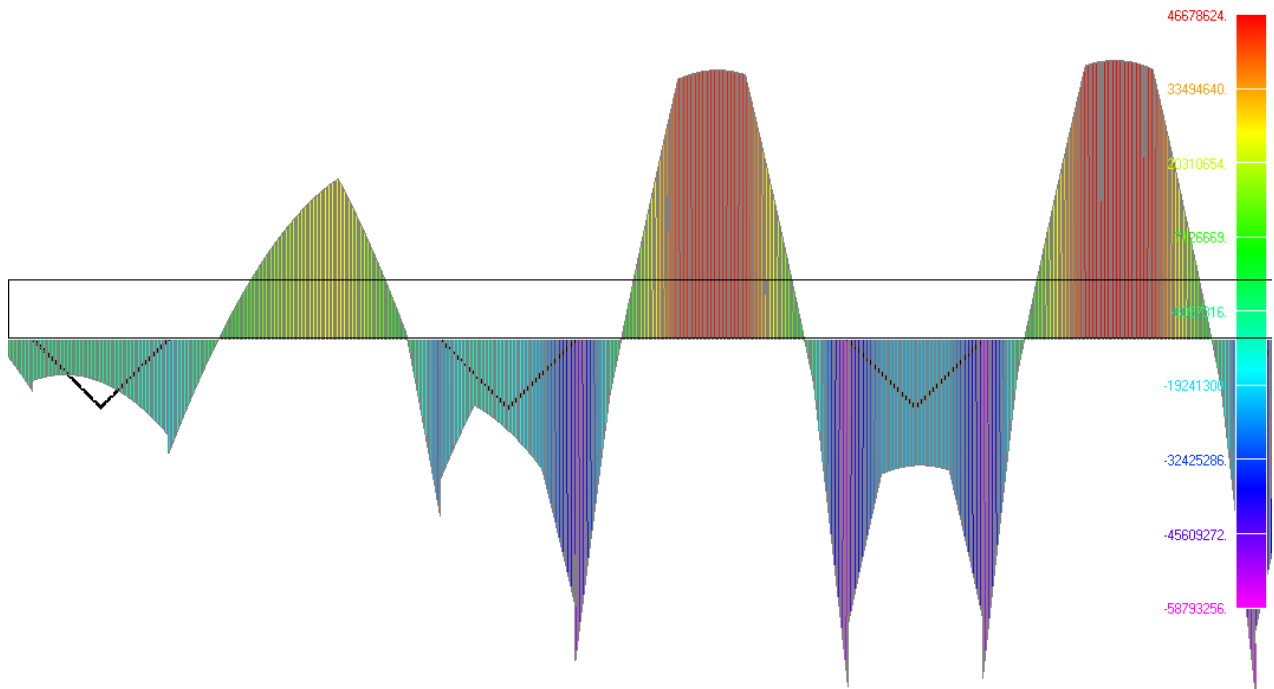


Fig. 2.52. The diagram of stress caused by bending (Pa) of a rail bottom.



2.11.2. Endurance Analysis

Endurance analysis is carried out towards the most weakened cross section of a string-rail which is crosscut welds in the rail top and in the rail body. Temperature difference analysis: $\Delta t = 80 \text{ }^\circ\text{C}$.

$$\sigma_t = \alpha \cdot E \cdot \Delta t = 1.2 \cdot 10^{-5} \cdot 2 \cdot 10^{11} \cdot 80 = 192 \cdot 10^6 \text{ Pa} = 192 \text{ MPa} \quad (2.1)$$

Endurance Analysis in Accordance with Russian Standard SNiP2.05.03-84 (Bridges and Pipes)*

Endurance analysis of steel structure elements of bridges and their connections should be carried out by the following formulas:

$$\sigma_{\max,ef} \leq \gamma_w \cdot R_y \cdot m \quad (2.2)$$

$$\tau_{\max,ef} \leq 0.75 \gamma_w \cdot R_y \cdot m \quad (2.3)$$

$\sigma_{\max,ef}$ is maximum in absolute value stress (positive in compression). Stress is calculated from the effect of permanent and temporary loads.

$\tau_{\max,ef}$ is maximum in absolute value contact stress in the calculation of fillet welds shear (its direction is taken as positive).

Stress is calculated from the effect of permanent and temporary loads.

γ_w is the coefficient of reduction of steel design stress due to steel fatigue.

m is the coefficient of working conditions (Tab.60 SNiP).

$$\gamma_w = \frac{1}{\zeta \cdot \vartheta \cdot [(\alpha\beta \pm \delta) - (\alpha\beta m \delta)\rho]} \leq 1, \quad (2.4)$$

where:

ζ is the coefficient equal to 1 for railway bridges and equal to 0,7 for road and city bridges;

ϑ - coefficient depends on the length of influence line loading in determining $\sigma_{\max,ef}$.

At the influence line length of $\lambda \geq 22\text{m}$ the coefficient is $\vartheta = 1$; at $\lambda < 22\text{m}$, $\vartheta = \nu - \xi \cdot \lambda$, where ξ and ν values are accepted depending on steel grade and effective coefficient of β concentration.

ϑ coefficient for the influence lines lengths less than 22 m can be determined from the formulas:

- for carbon steel:

$$\vartheta = \nu - \xi \cdot \lambda = (1.45 + 0.2917 \cdot (\beta - 1)) - (0.0205 + 0.01325 \cdot (\beta - 1) \cdot \lambda) \quad (2.5)$$

- for low alloy steel:

$$\vartheta = \nu - \xi \cdot \lambda = (1.65 + 0.44 \cdot (\beta - 1)) - (0.0295 + 0.02006 \cdot (\beta - 1) \cdot \lambda) \quad (2.6)$$

where:

α and δ coefficients considering steel grade and non-stationary mode of loading are taken from Tab.2.17.

Table 2.17

Steel Grade	α	δ
16Д	0.64	0.20
15ХСНД; 09Г2СД	0.72	0.24
10ХСНД; 15ХСНД-40; 14Г2АФД; 15Г2АФДпс	0.81	0.20



β is effective coefficient of stress concentration. The values are taken from Tab. 1 Appendix 17 SNiP 2.05.03-84*, pages 181 – 186. The drawings of compounds are not given in the table, and the coefficients are taken from the description of construction details.

$$\rho \text{ is the cycle asymmetry coefficient } \rho = \frac{\sigma_{\min}}{\sigma_{\max}} \quad \rho = \frac{\tau_{\min}}{\tau_{\max}}$$

σ_{\min} , σ_{\max} and τ_{\min} , τ_{\max} are minimum and maximum absolute values of stress with their signs, defined in the same sections as $\sigma_{\max,ef}$ and $\tau_{\max,ef}$. The worst is a symmetrical cycle where $\rho = -1$. When $\rho = +1$ there are no stress changes and endurance testing is not required.

In the formula (2.4) the upper signs in brackets should be taken when calculating the formula (2.2) if $\sigma_{\max,ef} > 0$, and always according to the formula (2.3).

For string construction the values of the coefficients are accepted as:

$$\zeta = 1.0$$

$$\vartheta = 1.0$$

$$\alpha = 0.72 \text{ and } \delta = 0.24$$

$\beta = 1.8$ for basic metal of a detail on the boundary of raw butt weld with a smooth transition to the basic metal.

At the maximum temperature there is neither compression nor extension in the rail:

$$\text{Rail } \sigma_{\max} = 60 \text{ MPa } \sigma_{\min} = 0 \text{ MPa (midspan) } \rho = 0$$

$$\gamma_w = \frac{1}{\zeta \cdot \vartheta \cdot [(\alpha\beta \pm \delta) - (\alpha\beta \mp \delta)\rho]} = \frac{1}{1 \cdot [(0.72 \cdot 1.8 + 0.24)]} = 0.651 \quad (2.7)$$

$$60 \text{ MPa} \leq 0.651 \cdot 300 \cdot 0.9 = 175 \text{ MPa}$$

At the minimum temperature in the rail there is maximum extension:

$$\text{Rail } \sigma_{\max} = 192 + 60 = 252 \text{ MPa } \sigma_{\min} = 192 \text{ MPa (midspan)}$$

$$\rho = 192/252 = 0.76$$

$$\gamma_w = \frac{1}{\zeta \cdot \vartheta \cdot [(\alpha\beta \pm \delta) - (\alpha\beta \mp \delta)\rho]} = \frac{1}{1 \cdot [(0.72 \cdot 1.8 + 0.24) - (0.72 \cdot 1.8 - 0.24) \cdot 0.76]} = 1.36 > 1 \quad (2.8)$$

$$252 \text{ MPa} \leq 1.0 \cdot 300 \cdot 0.9 = 270 \text{ MPa}$$

Rail endurance is provided.

Endurance Analysis in Accordance with Russian Standard SNiP II-23-81* (Steelwork)

Endurance analysis should be determined from the formula:

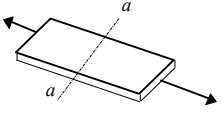
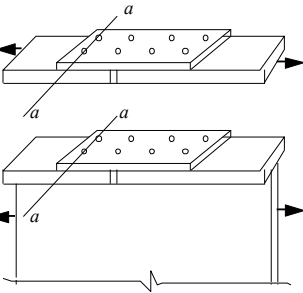
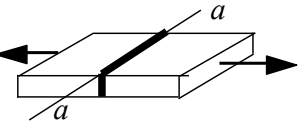
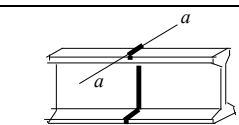
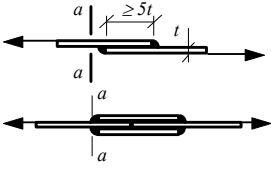
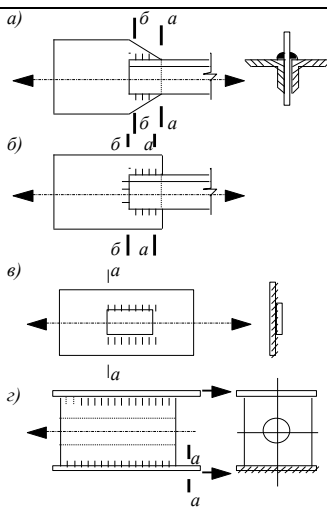
$$\sigma_{\max} \leq \alpha \times R_v \times \gamma_v, \quad (2.9)$$

where:

R_v is estimated fatigue resistance taken from the Tab. 32* (SNiP) depending on the tensile strength of steel and structural elements given in the Tab. 83* (SNiP) (See the Tab. 2.18 below); for transverse welds (butt rolling sections) does not depend on rail material and is equal to $R_v = 75 \text{ MPa}$ (the fourth group of elements).

Table 2.18

Groups of elements and connections in endurance analysis

Ser. No.	Schematic representation of the element and the location of design section	Element Specification	Groups of Element
1		Basic metal with rolled or mechanically processed edges The same with edges, cut off with gas cutting machine.	1 2
3		Basic metal in high-strength bolts connections Basic metal in bolt (bolts, accuracy class A) connections in sections across the aperture	1 4
9		Butt-jointed raw seam; the load is perpendicular to the weld; jointing elements are of the same width and thickness	2
14		Butt-jointing rolling sections	4
20		Basic metal in the place of transition to the transverse (frontal) corner weld	6
21		Basic metal in connections with side-lap welds (in the places of transition from the element to the ends of side-lap welds): a) with double side-lap welds b) with side-lap and frontal welds b) during force transfer through basic metal r) anchor jaws where steel ropes are attached	8 7 7 8



R_v coefficient values are represented in Fig. 2.19.

Table 2.19

R_v coefficient values (Tab. 32* SNiP II-23-81)

Groups of element	R_v values at temporary steel resistance to tearing R_{un} , MPa (kgf/cm ²)				
	Less than 420 (4300)	More than 420 (4300) Less than 440 (4500)	More than 440 (4500) Less than 520 (5300)	More than 520 (5300) Less than 580 (5900)	More than 580 (5900) Less than 635 (6500)
1	120 (1220)	128 (1300)	132 (1350)	136 (1390)	145 (1480)
2	100 (1020)	106 (1080)	108 (1100)	110 (1120)	116 (1180)
3	For all grades of steel 90 (920)				
4	For all grades of steel 75 (765)				
5	For all grades of steel 60 (610)				
6	For all grades of steel 45 (460)				
7	For all grades of steel 36 (370)				
8	For all grades of steel 27 (275)				

α is the coefficient taking into account the number of loading cycles n :

When $10^5 < n < 3.9 \cdot 10^6$ it is determined from the formulas:

-for groups of elements 1 and 2:

$$\alpha = 0.064 \left(\frac{n}{10^6} \right)^2 - 0.5 \left(\frac{n}{10^6} \right) + 1.75; \quad (2.10)$$

- for groups of elements 3-8:

$$\alpha = 0.07 \left(\frac{n}{10^6} \right)^2 - 0.64 \left(\frac{n}{10^6} \right) + 2.2; \quad (2.11)$$

when $n > 3.9 \cdot 10^6$ $\alpha = 0.77$.

For groups of elements 3 – 8 calculation by formula (2.11) results in:

when $n = 3.9 \cdot 10^6$ $\alpha = 0.77$;
 when $n = 2.5 \cdot 10^6$ $\alpha = 1.04$;
 when $n = 2.0 \cdot 10^6$ $\alpha = 1.2$;
 when $n = 1.0 \cdot 10^6$ $\alpha = 1.63$;
 when $n = 5.0 \cdot 10^5$ $\alpha = 1.9$;
 when $n = 1.0 \cdot 10^5$ $\alpha = 2.14$.

γ_v is the coefficient defined in the Tab. 33 SNiP depending on the type of stress state and coefficient of stresses asymmetry $\rho = \sigma_{min}/\sigma_{max}$. In this case σ_{min} и σ_{max} are maximum and minimum values of the stresses in the estimated element.

γ_v coefficient values are represented in Fig. 2.20.



Table 2.20

 γ_v coefficient values (Table 33 SNiP II-23-81)

σ_{max}	Coefficient of stresses asymmetry ρ	Formulas for calculating γ_v coefficient
Compression	$-1 \leq \rho \leq 0$	$\gamma_v = \frac{2.5}{1.5 - \rho}$
	$0 < \rho \leq 0.8$	$\gamma_v = \frac{2.0}{1.2 - \rho}$
	$0.8 < \rho < 1$	$\gamma_v = \frac{1.0}{1 - \rho}$
Extension	$-1 \leq \rho < 1$	$\gamma_v = \frac{2}{1 - \rho}$

At a maximum temperature (heating in the sun) there is neither compression nor extension in a cutless rail:

Rail: $\sigma_{max} = 60$ MPa, $\sigma_{min} = 0$ MPa (midspan), $\rho = 0$

$$\gamma_v = \frac{2.5}{1.5 - \rho} = 1.67 \quad (2.12)$$

When $n > 3.9 \cdot 10^6$ take $\alpha = 0.77$;

$$\alpha \times R_v \times \gamma_v = 0.77 \times 75 \times 1.67 = 96 \text{ MPa} > \sigma_{max} = 60 \text{ MPa.}$$

When $n = 1.0 \cdot 10^6$ take $\alpha = 1.63$;

$$\alpha \times R_v \times \gamma_v = 1.63 \times 75 \times 1.67 = 204 \text{ MPa} > \sigma_{max} = 60 \text{ MPa.}$$

When $n = 5.0 \cdot 10^5$ take $\alpha = 1.9$.

$$\alpha \times R_v \times \gamma_v = 1.9 \times 75 \times 1.67 = 238 \text{ MPa} > \sigma_{max} = 60 \text{ MPa.}$$

At a minimum temperature (in winter) there will be maximum extension in a cutless rail:

Rail: $\sigma_{max} = 192 + 60 = 252$ MPa, $\sigma_{min} = 192$ MPa (midspan), $\rho = 192/252 = 0.76$

$$\gamma_v = \frac{2.0}{1.2 - \rho} = 4.545 \quad (2.13)$$

When $n > 3.9 \cdot 10^6$ take $\alpha = 0.77$;

$$\alpha \times R_v \times \gamma_v = 0.77 \times 75 \times 4.545 = 262.5 \text{ MPa} > \sigma_{max} = 252 \text{ MPa.}$$

When $n = 1.0 \cdot 10^6$ take $\alpha = 1.63$;

$$\alpha \times R_v \times \gamma_v = 1.63 \times 75 \times 4.545 = 534 \text{ MPa} > \sigma_{max} = 252 \text{ MPa.}$$

When $n = 5.0 \cdot 10^5$ take $\alpha = 1.9$.

$$\alpha \times R_v \times \gamma_v = 1.9 \times 75 \times 4.545 = 648 \text{ MPa} > \sigma_{max} = 252 \text{ MPa.}$$

Endurance of the rail weld is provided.

Endurance Analysis According to ENV

Endurance estimate is calculated from the formula:

$$\Delta\sigma \leq \frac{\Delta\sigma_R}{\gamma_f} \quad (2.14)$$

where:

$\Delta\sigma = \sigma_{max} - \sigma_{min}$ is current stress range;

$\gamma_f = 1,15$ is reliability coefficient in accordance with endurance limit;

$\Delta\sigma_R$ is maximum permissible stress range at a given number of loading cycles N.



$$\text{When } N < 5\,000\,000 \quad \Delta\sigma_R = \frac{\Delta\sigma_C}{\sqrt[3]{\frac{N}{20\,000\,000}}} \quad (2.15)$$

N is predetermined number of stress cycles;

$\Delta\sigma_C$ is maximum permissible stress range at 2 000 000 of symmetric cycles of details and compounds (double endurance limit).

We accept $\Delta\sigma_C = 90\text{MPa}$ (detail category 90, transverse butt welds).

Thermal stresses are not taken into account, because this method of calculation does not account for the asymmetry of the cycle. The range is specified only by rail bending.

$$\Delta\sigma = \sigma_{\max} - \sigma_{\min} = 60 \text{ MPa}$$

when $N = 5\,000\,000$ cycles

$$\Delta\sigma_R = \frac{\Delta\sigma_C}{\sqrt[3]{\frac{N}{20\,000\,000}}} = \frac{90}{\sqrt[3]{\frac{5\,000\,000}{20\,000\,000}}} = \frac{90}{1.357} = 66.3\text{MPa}$$

$$\Delta\sigma = 60\text{MPa} \approx \frac{\Delta\sigma_R}{\gamma_f} = \frac{66.3}{1.15} = 57.7\text{MPa}$$

when $N = 2\,000\,000$ cycles

$$\Delta\sigma_R = 90\text{MPa} \quad \Delta\sigma = 60\text{MPa} \leq \frac{\Delta\sigma_R}{\gamma_f} = \frac{90}{1.15} = 78.3\text{MPa}$$

when $N = 1\,000\,000$ cycles

$$\Delta\sigma_R = \frac{\Delta\sigma_C}{\sqrt[3]{\frac{N}{20\,000\,000}}} = \frac{90}{\sqrt[3]{\frac{1\,000\,000}{20\,000\,000}}} = \frac{90}{0.793} = 113.5\text{MPa}$$

$$\Delta\sigma = 60\text{MPa} \leq \frac{\Delta\sigma_R}{\gamma_f} = \frac{113.5}{1.15} = 98.7\text{MPa}$$

when $N = 500\,000$ cycles

$$\Delta\sigma_R = \frac{\Delta\sigma_C}{\sqrt[3]{\frac{N}{20\,000\,000}}} = \frac{90}{\sqrt[3]{\frac{500\,000}{20\,000\,000}}} = \frac{90}{0.63} = 142.8\text{MPa}$$



$$\Delta\sigma = 60MPa \leq \frac{\Delta\sigma_R}{\gamma_f} = \frac{142.8}{1.15} = 124.2MPa$$

Endurance of a rail weld is provided up to 5 000 000 cycles.

When transporting 160 tons of cargo by one motorail, million loading cycles for string-rail track structure and supports will occur in the total transportation volume of 160 million tons. Five million cycles will occur in the total transportation volume of 800 million tons.

General view of double-track STS located on “the second level” is represented in Fig. 2.53 and 2.54.

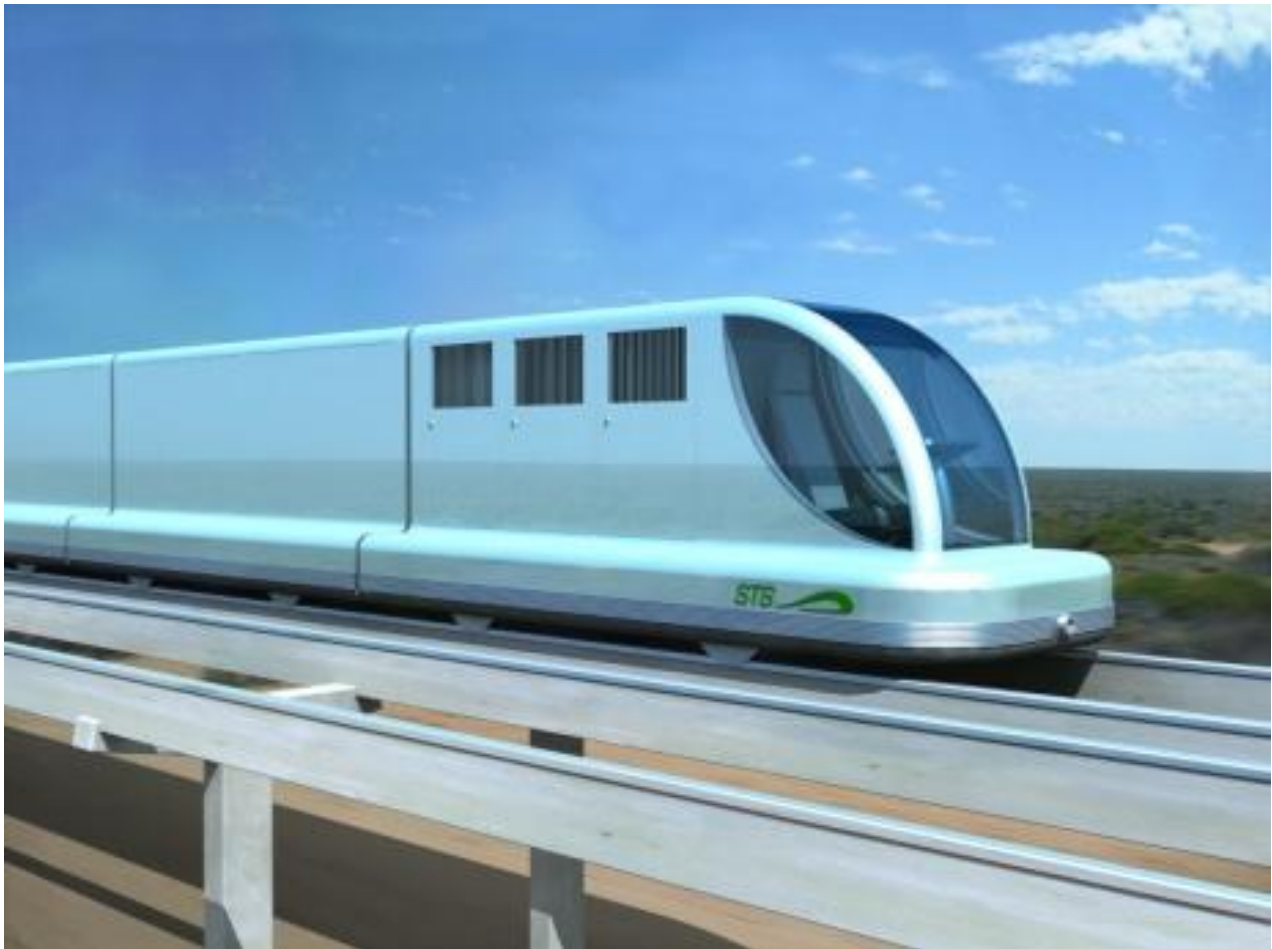


Fig. 2.53. General view of double-track STS located on “the second level”

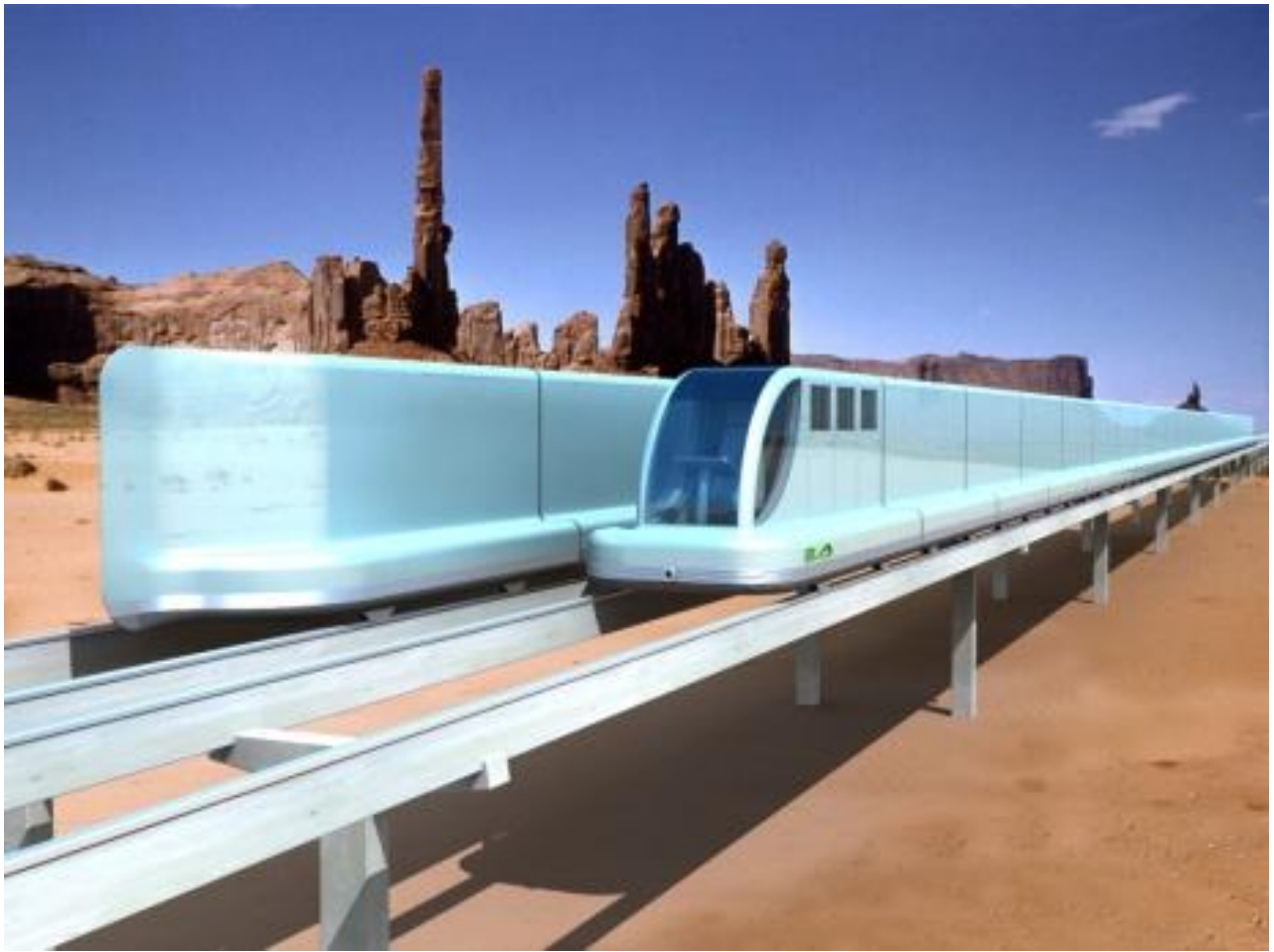


Fig. 2.54. General view of double-track STS located on “the second level”

2.11.3. Optimized Track Structure

To reduce the deformability of the track structure on the span and to improve the evenness of the way and, accordingly, the smoothness of a rolling stock, we shall consider an optimized design of supports which allows increasing the length span of up to 15 m. (see Fig. 2.55).

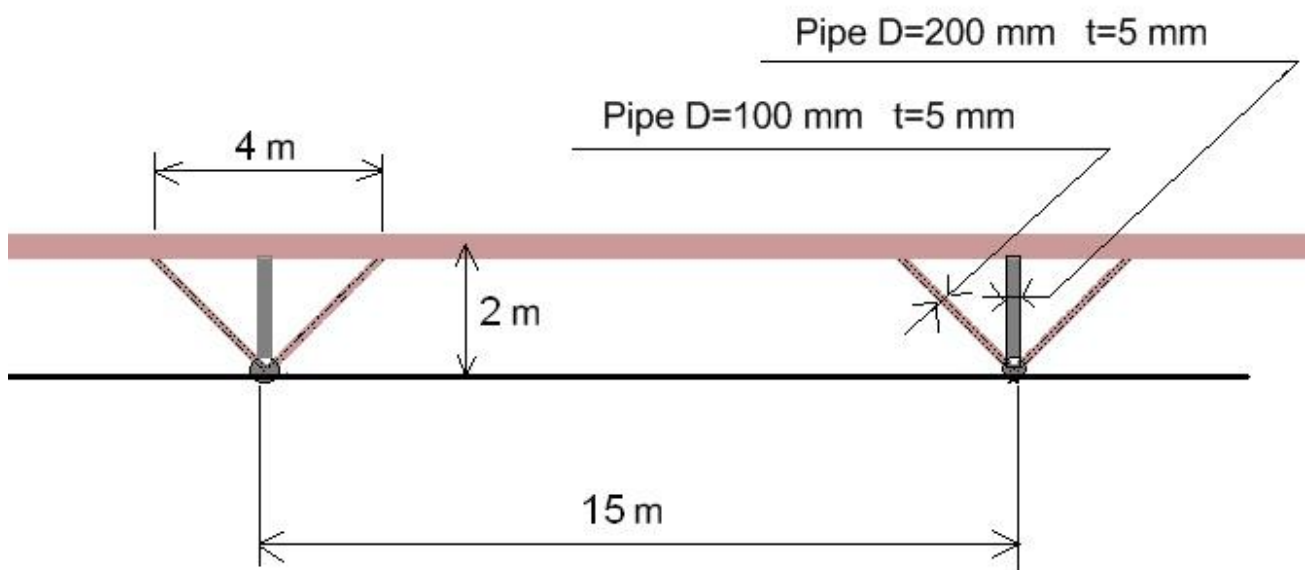


Fig. 2.55. Amended schematic view of STS elevated track section



The results of track structure (shown in Fig. 2.55) analysis are represented in Fig. 2.56 – 2.59.

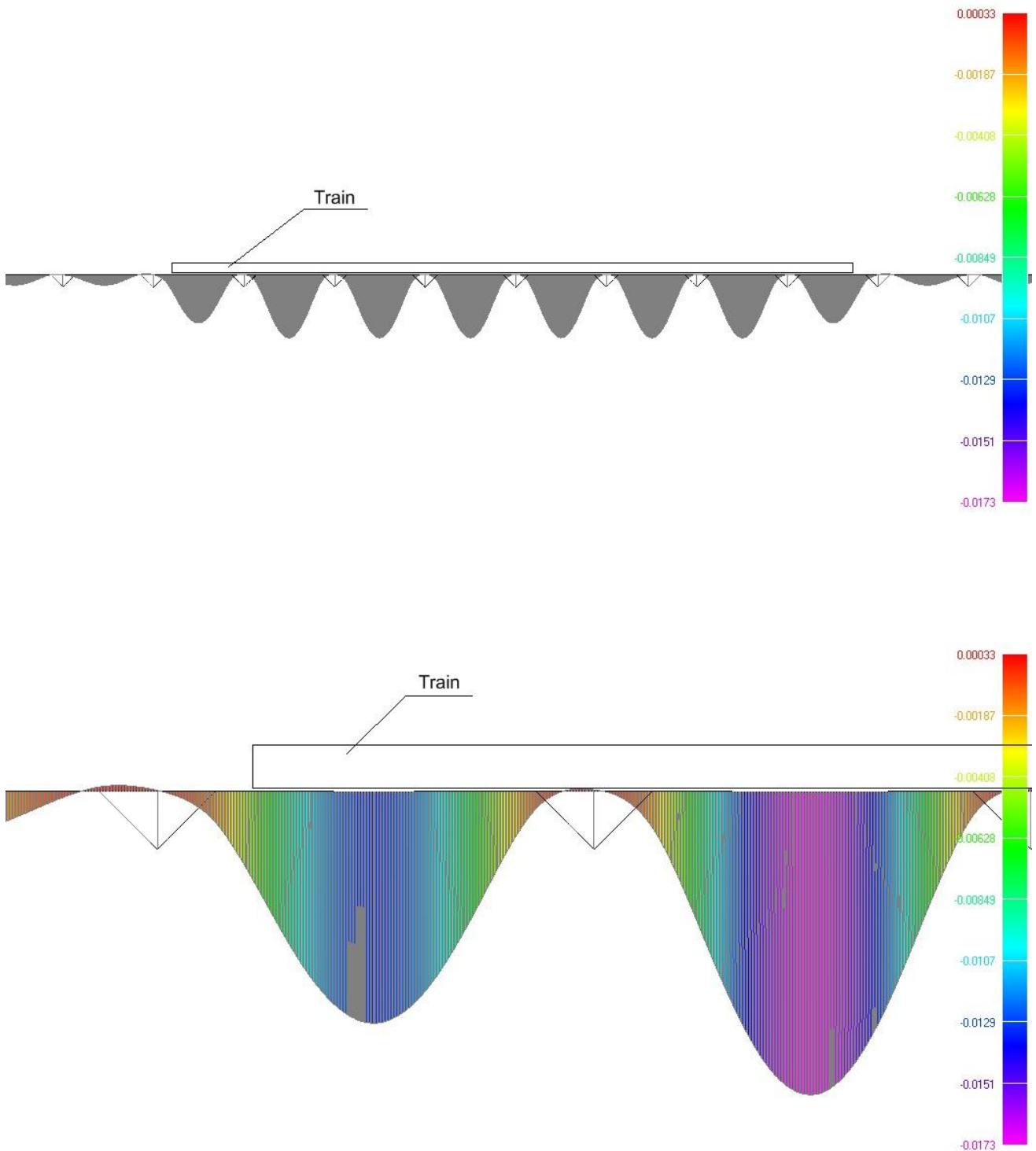


Fig. 2.56. The diagram of track bending (meters) along the whole length of a train: the upper diagram represents track bending above the whole train body, the lower diagram represents track bending above the forebody of a train. Maximum deflection is 17.3 mm.

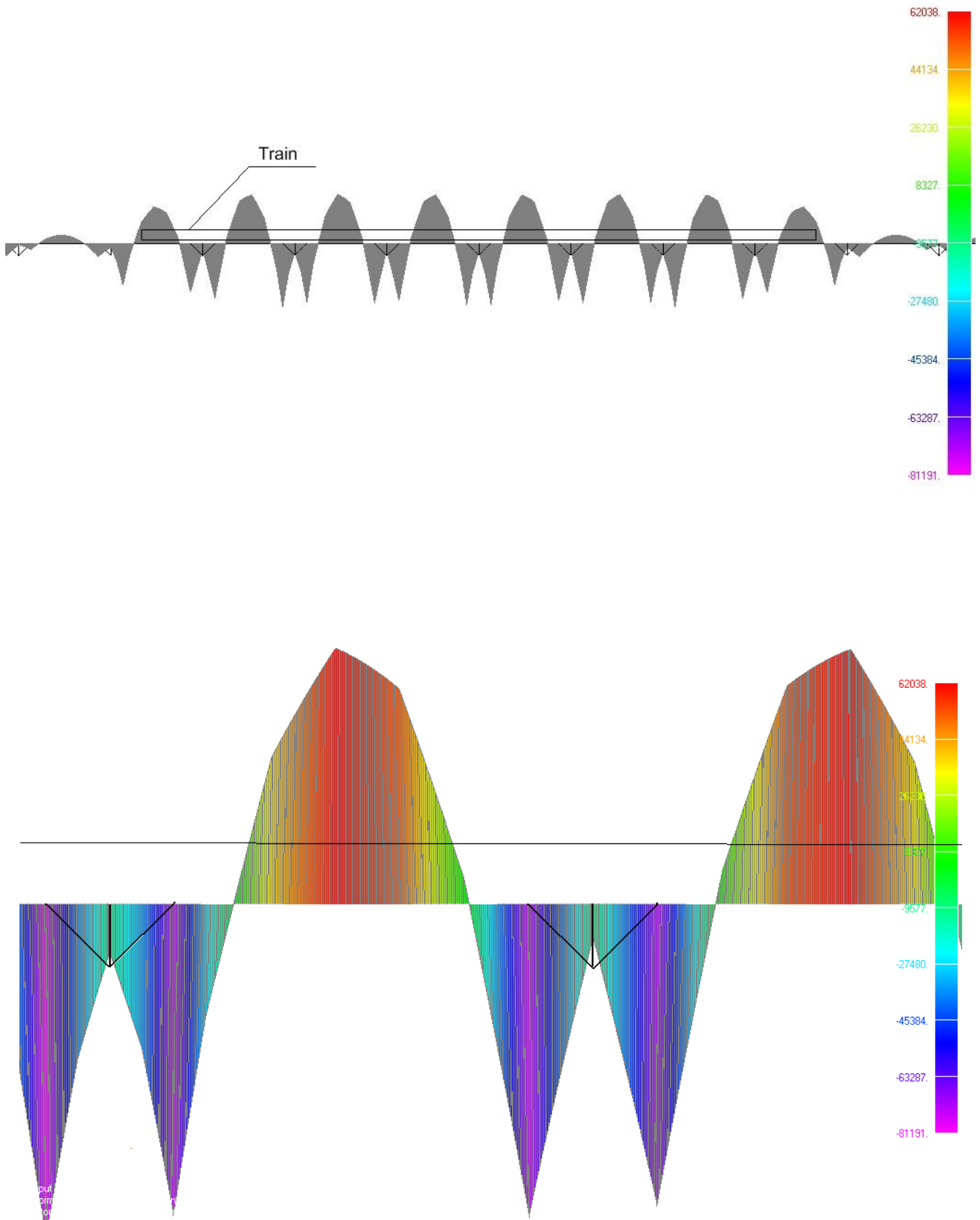


Fig. 2.57. The diagram of bending moments in a track structure along the whole length of a train.
Maximum moment is +62 038 N·m, minimum moment is -81 191 N·m

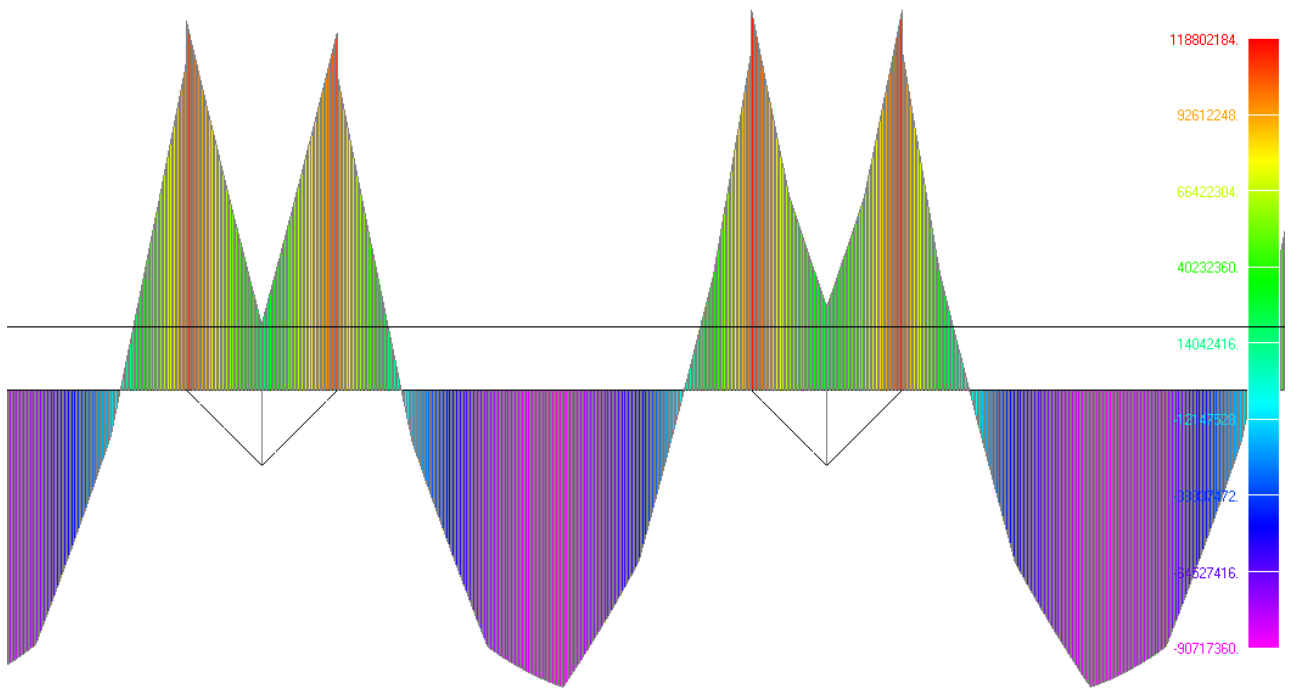


Fig. 2.58. The diagram of stress caused by bending (Pa) of a rail top

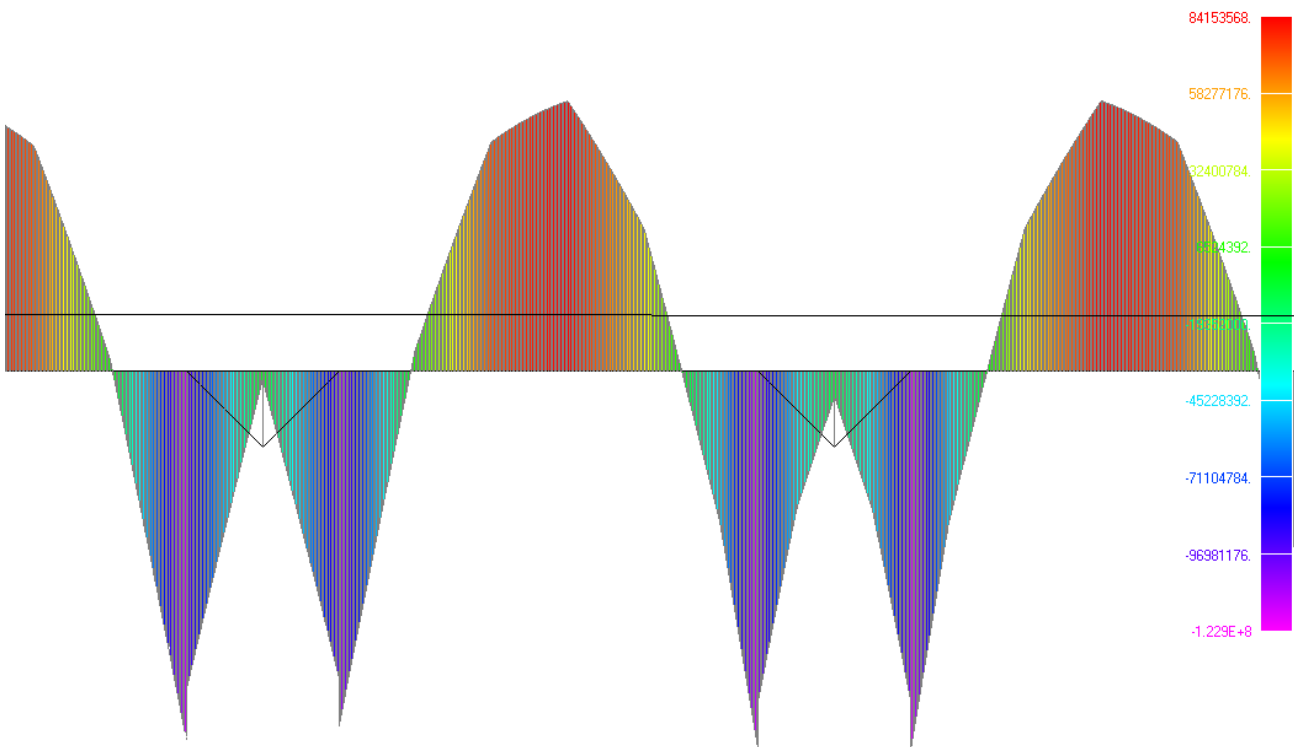


Fig. 2.59. The diagram of stress caused by bending (Pa) of a rail bottom



2.11.3.1. Strength Analysis

Strength analysis is carried out towards the most weakened cross section of a string-rail which is crosscut welds in a rail top and in a rail body. The analysis is carried out taking into account temperature differential with respect to temperature circuit: $\Delta t = 40 \text{ }^\circ\text{C}$.

$$\sigma_t = \alpha \cdot E \cdot \Delta t = 1.2 \cdot 10^{-5} \cdot 2 \cdot 10^{11} \cdot 40 = 96 \cdot 10^6 \text{ Pa} = 96 \text{ MPa}$$

Endurance analysis of steel structure elements and their compounds should be carried out by the following formulas:

$$\sigma_{\max} \leq R_y \cdot m$$

$\sigma_{\max} = \sigma_t + \sigma = 96 + 123 = 219 \text{ MPa}$ is maximum in absolute value stress. The stress is calculated from the effect of permanent and temporary loads.

$m = 0.9$ is the coefficient of working conditions.

$R_y = 315 \text{ MPa}$ is the rated yield resistance for steels with additions of manganese. The rail is produced of structural alloy steel 09Г2С after quenching and tempering at a rolled thickness of 15—20 mm of C345 class according to GOST 27772-88.

$$\sigma_{\max} = 211 \text{ MPa} \leq R_y \cdot m = 315 \cdot 0.9 = 283.5 \text{ MPa}.$$

Rail strength is provided.

2.11.3.2. Endurance Analysis

Strength analysis is carried out towards the most weakened cross section of a string-rail which is crosscut welds in a rail top and in a rail body. The analysis is carried out taking into account temperature differential with respect to temperature circuit: $\Delta t = 40 \text{ }^\circ\text{C}$.

$$\sigma_t = \alpha \cdot E \cdot \Delta t = 1.2 \cdot 10^{-5} \cdot 2 \cdot 10^{11} \cdot 40 = 96 \cdot 10^6 \text{ Pa} = 96 \text{ MPa}.$$

Endurance Analysis According to Russian Standard SNiP 2.05.03-84* (Bridges and Pipes)

At a maximum temperature there is neither axial compression nor axial extension in a rail (caused by temperature influence):

$$\text{Rail: } \sigma_{\max} = 119 \text{ MPa}, \sigma_{\min} = 0 \text{ MPa (midspan)}, \rho = 0$$

$$\gamma_w = \frac{1}{\zeta \cdot \vartheta \cdot [(\alpha\beta \pm \delta) - (\alpha\beta \mp \delta)\rho]} = \frac{1}{1 \cdot [(0.72 \cdot 1.8 + 0.24)]} = 0.651$$

$$119 \text{ MPa} \leq 0.651 \cdot 315 \cdot 0.9 = 184 \text{ MPa}.$$

At a minimum temperature there will be maximum extension in a rail (caused by temperature influence):

$$\text{Rail: } \sigma_{\max} = 96 + 119 = 215 \text{ MPa}, \sigma_{\min} = 96 \text{ MPa (midspan)}, \rho = 96/215 = 0.447,$$



$$\gamma_w = \frac{1}{\zeta \cdot \varrho \cdot [(\alpha\beta \pm \delta) - (\alpha\beta \mp \delta)\rho]} = \frac{1}{1 \cdot [(0.72 \cdot 1.8 + 0.24) - (0.72 \cdot 1.8 - 0.24) \cdot 0.447]} = 0.94,$$

$$215 \text{ MPa} \leq 0.94 \cdot 315 \cdot 0.9 = 266 \text{ MPa}.$$

Rail endurance is provided.

Endurance Analysis According to Russian Standard SNiP II-23-81* (Steelwork)

At a maximum temperature there is neither axial compression nor axial extension in a rail (caused by temperature influence):

Rail: $\sigma_{max} = 119 \text{ MPa}$, $\sigma_{min} = 0 \text{ MPa}$ (midspan), $\rho = 0$

$$\gamma_v = \frac{2.5}{1.5 - \rho} = 1.67.$$

When $n > 3.9 \cdot 10^6$ take $\alpha = 0.77$;

$$\alpha \times R_v \times \gamma_v = 0.77 \times 75 \times 1.67 = 96 \text{ MPa} < \sigma_{max} = 119 \text{ MPa}.$$

When $n = 2.0 \cdot 10^6$ take $\alpha = 1.2$;

$$\alpha \times R_v \times \gamma_v = 1.2 \times 75 \times 1.67 = 150 \text{ MPa} > \sigma_{max} = 119 \text{ MPa}.$$

When $n = 5.0 \cdot 10^5$ take $\alpha = 1.9$.

$$\alpha \times R_v \times \gamma_v = 1.9 \times 75 \times 1.67 = 238 \text{ MPa} > \sigma_{max} = 119 \text{ MPa}.$$

At a minimum temperature there will be maximum extension in a rail:

Rail: $\sigma_{max} = 96 + 119 = 215 \text{ MPa}$, $\sigma_{min} = 96 \text{ MPa}$ (midspan), $\rho = 96/215 = 0.447$

$$\gamma_v = \frac{2.0}{1.2 - \rho} = 2.656$$

When $n > 3.9 \cdot 10^6$ take $\alpha = 0.77$;

$$\alpha \times R_v \times \gamma_v = 0.77 \times 75 \times 2.656 = 153 \text{ MPa} < \sigma_{max} = 202 \text{ MPa}.$$

When $n = 2.0 \cdot 10^6$ take $\alpha = 1.2$;

$$\alpha \times R_v \times \gamma_v = 1.2 \times 75 \times 2.656 = 239 \text{ MPa} > \sigma_{max} = 202 \text{ MPa}.$$

When $n = 5.0 \cdot 10^5$ take $\alpha = 1.9$.

$$\alpha \times R_v \times \gamma_v = 1.9 \times 75 \times 2.656 = 378 \text{ MPa} > \sigma_{max} = 202 \text{ MPa}.$$

Endurance of a rail weld is provided up to 2 000 000 cycles.

Endurance Analysis According to ENV

We accept $\Delta\sigma_c = 90 \text{ MPa}$ (detail category 90, transverse butt welds). Thermal stresses are not taken into account, because this method of calculation does not account for the asymmetry of the cycle. The range is specified only by rail bending.

$$\Delta\sigma = \sigma_{max} - \sigma_{min} = 119 \text{ MPa}$$

when $N = 5\,000\,000$ cycles:

$$\Delta\sigma_R = \frac{\Delta\sigma_c}{\sqrt[3]{\frac{N}{2000000}}} = \frac{90}{\sqrt[3]{\frac{5000000}{2000000}}} = \frac{90}{1.357} = 66.3 \text{ MPa},$$



$$\Delta\sigma = 119MPa > \frac{\Delta\sigma_R}{\gamma_f} = \frac{66.3}{1.15} = 57.7MPa,$$

when $N = 2\,000\,000$ cycles:

$$\Delta\sigma_R = 90MPa, \quad \Delta\sigma = 119MPa > \frac{\Delta\sigma_R}{\gamma_f} = \frac{90}{1.15} = 78.3MPa,$$

when $N = 700\,000$ cycles:

$$\Delta\sigma_R = \frac{\Delta\sigma_C}{\sqrt[3]{\frac{N}{2000000}}} = \frac{90}{\sqrt[3]{\frac{700000}{2000000}}} = \frac{90}{0.7} = 128MPa,$$

$$\Delta\sigma = 119MPa \approx \frac{\Delta\sigma_R}{\gamma_f} = \frac{128}{1.15} = 111MPa,$$

when $N = 500\,000$ cycles:

$$\Delta\sigma_R = \frac{\Delta\sigma_C}{\sqrt[3]{\frac{N}{2000000}}} = \frac{90}{\sqrt[3]{\frac{500000}{2000000}}} = \frac{90}{0.63} = 142.8MPa,$$

$$\Delta\sigma = 106MPa \leq \frac{\Delta\sigma_R}{\gamma_f} = \frac{142.8}{1.15} = 124.2MPa.$$

Endurance of a rail weld is provided up to 700 000 cycles. To provide larger number of loading cycles transverse welds should be strengthened (for example, with the help of overlays).

2.12. Analysis of Rail Motor-Vehicle Train Dynamic Interaction on an Elevated Section of STS Track Structure

Basic data on a string-rail and its design for dynamic analysis was presented in the Article 2.11 (cross section of a rail see in Fig. 2.45).

Schematic view of STS elevated track section with spans of 15m for dynamic analysis was represented in the Article 2.11.3 (see Fig. 2.55).

2.12.1. Basic Data on Motor-Vehicle Train Loading

To reduce the time of engineering calculations and to simplify them, it is accepted that there are 8 wagons in the train and the train length is accepted as 50 m, i.e. exceeding the length of three spans. Accuracy of dynamic analysis of system vertical oscillations won't be affected (the length of the train affects the dynamics of train acceleration and deceleration, which are not analyzed in this Article). Loading diagram of a train is represented in Fig. 2.60.

Design speed of a train for steady motion is accepted as $V = 100 \text{ km/h} = 27.8 \text{ m/sec}$.

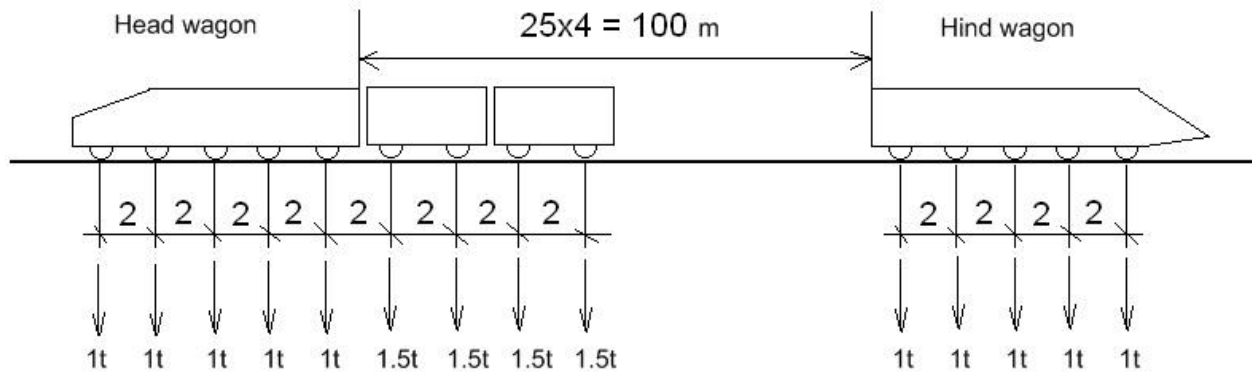


Fig. 2.60. Loading diagram of a train

The pressure resulted from one wheel of head and hind wagons is $P_1 = 10\,000 \text{ N}$.

The pressure resulted from one wheel of freight wagon is $P_2 = 15\,000 \text{ N}$.

Dynamic characteristics of a head wagon:

$M_L = 9800 \text{ kg}$ is the sprung mass;

$m_k = 20 \text{ kg}$ is the mass of one wheel;

$n_0 = 5$ is the number of axles;

$M_p = 9800 + 2 \cdot 20 \cdot 5 = 10000 \text{ kg}$ is gross weight;

$L_M = 8 \text{ m}$ is the distance between the first axle and the last axle;

$L_0 = 2 \text{ m}$ is the distance between the axles;

$Hod = 0.04 \text{ m}$ is static suspension movement;

$EJ = 5.92 \cdot 10^9 \text{ N} \cdot \text{m}^2$ is the bending stiffness of the wagon body.

Damping coefficient of shock absorbers on all wheels of a head wagon constitute 25% (see. [7], page 150) of critical coefficient (when non-periodic process with free vibrations of sprung mass takes place):

$$\beta = 0.25 \cdot \beta_{kp} = \frac{M}{2} \cdot \sqrt{\frac{g}{Hod}} = \frac{9800}{2} \cdot \sqrt{\frac{10}{0.04}} = 77476 \text{ N} \cdot \text{s/m},$$

where $\beta = 77476 \text{ N} \cdot \text{s/m}$ is the damping coefficient of shock absorbers on all wheels of a head wagon;
 $\beta_k = 77476/10 = 7747.6 \text{ N} \cdot \text{s/m}$ is the damping coefficient of shock absorbers per one wheel of a head wagon.

Dynamic characteristics of a freight wagon:

$M_V = 5920 \text{ kg}$ is the sprung mass;

$m_k = 20 \text{ kg}$ is the mass of one wheel;



$n_0 = 2$ is the number of axles;
 $M_p = 5920 + 2 \cdot 20 \cdot 2 = 6000$ kg is gross weight;
 $L_0 = 2$ m is the distance between the axles;
 $Hod = 0.04$ m is suspension movement;
 $EJ = 5.92 \cdot 10^9$ N·m² is the bending stiffness of a body.

Damping coefficient of shock absorbers on all wheels of a freight wagon:

$$\beta = 0.25 \cdot \beta_{kp} = \frac{M}{2} \cdot \sqrt{\frac{g}{Hod}} = \frac{5920}{2} \cdot \sqrt{\frac{10}{0.04}} = 46802 \text{ N·s/m.}$$

$\beta = 46802$ N·s/m is the damping coefficient of shock absorbers on all wheels of a freight wagon;
 $\beta = 46802/4 = 11700$ N·s/m is the damping coefficient of shock absorbers per one wheel of a freight wagon.

A string-rail consists of tensed strings which ensure its transverse and longitudinal stability (which maybe influenced by temperature drops or dynamics of motorail movement). In the dynamic analysis, due to the low transverse stiffness of tensed strings in comparison with bending stiffness of a rail, their tension is neglected. This tension is in the margin of rail's safety and stability.

2.12.2. Analysis of Wagon Bodies Resonant Speed when Driving on an Elevated Track Section

Frequency analysis of wagon body bouncing is carried out in a simplified analytical method.

Analytical analysis of the first frequency (see [6], page 236):

$Hod = 0.04$ m is suspension movement,

$$f_1 \approx f_2 = \frac{1}{2 \cdot \pi} \cdot \sqrt{\frac{g}{Hod}} = \frac{1}{2 \cdot \pi} \cdot \sqrt{\frac{10}{0.04}} = 2.516 \text{ Hz.}$$

The third mode of vibrations corresponds to the bending forms of a wagon body beam. Solving the problem of free frequency beam in zero gravity (see [6], pages 294 — 300). Wagon bodies are accepted in the analysis to be rather rigid; it results in large frequencies which correspond to their bending forms. Later, in the process of motorail designing, this bending stiffness should be clarified.

$$f_3 = \frac{1}{2 \cdot \pi} \cdot \sqrt{\frac{EJ}{m_L}} \cdot \left(\frac{k_1}{L_M}\right)^2 = \frac{1}{2 \cdot \pi} \cdot \sqrt{\frac{5.92 \cdot 10^9}{980}} \cdot \left(\frac{4.73}{10}\right)^2 = 87.5 \text{ Hz for the head wagon,}$$

where:

$EJ = 5.92 \cdot 10^9$ N·m² is bending stiffness of a head wagon body;
 $L_M = 10$ m is the length of a wagon body;
 $M = 9800$ kg is the sprung mass;
 $m_L = M/L_M = 9800/10 = 980$ kg/m is wagon body mass per unit;
 $k_1 = 4.73$ is the coefficient for calculation of the first bending frequency of beam free vibrations in zero gravity.

$$f_3 = \frac{1}{2 \cdot \pi} \cdot \sqrt{\frac{EJ}{m_L}} \cdot \left(\frac{k_1}{L_M}\right)^2 = \frac{1}{2 \cdot \pi} \cdot \sqrt{\frac{5.92 \cdot 10^9}{1480}} \cdot \left(\frac{4.73}{4}\right)^2 = 445 \text{ Hz for the freight wagon,}$$

where:

$EJ = 5.92 \cdot 10^9$ N·m² is bending stiffness of a freight wagon body;
 $L_M = 4$ m is the length of a wagon body;
 $M = 5920$ kg is the sprung mass of a wagon;
 $m_L = M/L_M = 5920/4 = 1480$ kg/m is wagon body mass per unit.

On the basis of numerical calculations of frequencies we find resonant speed of a motorail moving on an elevated track structure with span length of $L = 15$ m (see Tab. 2.21).

Table 2.21

Resonant speed of a motorail moving on an elevated track structure with span length of 15 m

Forms	Frequency, Hz	Resonant speed of a motorail, m/s $V_i = L \cdot f_i$
1 	$f_1 = f_2 = 2.516$ Hz	$V_1 = V_2 = 15 \cdot 2.516 = 37.7$ m/s (136 km/h)
2 	$f_3 = 87.5$ Hz for the head wagon $f_3 = 445$ Hz for the freight wagon	$V_3 = 15 \cdot 87.5 = 1312.5$ m/s $V_3 = 15 \cdot 445 = 6675$ m/s

The Table 2.21 shows that at a steady flow speed of $V = 100$ km/h = 27.8 m/s there won't be vertical resonances in wagon bodies (the first form of resonant oscillations occur at a higher speed of 136 km/h).

2.12.3. Finite Element Scheme of STS for the Analysis of Dynamic Processes

Patran 2007 r1b 19-May-10 10:25:48

Deform: Dinamika, A2: Dyn, Incr=57500, Time=5.75000, Displacement, Translation,

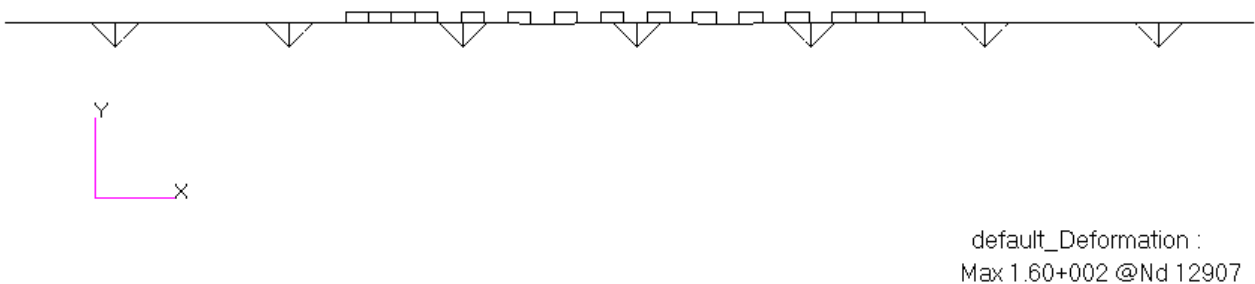


Fig. 2.61. Finite element scheme of a track structure for the analysis of dynamic processes (head wagon, freight wagons and hind wagon)

Modeling of the dynamic contact interaction of a motorail with STS track structure was carried out using program system MSC.Patran – MSC.Marc. This finite-element system is focused on efficient analysis of complex contact interaction. Constantly developing, it accumulates the best of new technologies, techniques and methods, and therefore remains the leading system of finite-element analysis in the world. The calculations were performed for the vertical transient dynamics. This was achieved by motorail prototype movement over the prototype of string-rail track structure consisting of 17 spans of 15 meters each at a constant speed of 100 km/h.



When driving on a track structure of a multiwheel motorail, vertical oscillations of motorail body and string-rail occur. They are the sum of free and forced oscillations. Free oscillations are determined by initial conditions of motion and appear due to a sudden entry of a train from the initial hard section to a deformable first flight. Dissipation of vertical oscillations energy by damping forces leads to decrease in the influence of free oscillations in a dynamic process. With further motorail movement there is increase in influence of forced oscillations, which are crucial for steady dynamic process.

2.12.4. The Results of Dynamic Analysis

2.12.4.1. The results of dynamic analysis in the absence of string-rail outward bend on the spans at a motorail speed of 100 km/h

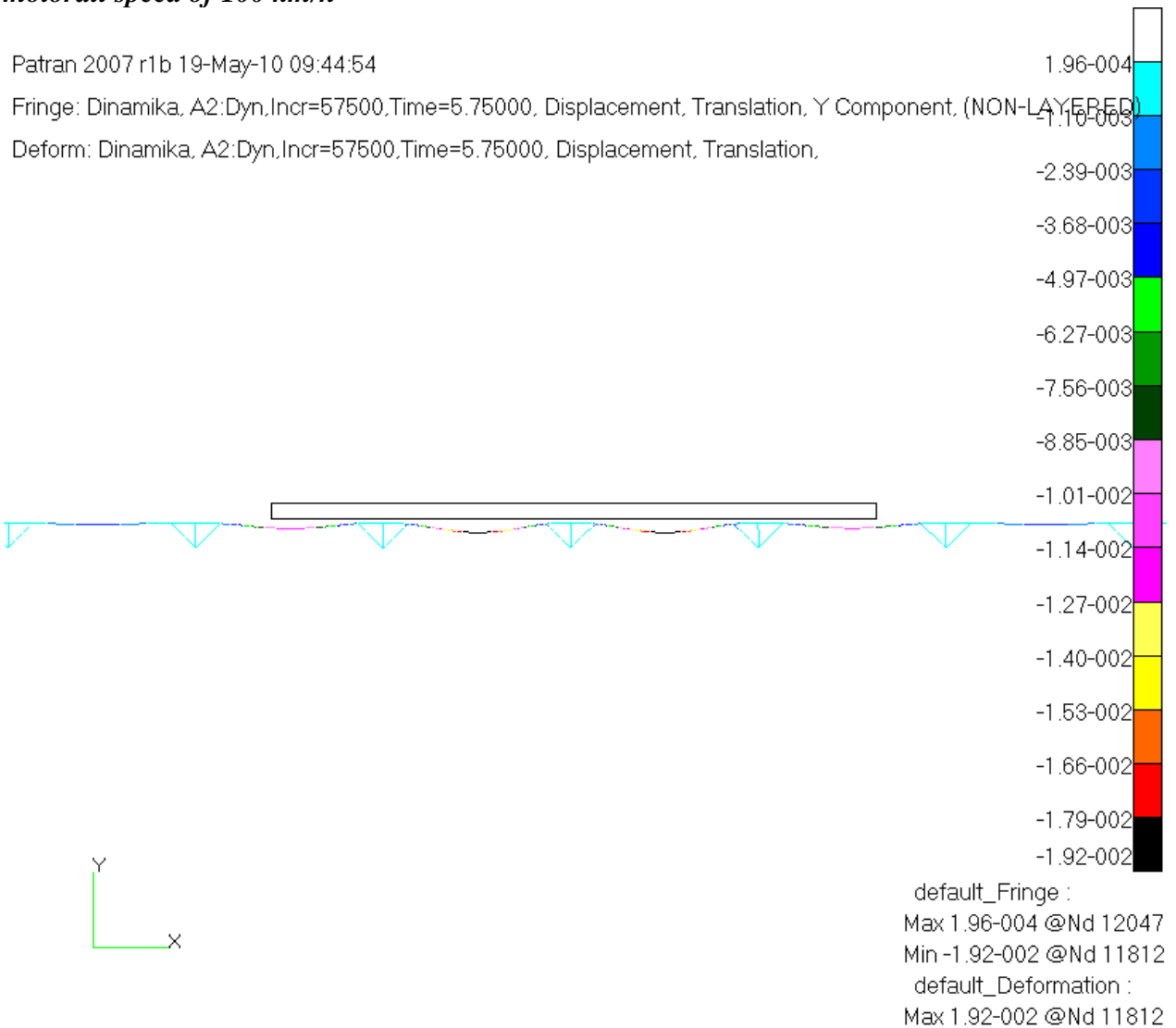


Fig. 2.62. Vertical deformations (meters) of an elevated track section. Maximum deflection is 19.2 mm.



Head wagon leading wheel
Central wagon wheel
Hing wagon rear wheel

LEGEND	
—	Node 12925: Displacement, Translation, YY
—	Node 12949: Displacement, Translation, YY
—	Node 12971: Displacement, Translation, YY

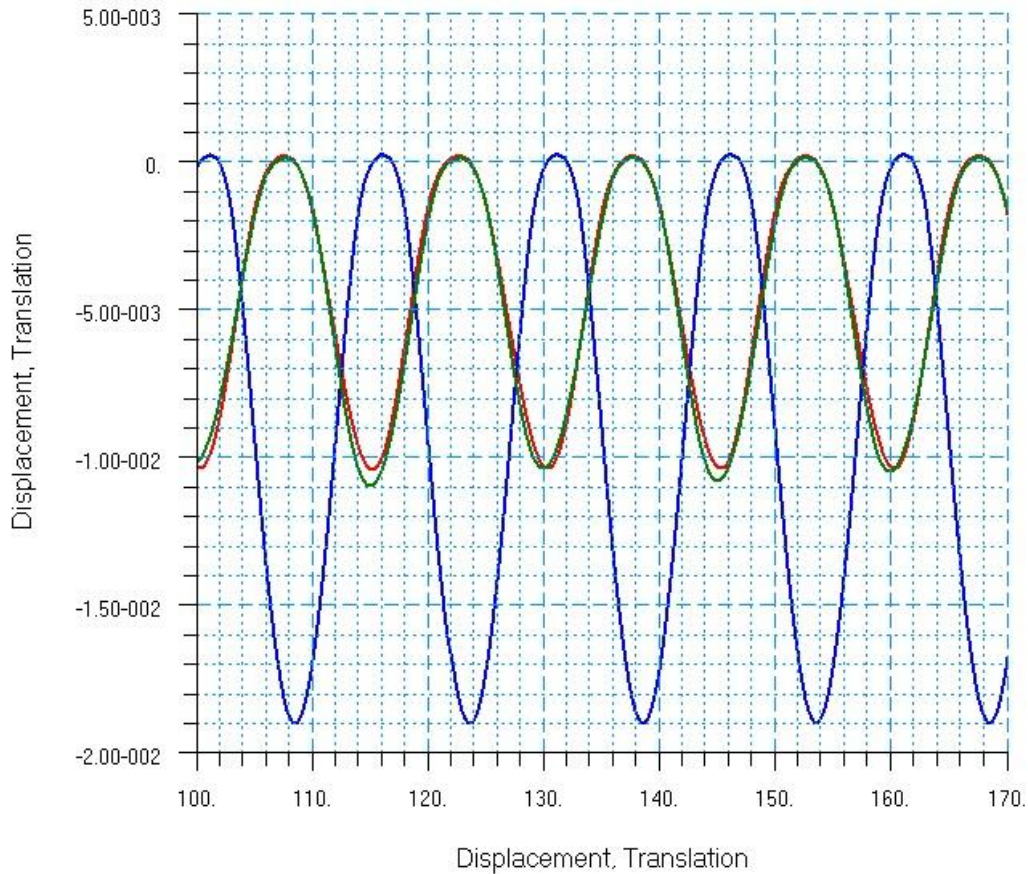


Fig. 2.63. The graph of vertical displacements (in meters) of motorail wheels.

Maximum deflection of the track under the wheel of the central wagon is 19.2 mm (1/781 of span length),
Maximum deflection of the track under the wheels of the head and the hind wagons is 12 mm (1/1250 of span length).

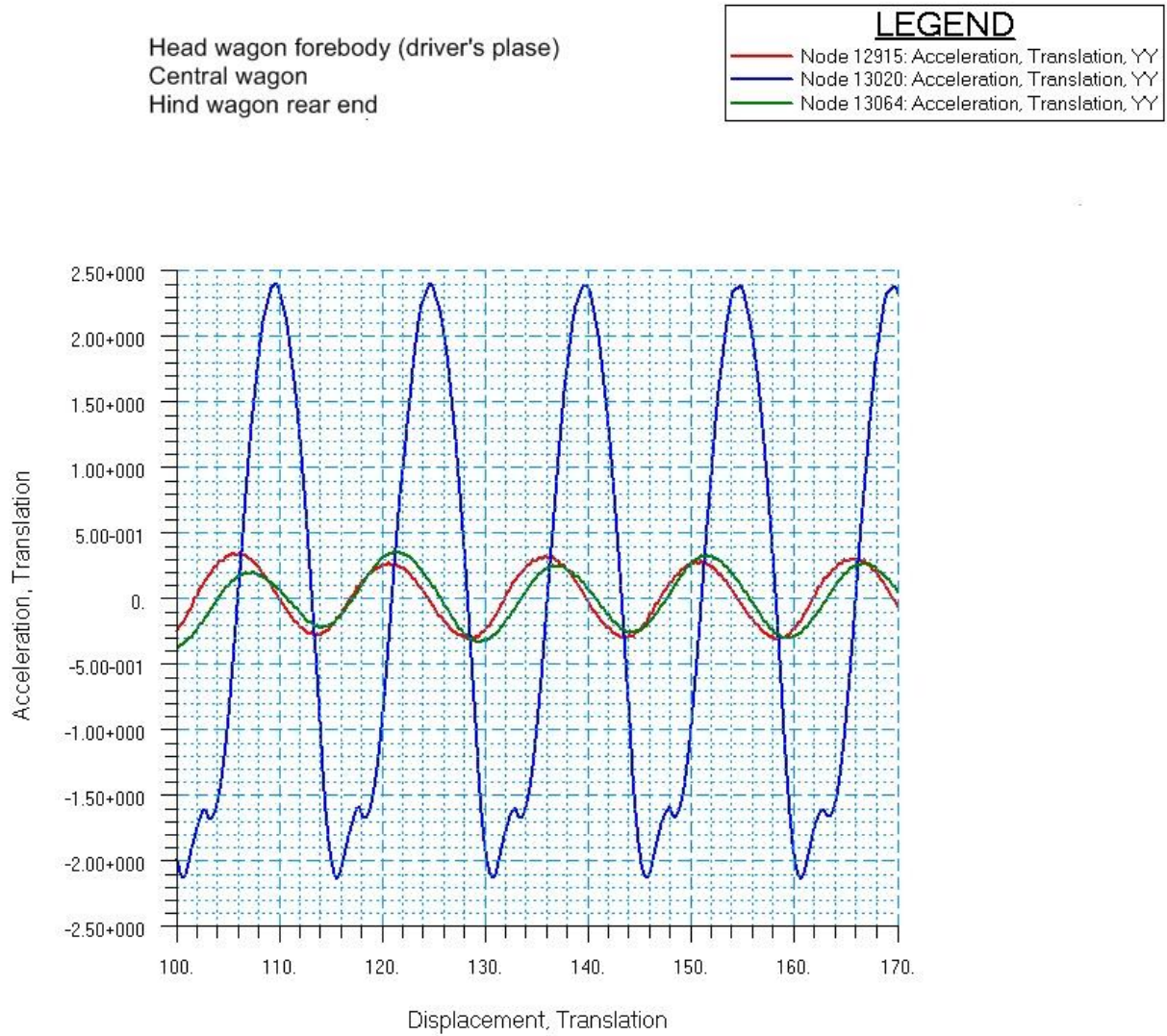


Fig. 2.64. The graphs of vertical accelerations (m/s^2) of motorail wagons. Maximum vertical acceleration of the driver's place (head wagon) is 0.3 m/s^2 , maximum vertical acceleration of a freight wagon is 2.4 m/s^2

2.12.4.2. The results of dynamic analysis when a string-rail outward bend occurs on each span at a motorail speed of 100 km/h

As the Fig. 2.64 shows, maximum vertical accelerations of a freight wagon can reach 2.4 m/s^2 . To reduce dynamic loads on a motorail and a track structure, it is necessary to make mounting upward bend (15.5mm) on a rail top in the middle of each span (curve close to sinusoid see Fig. 2.65).

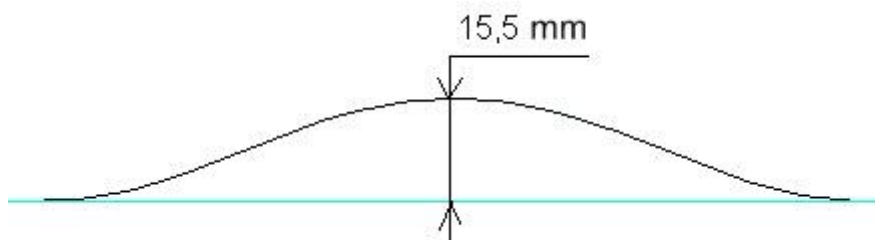


Fig. 2.65. The curve of a rail upward bend (100 times scaled up vertically)



Patran 2007 r1b 19-May-10 09:11:01

Fringe: Dinamika, A2:Dyn,Incr=57500,Time=5.75000, Displacement, Translation, Y Component, (NON-LAYERED)

Deform: Dinamika, A2:Dyn,Incr=57500,Time=5.75000, Displacement, Translation,

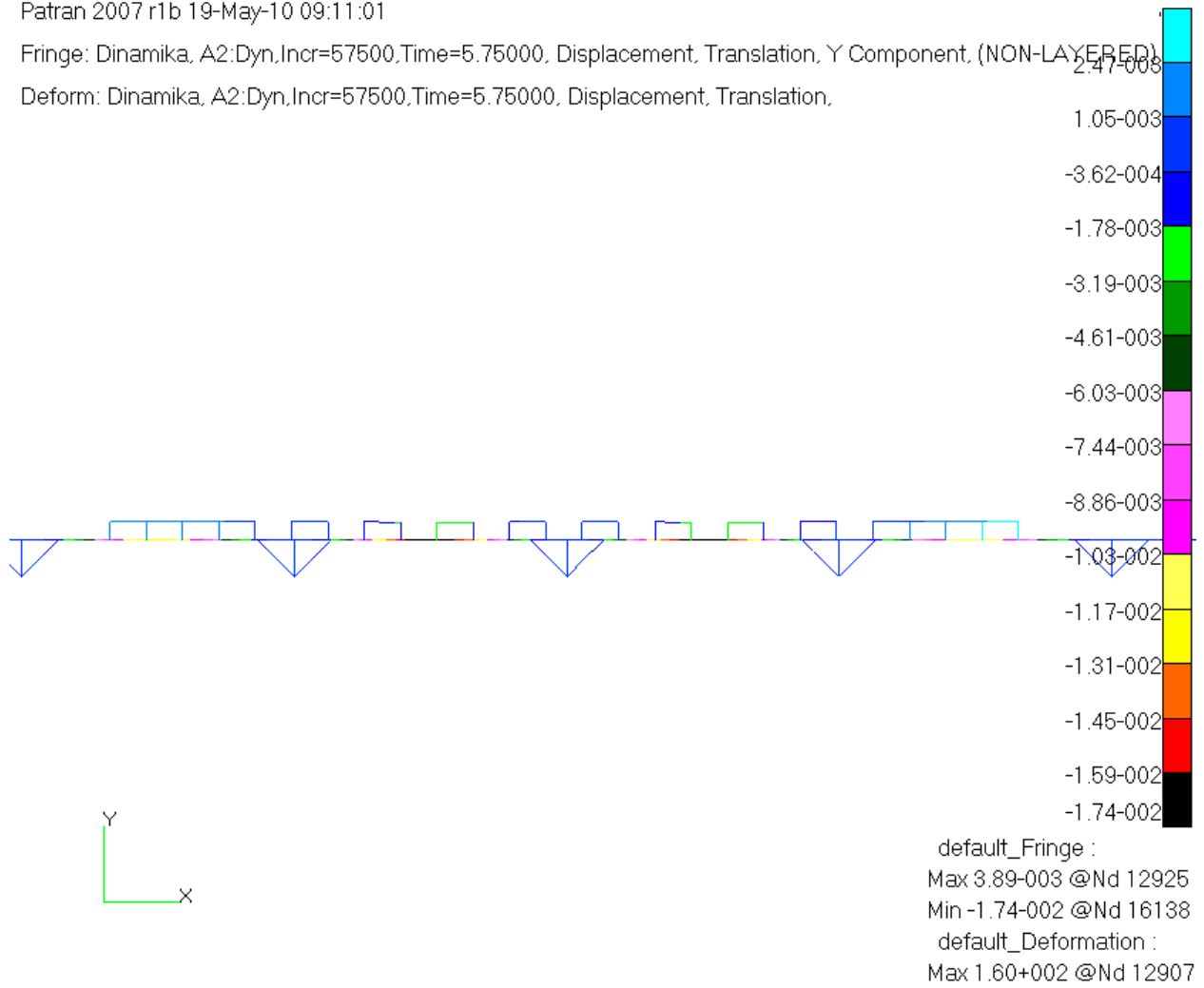


Fig. 2.66. Vertical deformations (meters) of an elevated track with a rail outward bend. Maximum deflection is 17.4 mm (in relation to the horizontal line maximum deflection will be:
 $15 - 17,4 = -2,4$ mm or $1/6250$ of the span length).



Head wagon leading wheel
Central wagon wheel
Hind wagon rear wheel

LEGEND	
—	Node 12925: Displacement, Translation, YY
—	Node 12949: Displacement, Translation, YY
—	Node 12971: Displacement, Translation, YY

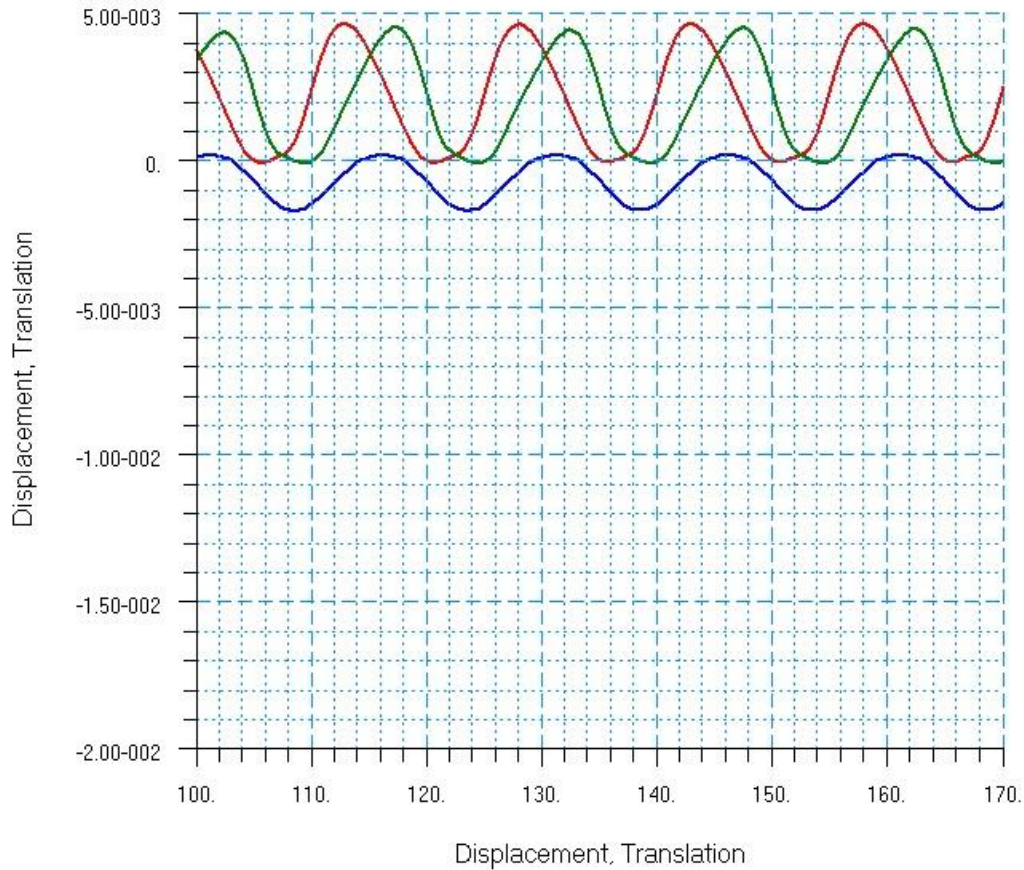


Fig. 2.67. The graph of vertical displacements (in meters) of motorail wheels.
Maximum deflection under the wheels of a central wagon is 1.9 mm (1/7890 of the span length);
Maximum rise under the wheels of a head wagon is 4.8 mm (1/3125 of the span length).



Head wagon forebody (driver's place)
 Central wagon
 Hind wagon rear end

LEGEND	
—	Node 12915: Acceleration, Translation, YY
—	Node 13020: Acceleration, Translation, YY
—	Node 13064: Acceleration, Translation, YY

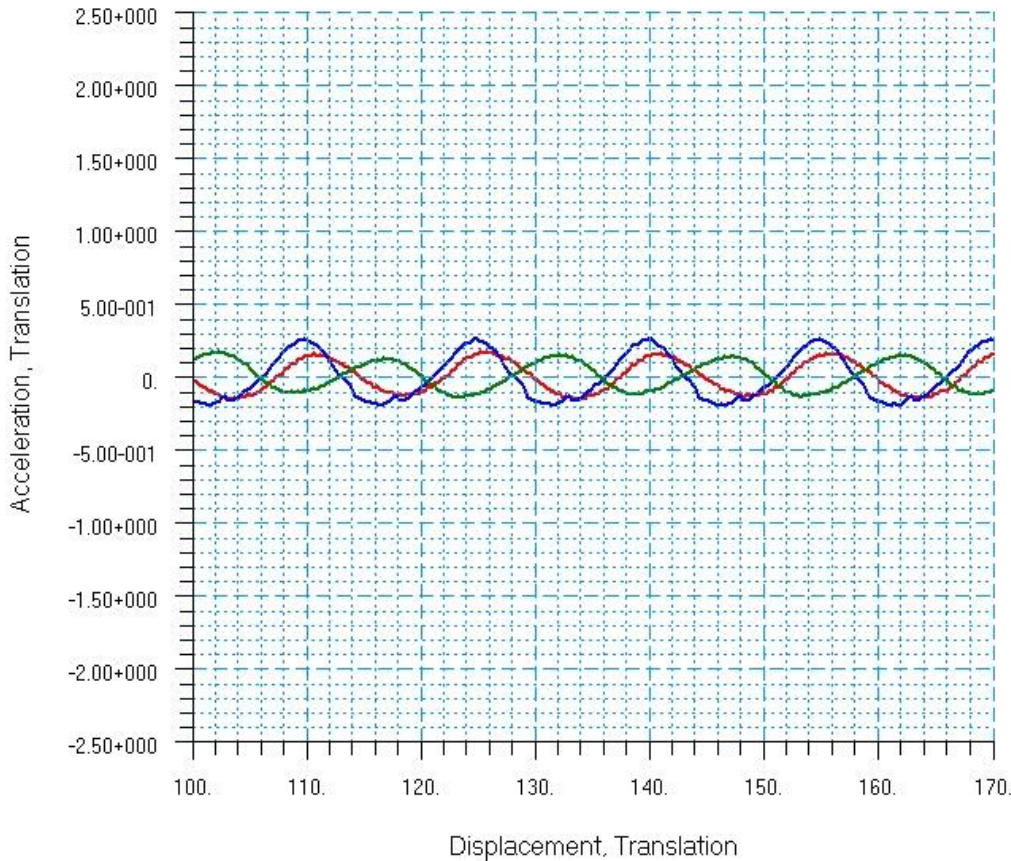


Fig. 2.68. The graphs of vertical accelerations (m/s²) of motorail wagons. Maximum vertical acceleration of the driver’s place (head wagon) is 0.2 m/s², maximum vertical acceleration of a freight wagon is 0.3 m/s²

2.12.4.3. Evaluation of Motorail’s Riding Comfort

Complex parameter W, which takes into account both speed fluctuations and their frequency (see [7], page 145) is accepted as the main parameter which estimates riding comfort of a motor-vehicle train. This parameter is widely used in rail transport today:

$$W = 0.9 \cdot k \cdot \sqrt[10]{\frac{z^3}{f}}$$

where:

- k is the proportionality coefficient, depending on the frequency of vertical oscillations (see Fig. 2.69);
- f is the frequency of the body vertical oscillations, Hz;
- Z is the amplitude of the body vertical acceleration (driver’s place), cm/s².



Fig. 2.69. Dependency of k coefficient on the frequency of vertical oscillations

The smaller is W parameter, the better is the vehicle riding comfort. Tab. 2.22 represents recommended and limit values of W parameter.

Riding Comfort Characteristics

Table 2.22

W parameter, used to evaluate riding comfort	
Very good	2
Good	2 – 2.5
Sufficient for passenger coaches	2.5 – 3
Maximum for passenger coaches	3 – 3.25
Maximum for a person from psychological point of view	4.5

With a steady motion (speed of 100 km/h) we find complex parameter W in a motor-vehicle train:

In a head wagon (driver’s place) the amplitude of the vertical acceleration is $Z = 20 \text{ cm/s}^2$ and global frequency is $f = 1.853 \text{ Hz}$:

$$W = 0.9 \cdot k \cdot 10 \sqrt{\frac{z^3}{f}} = 0.9 \cdot 0.98 \cdot 10 \sqrt{\frac{20^3}{1.853}} = 2.038.$$

Riding comfort in the driver’s place may be estimated as very good.

Besides, it should be taken into account that human fatigue depends not only on the mode of vehicle body vibrations (acceleration and frequency), but also on the duration of impact acceleration t_d (see Tab. 2.23, which represents the data for passengers; driver’s level of exposure to vibration may be considerably higher).



Table 2.23

Admissible Duration of Vibration Exposure on Man

Admissible Duration of Vibration Exposure on Human Body t_d			
a_G , m/s^2	t_d , min		Admission, %
	Standard ISO	Standard PN	
0.12	1 440	1 516	5.3
0.18	960	941	2
0.27	600	586	2.3
0.315	480	469	2.3
0.38	378	372	1.6
0.53	240	225	4.6
0.71	150	148	1.3
0.95	96	93.6	2.5
1.18	60	64.5	7
1.5	40	40	0
1.8	25	25.4	1.6
2.13	16	14.8	7.5
2.36	10	9.91	0.9
2.65	6.3	5.9	6.8

At the acceleration of $a_G = 0.2 \text{ m/s}^2$ permissible duration of a trip for a man is 900 minutes or 15 hours.

2.13. Analysis of Dynamic Interaction of a Rail Motor-Vehicle Train and Ground Sections of STS Track Structure

Basic data on a string-rail and its construction for dynamic analysis was presented in the Article 2.10.3 (string-rail cross section see in Fig. 2.31). The rail is viewed as a beam resting with its entire length on elastic foundation. The influence of elastic foundation on the rail is proportional to rail deflection. Proportionality (compliance) coefficient of the elastic foundation is numerically equal to the force, which should be attached to the foundation area unit of 1 cm^2 , to make its settling of 1cm.

The scheme of a ground section of a string-rail track structure consists of two sections. The first section is more rigid (for example, concrete foundation). Its length is 50 m and motorail movement starts from this section. And the second ground section has the length of 250 m. Analyses of motorail dynamic interaction were carried out taking into account three types of grounds with different proportionality (compliance) coefficient k of elastic foundation: firm ground 10 kgf/cm^3 , moderately firm ground 2.5 kgf/cm^3 and loose ground 0.5 kgf/cm^3 . Basic data on motorail loading was presented in the paragraph 2.12.1. Design speed for steady motion is accepted as $V = 100 \text{ km/h} = 27.8 \text{ m/sec}$.

2.13.1. Finite Element Scheme of STS for the Analysis of Dynamic Processes on Grounds

The ground is modeled by a set of springs of constant stiffness (see Fig. 2.70). It is an approximate assumption, but it is close to reality and it is widely used in railroads.

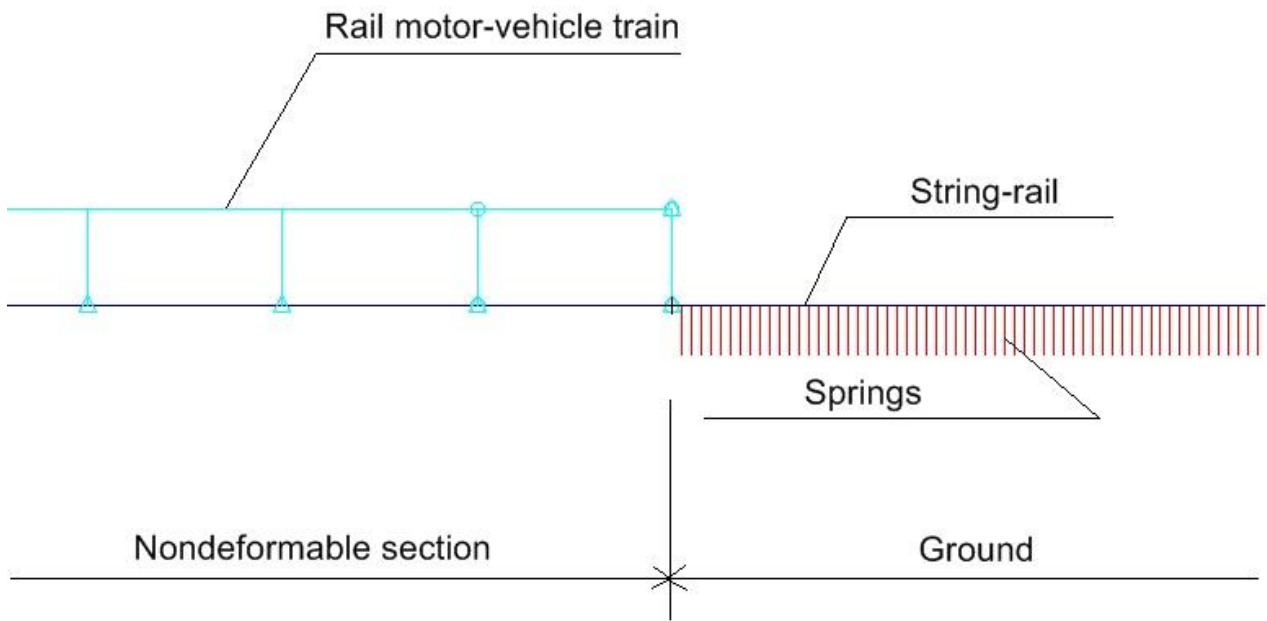


Fig. 2.70. The part of the finite element scheme of a track structure for dynamic analysis on grounds.

Modeling of dynamic contact interaction of a motorail with STS track structure was carried out similarly to what was mentioned in the paragraph 2.12.3 using the programming system MSC.Patran – MSC.Marc.



2.13.2. The Results of Dynamic Analysis

2.13.2.1. The results of dynamic analysis of the motion on a firm ground at a motorail speed of 100 km/h.

Patran 2007 r1b 26-May-10 09:26:08

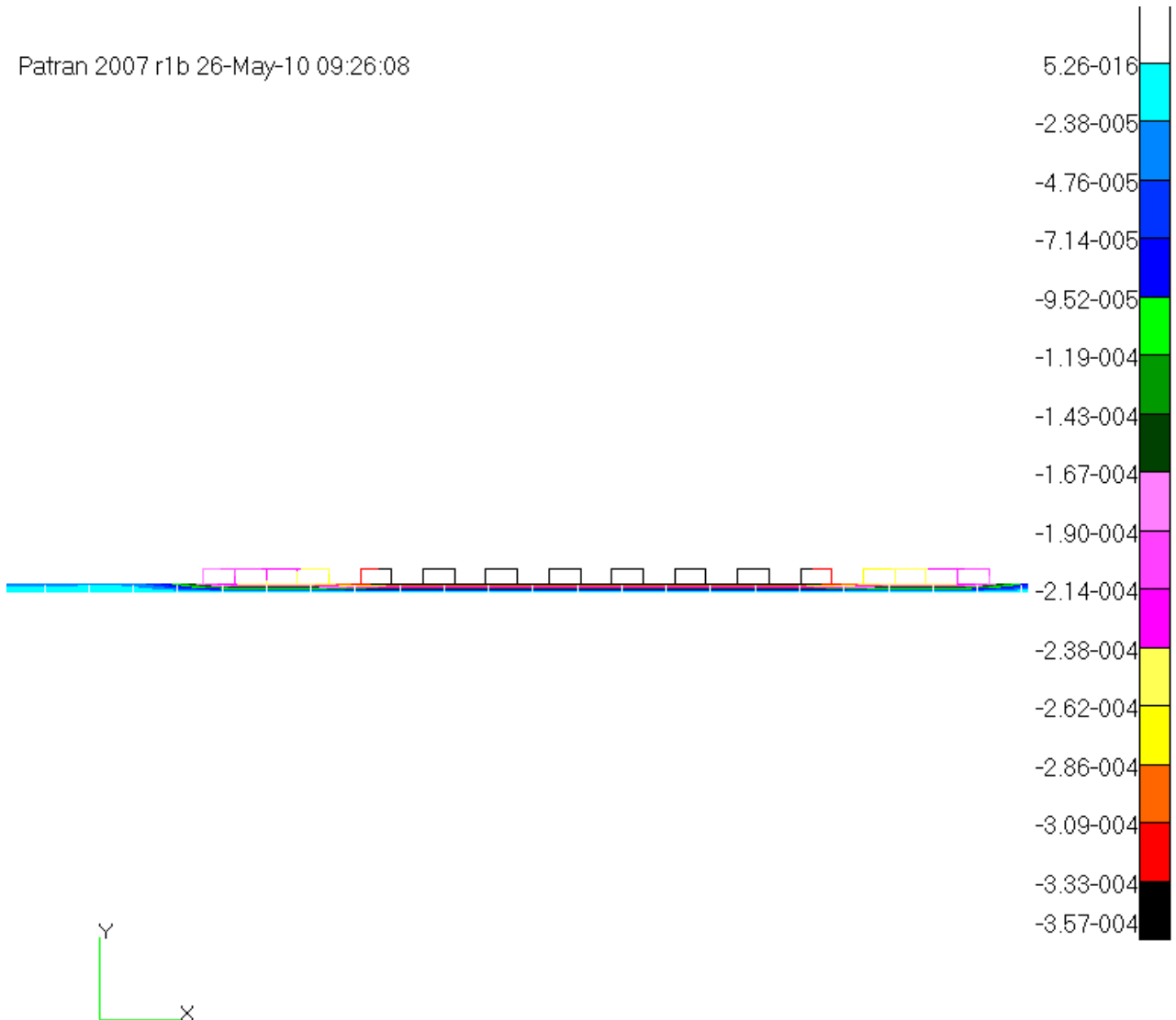


Fig. 2.71. Vertical deformations (meters) while moving on a firm ground.
Maximum rail deflection is 0.357mm.

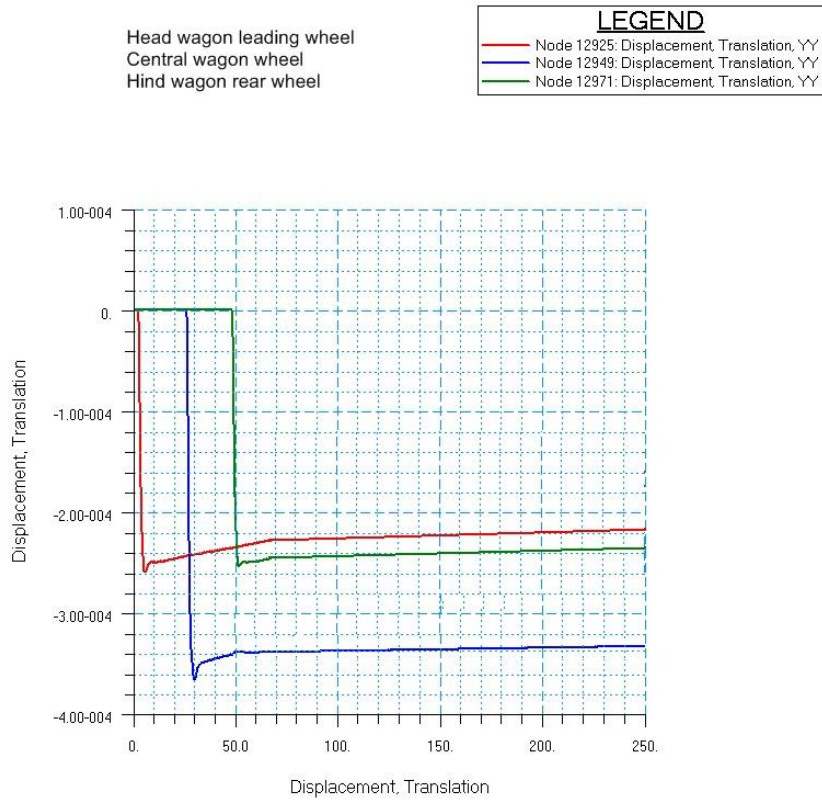


Fig.2.72. The graph of vertical displacements (in meters) of motorail wheels when riding from rigid section of a track to a firm ground and moving over it.

Maximum deflection of the track under the wheel of the central wagon is 0.362 mm,
Maximum deflection of the track under the wheels of the head wagon is 0.26 mm.

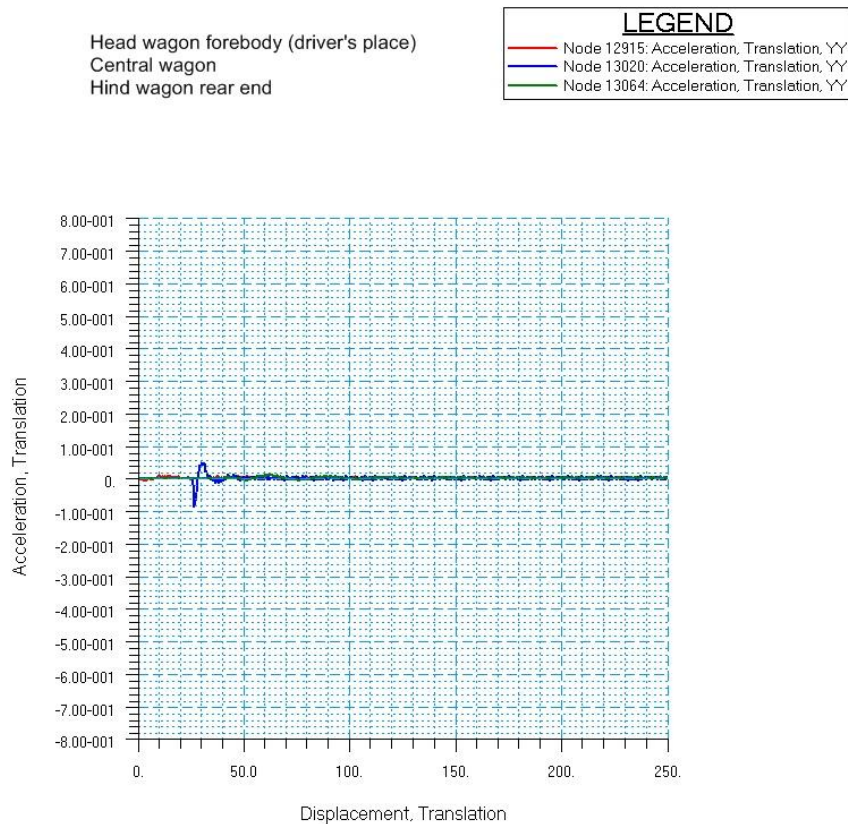


Fig. 2.73. The graph of vertical accelerations (m/s^2) of a motorail head wagon (driver's place) and of a central freight wagon when riding from rigid section of a track to a firm ground and moving over it.

Maximum vertical acceleration of driver's place is $0.01 m/s^2$,
Maximum vertical acceleration of a freight wagon is $0.08 m/s^2$



2.13.2.2. The results of dynamic analysis of the motion on a moderately firm ground at a motorail speed of 100 km/h.

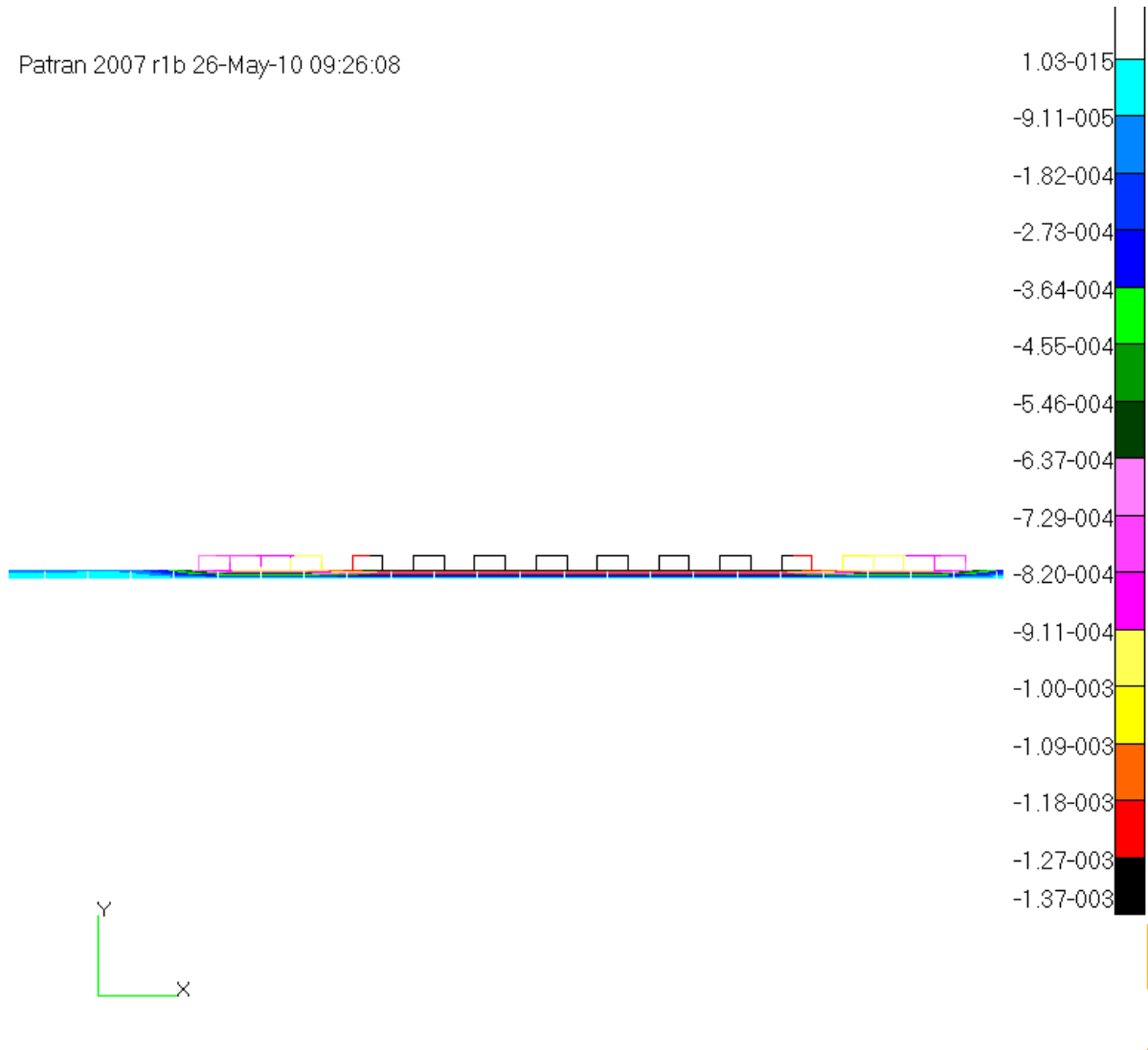


Fig. 2.74. Vertical deformations (meters) while moving on a moderately firm ground.
Maximum rail deflection is 1.37mm.

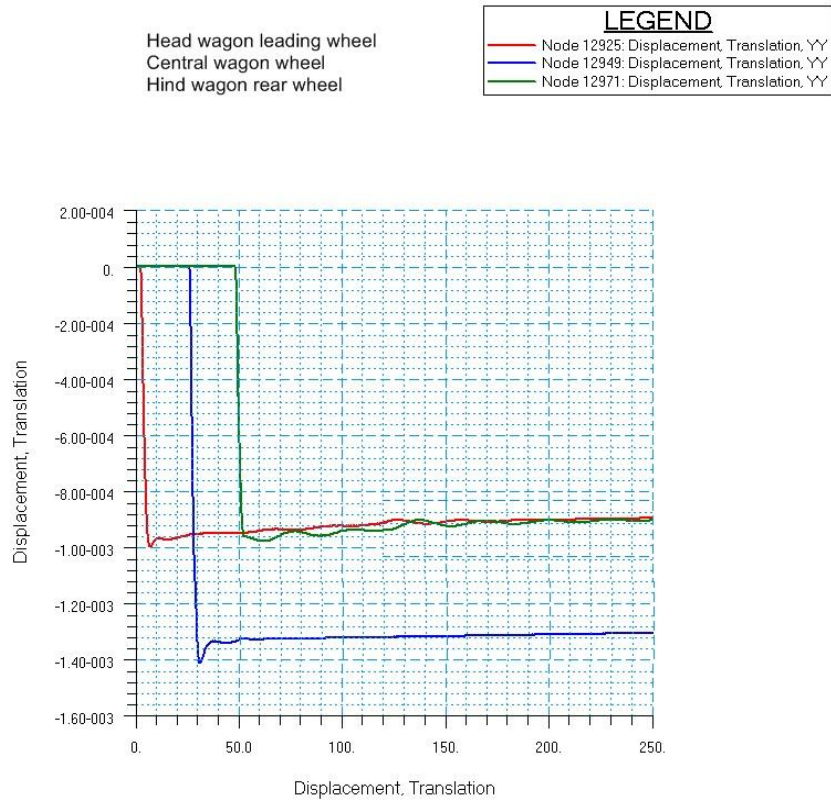


Fig. 2.75. The graph of vertical displacements (in meters) of motorail wheels when riding from rigid section of a track to a moderately firm ground and moving over it.

Maximum deflection of the track under the wheel of the central wagon is 1.4 mm,
Maximum deflection of the track under the wheels of the head wagon is 1.0mm.

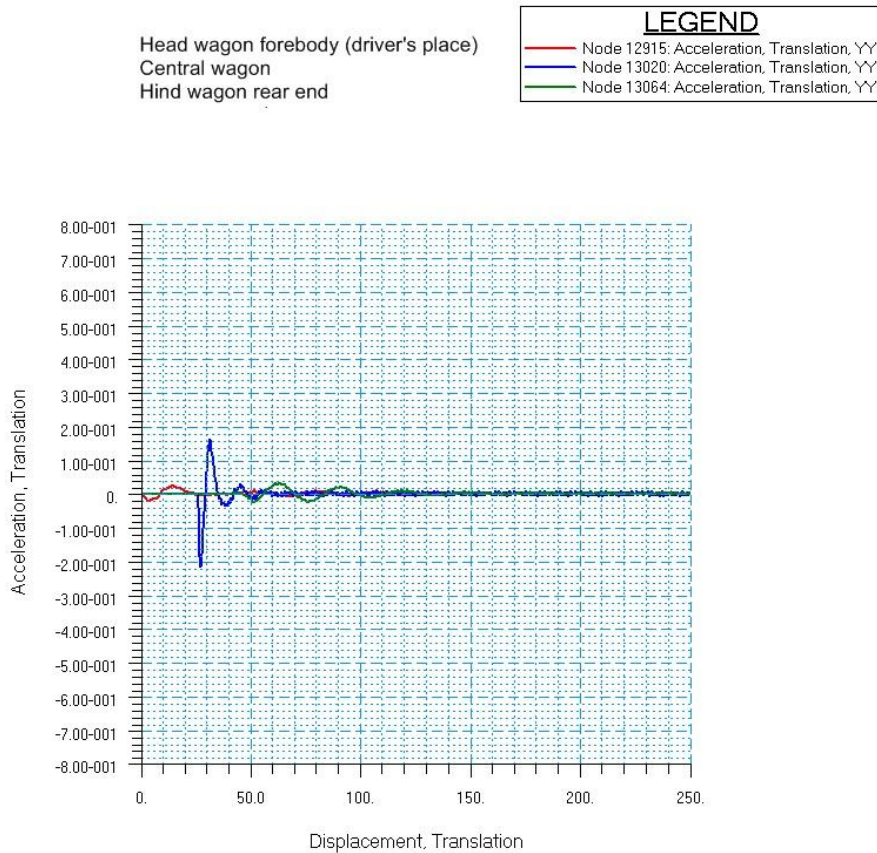


Fig.2.76. The graph of vertical accelerations (m/s^2) of a motorail head wagon (driver's place) and of a central freight wagon when riding from rigid section of a track to a moderately firm ground and moving over it. Maximum vertical acceleration of driver's place is $0.04 m/s^2$, Maximum vertical acceleration of a freight wagon is $0.22 m/s^2$



2.13.2.3. The Results of dynamic analysis of the motion on a loose ground at a motorail speed of 100 km/h

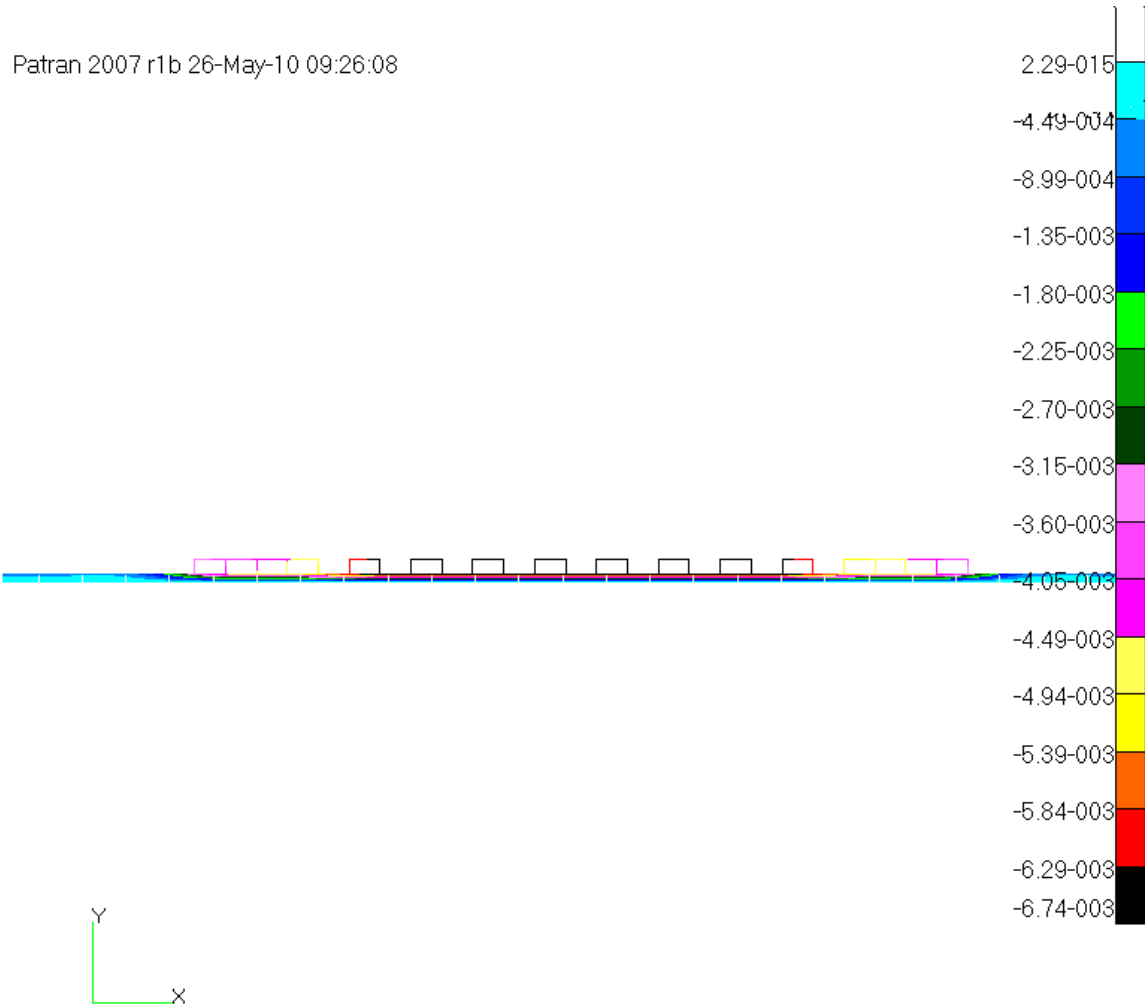


Fig. 2.77. Vertical deformations (meters) while moving on a loose ground.
Maximum rail deflection is 6.74mm.

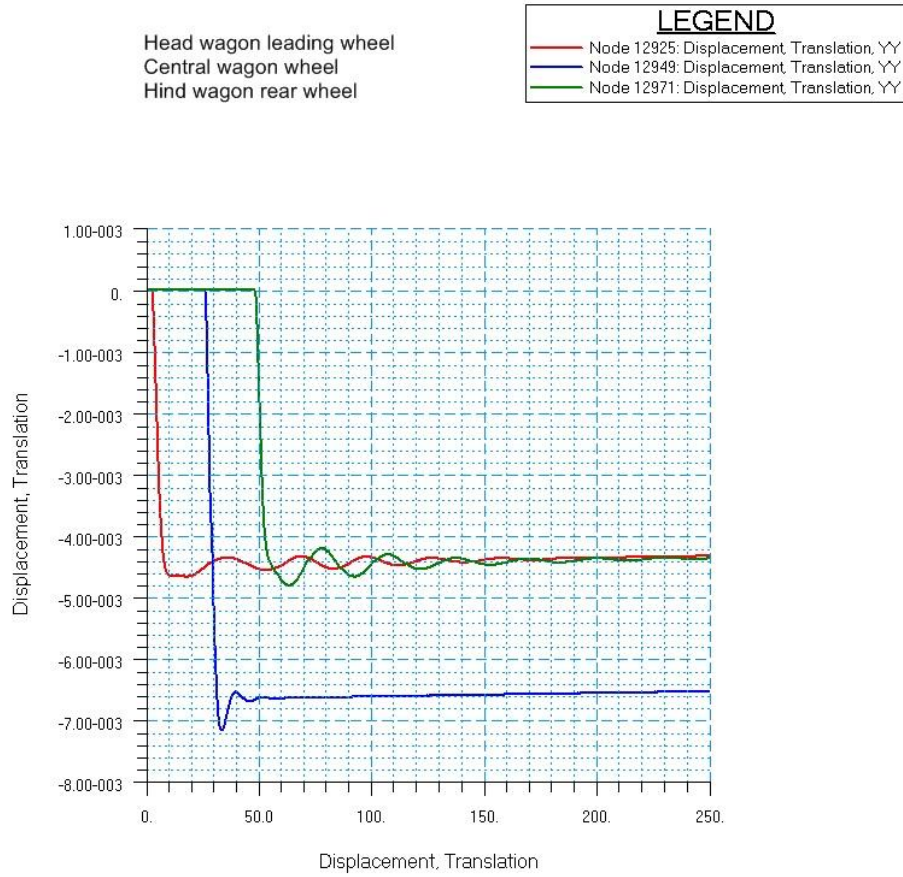


Fig. 2.78. The graph of vertical displacements (in meters) of motorail wheels when riding from rigid section of a track to a loose ground and moving over it. Maximum deflection of the track under the wheel of the central wagon is 7.2 mm, Maximum deflection of the track under the wheels of the head wagon is 4.8mm.

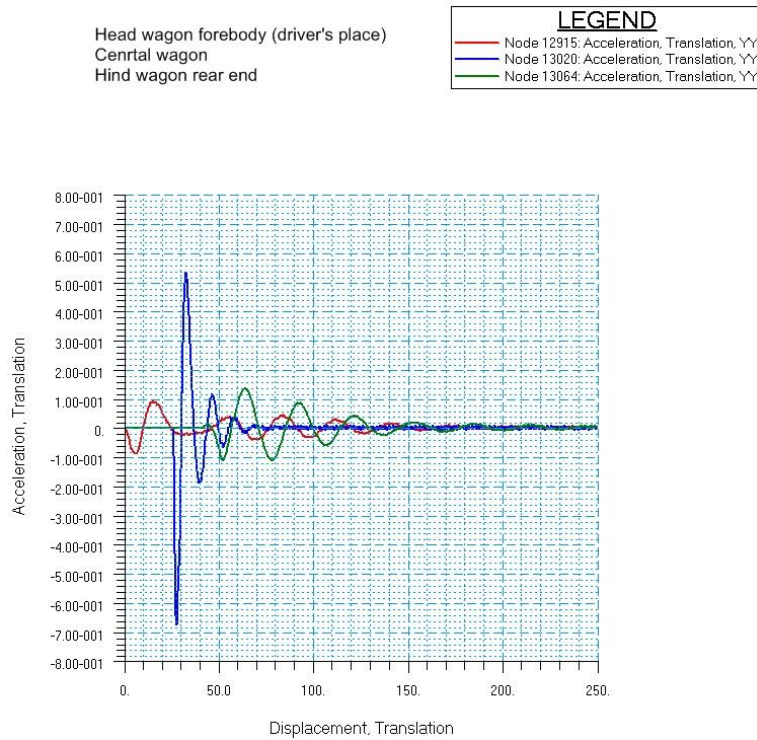


Fig.2.79. The graph of vertical accelerations (m/s^2) of a motorail head wagon (driver's place) and of a central freight wagon when riding from rigid section of a track to a loose ground and moving over it. Maximum vertical acceleration of driver's place is $0.14 m/s^2$, Maximum vertical acceleration of a freight wagon is $0.68 m/s^2$



2.13.2.4. Evaluation of Motorail's Riding Comfort on a Loose Ground

Motorail riding on rigid sections will occur rarely, the calculation of the basic parameter of riding comfort W see in paragraph 2.12.4.3. Riding comfort in the driver's place may be estimated as very high.

It should be taken into account that human fatigue depends not only on the mode of vehicle body vibrations (acceleration and frequency), but also on the duration of impact acceleration t_d (see Tab. 2.23, which represents the data for passengers; driver's level of exposure to vibration may be considerably higher). At acceleration of $a_G = 0,14 \text{ m/s}^2$ permissible duration of uninterrupted travel for the driver is 1200 minutes or 20 hours.

2.14. Conclusions on Mounted STS

Summarizing the results of the preliminary design work, analysis and concept evaluation of ore transportation by mounted STU in conditions of Australia, we can draw the following conclusions:

- high bulk density of iron ore ($2,4 - 2,8 \text{ t/m}^3$) and the height of the freight wagon cabin, which is equal to 1205mm and which is determined by the driver's cabin, result in small width of a freight wagon cabin (470 mm) and motorail gauge (1000 mm);

- to ensure annual productivity of about 50 million tons per year (when working in three shifts with 20 minutes breaks between them) transport system should be equipped with motorails with load capacity of 160 tons; motorails loading and off-loading should be performed on terminal stations on the fly at a speed of about 2 m/s;

- not less than 77 motorails with load capacity of 160 tons should be involved in ore transportation process at a distance of 100 km/h with annual productivity of 51 million tons per year (i.e. 1.5 motorails per 1 million tons);

- fuel consumption of a motorail (with load capacity of 160 tons) per 1 ton of ore transportation at a distance of 1km is $42 \text{ g/t} \times \text{km}$, which is lower than the level of fuel consumption of ore transportation by conventional rail (for example, fuel consumption of a train consisting of 40 dumpcars with load capacity of 60 tons at an average speed of 100 km/h will be 15 percent higher and will be $4.8 \text{ g/t} \times \text{km}$);

- fuel consumption of ore transportation by motor vehicle on an asphalt road at a speed of 100 km/h will be 3.6 times higher and on a gravel road will be 4.8 times higher;

- additional calculations prove that if motorail load capacity will be 2 times increased (up to 320 tons) fuel consumption will be 4.5 percent lower;

- additional calculations prove that decrease of the coefficient of freight wagons tare to the level of rail hoppers ($kt = 0.4$) allows to increase motorail load capacity approx. by 7 percent;

- to ensure acceleration of a loaded motorail in head wind without decrease of fuel efficiency and power equipment resources, total capacity of power equipment should be not less than 600 kW;

- maximum allowable speed of head wind, when a motorail loses its lateral stability, is 259km/h for empty motorail and 352 km/h for loaded motorail, which corresponds to the highest grade storm according to Saffir-Simpson storm scale;



- motorail driving comfort at a driver's place can be estimated as very high ($W = 2.04$);
- the results of analysis of motorail dynamic interaction on ground sections of STS track are satisfactory (for different types of ground). In the worst case (when a motorail drives from the hard section to loose ground and moves over it) maximum vertical acceleration on a driver's place is 0.14m/s^2 , and maximum rail deflection (under the wheels of a central wagon) is 7.2 mm;
- when a string-rail of mounted STS is wired to the ground, ground pressure under a rail bottom is not high ($0.33 - 0.36 \text{ kgf/cm}^2$). In conventional rail roads there is larger pressure on the ground ($0.6-0.8 \text{ kgf/cm}^2$), though there are assembled rails and sleepers and sand and road cap. The abovementioned ground pressure is much lower in comparison with ground pressure caused by foundations of buildings, which have lifetime of dozens and hundreds of years. It assumes high reliability and durability of STS string-rail track structure wired to the ground;
- the absence of expensive sleepers, sand and crush-stoned cap and earth embankment will help to decrease the cost of mounted STS track structure by 3-5 times for the version, when the string-rail is wired to the ground and by 2-3 times for the version, when the strings are mounted on supports, which will provide high productivity of transport system (50 million tons per year and even more);
- the version of mounted STS with longitudinal sleeper wired to the ground will be 1.5-2 times less resource demanding, and as a result cheaper in comparison with string-rail on supports;
- the proposed string-rail track structure will provide construction durability of at least 5 million of load cycles. Taking into account motorail load capacity of 160 tons, it will provide mounted STS with total capacity of 800 million tons;
- placing of a string-rail to the ground helps to reduce its temperature range by $40-50^\circ\text{C}$ throughout a year (by reducing rail heating during a day in the sun in summer and increasing of rail temperature at night in winter, because minimum temperature of the ground in winter is higher than minimum ambient temperature due to thermal inertia). It helps to design a string rail with reduced by 1000 kgf/cm^2 stress range in continuous structural elements, which will improve the reliability and durability of the whole STS transport system;
- mounted STS has high ecological compatibility due to:
 - lower fuel (energy) consumption (it is 10-20 percent lower in comparison with rail road and 3-5 times lower in comparison with motor road);
 - 3-5 times lower resource intensity, i.e. fewer concrete, road metal, sand and gravel is needed to build a track; it results in reduction of negative impacts on Nature throughout the whole operational life of transportation system (production, transportation, installation and restoration of degraded mineral resources, which is the integral part of any transportation system construction);
 - the absence of embankment and assembled rails and sleepers of rail road and the absence of roadway covering provides environmental friendliness of STS track, it won't destroy flora and fauna of the area; green plants will restore oxygen, burned in the engines of a rolling stock;
 - the absence of embankment with compact ground won't turn mounted STS into low-head dam, which disrupts the flow of ground waters and surface waters and migration of animals, particularly small ones (reptiles, rodents, insects, etc.).



3. Suspended STS

The concept of suspended STS is transportation of bulk materials over a string-rail track structure with the help of rail cars (unicars), adapted for loading and off-loading of cargo on the move in special terminals in autonomous mode.

Unicar is a motorized hopper with autonomous power system in the form of diesel-electric aggregates.

The concept assumes complete automation of transportation process.

String-rail track structure of suspended STS is the form of wire or cable bridges with prestressed cable, wired to the stiffening truss which serves as a string railway for unicars.

3.1. Unicars Weight and Dimensional Parameters

Admissible axial load on track (taking into account calculated norms of freight suspended STU-STTS) is accepted as initial data for evaluative definition of weight and dimensional parameters of a unicar.

Admissible moving load on a track structure at acceptable values of string-rail deflection (4-6mm) on 250m span is 25 tons (moving load per one string rail is 12,5 tf).

3.1.1. Unicar Load Capacity

Unicar load capacity is determined from the formula:

$$P = Z / (1 + k_t) \cdot g = 250000 / (1 + 0.65) \cdot 9.8 = 15460 \text{ kg,}$$

where:

$Z = 250\,000 \text{ N}$ is admissible moving load on a track;

$g = 9.8 \text{ m/s}^2$ is acceleration of free-fall;

$k_t = 0.65$ is tare coefficient (on pre-design stage is accepted as equal to the tare coefficient of dump trucks).

Wagon load capacity is accepted equal to $P = 15$ tons.

3.1.2. Weight of a Unicar

Dead weight of a unicar (tare) will be: $T = P \cdot k_t = 15 \cdot 0.65 = 9.75$ tons.

Total weight (gross weight) of a unicar will be: $M = P + T = 15 + 9.75 = 24.75$ tons.

3.1.3. The Volume of the Iron Ore Loaded to the Unicar Body

The calculated volume v of ore loaded to the unicar body can be determined from the following formula:

$$v = P / \rho, \text{ m}^3,$$

where ρ is a bulk density, t/m^3 .



To calculate the body volume we take the density of $2,5 \text{ t/ m}^3$ which is relevant for fine-crushed ore (fineness of approx. 25 mm), which is largely distributed by Australian mine companies.

In this case calculated volume of the iron ore loaded to the unicar body will be:

$$v = 15 / 2.5 = 6 \text{ m}^3.$$

3.1.4. Wheel Tread Diameter

Wheel diameter can be determined on the basis of contact resistance. There are two contact versions depending on the wheel rim and rail form:

- line contact (contact patch is close to rectangular shape);
- point contact (contact patch is close to ellipse shape).

Ropeway operational back-ground [2] shows that track resistance at point contact is 1.5 times higher than it is at line contact (with the same load and wheel diameter). However, it should be mentioned that it is quite difficult to achieve large values of contact length in “wheel-rail” pair. Of course, due to string-rail compliance this problem doesn't exist when the unicar moves between supports. To provide line contact of a unicar on support shoes additional measures should be taken (the accuracy of wheel and rail top relative position should be improved, “self-setting” wheel solution should be implemented, etc).

Below is the analysis of contact resistance for both versions. The final choice of the wheel rim form will be made during project implementation process.

3.1.4.1. Line Contact Version

Taking into account the recommendations [2], unicar wheels should be at least of 450 mm diameter. Rail top width is 60mm. The scheme of wheel and rail top contact is represented in Fig. 3.1.

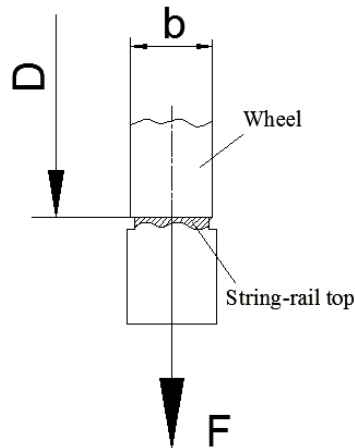


Рис. 3.1. Wheel and rail top line contact

In this case contact stress will be the following:

$$\sigma_k = 272 \cdot 10^3 (F/(D \cdot b))^{1/2} = 272 \cdot 10^3 (30318.75/(0.45 \cdot 0.06))^{1/2} = 288232314 \text{ Pa} = 288.2 \text{ MPa},$$

where:

$F = M \cdot g / n_k = 24750 \cdot 9.8 / 8 = 30318.75 \text{ N}$ is load per wheel;

$D = 0.45 \text{ m}$ is wheel rolling surface diameter;

$b = 0.06 \text{ m}$ is the width of a flat strip on the rail top (the length of a contact line);

$M = 24750 \text{ kg}$ is the total (gross) weight of a freight wagon;



$n_k = 8$ is the number of wheels (which is determined by pre-design).

Admissible contact stress rates for steel rails in case of line contact are represented in Tab. 3.1.

Admissible contact stress rates for steel wheels in case of line contact are represented in Tab. 3.2.

Table 3.1

Admissible contact stress rates for steel rails (line contact)

Steel Grade	Hardness, HB, not less than	$[\sigma_k]$, MPa
Carbonaceous of ordinary quality		
Cr3	130	400
Cr5	140	450
14Г	130	460
14Г2	140	480
24Г	140	500
Carbonaceous and manganous of high quality		
45	229	570
60Г	260	650
35Г2	225	650
Rail		
M71	217	600
M75	245	770

Table 3.2

Admissible contact stress rates for steel wheels (line contact)

Steel Grade	Rim hardness (normalization), HB	$[\sigma_k]$, MPa
45	217	450
50Г2	241	550
65Г	260	600
40XH	255	550

In the presence of tangential forces (tractive or breaking force) the rates represented in Tab. 3.1 and 3.2 must be decreased. Reduction value depends on tangential to normal force ratio (see Tab. 3.3).

Table 3.3

Decrease of admissible contact stresses

Tangential to normal force ratio	0.0	0.1	0.15	0.2	0.25	0.3
Admissible stresses decrease, %	0.0	2	4	6	10	15-20

Wheel and rail adhesive coefficient also depends on tangential to normal force ratio. For “steel-steel” pair the largest coefficient value will be approx. 0.3 – 0.35. It follows that admissible contact stresses values represented in Tab. 3.1 and 3.2 should be decreased by 20%. In this case the wheels of the unicar might be produced of any abovementioned steel grade. The rail top might be produced of Cr3, Cr5, 14Г, 14Г2 и 24Г steel grades, which have no limitations to welding. The other steel grades are difficult-to-weld. They need heating and thermal processing or they are not used in production of weld-fabricated constructions.

3.1.4.2. Point Contact Version

In case of rolling of a steel wheel with a curved rim on a flat surface of a steel rail (see Fig. 3.2) local contact stresses might be determined from the formula suggested by Research Institute of Handling Machinery of Russian Federation [2]:

$$\sigma_k = 35 \cdot k \cdot (F / r_{\max}^2)^{1/3} = 35 \cdot 0.49 \cdot (30318.75 / 0.6^2)^{1/3} = 752 \text{ MPa,}$$

where:

$F = 30318.75 \text{ N}$ is load per wheel;

$r_{\max} = 0.6 \text{ m}$ (maximum values of radii $R = 0.6 \text{ m}$ and $r = 0.3 \text{ m}$);

$k = 0.49$ is the coefficient depending on the relation of r_{\min} / r_{\max} (see Tab. 3.4).

Table 3.4

k-coefficient

r_{\min} / r_{\max}	1.0	0.9	0.8	0.7	0.6	0.5	0.4	0.3	0.2	0.15	0.1	0.05
k	0.388	0.400	0.420	0.440	0.468	0.490	0.536	0.600	0.716	0.800	0.970	1.280

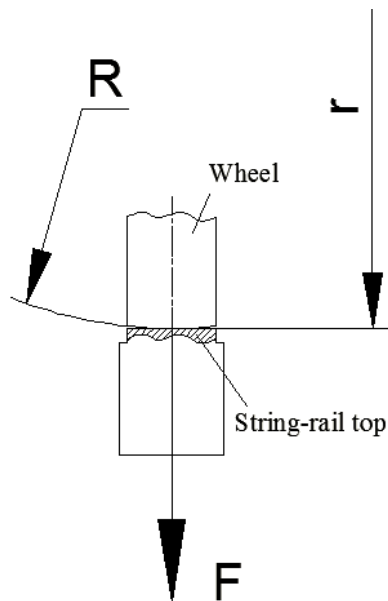


Fig. 3.2. Wheel and rail top point contact

Admissible contact stress rates for steel rails in case of point contact are represented in Tab. 3.5.

Admissible contact stress rates for steel wheels in case of point contact are represented in Tab. 3.6.



Table 3.5

Admissible contact stress rates for steel rails (point contact)

Steel Grade	Hardness, HB, not less than	$[\sigma_k]$, MPa
Carbonaceous of ordinary quality		
Ст3	130	960
Ст5	140	1100
14Г	130	1100
14Г2	140	1150
24Г	140	1200
Carbonaceous and manganese of high quality		
45	229	1400
60Г	260	1500
35Г2	225	1500
Rail		
M71	217	1450
M75	245	1800

Table 3.6

Admissible contact stress rates for steel wheels (point contact)

Steel Grade	Rim hardness (normalization), HB	$[\sigma_k]$, MPa
45	217	1100
50Г2	241	1300
65Г	260	1400
40XH	255	1300

In the presence of tangential forces (tractive or breaking force) the rates represented in Tab. 3.5 and 3.6 must be decreased. Reduction value depends on tangential to normal force ratio (see Tab. 3.7).

Table 3.7

Decrease of admissible contact stresses

Tangential to normal force ratio	0.0	0.1	0.15	0.2	0.25	0.3
Admissible stresses decrease, %	0.0	2	4	6	10	15-20

Wheel and rail adhesive coefficient also depends on tangential to normal force ratio. For “steel-steel” pair the largest coefficient value will be approx. 0.3 – 0.35. It follows that admissible contact stresses values represented in Tab. 3.5 and 3.6 should be decreased by 20 percent. In this case the wheels of the unicar might be produced of any abovementioned steel grade. The rail top might be produced of Ст5, 14Г, 14Г2 и 24Г steel grades, which have no limitations to welding. The other steel grades are difficult-to-weld. They need heating and thermal processing or they are not used in production of weld-fabricated constructions.

3.1.5. Gauge and Unicar Cross-Sectional Dimensions

Overall width of a unicar, its body and gauge are determined by pre-design taking into account the following data:

- minimum radius of curves passing is 20 m;
- overall length of DKWBZ traction electric motor is 385 mm;
- overall width of GMT resilient member is 197 mm;



- wheel overall width is 60mm;
- overall width of GEKO (32-48kW) diesel-electric aggregate is up to 900mm.

The most appropriate gauge width, corresponding to the norms of freight suspended STS is 1750mm. Overall height of a unicar is accepted as 2150mm to provide unicar windage centre in a plane of a string-rail.

Pre-design of a suspended unicar with load capacity of 15 tons is represented in Fig. 3.3.

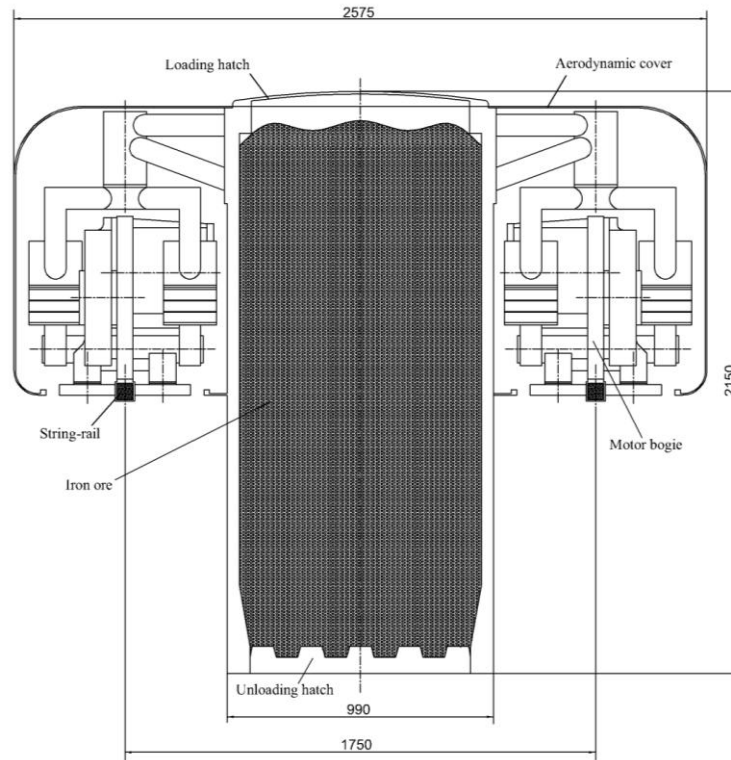


Fig. 3.3. Unicar cross section

3.1.6. Inner Length of a Unicar Body

Ore volume loaded to the unicar body is equal to 6 m^3 (see Art. 3.1.3). To use totally unicar nominal load capacity its body volume should exceed the volume of loaded ore. As it was already mentioned, rail transport operational back-ground shows that even at the most accurate loading the volume of the wagon is utilized at only 90 – 95 percent of its potential. It happens because the wagon is not fully loaded at its flank sides and to their whole height due to the load angle of repose [4]. The unicar body volume can be determined from the formula which is also used to determine the volume of rail dump wagons:

$$v_r = v \cdot k_H = 6 \cdot 1.25 = 7.5 \text{ m}^3 \text{ is the freight wagon body volume,}$$

where:

$k_H = 1.1 - 1.25$ is dump wagons coefficient of fullness [4] (on pre-design stage the coefficient of 1.25 is accepted).

In this case the inner length of a unicar body can be determined:

$$L = v_r / (b \cdot h) = 7.5 / (0.9 \cdot 1.99) = 4.2 \text{ m,}$$

where:

$b = 0.9 \text{ m}$ is inner width of a unicar body;



$h = 1.99$ is inner height of a unicar body.

3.1.7. Longitudinal Size of a Unicar

To obtain the optimal values of bending stresses in a string-rail body (regardless the stresses arising in a rail body due to adjacent wheels), the distance between unicar wheels should not be less than 1500 mm. At that there should be eight support traction wheels in accordance with the analysis of “rail-wheel” contact resistance. Thus motorcar undercarriage consists of two two-wheels motor bogies on each side (see Fig. 3.4). Motor bogies may be rotated in the horizontal and vertical planes, when the unicar is passing radius curves.

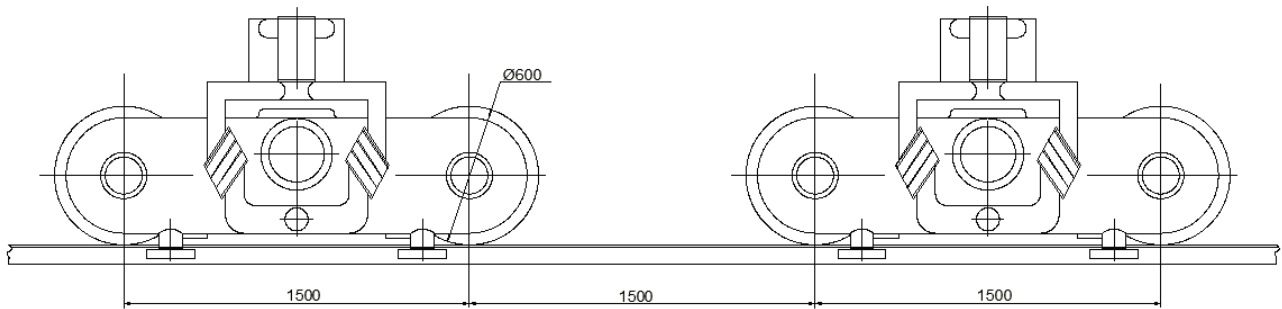


Fig. 3.4. The scheme of a suspended unicar undercarriage

Unicar overall length of 7850mm is determined by pre-design taking into account overall sizes of basic compounds. Overall length of a unicar and its total weight depends on the overall sizes of the following compounds: cargo sections #1, 2 (see Fig. 3.5), diesel-electric aggregate #3 and fuel tank #4. Optimal sizes of abovementioned compounds, which will provide uniform loading of motor bogies to wheel pairs, will be determined in the process of project implementation.

The results of pre-design are represented in Fig. 3.5.

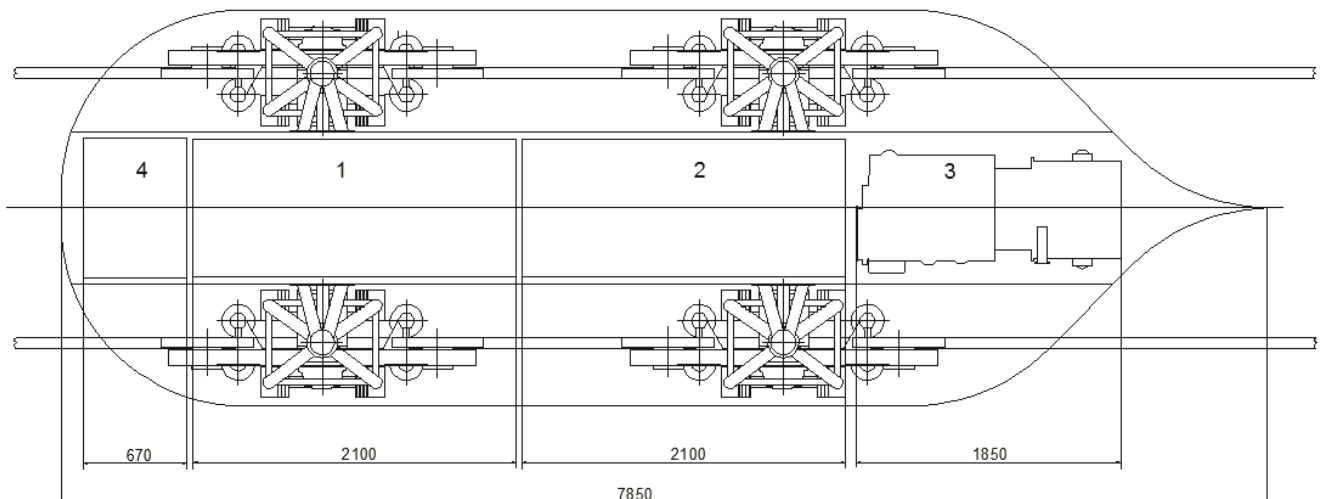


Fig. 3.5. The scheme of a unicar overall length determination



3.2. The Provision of Ore Carriage in the Volume of 50 mln t/year

There are four stages in the process of ore transportation:

- loading of ore to a moving at a low speed unicar at a loading terminal station (0.5–1.5 m/sec);
- transportation of ore by a unicar to the off-loading terminal station (65–75 km/h);
- off-loading of ore by a moving at a low speed unicar at an off-loading terminal station (0.5–1.5 m/sec);
- moving of an empty unicar to a loading terminal station (65–75 km/h).

To carry 50 million tons of ore per year unicar loading and off-loading on terminal stations should be provided with a productivity of at least 1.5 t/sec. Unicars with load capacity of 15 tons will provide such productivity moving on a track with 10 seconds intervals. At that the process of ore transportation in such volumes should be fully automated.

3.2.1. Loading

Continuous automatic mode of transportation of ore in large quantities involves the process of ore loading to a unicar on the move. There are many solutions of bulk cargo loading on the move. As an example the most well-known method, which is widely used in ropeways loading process, might be considered. Ore with the help of conveyor belt (one or more) is fed to a rotating set of cones. When the cone flap is opened the ore is supplied to the trucks (in our case to the unicars) moving at rotational speed (see Fig. 3.6). Volume productivity of transport system can be determined from the formula:

$$Q_2 = Q_1 / \rho = 1.5 / 2.5 = 0.6 \text{ m}^3/\text{sec},$$

where:

$Q_1 = 1.5 \text{ t/sec}$ is transport system productivity;

$\rho = 2.5 \text{ t/m}^3$ is bulk density of ore,

Thus, the speed of a unicar at a loading terminal station might be determined.

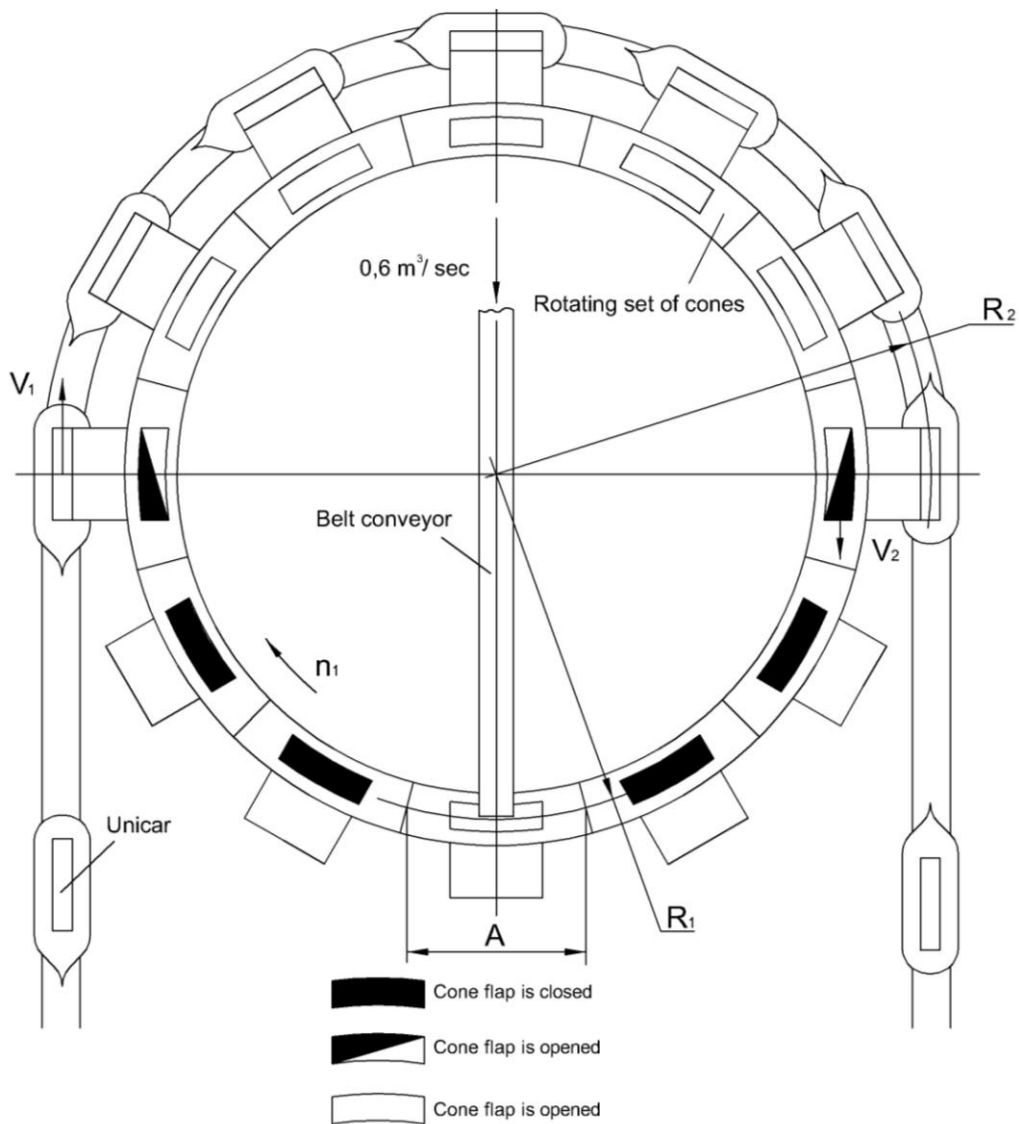


Fig. 3.6. The scheme of ore loading to the moving unicar (a version)

The volume of each cone in the rotating set is equal to the volume of ore loaded to a unicar. The time needed for loading of one cone will be:

$$t_1 = v / Q_2 = 6 / 0.6 = 10 \text{ sec,}$$

where:

$v = 6 \text{ m}^3$ is an estimated volume of ore loaded to a unicar.

Linear speed of cones in the rotating set can be determined from the formula:

$$V_1 = A / t_1 = 8.3 / 10 = 0.83 \text{ m/sec,}$$

where:

$A = 8.3 \text{ m}$ is the length of a cone of radius $R_1 = 15.9 \text{ m}$

Linear speed of a unicar at a terminal station might be determined from the formula:

$$V_2 = V_1 \cdot R_2 / R_1 = 0.83 \cdot 20 / 15.9 = 1.044 \text{ m/sec}$$

where:



$R_2 = 20$ m is an average radius of a turning circle of a loading terminal station (on the central line of the track structure at the terminal station).

In this case the angular speed of the rotating set of cones will be:

$$n_1 = V_1 \cdot 30 / R_1 \cdot \pi = 0.83 \cdot 30 / 15.9 \cdot 3.14 = 0.5 \text{ rpm.}$$

3.2.2. Off-Loading

Motorail off-loading is implemented on the move by opening hatches on a signal to hatch hold-down (or by runover to the hatches). Hatch doors return to their initial position on the move by runover to hold-down rolling batteries. The ore can be off-loaded in piles of the pier or to the storage bins of the loading terminal, which can be built directly in the sea in case when the ore is delivered to a consumer by bulk carriers (see Fig. 3.7).

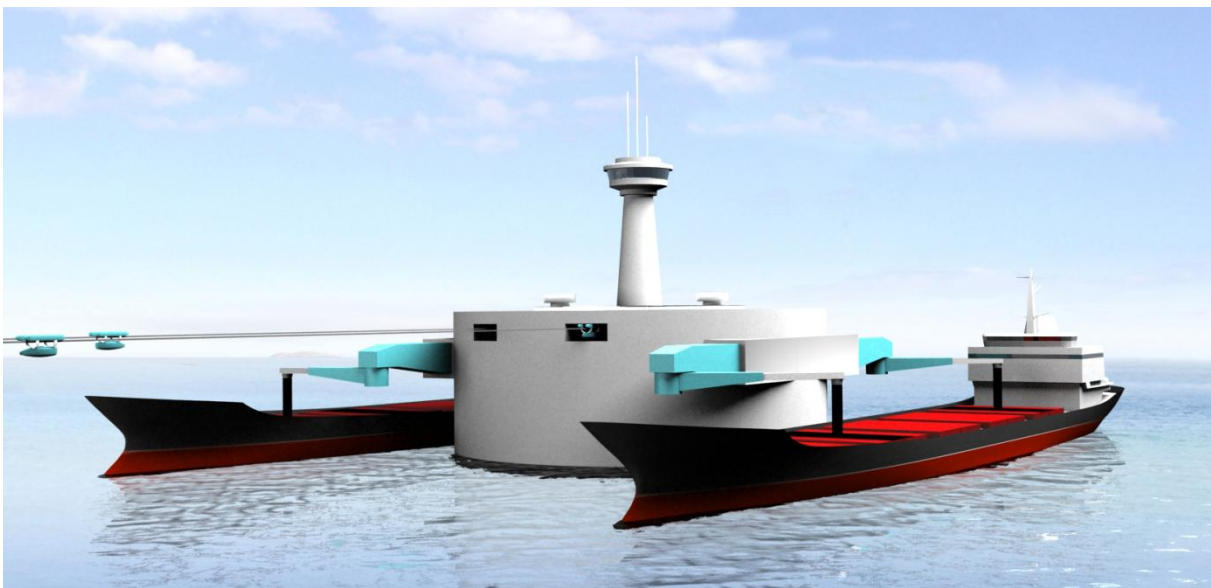


Fig. 3.7. STS loading terminal station built in the sea (version)

If necessary, ore delivered to the off-loading terminal station might be sorted and dumped to different bins. There are at least two ways of ore transfer from bins to bulk carriers:

- each bin is equipped with its transfer device (see Fig. 3.8);
- ore is transferred by one transfer device, which is able to move along all the bins (see Fig.3.9).

Both versions assume that the ore is loaded to the bins through the hatches. Minimum length of the hatches might be calculated by the formula [1]:

$$B = t_{ul} \cdot V_{ul} + X = 3 \cdot 1 + 4 = 7 \text{ m,}$$

where:

$t_{ul} = 3$ sec is off-loading time (taking into account operational back-ground of freight ropeways [1]);

$V_{ul} = 1$ m/sec is unicar speed within a terminal station;

$X = 4$ m is the total length of unicar off-loading hatches.

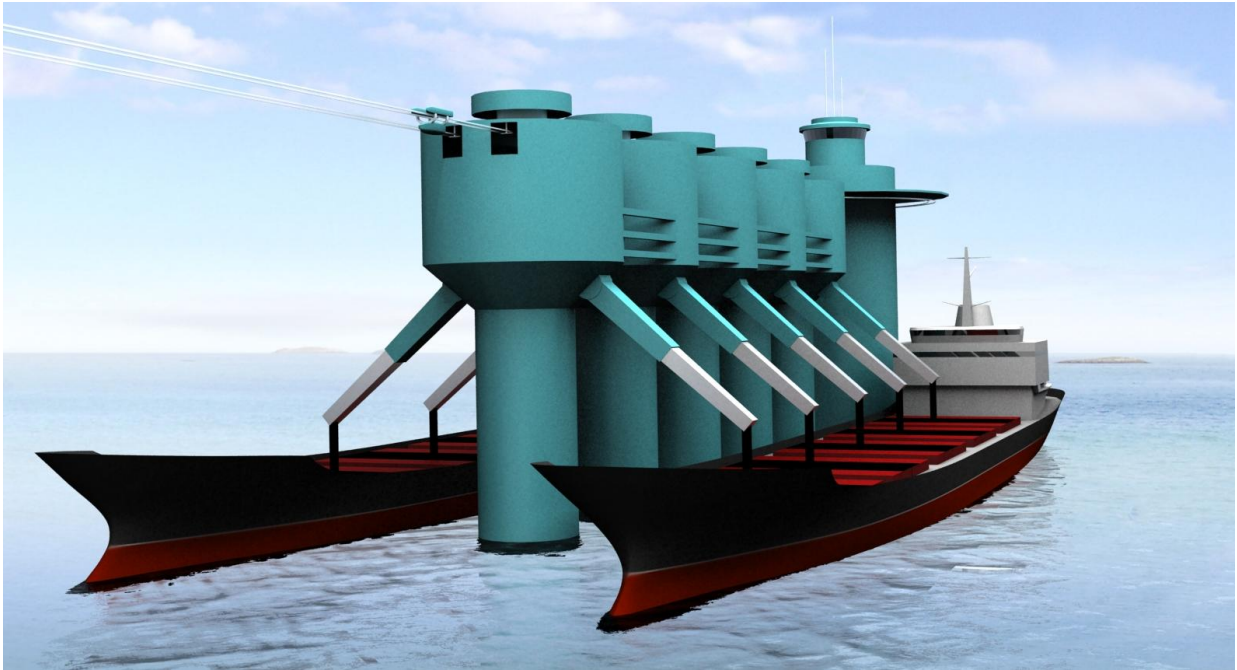


Fig. 3.8. The version of ore transfer to the bulk carrier (each bin is equipped with its transfer device)

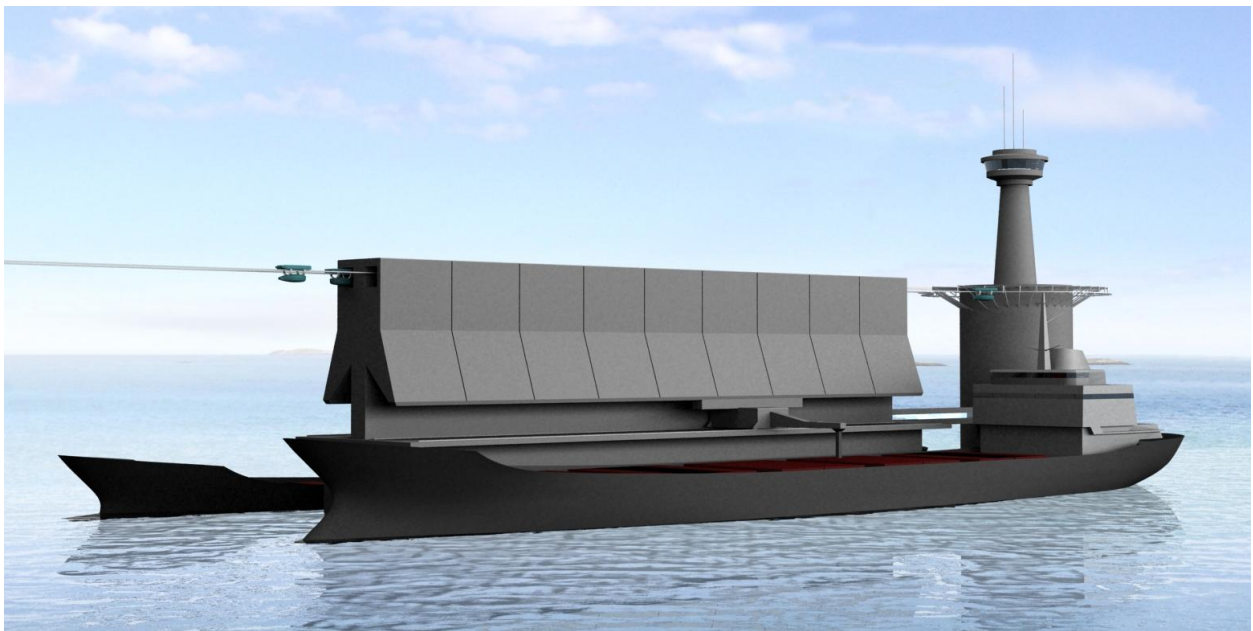


Fig. 3.9. The version of ore transfer to the bulk carrier (ore is transferred by one transfer device, which is able to move along all the bins and choose the necessary one)

3.2.3. Number of Unicars and Their Average Speed on a Track

An average speed of the unicars on a track depends on their traffic intervals, which may be determined taking into account annual volume of ore transportation, the distance between intermediate supports. On the basis of it minimum distance between the unicars on a track is set. With an annual volume of ore transportation of 50 million tons traffic interval between the unicars will be 10 sec. Admissible moving load on a track structure is 25 tons. It provides the distance between intermediate supports up to 250 meters. In this case the distance between the unicars on a track will be 200 meters. Thus, with an annual volume of ore transportation of 50 million tons an



average speed of the unicars on a track will be 20 m/sec. The number of unicars involved in the transportation process depends on the distance of transportation. Approx. 1010 unicars will be of use in the process of ore transportation at a distance of 100 km/h with annual productivity of 50 million tons per year.

3.3. Capacity of Autonomous Power Supply System

In the article the analysis of an installed capacity of autonomous power equipment (diesel internal combustion engine) was carried out on the basis of traction-dynamic analysis for a unicar with load capacity of 15 tons providing an average speed of ore transportation of 72 km/h in a headwind of 15 m/sec.

3.3.1. The Power Required for Moving of a Loaded Unicar

Power required for moving (effective power) can be determined from the formula:

$$N_{\pi} = (F_1 + F_2) \cdot V = (485 + 359.5) \cdot 20 = 16890 \text{ W},$$

where:

$V = 20$ m/s is design speed of a unicar.

Analysis of the values used in the N_{π} determination formula:

$$1) \quad F_1 = M \cdot g \cdot f = 24750 \cdot 9.8 \cdot 0.002 = 485 \text{ N is unicar wheels drag force},$$

where:

$M = 24750$ kg is the total weight of a unicar;

$f = 0.002$ is the coefficient of rolling resistance at point contact when $D > 600$ mm;

$$2) \quad F_2 = 0,5 \cdot \rho_B \cdot A_M \cdot C_x \cdot V_a^2 = 0.5 \cdot 1.204 \cdot 3.75 \cdot 0.13 \cdot 35^2 = 359.5 \text{ N is unicar air resistance},$$

where:

$\rho_B = 1.204$ kg/m³ is sea level atmospheric density at a temperature of + 20° C;

$A_M = 3.75$ m² is the largest area of middle section;

$C_x = 0.13$ is air resistance coefficient (according to design standards of suspended STU);

$V_a = 20 + 15 = 35$ m/sec is the speed of a flowing air.

3.3.2. Capacity on Crankshaft of Power Equipment

Capacity on crankshaft of power equipment can be determined from the formula:

$$N = N_{\pi} / (\eta_p \cdot \eta_d \cdot \eta_n \cdot \eta_r \cdot (1 - \eta_B) \cdot \cos\varphi) = 16890 / (0.94 \cdot 0.92 \cdot 0.94 \cdot 0.92 \cdot (1 - 0.1) \cdot 0.95) = 26414 \text{ W} \approx 27 \text{ kW},$$

where:

$\eta_p = 0.94$ is reducing gear efficiency coefficient (three gearings);

$\eta_d = 0.92$ is traction motor efficiency coefficient;

$\eta_n = 0.94$ is traction converter efficiency coefficient;

$\eta_r = 0.92$ is generator efficiency coefficient;

$\eta_B = 0.1$ is power equipment ventilating losses;

$\cos\varphi = 0.95$ is phase shift.



Installed capacity of power equipment is rather large for the reasons of fuel economy. In particular, an average capacity of GEKO diesel-electric aggregate for 24 hours should not exceed 60 percent of its installed capacity. As a result, installation capacity of autonomous power supply system should not be less than 45 kW. Making autonomous power supply system of GEKO diesel-electric aggregates, it is reasonable to choose 60000 ED-SDEDA model with power equipment capacity of 48 kW.

3.3.3. The Dynamics of Unicar Acceleraton

The dynamics of loaded unicar acceleration is determined on the basis of traction-dynamic analysis. The results of analysis (time and starting distance, changes of speed rates and acceleration) are represented in Tab. 3.8.

Table 3.8

Changes of speed rates, acceleration,
starting time and starting distance of a loaded unicar

V, km/h	V, m/s	a, m/s ²	t _v , sec	S _v , m
0	0	0	0	0
2	0.556	0.600	0.926	0.257
4	1.111	0.600	1.852	1.029
6	1.667	0.600	2.778	2.315
8	2.222	0.527	3.764	4.232
10	2.778	0.417	4.941	7.175
12	3.333	0.344	6.399	11.631
14	3.889	0.292	8.144	17.931
16	4.444	0.253	10.180	26.414
18	5.000	0.223	12.513	37.432
20	5.556	0.199	15.149	51.345
22	6.111	0.179	18.095	68.529
24	6.667	0.162	21.357	89.370
26	7.222	0.148	24.943	114.272
28	7.778	0.136	28.860	143.650
30	8.333	0.125	33.117	177.938
32	8.889	0.116	37.721	217.588
34	9.444	0.108	42.683	263.071
36	10.000	0.101	48.012	314.879
38	10.556	0.094	53.718	373.527
40	11.111	0.088	59.813	439.557
42	11.667	0.083	66.309	513.537
44	12.222	0.078	73.218	596.067
46	12.778	0.073	80.555	687.781
48	13.333	0.069	88.335	789.347
50	13.889	0.066	96.573	901.480
52	14.444	0.062	105.288	1024.935
54	15.000	0.059	114.497	1160.522
56	15.556	0.056	124.223	1309.107
58	16.111	0.053	134.487	1471.617
60	16.667	0.050	145.313	1649.054
62	17.222	0.047	156.730	1842.497
64	17.778	0.045	168.765	2053.116
66	18.333	0.043	181.452	2282.186



V, km/h	V, m/s	a, m/s ²	t _v , sec	S _v , m
68	18.889	0.040	194.826	2531.093
70	19.444	0.038	208.927	2801.360
72	20.000	0.036	223.799	3094.658

3.4. Specifications of Suspended STS Unicar with Load Capacity of 15 Tons Intended for Ore Transportation

Specifications of suspended STS unicar with load capacity of 15 tons are represented in Tab. 3.9. Front view and plan view of a unicar are represented in Fig. 3.10.

Table 3.9

Specifications of suspended STS unicar

No.	Specification	Specification values (description)
1	Load capacity, t	15
2	Dead weight, t	9.75
3	Body capacity, m ³	7.5
4	Overall dimensions, mm: - length - width -height	8200 2575 2150
5	Gauge, mm	1750
6	Base of a bogie, mm	1500
7	Wheel arrangement	8 x 8
8	Load on a track: - axial, ton-force - linear, ton-force/m	6.2 4.2
9	The number of freight sections	2
10	Maximum operational speed, km/h	85
11	Time of acceleration to the speed 70 km/h , minutes	3.5
12	Maximum climbing ability, %: - loaded with 15 t - empty	8.0 13.0
13	Braking distance (initial speed of 72 km/h), m	200
14	Driving system	Diesel-electric (the version manufactured by GEKO , VEM, Germany)
15	Fuel consumption (1 ton of ore transportation at a distance of 1 km, g /t ×km)	3.9
16	Brake system: - service - parking (emergency)	electrodynamic electromechanical (the version manufactured by Mayr, Germany)
17	Ore loading	Through upper hatches
18	Ore off-loading	Through bottom hatches
19	Minimum radius of turnaround section, m	20
20	Control system	automatic

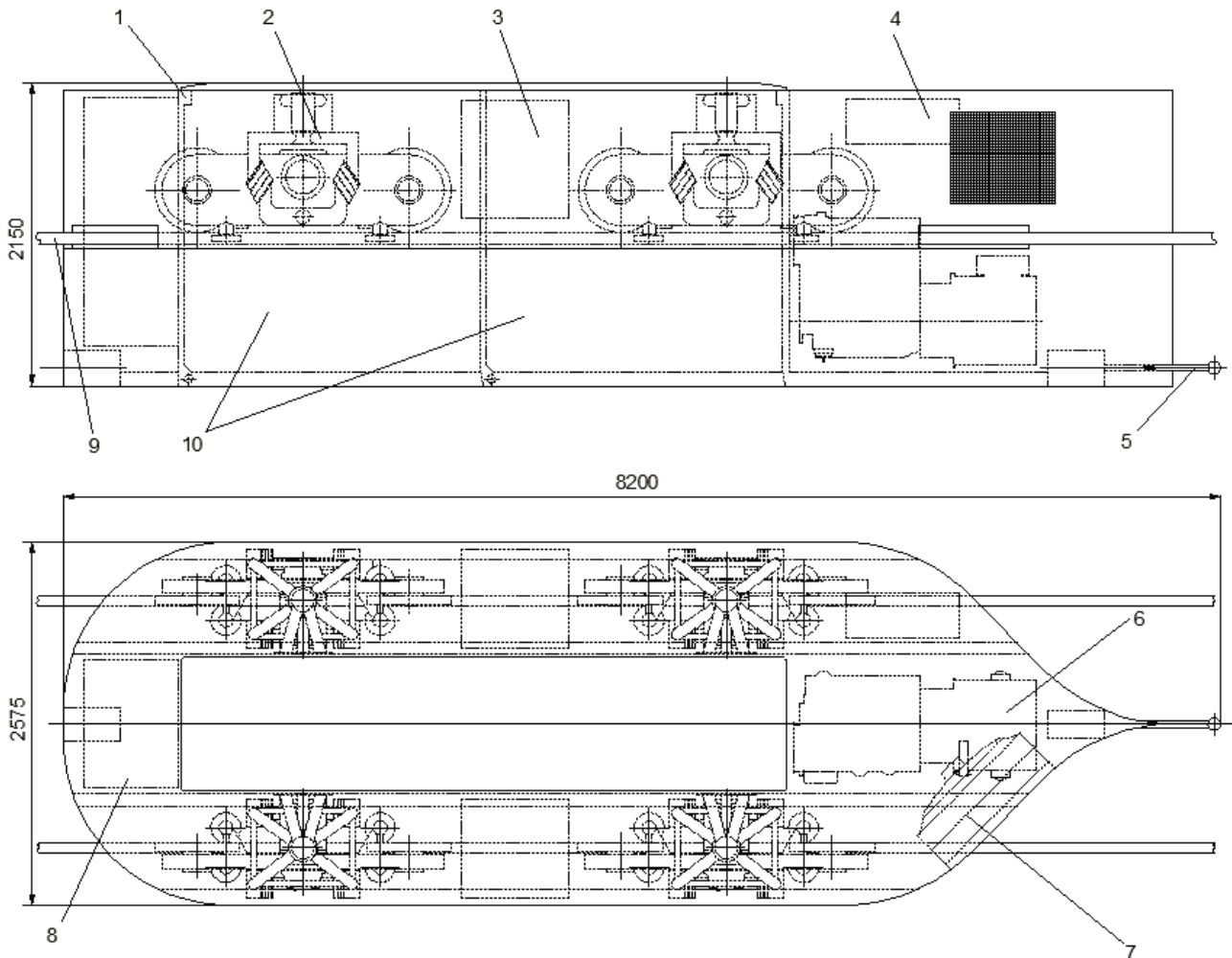


Fig. 3.10. Suspended STS unicar with load capacity of 15 tons intended for ore transportation:
1 – body; 2 – motor bogie; 3 – power converter; 4 – on-board control device; 5 – coupling unit; 6 – diesel-electric aggregate; 7 – cooling unit;
8 – main fuel tank; 9 – string rail; 10 – cargo sections

3.5. Fuel Efficiency of a Suspended STS Unicar

Fuel consumption during transportation of 1 ton of iron ore at a distance of 1 km for STS suspended unicar with load capacity of 15 tons is 3.9 g/t×km. This rate is approx. 16 percent lower than an average fuel consumption of ore transportation by a conventional railroad. And it is much lower in comparison with “Road trains” which are widely used in Australia in mining transportation (see Fig. 3.11).



Fig. 3.11. “Road trains” are widely used in Australia in mining transportation

Tab. 3.10 represents fuel consumption of “Road train” and suspended STS unicars while transporting 1 mln tons of load at a distance of 100 km.

Table 3.10
Comparative table of “Road train” and suspended STS unicars fuel consumption while transporting 1 mln tons of load at a distance of 100 km

Motorail	Fuel consumption while transporting 1 mln tons of load at a distance of 100 km, tons		
	Asphalt covering	Pressed gravel surfacing	STS track
«Road train»	2375*	3125*	-
STS	-	-	590*

*taking into account diesel motors fuel consumption of 210 g/kW×h

3.6. Automatic Control System of Suspended STS

Nowadays rail roads, including STU are the systems which might be controlled in an automated mode. Therefore it’s quite easy to implement automatic control of rail vehicles. In comparison with road transport, where all decisions are taken by a driver, a driver of a train or a motorail is strictly guided by system instructions, signals and running time. Such system might be easily automated. There are two types of traffic automation: manned and unmanned.

Currently both types of automation have been implemented. Operational experience proves that high traffic density of small trains is paid back only in case of unmanned control. Automatic control system (hereinafter ACS) of STS suspended transport system with productivity of 50 million tons per year and unicar traffic intervals of 10 seconds should correspond to the second level of automation, i.e. unmanned driving. Structural arrangement of ACS of “the second level” rail transport system is represented in Fig. 3.12.

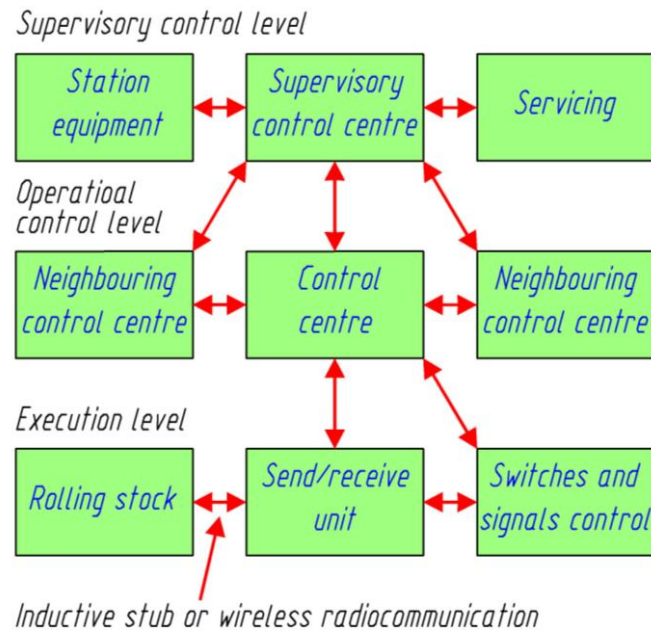


Fig. 3.12. ACS structural arrangement at unmanned driving

The main task of control centers (they are fully automatic) is traffic control of a rolling stock. They control its speed in accordance with traffic schedule on a track, provide safe distance between the motorails and set motorail stops. A rolling stock is equipped with on-board ACS devices. The main task of on-board device is to analyze and control a target speed.

Target speed of a rolling stock is analyzed on the basis of control data transmitted from the control centre. It includes the data of braking speed, deceleration rate (taking into account decline of a track), places of irregularities on a track, and speed rate in these places. In addition to speed control ACS should also control traction motors and brakes. This function is integrated into the software of on-board device. ACS of the suspended STS will also implement support functions, such as opening of loading and off-loading hatches and their control. Supervisory control centre is equipped with computer system, which does not implement critical functions. There will be only one supervisory control centre, which will perform the overall coordination of the operational process. Supervisory control centre is in connection with all control centers (on a track, on loading and off-loading terminal stations) and assigns supervisory tasks to these centers. It also is interfaced with the staff of the supervisory centre, providing control of data output to the monitors and processing regulatory tasks of traffic controllers.

3.7. Static Analysis of a String-Rail on a Suspended Section of a Track Structure

3.7.1. Basic Data on a Suspended Track Structure

Pre-design analysis of a suspended track string-rail in conditions of Australia should be implemented. On a suspended section of a track string-rail's stiffness, strength and endurance are tested.

The scheme of a track section with spans of 250 meters each is represented in Fig.3.13. The construction of suspended string track is mounted on intermediate and anchor supports (anchor supports are not represented in Fig.3.13).

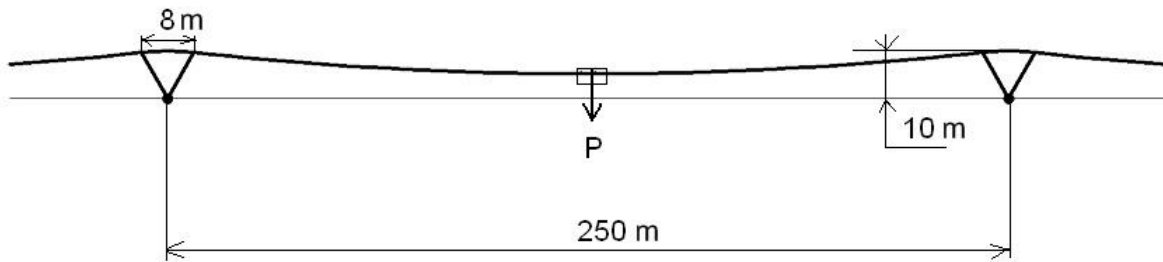


Fig. 3.13. The scheme of a suspended string track

Track structure consists of two string rails. Inside of each rail there are pre-stressed strings (steel wires) and a filling material (binding rail body and the strings). Cross section of a rail and internal strings is represented in full scale in Fig. 3.14.

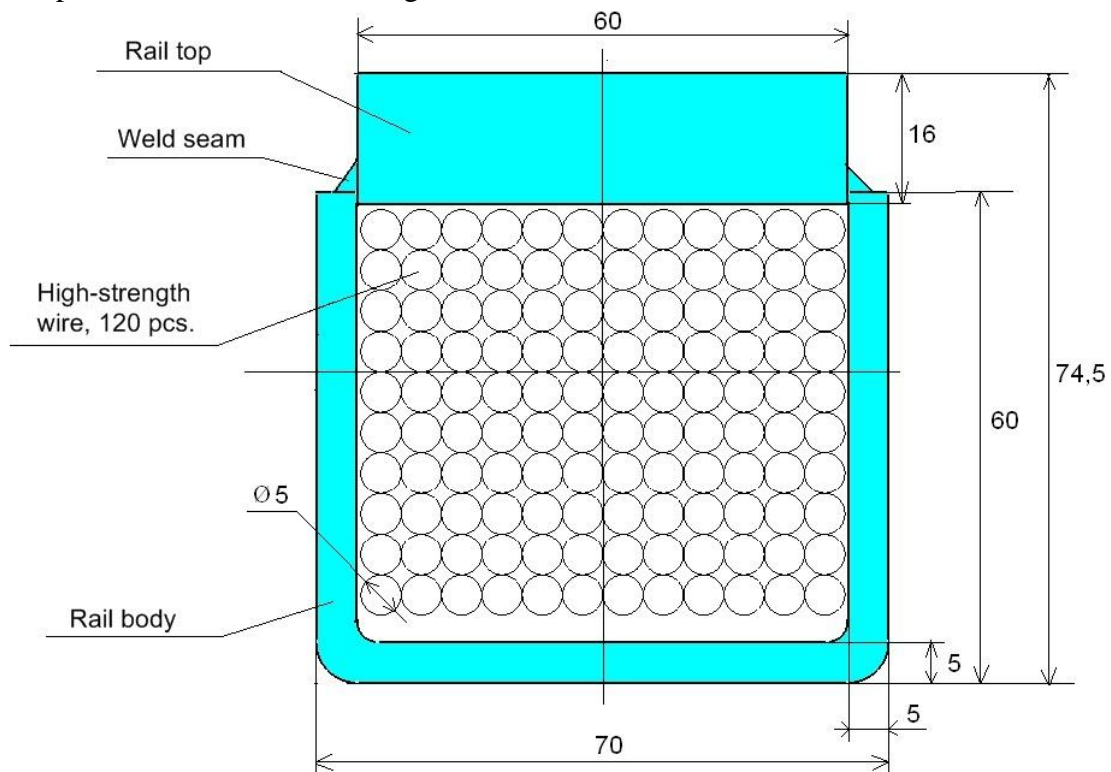


Fig. 3.14. Cross section of a rail and internal strings

Rail weight per suspended track length is 35 kg/m (7.5 kg/m is rail top weight, 7 kg/m is rail body weight, 18.5 kg/m is the weight of the strings (5mm diameter, 120 pieces in each rail) and 2 kg/m is the weight of a filling material).

The strings are made of 5 mm in diameter steel wires. The wires should be produced of carbon steel grades 75, 80, 85 and should have yield limit of not less than 1336 MPa and strength limit of not less than 1670 MPa.

Rail body and rail top should be produced of 09Г2 steel grade. At a steel gauge of 2-20mm its yield limit is 335 – 315 MPa and its strength limit is 490 – 470 MPa.

Filler might be produced of different materials. In strength analysis of a string rail mechanical characteristics of filler are not taken into account. The main function of filler is to provide uniform load transmission of unicar weight to the strings through rail top and rail body.

3.7.2. Design Section of a String-Rail

Cross section area of a string-rail body is $A = 18.5 \text{ cm}^2$;
 $E = 2 \cdot 10^{11} \text{ Pa}$ is elasticity modulus of string-rail steel;
Inertia moment of rail body section is $J = 1.305 \cdot 10^{-6} \text{ m}^4$;
 $E \cdot J = 2.61 \cdot 10^5 \text{ N} \cdot \text{m}^2$;
 $\rho = 35 \text{ kg/m}$ is linear density (mass) of a string-rail.

Design cross-section of string-rail body is represented in Fig. 3.15.

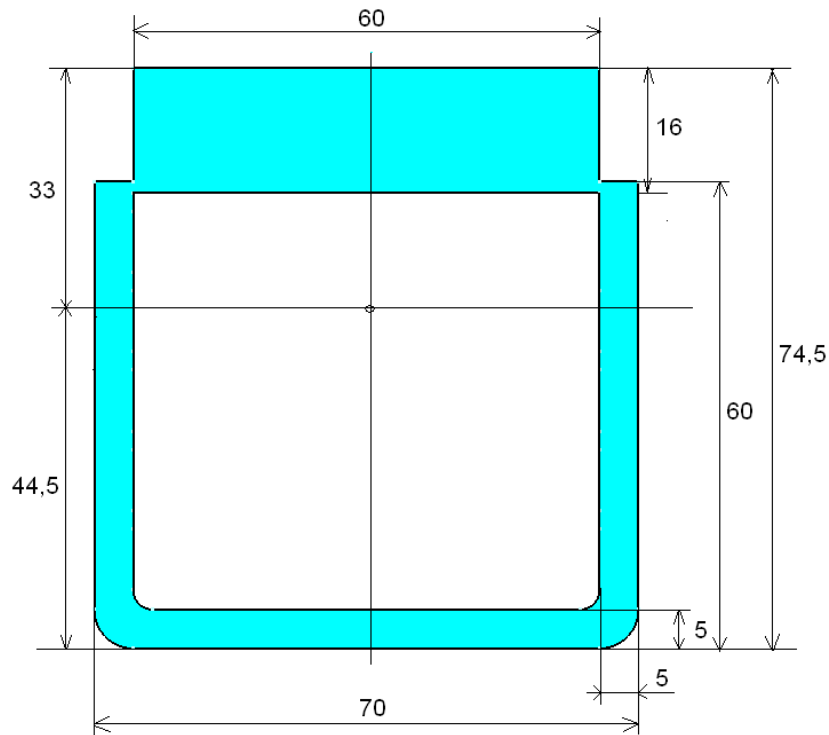


Fig. 3.15. Cross-section of string-rail body

Filling material was supposed to provide uniform transmission of load from rail top and rail body to the strings. Local bending is caused by rigidly connected rail top and rail body, which are supported on the strings (the shift between the body section and the strings takes place). In this case, local bending stresses in rail body and in a rail increase and force strength margin of rail top and rail body. The strength of the strings is slightly influenced by this assumption.

3.7.3. Initial Data on the Load of Unicar Weight

The schematic view of string-rail loading by a unicar is represented in Fig. 3.16.

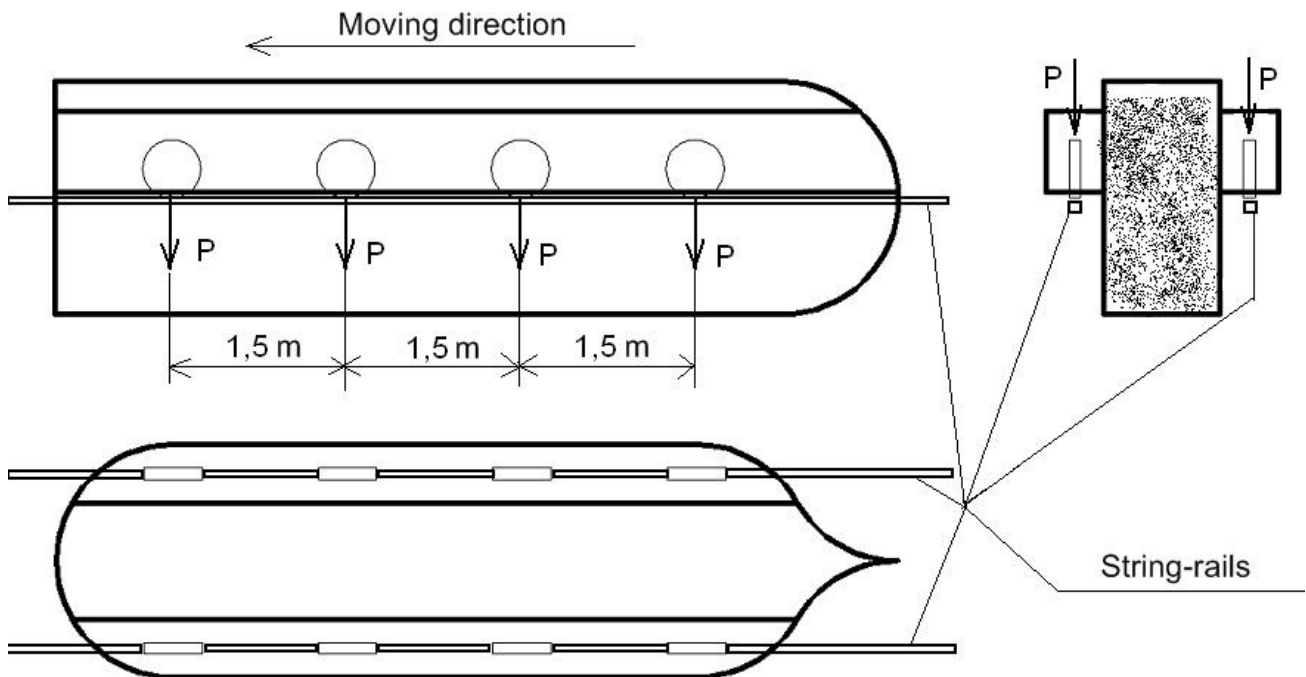


Fig. 3.16. The schematic view of string-rail loading by a unicar
(the pressure resulted from one wheel of a unicar is $P = 32000 \text{ N}$)

To make stiffness and endurance analysis of a track a unicar is supposed to create vertical force of 25.6 ton-force (half of a string-rail track (one line) is loaded by 12.8 ton-force and there is a load of 3.2 ton-force per each wheel).

To make strength analysis two unicars are supposed to move in coupling and each of them is assumed to create vertical force of 25.6 tons. To make strength analysis two unicars created vertical force of 51.2 tons (half of a string-rail track (one line) is loaded by 25.6 ton-force and there is a load of 3.2 ton-force per each wheel).

3.7.4. The Description of a Design Model and the Stages of Analysis

The calculation was carried out on the basis of finite-element analysis. The models were processed on PC using the finite-element complex Femap with NX Nastran. The finite-element model is string-rail track structure consisting of 5 spans, which total length is $250 \cdot 5 = 1250 \text{ m}$. As the finite elements linear-type elements were used. The design model consists of 11782 of assembly units and 11784 of elements. The finite-element model of suspended STS string-rail track structure is represented in Fig.3.17.

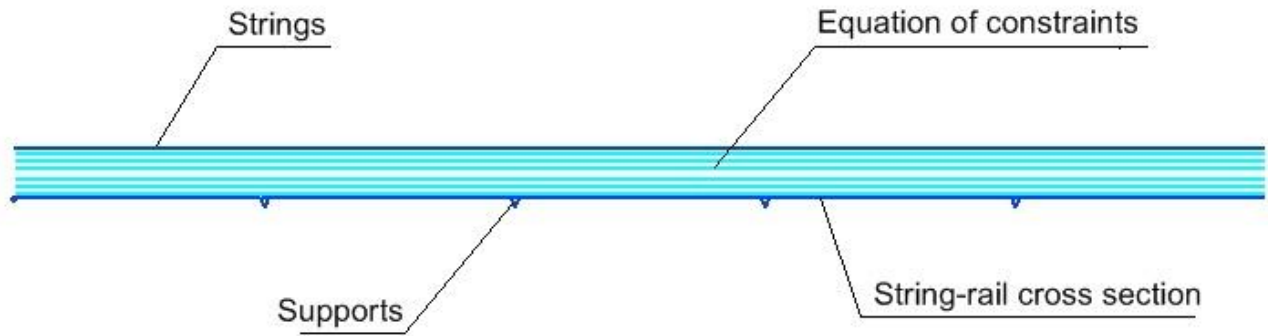


Fig. 3.17. The finite-element model of suspended STS string-rail track structure

Boundary data of the finite-element model was divided into four stages of force gaining and fixing to provide provisional assembly of a track structure and its loading.

The first stage of analysis is loading of strings under track structure weight (under rail top, rail body and filler weight) at an assembly temperature of $+40^{\circ}\text{C}$. Under gravity the strings are sagged, at that string tension is 225 ton-force. With the use of technological operations rail top and rail body are connected with the sagged strings. When assembling rail top and rail body internal forces don't occur.

The second stage of analysis includes recalculation of tension forces and sagging of a track structure under gravity depending on temperature conditions ($+100^{\circ}\text{C}$ and 0°C).

The third stage of analysis includes track structure loading by vertical forces of one unicar during performing of stiffness and endurance analysis and by vertical forces of two unicars during performing of strength analysis taking into account two temperature conditions ($+100^{\circ}\text{C}$ и 0°C).

The fourth stage of analysis includes further calculations of string-rail strength and endurance on the basis of intensively strained track analysis.

3.7.5. The Results of Analysis

The diagram of track deflection and internal forces under its own weight and the weight of a unicar at assembly temperature of $+40^{\circ}\text{C}$ are represented in Fig. 3.18 – 3.25.

The diagram of track deflection and internal forces under its own weight and the weight of a unicar at maximum temperature of $+100^{\circ}\text{C}$ are represented in Fig. 3.26 – 3.33.

The diagram of track deflection and internal forces under its own weight and the weight of a unicar at minimum temperature of 0°C are represented in Fig. 3.34 – 3.42.

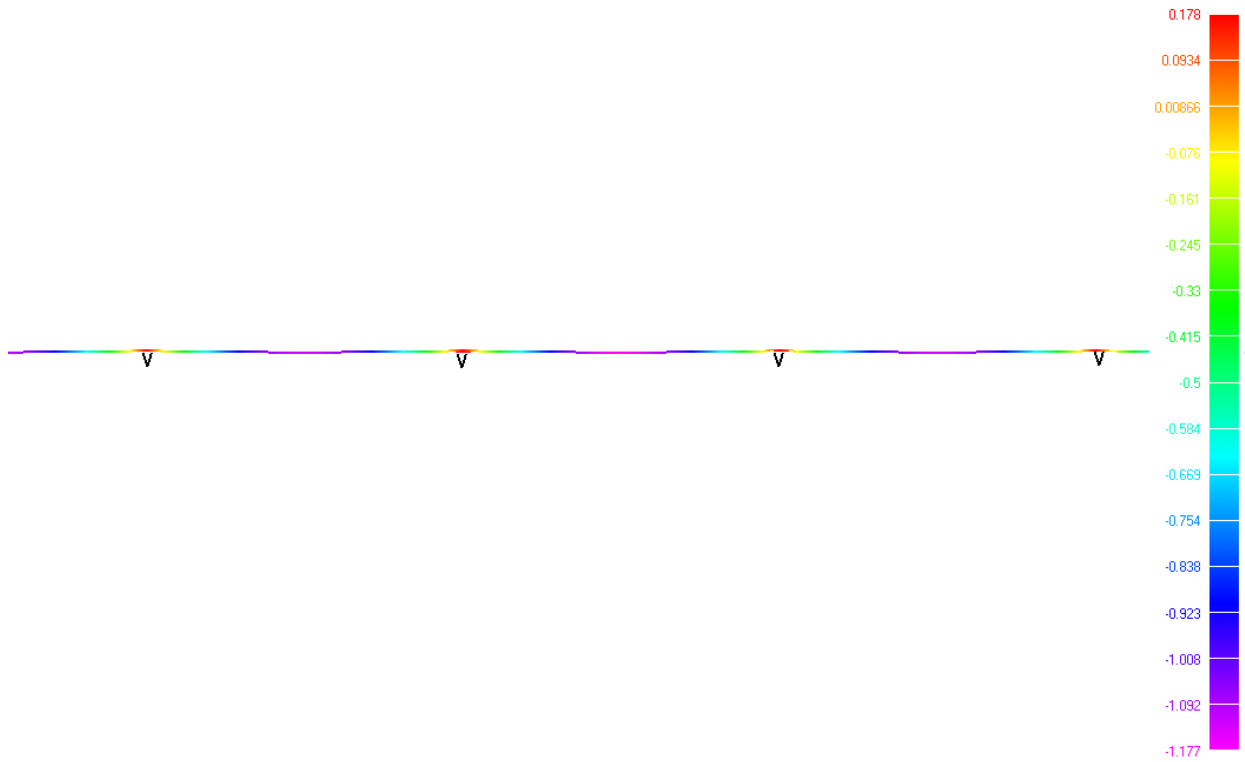


Fig. 3.18. The diagram of track deflections (meters) under its own weight at assembly temperature of +40°C (maximum deflection is 1.177 m)

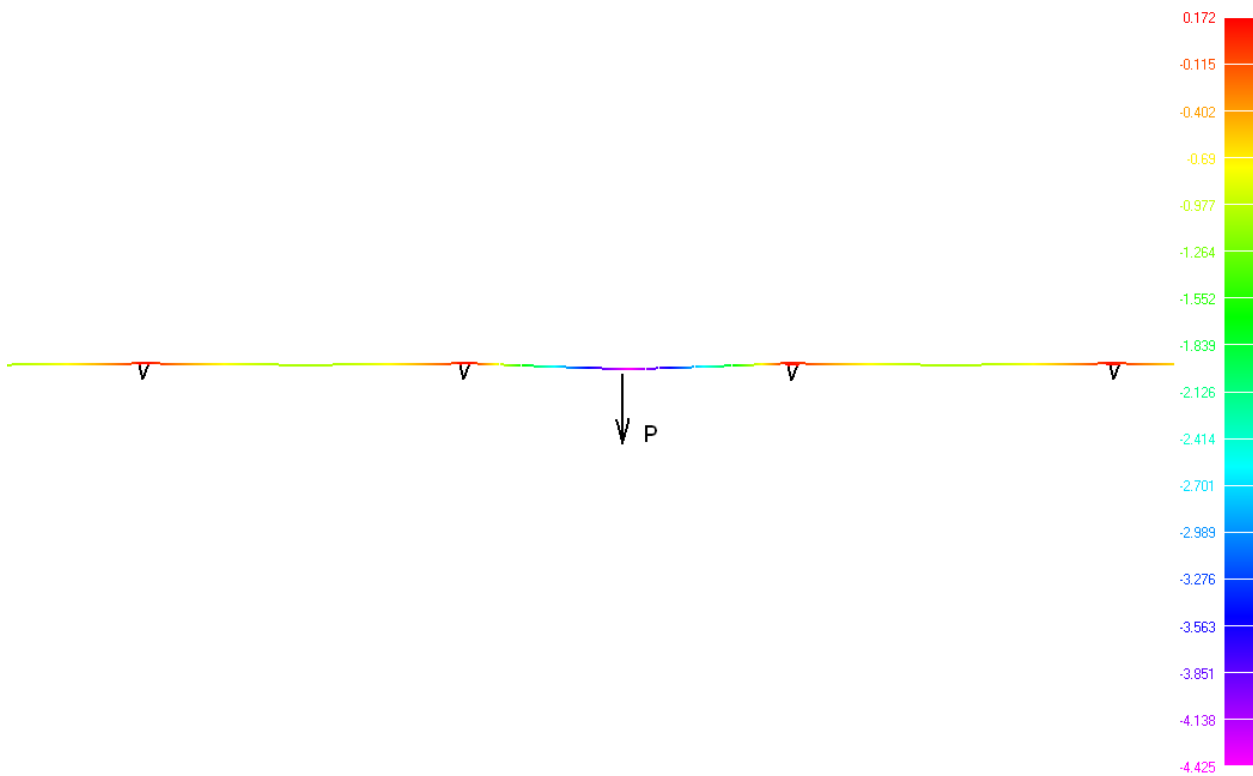


Fig. 3.19. The diagram of track deflections (meters) under its own weight and the weight of a unicar at assembly temperature of +40°C (maximum deflection is 4.425 m)

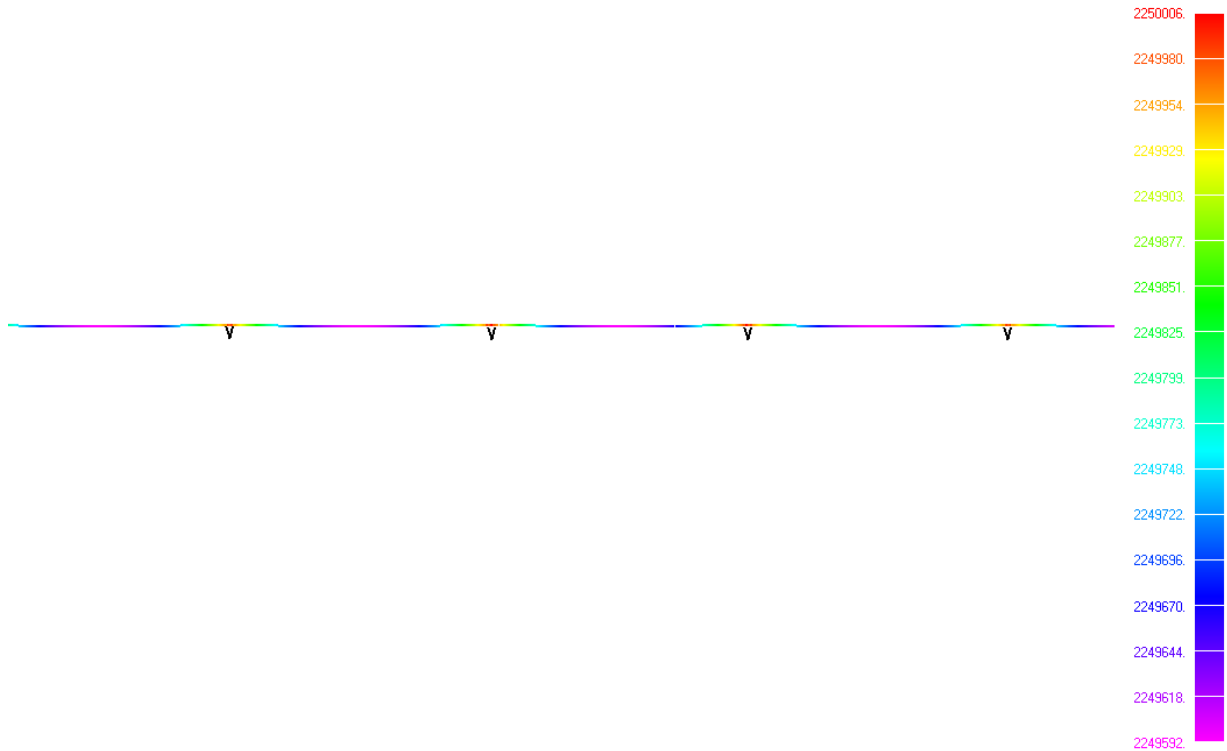


Fig. 3.20. The diagram of forces in a string (N) under its own weight at assembly temperature of +40°C (tension force along the whole length of a string is approx. uniform and is equal to 225 ton-force)

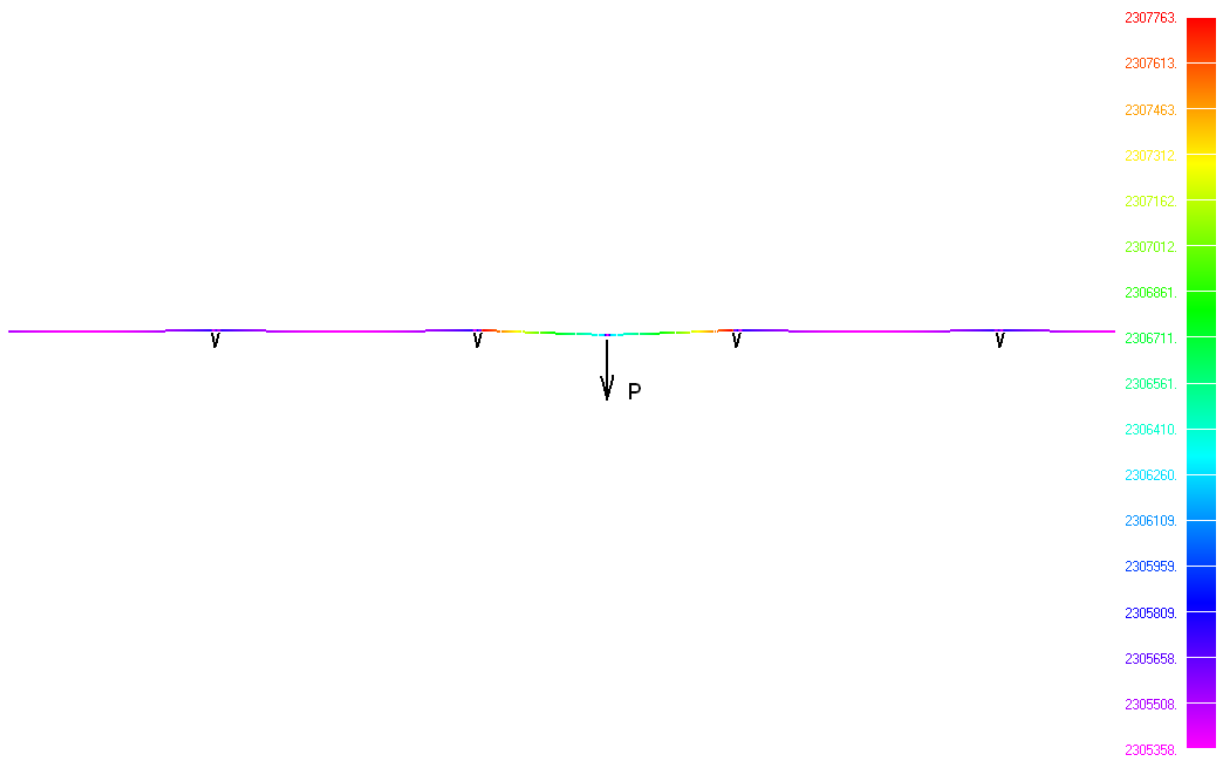


Fig. 3.21. The diagram of forces in a string (N) under its own weight and the weight of a unicar at assembly temperature of +40°C (tension force along the whole length of a string is approx. uniform and is equal to 230.7 ton-force)

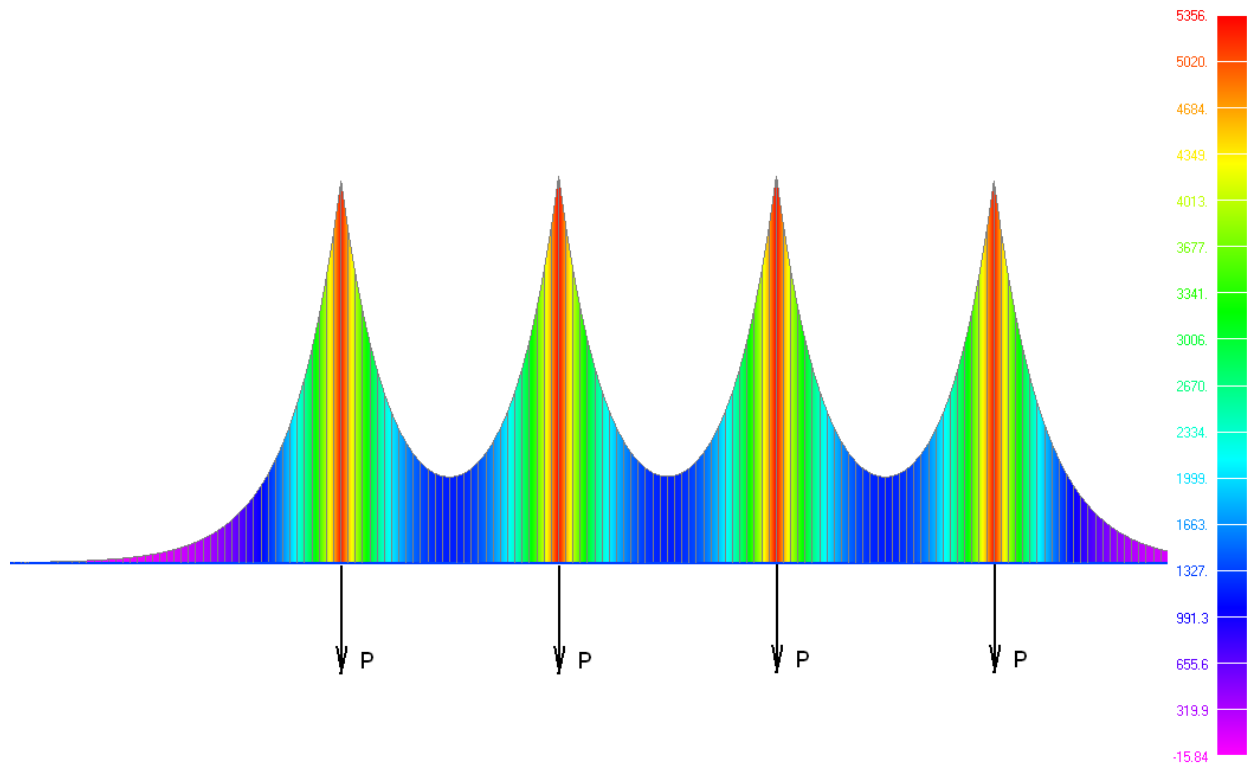


Fig. 3.22. The diagram of bending moments in string-rail cross section (N·m) under its own weight and the weight of a unicar at assembly temperature of +40°C (maximum bending moment is 5356 N·m)

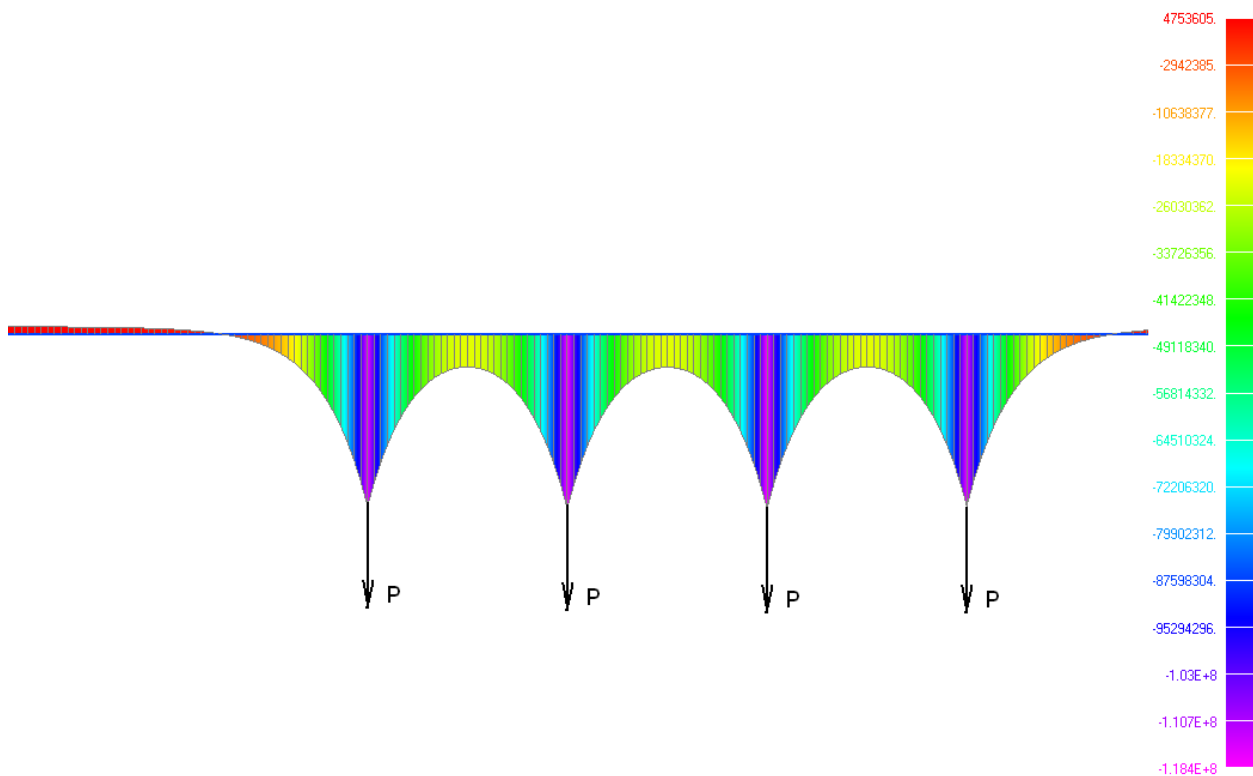


Fig. 3.23. The diagram of stresses (extension + bending) in an upper part of a rail top (Pa) under its own weight and the weight of a unicar at assembly temperature of +40°C (maximum compression stress is 118.4 MPa)

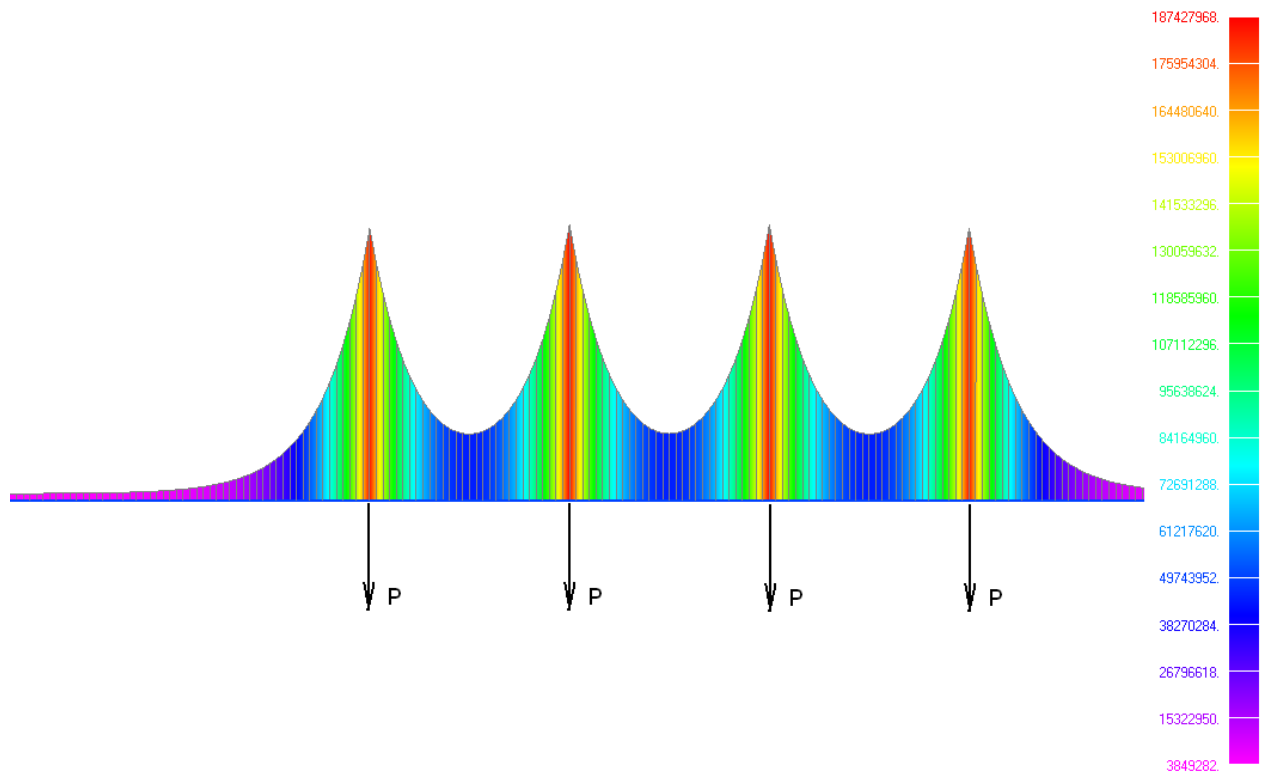


Fig. 3.24. The diagram of stresses (extension + bending) in the bottom of a rail top (Pa) under its own weight and the weight of a unicar at assembly temperature of +40°C (maximum compression stress is 187.4 MPa)

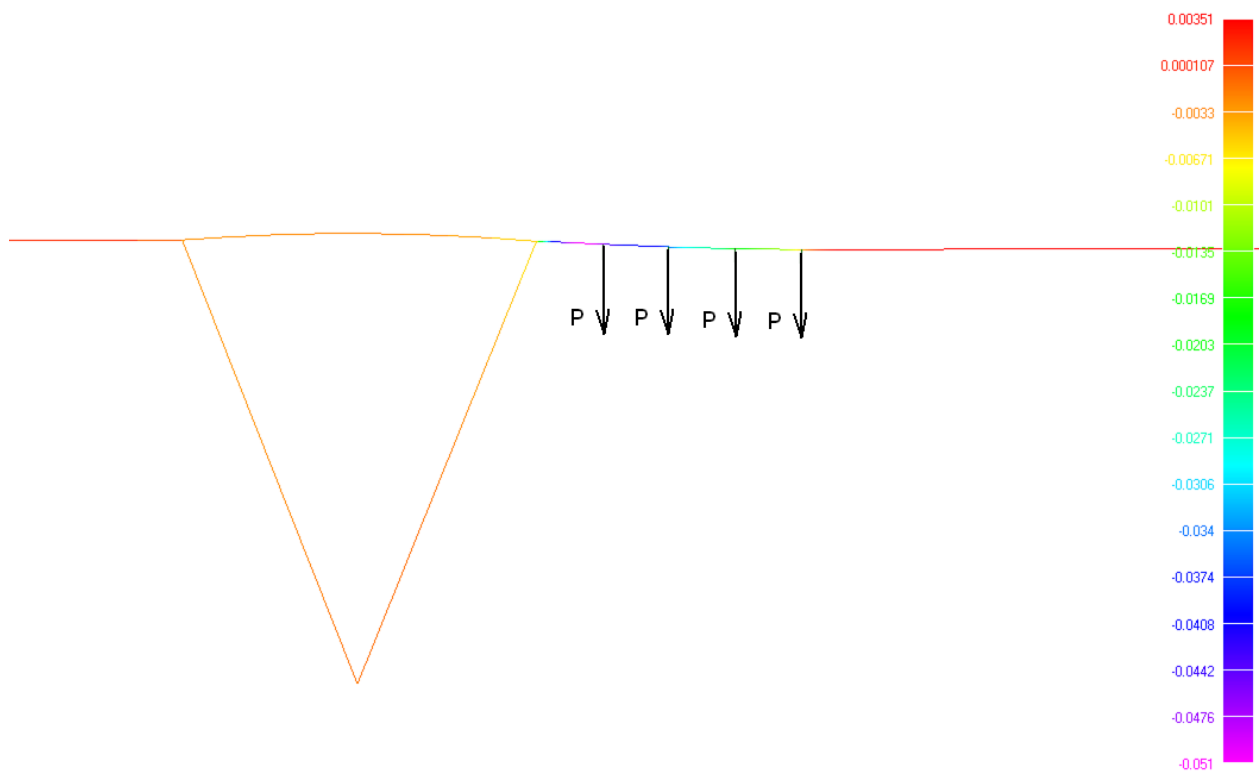


Fig. 3.25. The diagram of inclinations (deflection angle is specified in radians) under wheels caused by track weight and the weight of a unicar, located near the support, at assembly temperature of +40°C (the largest gradient of a track under the front wheel is 0.051)

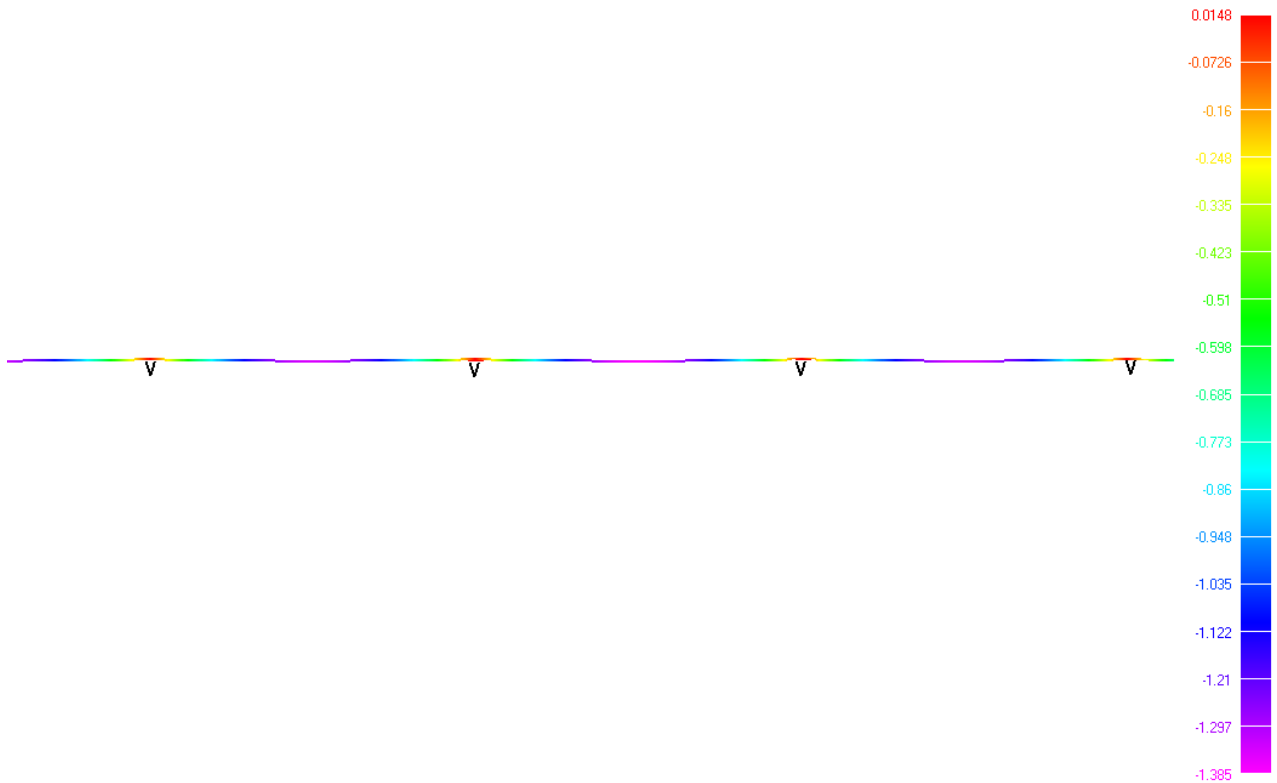


Fig. 3.26. The diagram of track deflections (meters) under its own weight at maximum temperature of +100°C (maximum deflection of a track on a span is 1.385 m)

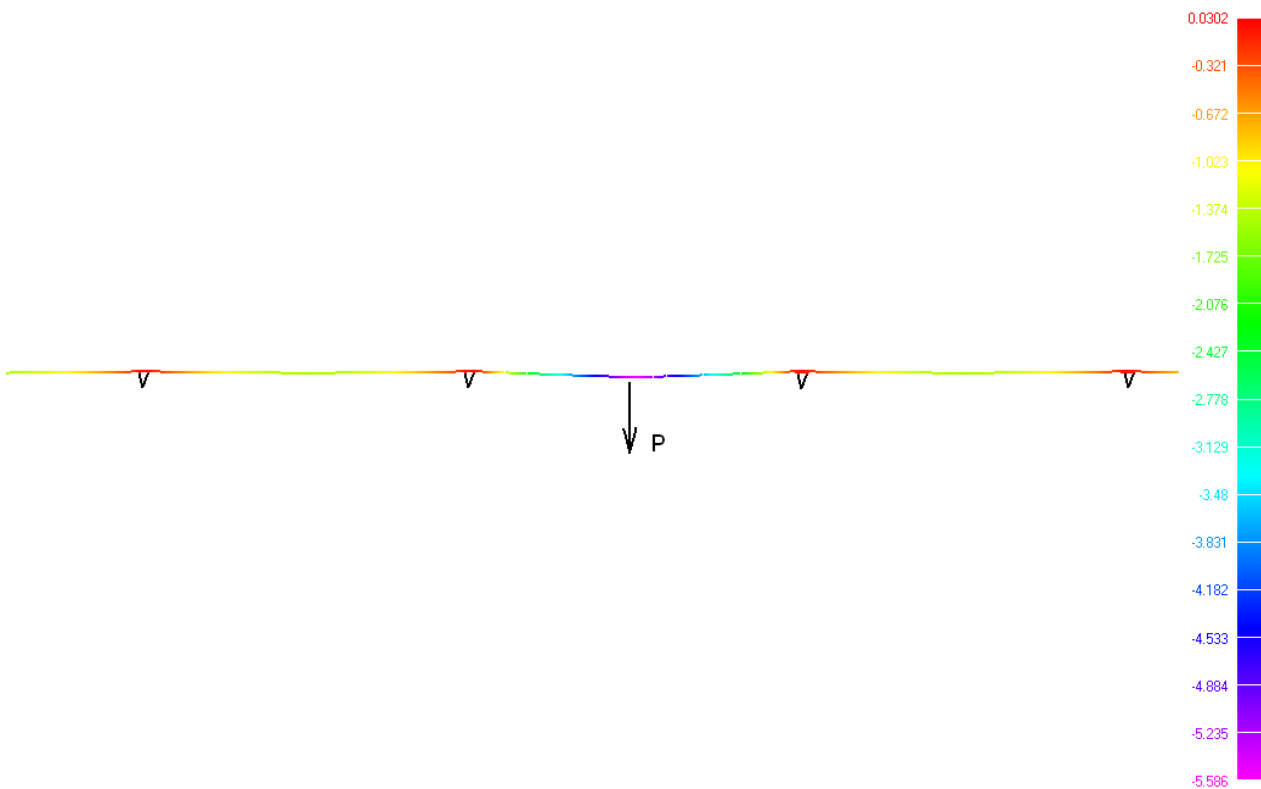


Fig. 3.27. The diagram of track deflections (meters) under its own weight and the weight of a unicar at maximum temperature of +100°C (maximum deflection of a track on a span is 5.586 m)

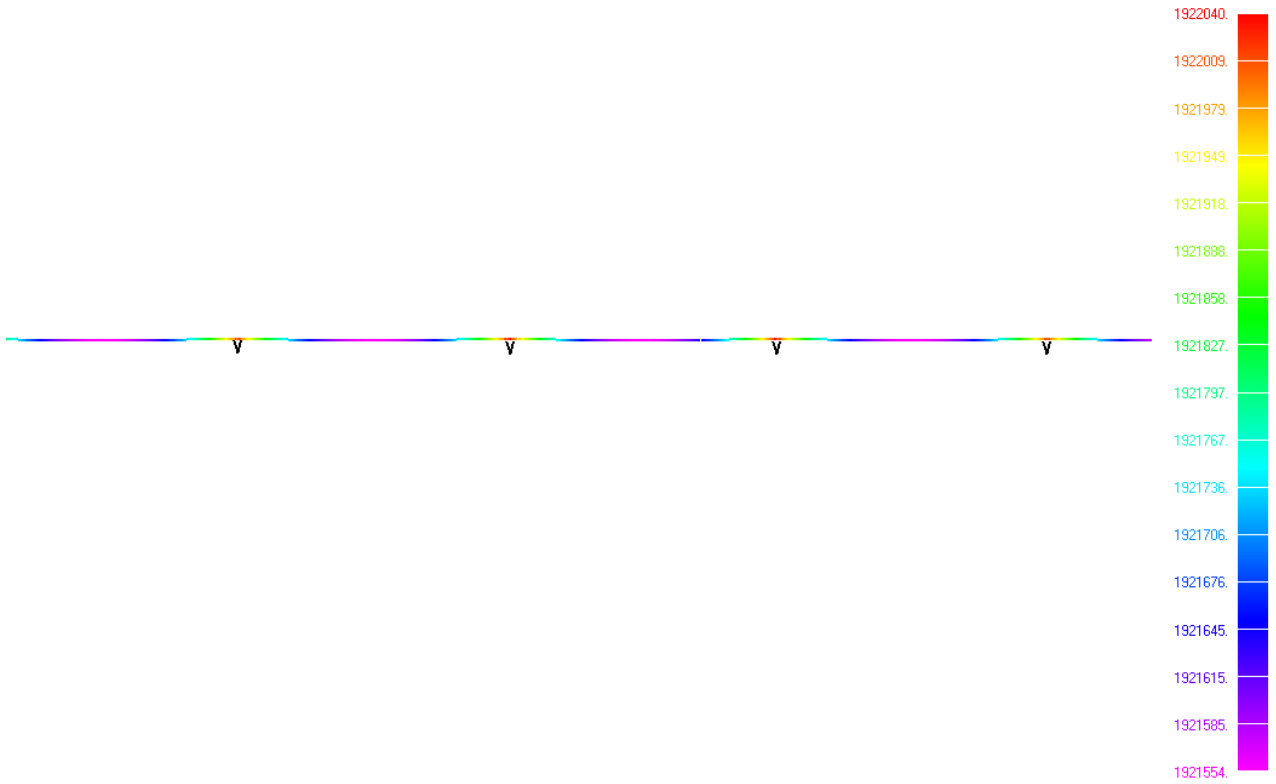


Fig. 3.28. The diagram of forces in a string (N) under its own weight at maximum temperature of +100°C (tension force along the whole length of a string is approx. uniform and is equal to 192 ton-force)

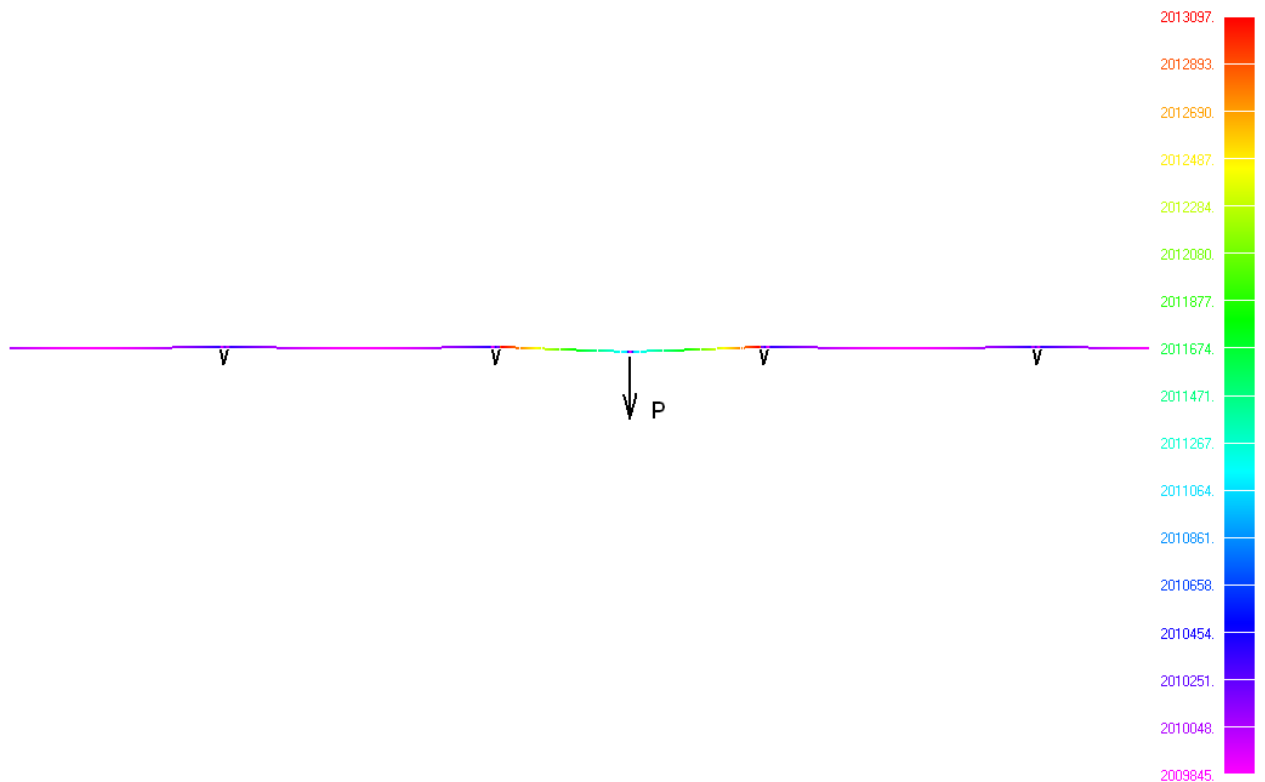


Fig. 3.29. The diagram of forces in a string (N) under its own weight and the weight of a unicar at maximum temperature of +100°C (tension force along the whole length of a string is approx. uniform and is equal to 201 ton-force)

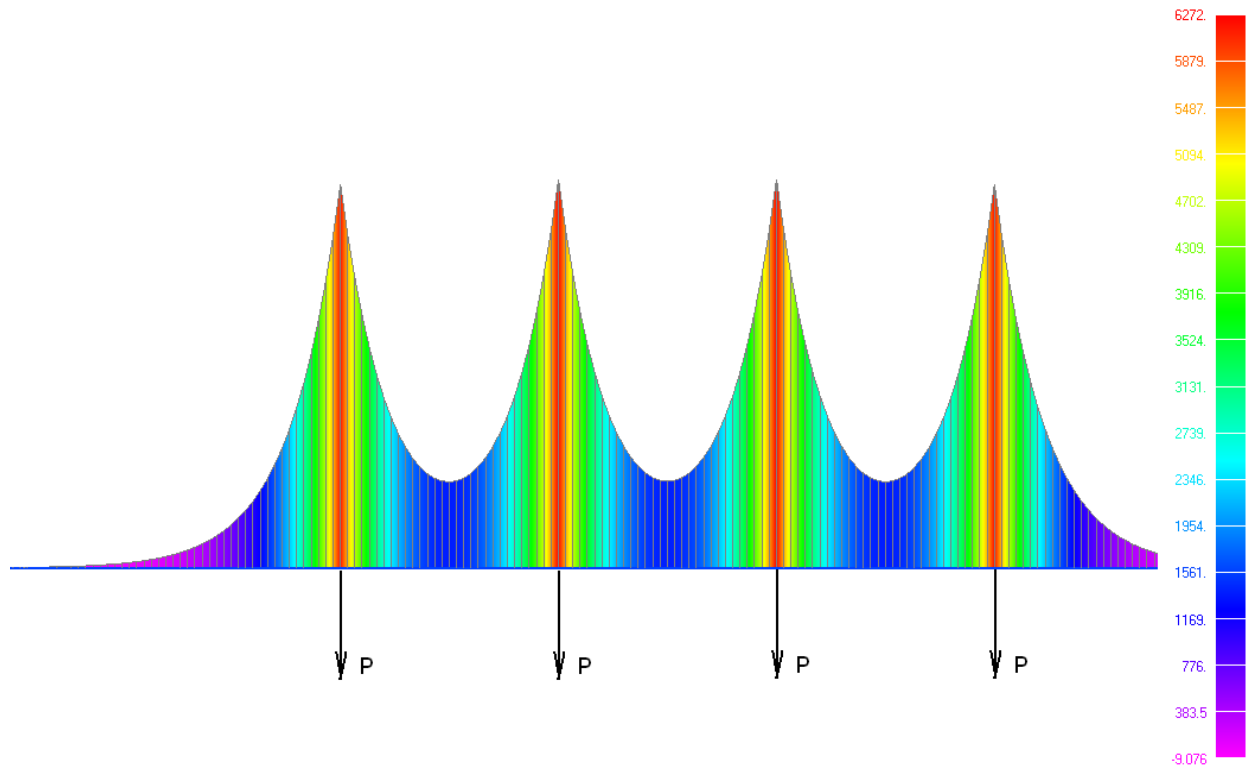


Fig. 3.30. The diagram of bending moments in string-rail cross section (N·m) under its own weight and the weight of a unicar at maximum temperature of +100°C (maximum bending moment is 6272 N·m)

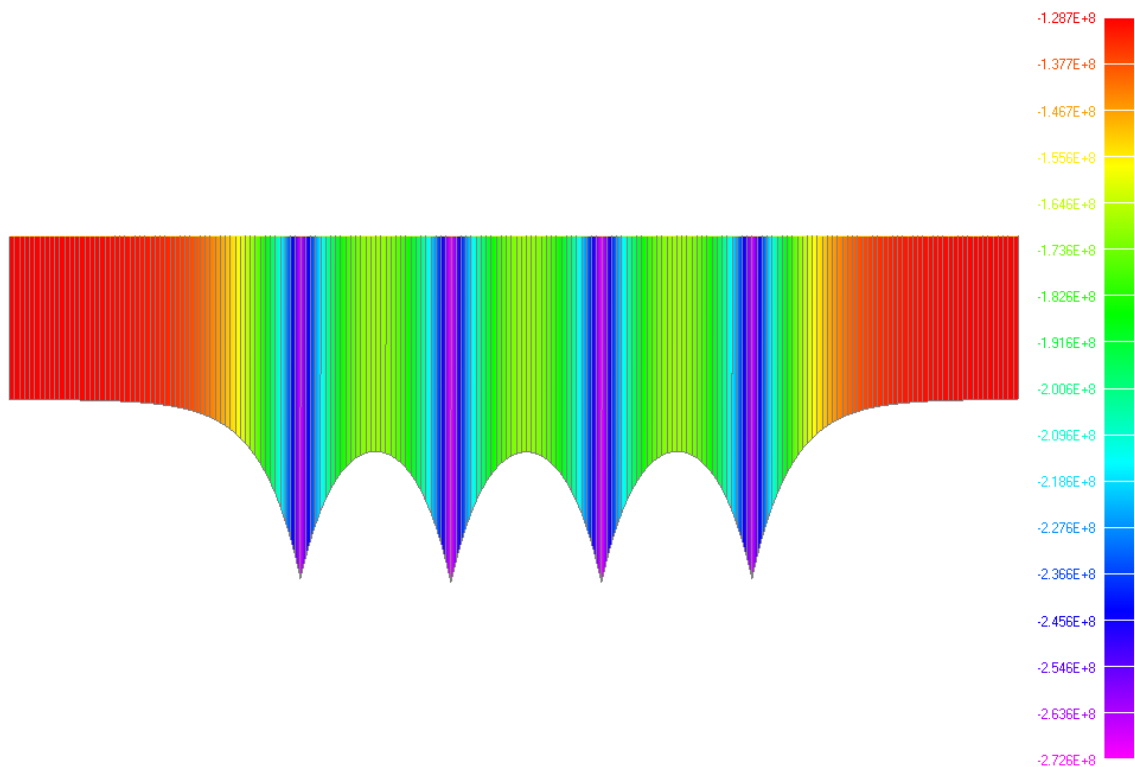


Fig. 3.31. The diagram of stresses (extension + bending) in an upper part of a rail top (Pa) under its own weight and the weight of a unicar at maximum temperature of +100°C (maximum compression stress is 272.6 MPa)

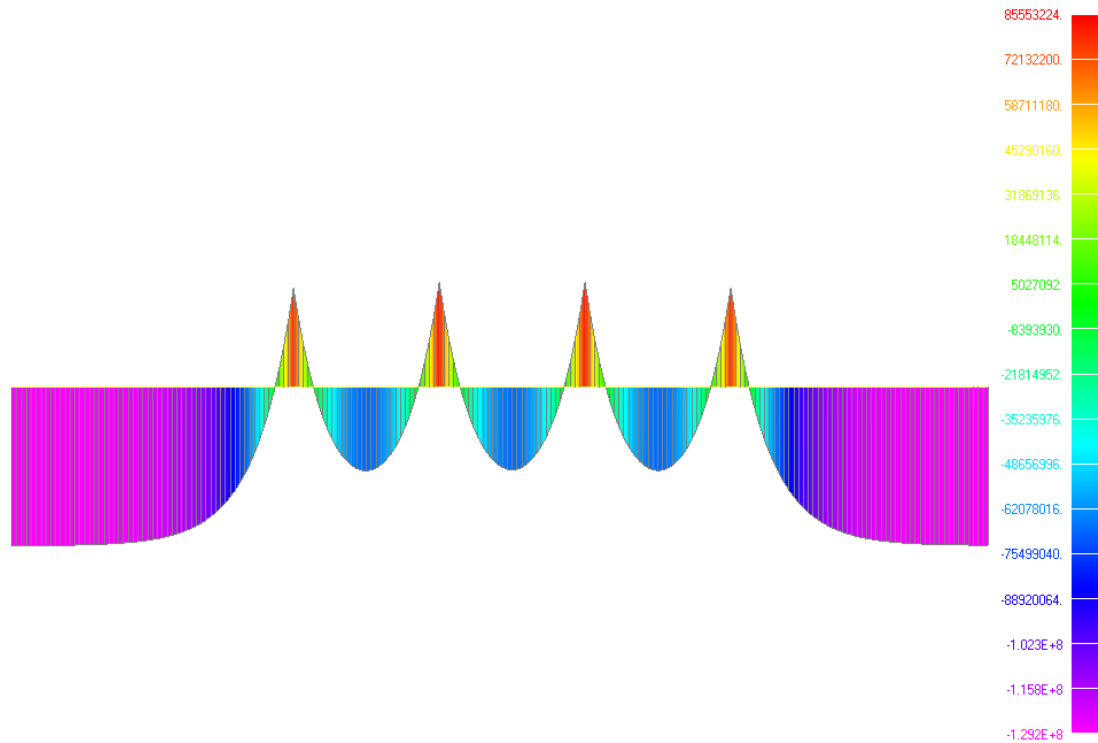


Fig. 3.32. The diagram of stresses (extension + bending) in the bottom of a rail top (Pa) under its own weight and the weight of a unicar at maximum temperature of +100°C (maximum compression stress is 129.2 MPa)

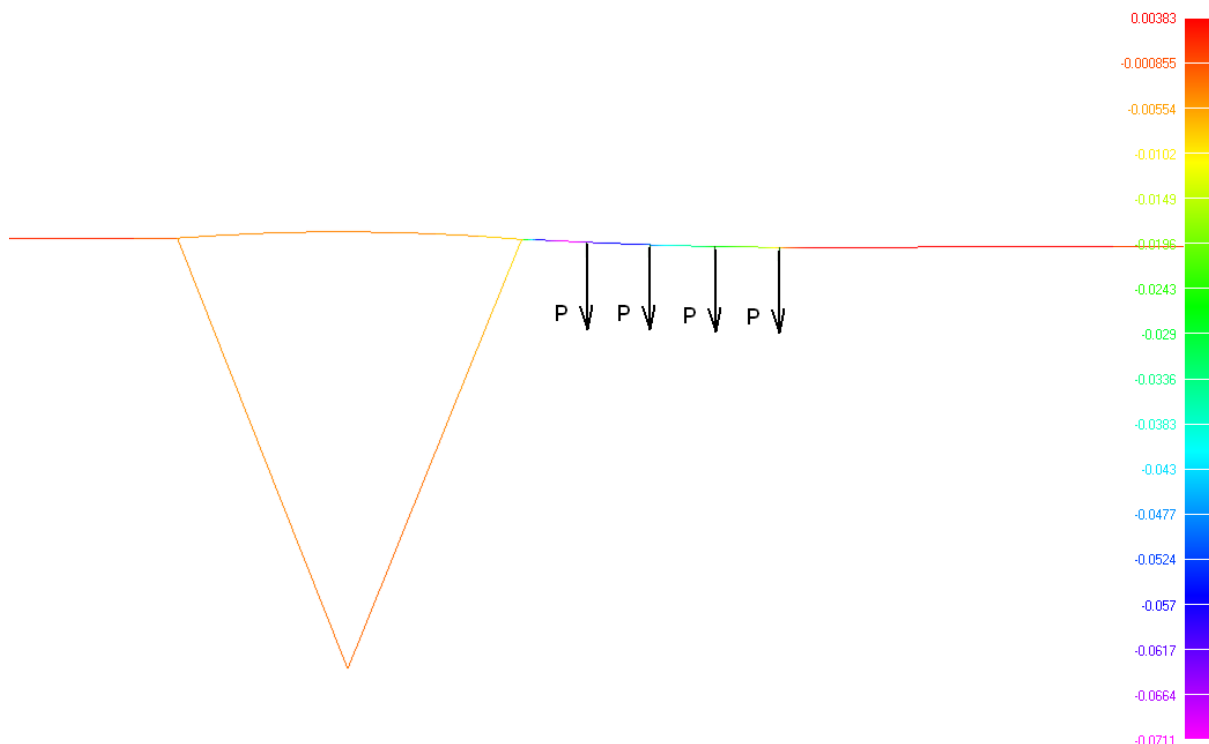


Fig. 3.33. The diagram of inclinations (deflection angle is specified in radians) under wheels caused by track weight and the weight of a unicar, located near the support at maximum temperature of +100°C (the largest gradient of a track under the front wheel is 0.071)

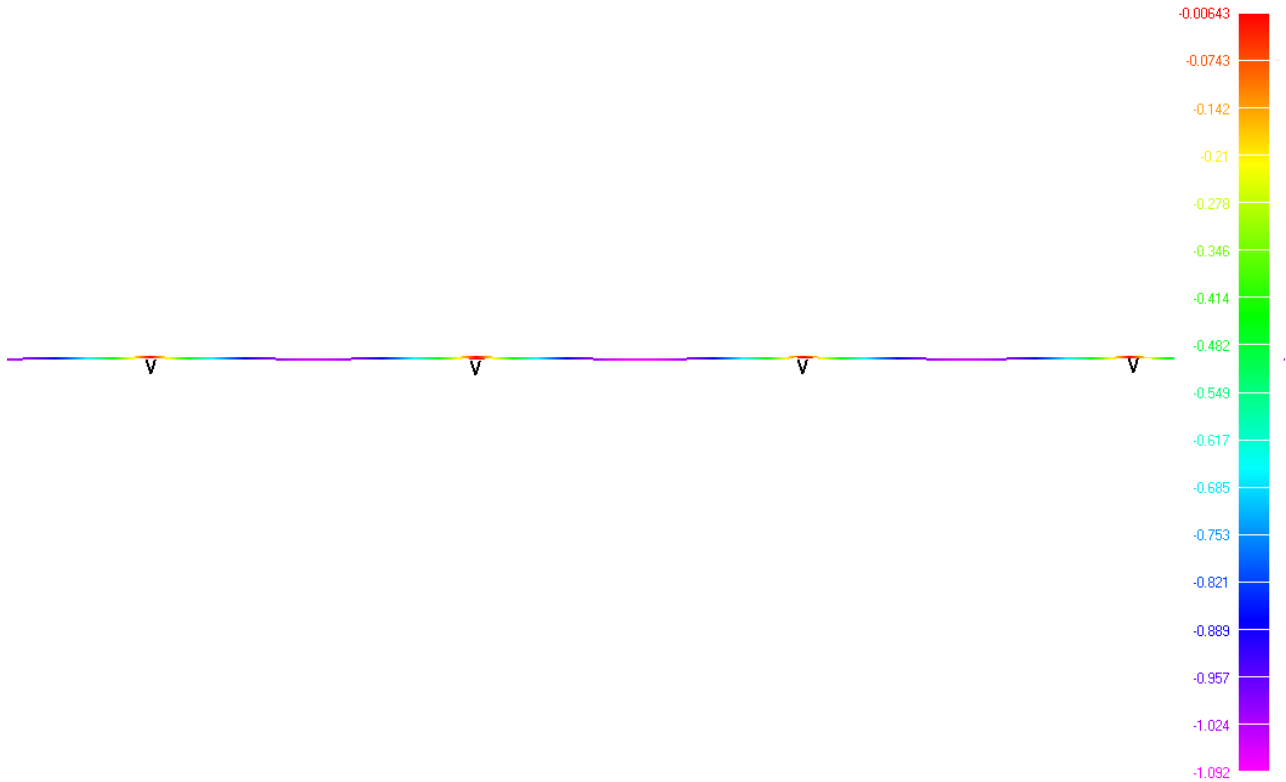


Fig. 3.34. The diagram of track deflections (meters) under its own weight at minimum temperature of 0°C (maximum track deflection is 1.092 m)

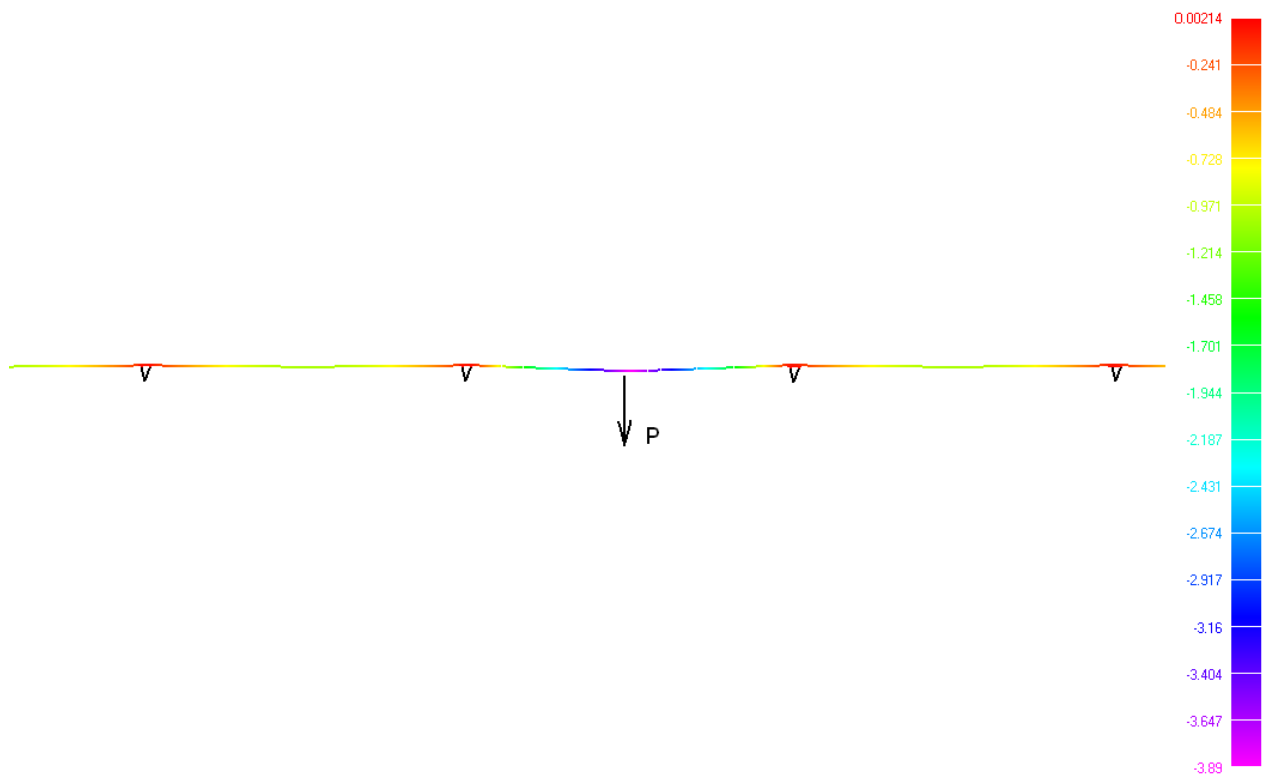


Fig. 3.35. The diagram of track deflections (meters) under its own weight and the weight of a unicar at minimum temperature of 0°C (maximum track deflection is 3.89 m)

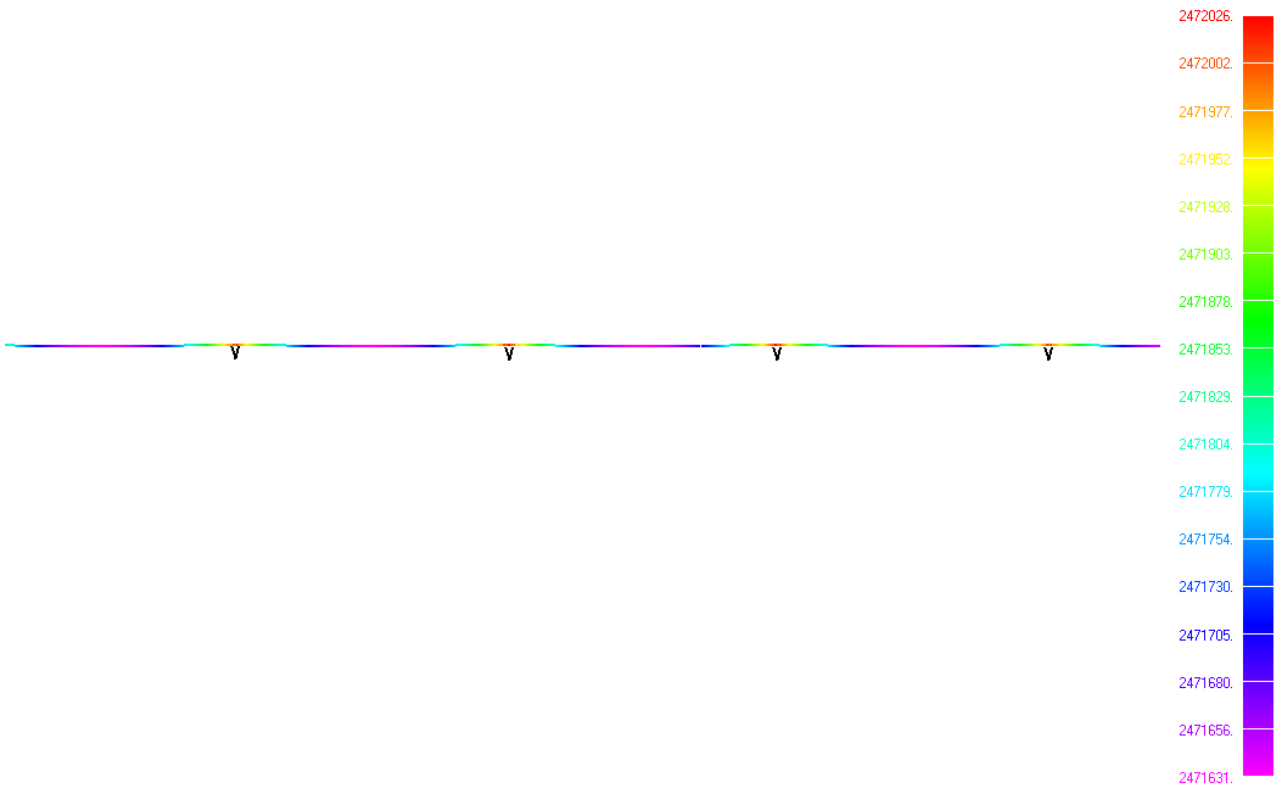


Fig. 3.36. The diagram of forces in a string (N) under its own weight at minimum temperature of 0°C (tension force along the whole length of a string is approx. uniform and is equal to 247.2 ton-force)

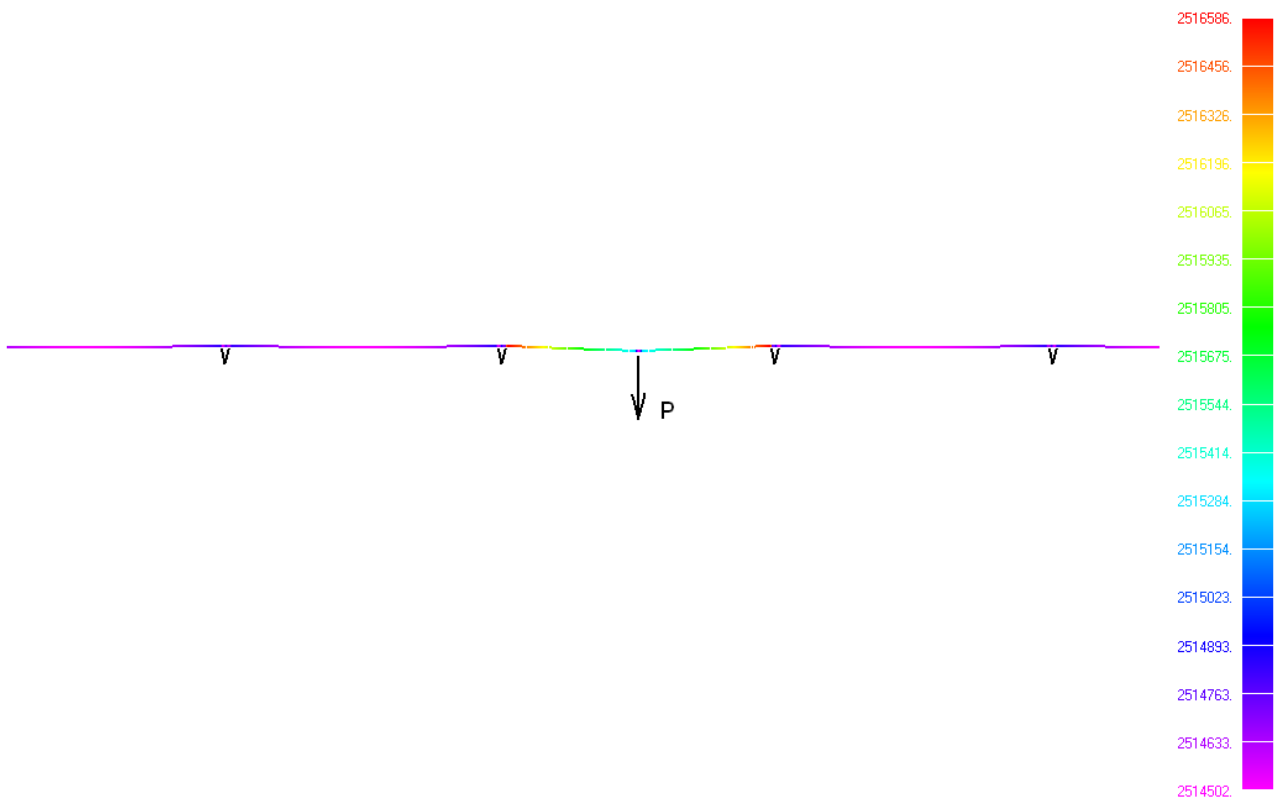


Fig. 3.37. The diagram of forces in a string (N) under its own weight and the weight of a unicar at minimum temperature of 0°C (tension force along the whole length of a string is approx. uniform and is equal to 251.5 ton-force)

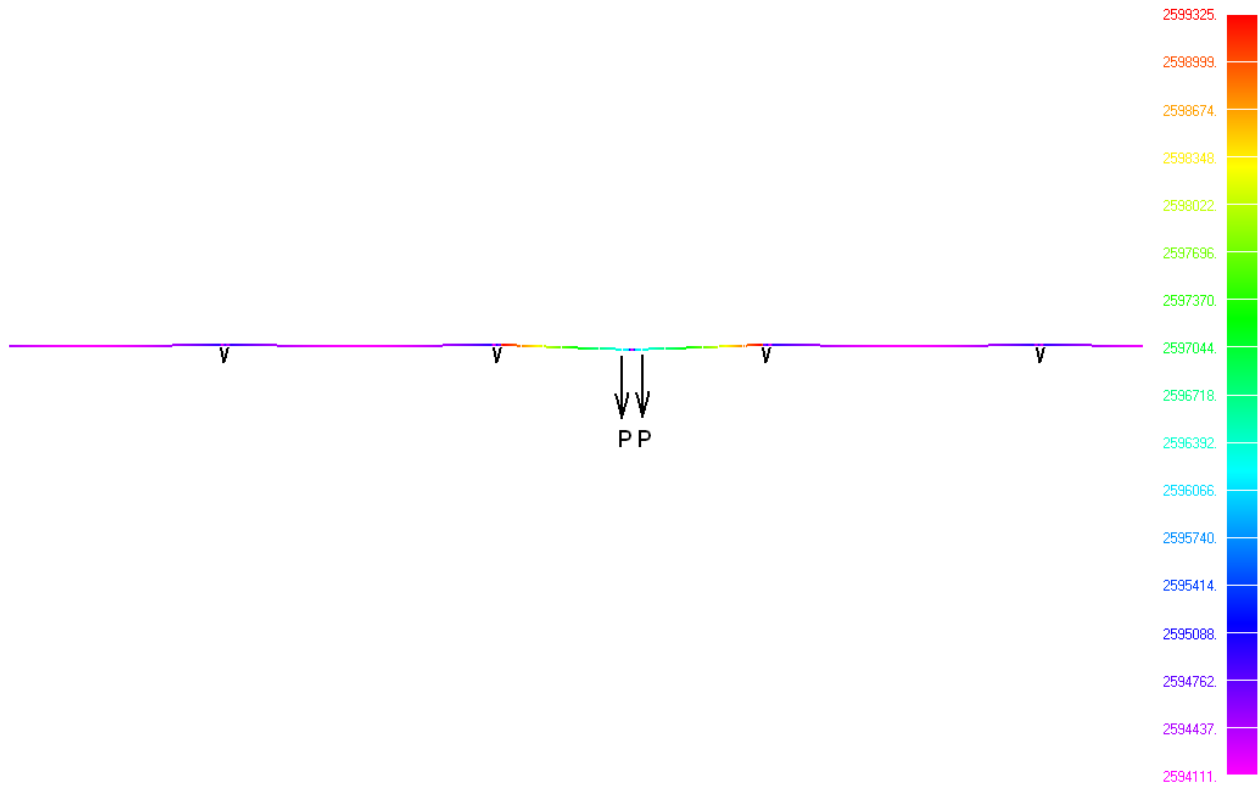


Fig. 3.38. The diagram of forces in a string (N) under its own weight and the weight of two unicars at minimum temperature of 0°C (tension force along the whole length of a string is approx. uniform and is equal to 260 ton-force)

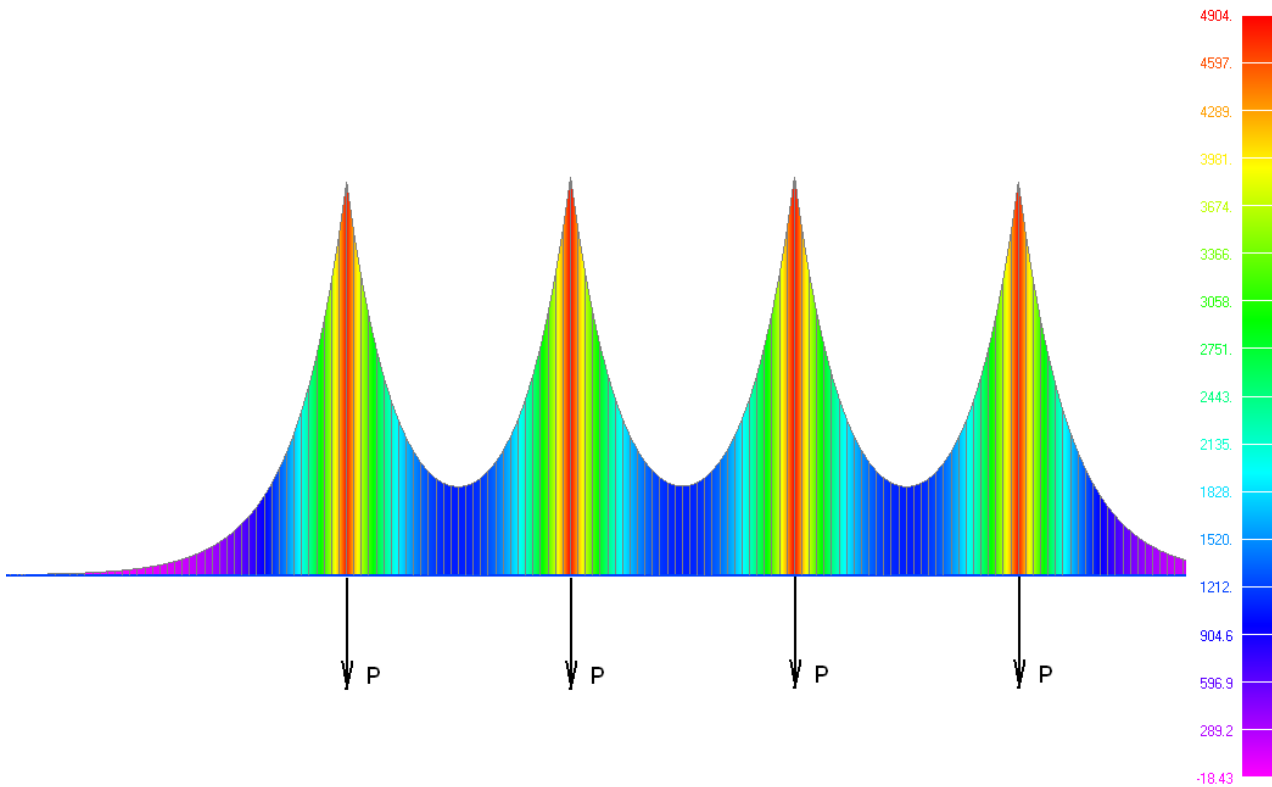


Fig. 3.39. The diagram of bending moments in string-rail cross section (N·m) under its own weight and the weight of a unicar at minimum temperature of 0°C (maximum bending moment is 4904 N·m)

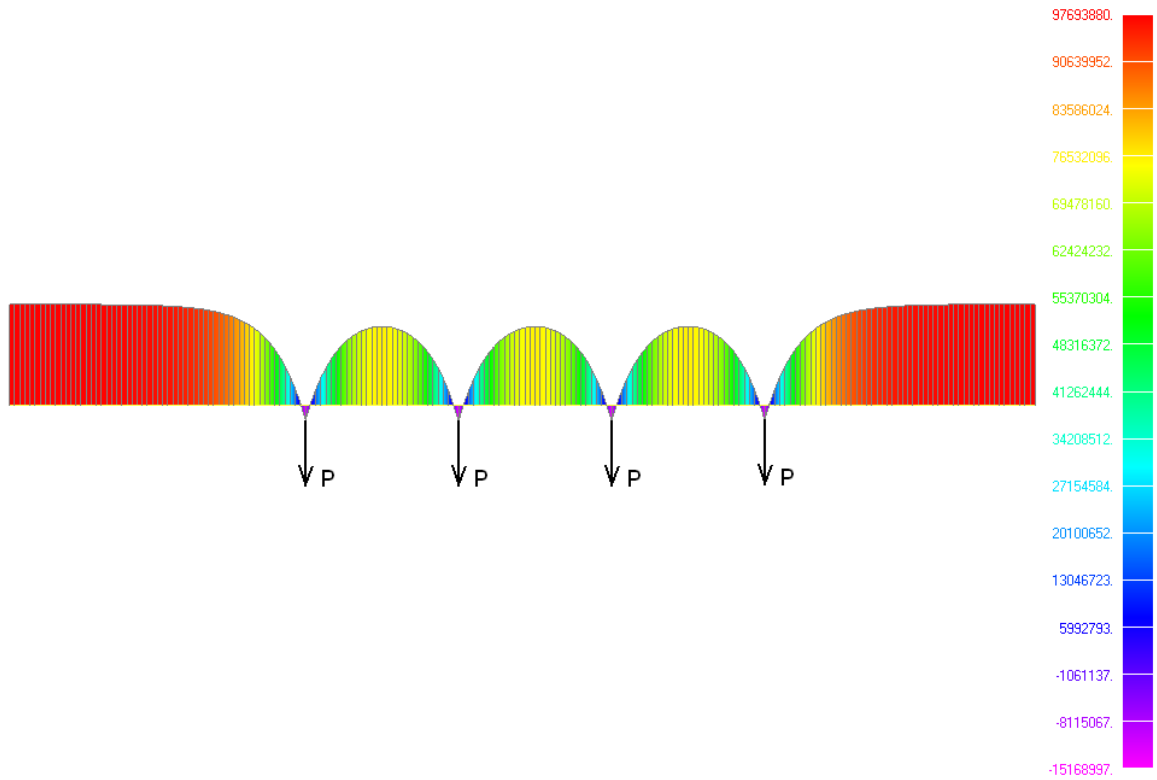


Fig. 3.40. The diagram of stresses (extension + bending) in an upper part of a rail top (Pa) under its own weight and the weight of a unicar at minimum temperature of 0°C (maximum compression stress is 97.7 MPa)

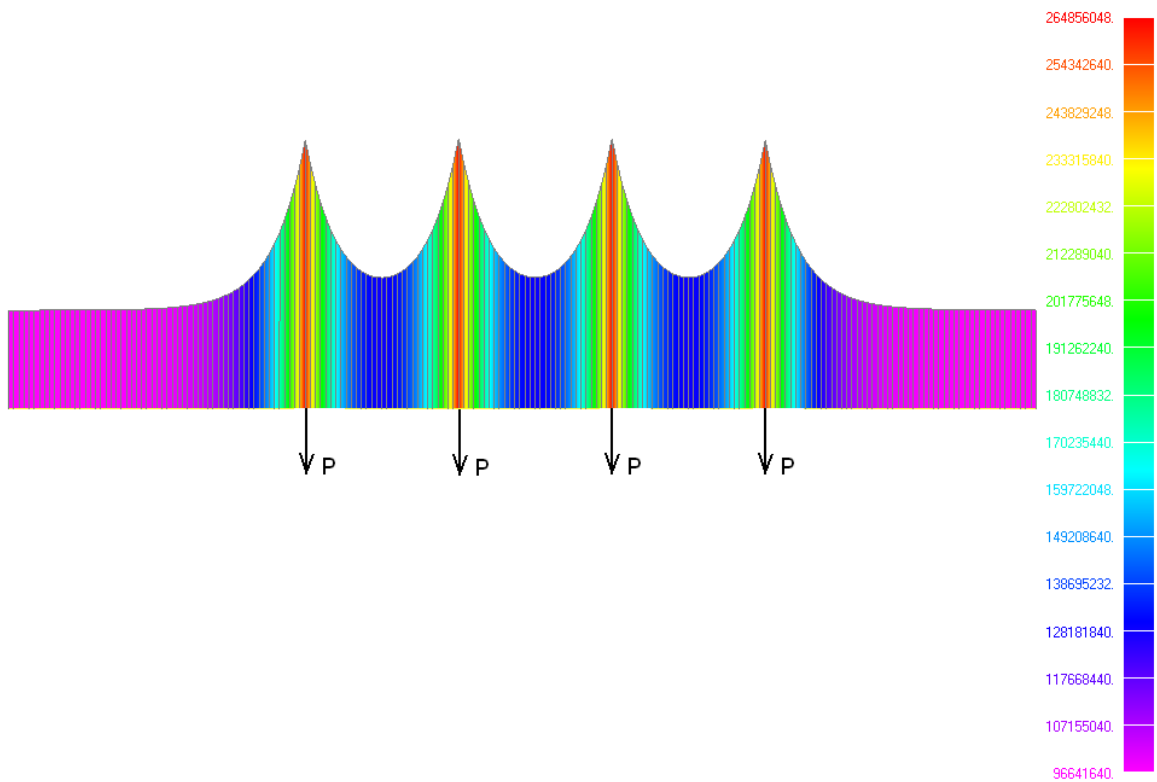


Fig. 3.41. The diagram of stresses (extension + bending) in the bottom of rail body (Pa) under its own weight and the weight of a unicar at minimum temperature of 0°C (maximum compression stress is 264.9 MPa)

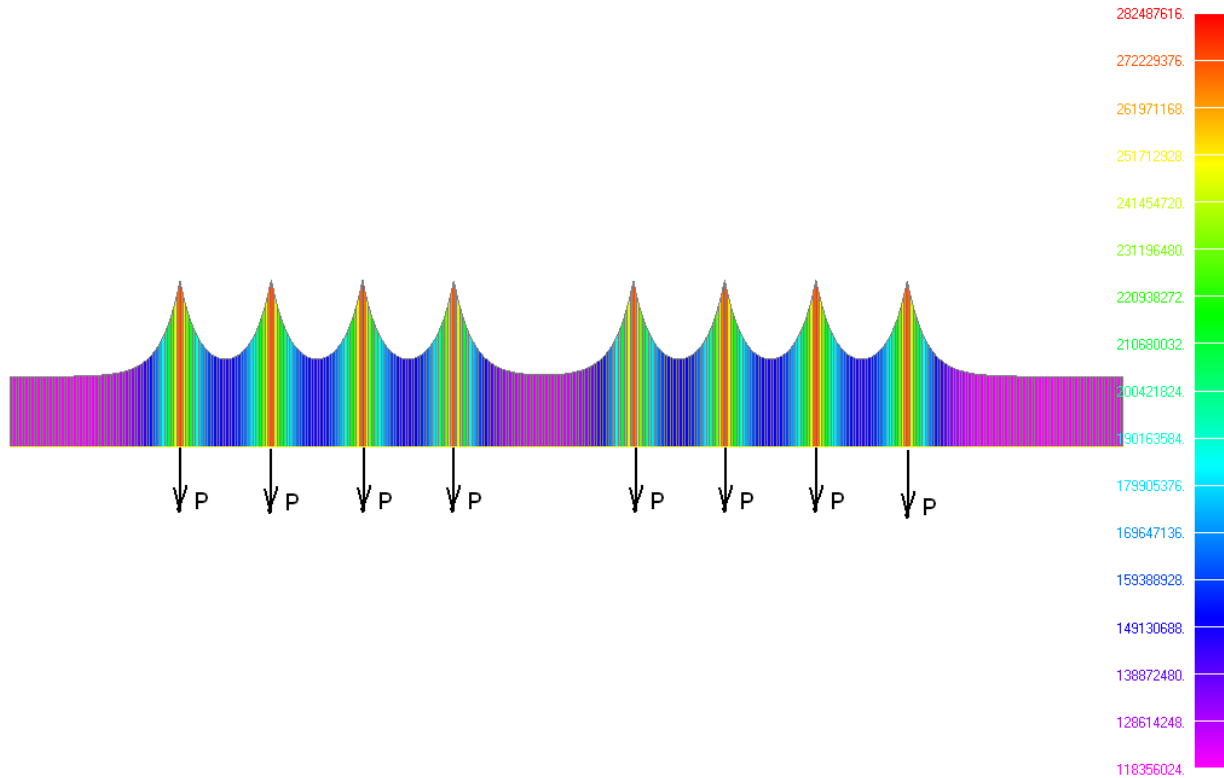


Fig. 3.42. The diagram of stresses (extension + bending) in the bottom of rail body (Pa) under its own weight and the weight of two unicars at minimum temperature of 0°C (maximum compression stress is 282.5 MPa)

3.7.6. Strength and Endurance Analysis of Strings

3.7.6.1. Strength Analysis of Strings

Strings produced of high strength wire will be analyzed. To carry out strength analysis of the strings two unicars (in mechanical coupling) should be located on a span.

Strength analysis of the strings should be carried out in accordance with the formula:

$$\sigma_{\max} \leq R_y \cdot m \quad (3.1.)$$

$$\sigma_{\max} = \frac{T_{\max}}{A_{strun}} = \frac{260 \cdot 10^4}{0.002356} = 1104 \cdot 10^6 = 1104 \text{ MPa} \text{ (see Fig. 3.38) is the largest tensile strength of the}$$

strings under the weight of two unicars;

$A_{strun} = 0.002356 \text{ m}^2$ is the cross section of one rail string;

$m = 0.95$ is the coefficient of working conditions;

$R_y = 1336 \text{ MPa}$ is yield resistance of string material (taking into account anchor mounting).

$$\sigma_{\max} = 1104 \text{ MPa} \leq R_y \cdot m = 1336 \cdot 0.95 = 1269 \text{ MPa}$$

The strength of the strings is provided.



3.7.6.2. Endurance Analysis of Strings

Endurance Analysis in Accordance with Russian Standard SNiP2.05.03-84* (Bridges and Pipes)

Endurance of strings (high-strength wires) is not less than endurance of steel ropes. Endurance analysis of bridge ropes in accordance with SNiP is carried out by the formula:

$$\sigma_{\max} \leq m_1 \gamma_{ws} R_y m \quad (3.2)$$

γ_{ws} is the coefficient of stresses variability.

$$\gamma_{ws} = \frac{0.15}{\zeta \cdot \mathcal{G} \cdot [(0.884 \cdot \beta_s - 0.387) - (0.884 \cdot \beta_s - 0.455) \cdot \rho]} \quad (3.3)$$

ρ is the coefficient of cycle asymmetry $\rho = \frac{\sigma_{\min}}{\sigma_{\max}}$;

$m_1 = 1.0$ is the coefficient of rope working conditions in endurance analysis for flexible bearing elements when the stress in a rope is regulated;

$\mathcal{G} = 1.1$ the coefficient depends on load length of influence line;

$\zeta = 1.0$ is the same as for railway bridge;

$\beta_s = 1.3$ is the effective coefficient of stress concentration at anchoring in clamp;

$m = 0.9$ is the coefficient of working conditions.

At maximum temperature of +100°C the following extension will occur in the strings:

$$\sigma_{\max} = \frac{T}{A_{ctrun}} = \frac{201 \cdot 10^4}{0.002356} = 853 \cdot 10^6 = 853 \text{ MPa} \quad (\text{see Fig. 3.28})$$

$$\sigma_{\min} = \frac{T}{A_{ctrun}} = \frac{192 \cdot 10^4}{0.002356} = 815 \cdot 10^6 = 815 \text{ MPa} \quad (\text{see Fig. 3.29})$$

$$\rho = 815/853 = 0.955$$

$$\gamma_{ws} = \frac{0.15}{1.1[(0.884 \cdot 1.3 - 0.387) - (0.884 \cdot 1.3 - 0.455) \cdot 0.955]} = 1.378 > 1.0 \quad \text{take } \gamma_{ws} = 1.0$$

At lower temperatures the coefficient of cycle asymmetry $\rho > 0.955$ and thus $\gamma_{ws} > 1$. At temperature

of 0°C find $\sigma_{\max} = \frac{T}{A_{ctrun}} = \frac{251.5 \cdot 10^4}{0.002356} = 1067.5 \cdot 10^6 = 1067.5 \text{ MPa}$ (see Fig. 3.37)

Prove of assumption:

$$\sigma_{\max} = 1067.5 \text{ MPa} \leq m_1 \gamma_{ws} R_y m = 1.0 \cdot 1.0 \cdot 1336 \cdot 0.9 = 1202.4 \text{ MPa}$$

Endurance is provided.



Endurance Analysis According to ENV

Endurance estimate is calculated from the formula:

$$\Delta\sigma \leq \frac{\Delta\sigma_c}{\gamma_f} \quad (3.4)$$

where:

$\Delta\sigma = \sigma_{\max} - \sigma_{\min}$ is current stress range;

$\gamma_{Mf} = 1.25$ is reliability coefficient in accordance with endurance limit;

$\Delta\sigma_R$ is maximum permissible stress range at a given number of loading cycles N.

$$\text{When } N < 5\,000\,000 \quad \Delta\sigma_R = \frac{\Delta\sigma_c}{\sqrt[3]{\frac{N}{20\,000\,000}}} \quad (3.5)$$

N is predetermined number of stress cycles ;

$\Delta\sigma_c$ is maximum permissible stress range at 2 000 000 of symmetric cycles of details and compounds (double endurance limit). To assess the endurance of rope strands, the knot with the largest stress is considered. It is the knot of strand fixing in wedge clamp. According to Eurocode maximum permissible stress range at 2 000 000 of cycles is $\Delta\sigma_c = 112$ MPa.

when N = 5 000 000 cycles

$$\Delta\sigma_D = \frac{\Delta\sigma_c}{\sqrt[3]{\frac{N}{20\,000\,000}}} = \frac{112}{\sqrt[3]{\frac{5\,000\,000}{20\,000\,000}}} = \frac{112}{1.357} = 82.5 \text{ MPa}$$

when N = 100 000 000 cycles

$$\Delta\sigma_R = \frac{\Delta\sigma_D}{\sqrt[5]{\frac{N}{50\,000\,000}}} = \frac{82.5}{\sqrt[5]{\frac{100\,000\,000}{50\,000\,000}}} = \frac{82.5}{1.82} = 45.3 \text{ MPa}$$

The largest stress range will occur at maximum temperature of +100°C.

$$\Delta\sigma = \sigma_{\max} - \sigma_{\min} = 853 - 815 = 38 \text{ MPa.}$$

$$\Delta\sigma = 38 \text{ MPa} \leq \frac{\Delta\sigma_c}{\gamma_{Mf}} = \frac{82.5}{1.25} = 45.3 \text{ MPa}$$

String endurance is provided for more than 100 million cycles, i.e. has no limit (total volume of carriage by 15 ton unicars on STS track is 1.5 billion tons).



3.7.7. Strength and Endurance Analysis of String-Rail Section

3.7.7.1. Strength Analysis of String-Rail Section

Strength analysis is carried out towards the most weakened cross section of a string-rail which is crosscut welds in the rail top and in the rail body. To make strength analysis two unicars are located on the span (in mechanical coupling).

Endurance analysis of steel structure elements and their connections should be carried out by the following formula:

$$\sigma_{\max} \leq R_y \cdot m \quad (3.6)$$

$\sigma_{\max} = 282.5 \text{ MPa}$ (see Fig. 3.42) is maximum stress of bottom extension of two unicars;

$m = 0.9$ – is the coefficient of working conditions;

$R_y = 335 \text{ MPa}$ is estimated yield resistance of body material. Due to good weldability of 09Г2 steel, the strength of weld material is accepted the same as the strength of body material.

$$\sigma_{\max} = 282.5 \text{ MPa} \leq R_y \cdot m = 335 \cdot 0.9 = 301.5 \text{ MPa}$$

Strength of string-rail section is provided.

3.7.7.2. Endurance Analysis of String-Rail Section

Strength analysis is carried out towards the most weakened cross section of a string-rail which is crosscut welds in the rail top and in the rail body. The analysis is carried out at three temperature rates:

1) At maximum temperature of $+100^\circ\text{C}$ compression of body is $\Delta t = 100 - 40 = 60^\circ\text{C}$.

$$\sigma_{100} = \alpha \cdot E \cdot \Delta t = 1.2 \cdot 10^{-5} \cdot 2 \cdot 10^{11} \cdot 60 = 144 \cdot 10^6 \text{ Pa} = 144 \text{ MPa}$$

2) At assembly temperature of $+40^\circ\text{C}$ (statistically most frequent) $\Delta t = 40 - 40 = 0^\circ\text{C}$.

$$\sigma_{40} = 0 \text{ MPa}$$

3) At minimum temperature of 0°C compression of body is $\Delta t = 40 - 0 = 40^\circ\text{C}$.

$$\sigma_0 = \alpha \cdot E \cdot \Delta t = 1.2 \cdot 10^{-5} \cdot 2 \cdot 10^{11} \cdot 40 = 96 \cdot 10^6 \text{ Pa} = 96 \text{ MPa}$$

Endurance Analysis in Accordance with Russian Standard SNiP2.05.03-84* (Bridges and Pipes)

Endurance analysis of steel structure elements of bridges and their connections should be carried out by the following formulas:

$$\sigma_{\max,ef} \leq \gamma_w \cdot R_y \cdot m, \quad (3.7)$$

$$\tau_{\max,ef} \leq 0.75 \gamma_w \cdot R_y \cdot m, \quad (3.8)$$

where:



$\sigma_{\max,ef}$ is maximum in absolute value stress (positive in compression). Stress is calculated from the effect of permanent and temporary;

$\tau_{\max,ef}$ is maximum in absolute value contact stress in the calculation of fillet welds shear (its direction is taken as positive);

Stress is calculated from the effect of permanent and temporary loads.

γ_w is the coefficient of reduction of steel design stress due to steel fatigue;

m is the coefficient of working conditions (Tab.60 SNiP);

$$\gamma_w = \frac{1}{\zeta \cdot \mathcal{G} \cdot [(\alpha\beta \pm \delta) - (\alpha\beta \mp \delta)\rho]} \leq 1, \quad (3.9)$$

where:

ζ is the coefficient equal to 1 for railway bridges and equal to 0,7 for road and city bridges;

\mathcal{G} - coefficient depends on the length of influence line loading in determining $\sigma_{\max,ef}$.

At the influence line length of $\lambda \geq 22\text{m}$ the coefficient is $\mathcal{G} = 1$; at $\lambda < 22\text{m}$, $\mathcal{G} = \nu - \xi \cdot \lambda$, where ν and ξ values are accepted depending on steel grade and effective coefficient of β concentration.

\mathcal{G} coefficient for the influence of lines lengths less than 22 m can be determined from the formulas:

- for carbon steel:

$$\mathcal{G} = \nu - \xi \cdot \lambda = (1.45 + 0.2917 \cdot (\beta - 1)) - (0.0205 + 0.01325 \cdot (\beta - 1) \cdot \lambda), \quad (3.10)$$

- for low alloy steel:

$$\mathcal{G} = \nu - \xi \cdot \lambda = (1.65 + 0.44 \cdot (\beta - 1)) - (0.0295 + 0.02006 \cdot (\beta - 1) \cdot \lambda), \quad (3.11)$$

where:

α and δ -coefficients considering steel grade and non-stationary mode of loading are taken from Tab.3.11

Table 3.11

Steel Grade	α	δ
16Д	0.64	0.20
15ХСНД; 09Г2СД	0.72	0.24
10ХСНД; 15ХСНД-40; 14Г2АФД; 15Г2АФДпс	0.81	0.20

β is effective coefficient of stress concentration. The values are taken from Tab. 1 Appendix 17 SNiP 2.05.03-84*, pages 181 – 186. The drawings of compounds are not given in the table, and the coefficients are taken from the description of construction details.

ρ is the cycle asymmetry coefficient: $\rho = \frac{\sigma_{\min}}{\sigma_{\max}}$, $\rho = \frac{\tau_{\min}}{\tau_{\max}}$,

σ_{\min} , σ_{\max} and τ_{\min} , τ_{\max} are minimum and maximum absolute values of stress with their signs, defined in the same sections as $\sigma_{\max,ef}$ and $\tau_{\max,ef}$. The worst is a symmetrical cycle where $\rho = -1$. When $\rho = +1$ there are no stress changes and endurance testing is not required.

In the formula (3.4) the upper signs in brackets should be taken when calculating by the formula (3.2) if $\sigma_{\max,ef} > 0$, and always by the formula (3.3).

For string construction the values of the coefficients are accepted as:

$$\zeta = 1.0$$

$$\mathcal{G} = 1.0$$

$$\alpha = 0.72 \text{ и } \delta = 0.24 \text{ for } 09\text{Г}2\text{СД}\text{-steel};$$



$\beta = 1,8$ – for basic metal of a detail on the boundary of raw butt weld with a smooth transition to the basic metal.

At a maximum temperature of $+100^{\circ}\text{C}$ there is maximum compression in a rail top:

Rail top is compressed (Fig. 3.31) $\sigma_{max} = 273$ MPa $\sigma_{min} = \sigma_{100} = 144$ MPa (midspan)
 $\rho = 144/273 = 0.527$

$$\gamma_w = \frac{1}{\zeta \cdot \vartheta \cdot [(\alpha\beta \pm \delta) - (\alpha\beta \mp \delta)\rho]} = \frac{1}{1 \cdot [(0.72 \cdot 1.8 - 0.24) - (0.72 \cdot 1.8 + 0.24) \cdot 0.527]} = 4.05 \geq 1$$

$$273\text{MPa} \leq 1.0 \cdot 315 \cdot 0.9 = 283.5\text{MPa}$$

At a temperature of $+40^{\circ}\text{C}$ there is neither compression, nor extension in a string-rail body:

Rail body is extended (Fig. 3.33) $\sigma_{max} = 187$ MPa, $\sigma_{min} = \sigma_{40} = 0$ MPa (midspan), $\rho = 0$.

$$\gamma_w = \frac{1}{\zeta \cdot \vartheta \cdot [(\alpha\beta \pm \delta) - (\alpha\beta \mp \delta)\rho]} = \frac{1}{1 \cdot [(0.72 \cdot 1.8 + 0.24)]} = 0.651$$

$$187\text{MPa} \leq 0.651 \cdot 335 \cdot 0.9 = 196\text{MPa}$$

Endurance of a rail body is provided.

At a minimum temperature of 0°C there is maximum extension in a string-rail body:

Rail body is extended (Fig. 3.41) $\sigma_{max} = 265$ MPa, $\sigma_{min} = \sigma_0 = 96$ MPa (midspan),
 $\rho = 96/265 = 0.362$.

$$\gamma_w = \frac{1}{\zeta \cdot \vartheta \cdot [(\alpha\beta \pm \delta) - (\alpha\beta \mp \delta)\rho]} = \frac{1}{1 \cdot [(0.72 \cdot 1.8 + 0.24) - (0.72 \cdot 1.8 - 0.24) \cdot 0.362]} = 0.867$$

$$265\text{MPa} \approx 0.867 \cdot 335 \cdot 0.9 = 261\text{MPa}$$

Statistically minimum temperature is quite rare. Endurance of a rail body is provided.

Endurance Analysis in Accordance with Russian Standard SNIIP II-23-81* (Steelwork)

Endurance analysis should be determined from the formula:

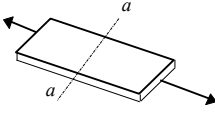
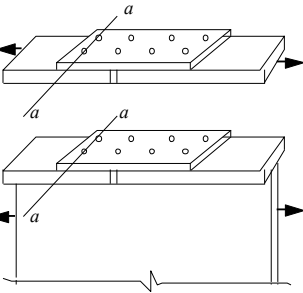
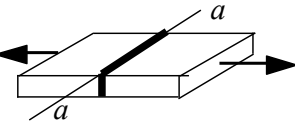
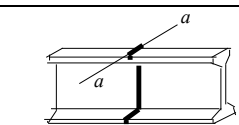
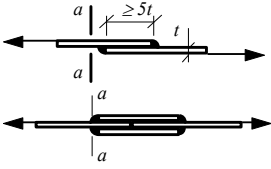
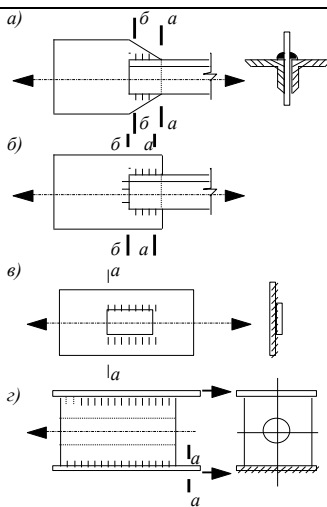
$$\sigma_{max} \leq \alpha \times R_v \times \gamma_v, \quad (3.12)$$

where:

R_v is estimated fatigue resistance taken from the Tab. 32* (SNIIP) depending on the tensile strength of steel and structural elements given in the Tab. 83* (SNIIP) (See the Tab. 3.12 below); for transverse welds (butt rolling sections) does not depend on rail material and is equal to $R_v = 75$ MPa (the fourth group of elements, No.14).

Table 3.12

Groups of elements and connections in endurance analysis

Ser. No.	Schematic representation of the element and the location of design section	Element Specification	Groups of Element
1		Basic metal with rolled or mechanically processed edges The same with edges, cut off with gas cutting machine.	1 2
3		Basic metal in high-strength bolts connections Basic metal in bolt (bolts, accuracy class A) connections in sections across the aperture	1 4
9		Butt-jointed raw seam; the load is perpendicular to the weld; jointing elements are of the same width and thickness	2
14		Butt-jointing rolling sections	4
20		Basic metal in the place of transition to the transverse (frontal) corner weld	6
21		Basic metal in connections with side-lap welds (in the places of transition from the element to the ends of side-lap welds): a) with double side-lap welds b) with side-lap and frontal welds b) during force transfer through basic metal r) anchor jaws where steel ropes are attached	8 7 7 8



R_v coefficient values are represented in Fig. 3.13.

Table 3.13

 R_v coefficient values (Tab. 32* SNiP II-23-81)

Groups of element	R_v values at temporary steel resistance to tearing R_{un} , MPa (kgf/cm ²)				
	Less than 420 (4300)	More than 420 (4300) Less than 440 (4500)	More than 440 (4500) Less than 520 (5300)	More than 520 (5300) Less than 580 (5900)	More than 580 (5900) Less than 635 (6500)
1	120 (1220)	128 (1300)	132 (1350)	136 (1390)	145 (1480)
2	100 (1020)	106 (1080)	108 (1100)	110 (1120)	116 (1180)
3	For all grades of steel 90 (920)				
4	For all grades of steel 75 (765)				
5	For all grades of steel 60 (610)				
6	For all grades of steel 45 (460)				
7	For all grades of steel 36 (370)				
8	For all grades of steel 27 (275)				

α is the coefficient taking into account the number of loading cycles n :

When $10^5 < n < 3.9 \cdot 10^6$ it is determined from the formulas:

-for groups of elements 1 and 2:

$$\alpha = 0.064 \left(\frac{n}{10^6} \right)^2 - 0.5 \left(\frac{n}{10^6} \right) + 1.75; \quad (3.13)$$

- for groups of elements 3-8:

$$\alpha = 0.07 \left(\frac{n}{10^6} \right)^2 - 0.64 \left(\frac{n}{10^6} \right) + 2.2; \quad (3.14)$$

when $n > 3.9 \cdot 10^6$ $\alpha = 0.77$.

For groups of elements 3 – 8 calculation by formula (2.11) results in:

when $n = 3.9 \cdot 10^6$	$\alpha = 0.77;$
when $n = 2.5 \cdot 10^6$	$\alpha = 1.04;$
when $n = 2.0 \cdot 10^6$	$\alpha = 1.2;$
when $n = 1.0 \cdot 10^6$	$\alpha = 1.63;$
when $n = 5.0 \cdot 10^5$	$\alpha = 1.9;$
when $n = 1.0 \cdot 10^5$	$\alpha = 2.14.$

γ_v is the coefficient defined in the Tab. 33 SNiP depending on the type of stress state and coefficient of stresses asymmetry $\rho = \sigma_{\min}/\sigma_{\max}$. In this case σ_{\min} and σ_{\max} are maximum and minimum values of the stresses in the estimated element.

γ_v coefficient values are represented in Fig. 3.14.



Table 3.14

 γ_v coefficient values (Table 33 SNiP II-23-81)

σ_{max}	Coefficient of stresses asymmetry ρ	Formulas for calculating γ_v coefficient
Compression	$-1 \leq \rho \leq 0$	$\gamma_v = \frac{2.5}{1.5 - \rho}$
	$0 < \rho \leq 0.8$	$\gamma_v = \frac{2.0}{1.2 - \rho}$
	$0.8 < \rho < 1$	$\gamma_v = \frac{1.0}{1 - \rho}$
Extension	$-1 \leq \rho < 1$	$\gamma_v = \frac{2}{1 - \rho}$

At maximum temperature of +100°C there is maximum compression in a string-rail top: rail top is compressed (Fig. 3.31): $\sigma_{max} = 273$ MPa, $\sigma_{min} = \sigma_{100} = 144$ MPa (midspan), $\rho = 144/273 = 0.527$,

$$\gamma_v = \frac{2}{1 - \rho} = 2.1.$$

When $n = 5.0 \cdot 10^5$ take $\alpha = 1.9$.

$$\alpha \times R_v \times \gamma_v = 1.9 \times 75 \times 2.1 = 299 \text{ MPa} > \sigma_{max} = 273 \text{ MPa}.$$

At a temperature of +40°C there is neither compression, nor extension in a rail body:

rail bottom is extended: (Fig. 3.33) $\sigma_{max} = 187$, MPa $\sigma_{min} = \sigma_{40} = 0$ MPa (midspan), $\rho = 0$

$$\gamma_v = \frac{2.5}{1.5 - \rho} = 1.67$$

When $n = 1.3 \cdot 10^6$ take $\alpha = 1.49$.

$$\alpha \times R_v \times \gamma_v = 1.49 \times 75 \times 1.67 = 187 \text{ MPa} \approx \sigma_{max} = 187 \text{ MPa}.$$

At minimum temperature of 0°C there is maximum extension in a rail body:

rail bottom is extended (Fig. 3.41): $\sigma_{max} = 265$ MPa, $\sigma_{min} = \sigma_0 = 96$ MPa (midspan),

$$\rho = 96/265 = 0.362.$$

$$\gamma_v = \frac{2.0}{1.2 - \rho} = 2.39$$

When $n = 1.3 \cdot 10^6$ take $\alpha = 1.49$.

$$\alpha \times R_v \times \gamma_v = 1.49 \times 75 \times 2.39 = 267 \text{ MPa} \approx \sigma_{max} = 265 \text{ MPa}$$

According to the statistics minimum and maximum temperatures occur rarely.

It should be mentioned that the analysis was carried out taking into account safety margin. As the filler will resist the shift, rail bottom extension will be decreased (part of the bending moment will be transferred to the strings). Analysis prove that in the absence of shift and at a temperature of 40°C rail bottom tension might be decreased by 36 per cent. Analysis for this case:

At temperature of +40°C there is neither compression, nor extension in a rail body:

rail bottom is extended (Fig. 3.33): $\sigma_{max} = 137$ MPa, $\sigma_{min} = \sigma_{40} = 0$ MPa (midspan), $\rho = 0$.

$$\gamma_v = \frac{2.5}{1.5 - \rho} = 1.67$$

When $n = 2.3 \cdot 10^6$ take $\alpha = 1.098$.

$$\alpha \times R_v \times \gamma_v = 1.098 \times 75 \times 1.67 = 137 \text{ MPa} \approx \sigma_{\max} = 137 \text{ MPa.}$$

Endurance of a rail body is increased up to 2 300 000 cycles. To increase the number of 2 300 000 cycles it is recommended to make use of filler with larger internal friction (to reduce the shift between cross section and the strings) and at the same time to reinforce the place of transverse welds. In fact, according to analysis procedure, it assumes the use of another group of elements (see. Tab. 3.12 and Tab. 3.13).

General view of suspended STS is represented in Fig. 3.43.



Fig. 3.43. General view of suspended STS (on the left there is front view of a unicar; on the right there is rear view of a unicar)

3.8. Conclusions on Suspended STS

Summarizing the results of the preliminary design work, analysis and assessment of the concept of iron ore transportation by suspended STS in Australia, the following conclusions might be drawn:

-unicars with load capacity of 15 tons provide ore transportation in the volume of 50 million tons per year on the following conditions: an average speed on a track is 72 km/h; the speed at loading and off-loading of ore at terminal stations is 1 m/s; traffic interval on a track is 10 seconds; the distance between the adjacent unicars is 200 m;

-the process of ore transportation should be fully automated;

-approx. 1010 unicars will be of use in the process of ore transportation at a distance of 100 km/h to achieve annual productivity of 50 million tons per year;

-fuel consumption during transportation of 1 ton of iron ore at a distance of 1 km for STS suspended unicar with load capacity of 15 tons is 3.9 g/t×km. This rate is approx. 16 percent lower than an average fuel consumption of ore transportation by a train, consisting of 40 dumpcars with load capacity of 60 tons at an average speed of 100 km/h;

-fuel consumption of ore transportation by motor vehicles on asphalt road will be 4 times higher and on gravel road fuel consumption will be 5.3 times higher;

-to provide fuel efficiency and energy saving installation capacity of autonomous power supply system should not be less than 45 kW;



- the results of contact strength analysis in “rail-wheel” pair prove that both linear and point contact might be implemented in suspended STS as wheel and rail top contact (a unicar might be equipped with eight wheels of 450 diameter (linear contact) or of 600 mm (point contact));
- a unicar of 15 tons load capacity will be approx. of the following linear dimensions: body length (without coupling unit) of 7850 mm, width of 2575 mm, height of 2150 mm, gauge of 1750 mm;
- total weight of a unicar will be approx. 25 tons;
- suspended STS has high ecological compatibility due to:
 - lower fuel (energy) consumption (it is 10-20 percent lower in comparison with rail road and 4-6 times lower in comparison with motor road);
 - 3-5 times lower resource intensity, i.e. fewer concrete, road metal, sand and gravel is needed to build a track; it results in reduction of negative impacts on Nature throughout the whole operational life of transportation system (production, transportation, installation and restoration of degraded mineral resources, which is the integral part of any transportation system construction);
 - the absence of embankment and assembled rails and sleepers of rail road and the absence of roadway covering provides environmental friendliness of STS track structure.



4. Conclusions

Mounted STS (transportation of bulk materials over a string-rail track structure with the help of speed multijointed motorails with load capacity of 160 tons, adapted for loading and off-loading of cargo on the move at special terminal stations) and suspended STS (transportation of bulk materials over a string-rail track structure with the help of unicars with load capacity of 15 tons, adapted for loading and off-loading of cargo on the move at special terminal stations in autonomous mode) provide transportation volume of 50 million tons per year.

Thus:

- both mounted and suspended STS provide lower fuel consumption (it is 10-20 percent lower in comparison with rail road, and 3-5 times lower in comparison with motor road);
- both mounted and suspended STS provide lower resource intensity, i.e. fewer concrete, road metal, sand and gravel is needed to build a track; it results in reduction of negative impacts on Nature;
- another important advantage of the suspended STS is the possibility of putting it to sea at a distance of 5-10 km from the shore for unloading of bulk cargo in special terminals, which will at the same time serve as remote seaports.

5. List of References

1. Berkman M.B. and others «Suspended Ropeways». – M.: Mashinostroyenie, 1984.
2. Petrenko O.S. «Suspended Railways». – M.: Mashinostroyenie, 1981;
3. Robert Bosch GmbH. «Automotive handbook» 4th edition, 1999;
4. Loginov A.I. and others «Dumpcars». – M.: Mashinostroyenie, 1975.
5. Timoshenko S. P. "Oscillations in Engineering".- M.: Nauka, 1967.
6. Birger I. A., Panovko Y. G. "Durability. Stability. Oscillations". Handbook in three volumes. Vol. 3.- M.: Mashinostroyenie, 1968.
7. Vershinskiy S.V. "Wagon Dynamics". 2nd edition.- M.: Transport, 1978.